Report No. FAA-RD-70-71

ELECTROSPACE PLANNING AND ENGINEERING FOR THE AIR TRAFFIC ENVIRONMENT

G.D. Gierhart, R.W. Hubbard, and D.V. Glen
U.S. Department of Commerce
Office of Telecommunications
Institute for Telecommunication Sciences
Boulder, Colorado

December 1970

FINAL REPORT

Availability is unlimited. For sale by Superintendent of Documents, U.S. Government Printing Office, Washington, D.C. 20402

Prepared for
FEDERAL AVIATION ADMINISTRATION
Systems Research and Development Service
Washington, D.C. 20590

This report was prepared for the Spectrum Plans and Programs Branch, Frequency Management Division, Systems Research and Development Service, Federal Aviation Administration, under Contract No. FA 67 WAI-134. The views presented are not necessarily those of the FAA and do not reflect FAA Policy. This report does not constitute a standard, specification, or regulation.

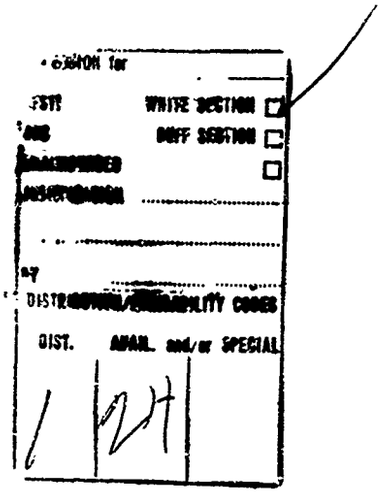

For sale by the Superintendent of Documents, U.S. Government Printing Office
Washington, D.C., 20402-Price $2.25

TECHNICAL REPORT STANDARD TITLE PAGE

1. Report No.	2. Government Accession No.	3. Recipient's Catalog No.
FAA-RD-70-71		

4. Title and Subtitle	5. Report Date
Electrospace Planning and Engineering for the Air Traffic Environment	December 1970
	6. Performing Organization Code
7. Author(s) G. D. Gierhart, R. W. Hubbard, D. V. Glen	8. Performing Organization Report No.
9. Performing Organization Name and Address U. S. Department of Commerce Office of Telecommunications (formerly ESSA Res. Labs) Institute for Telecommunication Sciences1 Boulder, Colorado 80302	10. Work Unit No.
	11. Contract or Grant No. FA67WAI-134
12. Sponsoring Agency Name and Address U. S. Department of Transportation Federal Aviation Administration Systems Research and Development Service Washington, D. C. 20590	13. Type of Report and Period Covered Final Report
	14. Sponsoring Agency Code

15. Supplementary Notes

16. Abstract

Service limitations imposed upon VHF/UHF/SHF radio communication links by cochannel and adjacent-channel interference is the primary subject, but limitations imposed by intermodulation and noise are also discussed. Methods for predicting available desired-to-undesired signal ratios (protection ratio) and determining the required protection ratio are summarized. Appendices on frequency sharing with air traffic control satellite, modulation characteristics, and system performance measurements are included.

17. Key Words	18. Distribution Statement
Air Traffic Control, Electrospace Frequency Sharing, Interference Protection Ratio Propagation, Satellite Communication, Transmission Loss.	For sale by the Superintendent of Documents, U.S. Government Printing Office, Washington, D.C. 20402

19. Security Classif. (of this report)	20. Security Classif. (of this page)	21. No. of Pages	22. Price
Unclassified	Unclassified	303	$2.25

Form DOT F 1700.7 (8-69)

TABLE OF CONTENTS

LIST OF FIGURES

LIST OF FIGURES (continued)

LIST OF FIGURES (continued)

LIST OF FIGURES (continued)

LIST OF FIGURES (continued)

LIST OF FIGURES (continued)

LIST OF TABLES

LIST OF SYMBOLS

This list includes most of the abbreviations, acronyms, and symbols used in this report. Many are identical to those used by Rice et al. (1967), Gierhart (1967) and / or Hubbard et al. (1970). The units given for symbols in this list are those required by or resulting from equations as given in this report and are applicable except when other units are specified. The following relationships are provided as a convenience to the reader.

1 ft	$= 3.048 \times 10^{-4}$ km
1 sm	= 5280 ft
1 sm	= 1.60934 km
1 nm	= 1.852 km
1 rad	$= 57.29577951^{\circ}$

In the following list the English alphabet precedes the Greek alphabet, letters precede numbers, and lower-case letters precede upper-case letters. Miscellaneous symbols and notations are given after the alphabetical items.

a(t)	normalized amplitude factor of a modulated signal as a dimensionless voltage ratio from (B-5).
A	defined by (A-8) and expressed in dBW (sec. A.2.3 only).
A	the peak value in V of the sinusoid in (B-33) and (B-34).
A(t)	amplitude factor of a modulated signal in V.
A_0	peak amplitude of carrier sinusoid in V.
A_e	effective area of an antenna in m^2 from (43).
A_Y	a conditional adjustment to L_{bs} in dB from (10).
AF	audio frequency.
AFC	automatic frequency control.
AGARD	Advisory Groups for Aerospace Research and Development.

AGC	automatic gain control.
AI	articulation index.
AM	amplitude modulation.
AM_D	desired AM signal.
ASK	amplitude shift keying.
ATC	air traffic control.
b(t)	normalized baseband or message signal as a dimensionless voltage ratio.
bit	binary digit.
B	receiver bandwidth in Hz.
B	a dimensionless distance ratio defined in fig. 35 (sec. 5.2 only).
B	transmission bandwidth in Hz (sec. B.2.1 only).
B_a	system bandwidth in Hz (sec. B.2.3 only).
B_c	single-channel bandwidth in kHz.
B_f	bandwidth of information signal in Hz, i.e., baseband (sec. B.2.3 only).
B_o	AF output bandwidth in Hz.
B_n	effective receiver noise bandwidth in Hz (footnote 10, sec. 4.2.3).
B_s	bandwidth of baseband signal in Hz.
B_M	approximate bandwidth of modulated spectrum in Hz.
B_R	RF bandwidth of the modulated signal in Hz.
$B_{3\,dB}$	bandwidth defined by half-power, 3 dB, points in kHz (sec. 4.2.3).
c	4.342944819 from (20).
C-MSG	C-message line weighting from fig. 16 (sec. 3.3.4 only).
C	a distance in nm defined in fig. 35 (sec. 5.2 only).
C_U	a parameter in dB defined by (55).
CCIF	International Frequency Consultative Committee
CCIR	International Radio Consultative Committee.

CEI	Communications Electronics, Inc..
COMSAT	Communications Satellite Corporation.
CW	continuous wave.
d	great circle path distance in nm.
d_e	effective distance in km from (14).
d_{s1}	a distance in km from fig. 3.
d_B	d in nm for "B" facility-to-aircraft "B" path (fig. 36).
d_D	d in nm for desired path (fig. 33).
d_K	d expressed in km.
d_L	path smooth-earth horizon distance in km from (15).
$d_{L1,2}$	either terminal smooth-earth horizon distance d_{L1} or d_{L2} in km (fig. 2).
d_U	d in nm for undesired path (fig. 33).
dB	decibels.
dB/kT_oB_n	dB greater than kT_oB_n (sec. 3.3.1).
dBm	dB greater than 1 mW.
dBW	dB greater than 1 W.
D(p)	desired signal power variability in W.
D/U	desired-to-undesired signal power ratio in dB.
D/U(min)	minimum value of D/U in dB from (A-16).
D/U(p, n)	D/U variability in dB for n undesired signals (sec. A.2.4 only).
$D/U(q_T)$	D/U variability in dB from (6).
$D_{dBW}(p)$	D(p) expressed in dBW.
DC	direct current.
DEI	Defense Electronics, Inc..
DM	delta modulation.
DPSK	differentially coherent PSK.
DSB	double sideband.

DSB/ SC	DSB/ suppressed carrier.
e	2.718281828.
$e_B(t)$	normalized baseband or message signal as a dimensionless voltage ratio from (B-7).
$e_M(t)$	normalized modulated signal as a dimensionless voltage ratio from (B-6).
$e_o(t)$	exponential or complex carrier signal function as a dimensionless voltage ratio from (B-27).
$erfc^{-1}$	inverse complementary error function.
E_n	rms noise field strength for bandwidth B_n in $\mu V/m - Hz$.
$E_{n_{dB}}$	E_n in dB greater than 1 $\mu V/m$.
$E_B(t)$	baseband or message signal in V.
$E_M(t)$	modulated carrier signal in V from (B-4).
EIRP	effective isotropic radiated power.
EPUT	event per unit time meter.
ERL	ESSA Research Laboratories.
ESSA	Environmental Science Services Administration.
f	frequency in MHz (in kHz for fig. B.3 only).
f(t)	modulating signal in V (sec. B.1.3).
f_a	effective antenna noise factor, a dimensionless power ratio (fig. 15).
f_c	antenna circuit noise factor, a dimensionless power ratio (fig. 15).
f_d	carrier offset frequency in kHz (sec. 5.4 only).
f_d	rms frequency deviation in kHz (fig. B.3).
f_D	Doppler frequency in Hz.
f_m	maximum baseband frequency in kHz (in Hz for sec. B.2.1 only).
f_n	network noise factor, a dimensionless power ratio from (35).

f_{1o}, f_{1o}'	assigned and actual LO frequency respectively, in Hz (sec. 5.4 only).
f_o, f_o'	assigned and actual carrier frequency respectively, in Hz (sec. 5.4 only).
f_p	frequency in kHz at which $S_{e_B}(f)$ peaks (fig. B.3).
f_r	receiver noise factor, a dimensionless power ratio (fig. 15).
f_s	effective system noise factor, a dimensionless power ratio from (40).
f_s	sampling frequency in Hz (sec. B.2.3 only).
f_t	test tone frequency in Hz (sec. B.2.3 only).
f_t	transmission line noise factor, a dimensionless power ratio (fig. 15).
f_1	f_t expressed in kHz (fig. B.2).
ft	feet.
F[ ]	Fourier transform operator.
F_a	antenna noise figure in dB/kT_oB_n from (fig. 9).
F_{an}	median antenna noise figure in dB/kT_oB_n from (fig. 8).
F_n	network noise figure in dB from (37).
F_r	receiver noise figure, f_r, in dB.
F_s	effective system noise factor in dB.
FAA	Federal Aviation Administration.
FCC	Federal Communications Commission.
FDM	frequency division multiplex.
FM	frequency modulation.
FM_D	desired FM signal.
FS	frequency shift.
FSK	frequency shift keying.
FIA	line weighting (fig. 16).
$g(q_T, f)$	dimensionless frequency factor from fig. 5.

$g(t)$	general complex time function from (B-11).
g_r	G_r expressed as a dimensionless power ratio.
g_s	required grade of service (sec. 2).
G	either G_r or G_t.
$G(\omega)$	spectrum of $g(t)$.
G_n	dimensionless network power gain ratio (sec. 3.3.2).
G_{pp}	path antenna power gain in dB greater than isotropic for (8)
G_r, G_t	maximum free-space gain in dB greater than isotropic for receiving and transmitting antennas, respectively.
GHz	gigahertz.
hr	hours.
h_A, h_B	altitude in ft above surface of aircraft "A" and aircraft "B", respectively.
$H[\ ]$	Hilbert transform operator from (B-17).
H_r, H_t	height of receiving or transmitting antenna in ft above surface.
$H_H(\omega)$	transfer function for Hilbert transform from (B-23).
H_1, H_2	antenna height for terminal 1 or 2 in ft above surface.
Hz	hertz or cycles per second.
IEEE	Institute of Electrical and Electronic Engineers.
IF	intermediate frequency.
Im	imaginary part operator.
IER	Institutes for Environmental Research.
ITS	Institute for Telecommunication Sciences.
ITT	International Telephone and Telegraph.
ITU	International Telecommunication Union.
j	imaginary operator, $\sqrt{-1}$.
$J_n(\ )$	Bessel function of first kind and order n.

JTAC	Joint Technical Advisory Committee.
k	1.374×10^{-23} joules/$^{\circ}$K, Boltzmann's constant.
k_p	gain factor dependent upon the distribution of the modulating signal.
km	kilometers.
kHz	kilohertz.
kW	kilowatts.
K	a power ratio in dB used in fig. A.6 and defined in footnote 2 of sec. 3.
K	degrees Kelvin.
ℓ_a	a dimensionless power loss ratio defined as 1 in fig. 15.
ℓ_c	antenna circuit coupling loss expressed as a dimensionless power ratio that is ≤ 1 (fig. 15).
ℓ_t	transmission line loss expressed as a dimensionless power ratio that is ≤ 1 (fig. 15).
log	common logarithm (base 10).
ln	natural logarithm (base e).
L	number of quantizing levels.
L_b	hourly median basic transmission loss in dB.
$L_b(q_T)$	a level of L_b in dB that is not exceeded for a fraction q_T of the time.
L_{bf}	L_b in dB for propagation through free space from (11)
L_{bm}	estimated long-term median of L_b in dB as given by Gierhart and Johnson (1969).
L_c	ℓ_c expressed in dB.
L_p	polarization loss in dB (table A.1).
L_t	line loss, ℓ_t, in dB.
LO	local oscillator.
m	meters.
min	minutes.

ms	milliseconds.
m(t)	general modulation function, the dimensionless voltage ratio of (B-28).
mW	milliwatt.
m_x	mean value of x.
m_y	mean value of y.
m_z	mean value of z from (A-2).
m_z'	mean value of z' from (A-3).
M	a constant used in sec. 5.2 only.
M	number of channels in a multichannel system for (B-38) only.
M	modulation index for linear modulation, a dimensionless voltage ratio.
M(ω)	spectrum of the modulation function m(t).
M_f	fading margin in dB (table A.1).
M_i	mean power in dBW of the i^{th} signal.
M_n	mean power in dBW resulting from n signals, obtained from (18), (A-5) or (A-7).
MHz	megahertz.
MRT	modified rhyme test.
n	number of undesired signal sources.
n	order of $J_n(\ )$ (sec. B.1.1 only).
n	number of elements the quantized signal is coded into (sec. B.2.1 only).
nm	nautical miles.
N	average noise power in W.
N	defined by (A-9) as a dB value (sec. A.2.3 only).
N	coding base (secs. B.2.1 and B.2.3 only).
N	positive integer for (A-1) only.
N_c	single channel available noise power in W for (47).

N_i	available input noise power in W.
N_o	available output noise power in W.
N_s	surface refractivity in N-units.
N_u	power density of white Gaussian noise in W/Hz.
NAFEC	National Aviation Facilities Experimental Center.
NATO	North Atlantic Treaty Organization.
p	time availability in % ($100 \times q_T$).
p_J	Johnson noise power in W/Hz from (27).
p_n	noise power available from an equivalent lossless antenna in W (sec. 3.3.1).
p.d.f.	probability density function.
pps	pulses per second.
P_e	probability of error.
P_r	total system noise power or system threshold dBW for applicable B_n.
P_s	system noise power density in dB greater than 1 W/Hz.
P_s	total received signal power at antenna terminals in W for (42).
P_B	baseband signal power in W from (B-34).
P_J	Johnson's noise in dBW from (28).
P_M	allowable undesired satellite signal for microwave systems in dB greater than 1 W/m^2 for a 4-kHz bandwidth from (44).
P_0	average carrier power in W, table B.3.
P_S	total received power in W for use in (42) only.
P_{TF}	total system noise power flux density in dB greater than 1 W/m^2 for a 30-kHz bandwidth.
PAM	pulse amplitude modulation.
PB	phonetically balanced (words or messages).
PCM	pulse code modulation.
PDM	pulse duration modulation.

PEP	peak envelope power.
PFM	pulse frequency modulation.
PM	pulse modulation.
PPM	pulse position modulation.
PSK	phase shift keying.
PTM	pulse time modulation.
q	same as q_T (footnote 11, sec. 5.1).
q_L	location availability (sec. 2).
q_T	time availability, a fraction of time used in (12) and (13).
Q	service probability, a fraction between 0 and 1 (sec. 5.1).
r_D	a distance in nm defined in fig. 35.
r_U	a distance in nm defined in fig. 35.
rad	radians.
rms	root mean square.
R	a radius in nm defined in fig. 35.
$R_s(q_T)$	signal ratio available q_T of the time.
$R_r(g_s)$	signal or protection ratio required for g_s.
R_{IM}	dimensionless signal power-to-intermodulation power ratio.
R_N	normal range in nm for (A-14).
R_R	reduced range in nm for (A-14).
Re	real part operator.
Rec	recommendation.
RF	radio frequency.
s	seconds.
sgn( )	a dimensionless function defined by (B-23).
sm	statute miles.
S	station separation in nm (fig.'s 34 and 36).
S	signal level in dBW (sec. 4.2.3 only).

$S(f)$	spectral density function in W/Hz.
SF	shape factor of receiver IF bandwidth defined by (60).
S/N	dimensionless signal power-to-noise power ratio.
S/N_c	dimensionless ratio of signal-to-noise power in a 4 kHz channel.
$S/N(g_s)$	S/N required for a particular g_s.
S/N_W	signal power-to-noise power density ratio in Hz.
S_c	carrier portion of RF input power in W (fig. 28).
S_c/N	dimensionless carrier power-to-noise power ratio.
S_c/N_W	carrier power-to-noise power density ratio in Hz.
$S_{e_g}(f)$	baseband spectral density function (fig. B.3).
$S_s(f)$	modulated signal spectral density function (fig. B.3).
SCI	speech communication index.
SCIM	SCI meter.
SHF	superhigh frequency band, 3 to 30 GHz.
SSB/L	single sideband/lower.
SSB/U	SSB/upper.
t	time in s.
T_a	antenna noise temperature in ^{o}K from (32).
T_c	antenna circuit temperature in ^{o}K (fig. 15).
T_e	effective noise temperature in ^{o}K from (36).
T_o	reference temperature of 288^{o}K.
T_r	pulse transmission rate in pps.
T_t	transmission line temperature in ^{o}K (fig. 15).
TDM	time division multiplex.
TMR-5	a DEI receiver model.
TR-711	a DEI receiver model.
TRMS	true root mean square.
U	undesired signal power in W.

$U(p, n)$	U variability in W for n undesired AM networks (sec. A.2.4).
U_{dBW}	U expressed in dBW.
$U_{dBW}(p, n)$	U_{dBW} variability in dBW for n undesired AM networks (sec. A.2.4).
UHF	ultra high frequency band, 300 to 3,000 MHz.
v	rate of change of path length (m/s).
VHF	very high frequency band, 30 to 300 MHz.
VOR	VHF omnirange, an air navigation aid.
W	watts.
W	hourly median available power at the receiving antenna terminals in dBW.
W/m^2-Hz	power flux density per Hz.
$W(q_T)$	W in dBW exceeded for a fraction q_T of the time from (13).
W_m	long-term median of W in dBW from (8) or W(0.5).
W_t	power delivered to the terminals of the transmitting antenna in dBW.
$W_D(q_T)$	$W(q_T)$ in dBW for desired signal.
$W_U(q_T)$	$W(q_T)$ in dBW for undesired signal.
x	a random variable (sec. A.2.2).
x	multiplication.
x(t)	a general time function or signal (real).
x_i	value of x characterizing the i^{th} percentage range.
X	a dB value used in fig. A.7.
$X(\omega)$	spectrum of x(t).
y	a random variable (sec. A.2.3).
y(t)	a general time function or signal (real).
y_j	value of y characterizing the j^{th} percentage range.
$Y(q_T)$	long-term variability of W in dB greater than W_m.
$Y(q, d_e, 100\ MHz)$	same as $Y_o(q_T, d_e)$ (fig. 30).

$Y(\omega)$	spectrum of y(t) (app. B only).
$Y_i(q_T)$	$Y(q_T)$ in dB for i^{th} signal.
$Y_o(q_T)$	long-term power-fading in dB from fig. 4.
$Y_D(q_T)$	$Y(q_T)$ in dB for desired signal.
$Y_v(q_T)$	long-term variability of $D/U(q_T)$ in dB greater than $D/U(0.5)$.
$Y_U(q_T)$	$Y(q_T)$ in dB for undesired signal(s).
z	the random variable x + y.
z'	the random variable x - y.
z_n	a particular value of z, $x_i + y_j$.
z_{no}	(dimensionless) standard normal deviate (fig. 32).
960	CEI receiver model number.
6A3	emission B_R = 6 kHz, AM, f_s = 3 kHz.
15F3	emission B_R = 15 kHz, FM, f_s = 3 kHz.
α	mean value of undesired power in W available from a single AM network (sec. A.2.3).
α	(dimensionless) fraction of total RF power not included in B_R (app. B only).
α_i	mean value of power in W available from the i^{th} undesired signal source (sec. 3.2).
β	modulation index or deviation ratio for FM, a dimensionless frequency ratio.
β_F	same as β.
β_p	modulation index for PM, a dimensionless phase ratio.
γ	actual direct ray takeoff angle or look angle in degrees for (44) and fig. A.1.
$\delta_o(\ )$	dimensionless unit impulse function.
$\delta_{-1}(\ )$	dimensionless unit step function defined by (B-22).
Δf_0	$f_0 - f_0'$ in Hz (sec. 5.4 only).
Δf_{10}	$f_{10} - f_{10}'$ in Hz (sec. 5.4 only).
ΔD	desired power increase in dB from (A-14).

ΔF	peak frequency deviation in kHz.
ΔIF	shift of IF frequency from (57) in Hz (sec. 5.4 only).
ΔP	power margin in dB from (52).
ΔN	internal noise introduced by network in W for (34).
ΔR	range reduction in nm from (A-15).
$\Delta\Omega$	frequency deviation in rad/s.
θ	an angle defined in fig. 33.
$\theta(t)$	time variant angular frequency in rad for (B-5).
θ_o	initial phase angle of carrier wave in rad.
λ	wavelength of operating frequency in m for (43).
λ^2	one-half the variance of the Laplace distribution of sec. B.1.3.
Λ	(dimensionless) peak-to-average power ratio.
Λ_B, Λ_M	(dimensionless) peak-to-average power ratio of the baseband and modulated signal, respectively (B.1.3).
μ	variance in W^3 of undesired power available from a single AM network (sec. A.2.3).
uV	microvolts.
uV/m-10 kHz	field intensity for 10-kHz bandwidth.
μ_i	variance in W^2 of undesired power available from the i^{th} source.
π	3.141592654.
ρ	dimensionless imput carrier power-to-noise power ratio (fig. 29).
σ^2	the variance of the Gaussian distribution of sec. B.1.3.
$\sigma_c(q)$	standard error of prediction in dB from (53).
σ_i^2	variance in dB^2 of undesired received power for the i^{th} source from (24).
σ_n^2	variance in dB^2 of the normally distributed dBW resulting for n sources from (19) or (A-5).
σ_x^2, σ_y^2	variance of x and y, respectively.

σ_z^2, $\sigma_{z'}^2$	variance of z and z', respectively.
$\sigma_{D}^2{}_{,n}$	variance of D/U(p, n) in dB from (A-12).
Σ	summation.
τ	time lag in s.
$\varphi(t)$	general phase function in rad.
$\varphi_o(t)$	phase function of carrier wave in rad.
$\Phi_B(\omega)$	spectrum of the baseband function.
$\Phi_M(\omega)$	spectrum of the modulated carrier wave.
ω	angular frequency in rad/s.
ω_o	ω for carrier in rad/s.
Ω	ohms.
Ω	peak angular frequency deviation in rad.

$(\quad)_a$	available parameter value, e.g., $(D/U)_a$.
$(\quad)_a$	adjacent channel, e.g., $(\Delta f_o)_a$ (sec. 5.4 only).
$(\quad)_d$	desired channel, e.g., $(\Delta f_o)_d$ (sec. 5.4 only).
$(\quad)_{dB}$	parameter expressed in dB, e.g., $(S/N)_{dB}$.
$(\quad)_i$	input parameter value, e.g., $(S/N)_i$.
$(\quad)_o$	output parameter value, e.g., $(S/N)_o$.
$(\quad)_r$	required parameter, e.g., $(D/U)_r$.
$\underline{(\quad)}$	analytical signal, e.g., $\underline{b}(t)$.
$(\quad)^o$	degrees.
$(\quad)^*$	complex conjugate, e.g., $e_o^*(t)$.
$(\check{\ })$	Hilbert transform, e.g., $\check{X}(\omega)$.
$(\dot{\ })$	partial derivative, e.g., $\dot{\theta}(t)$.

$(\hat{\ })$	peak value, e.g., $\hat{E}_\theta$.
$-$	subtraction.
$+$	addition.
$\mp$	minus or plus.
$\boxtimes$	convolution via (B-19).
$\oplus$	convolution via $z = x + y$ process of sec. A.2.3.
$\ominus$	convolution via $z' = x - y$ process of sec. A.2.3.
%	percent.
$\sqrt{\ }$	positive square root.
$=$	is equal to.
$\simeq$	is approximately equal to.
$>$	is greater than.
$>>$	is much greater than.
$\geq$	is greater than or equal to.
$<$	is less than.
$\approx$	is proportional to.
$\sim$	approximately.
$\cdot$	multiplication.

ELECTROSPACE PLANNING AND ENGINEERING FOR THE AIR TRAFFIC ENVIRONMENT

G. D. Gierhart, R. W. Hubbard, and D. V. Glen

Service limitations imposed upon VHF/ UHF/ SHF radio communication links by cochannel and adjacent-channel interference is the primary subject of this report, but limitations imposed by intermodulation and noise are also discussed. Methods for predicting available desired-to-undesired signal ratios (protection ratio) and determining the required protection ratio are summarized. Appendices on frequency sharing with an air traffic control satellite, modulation characteristics, and system performance measurements are included.

Key Words: Air traffic control, electrospace, frequency sharing, interference, protection ratio, propagation, satellite communication, transmission loss.

1. INTRODUCTION

Electrospace is becoming more congested and more efficient use of this natural resource must be made if vital telecommunication requirements are to be satisfied (Norton, 1962; JTAC, 1964, 1968; Commerce Technical Advisory Board, 1966; Booker and Little, 1965). The term "electrospace" is used here only to emphasize that efficient use of the electromagnetic spectrum for radio telecommunication depends on parameters other than frequency, e.g., time , polarization, radiated power, antenna directivities, and terminal locations.

However, the eight-dimensional matrix concept of electrospace suggested by Hinchman (1969) is not used in this report.

Electrospace assigned to aeronautical radio must provide reliable services for an increasing air traffic density (IEEE, 1970). Potential interference between facilities operating on the same or on adjacent channels must be considered in expanding present services to meet future demands. Service quality depends on the desired-to-undesired signal ratio at the receiver, which varies with receiver location and time even when other parameters, such as antenna gain and radiated powers, are fixed (Kirby et al., 1952).

This report provides information applicable to services operating from about 100 MHz to about 15 GHz. At these frequencies, propagation of radio frequency energy is affected by the lower, nonionized atmosphere (troposphere), specifically by variations in the refractive index (Bean and Dutton, 1966) of the atmosphere. Atmospheric absorption and attenuation or scattering due to rain becomes important at SHF (Rice et al., 1967, chs. 3 and 10; Gierhart and Johnson, 1969, app. B; Kerr, 1964, ch. 7; Skerjanec and Samson, 1970). The terrain along and in the vicinity of the great-circle path between transmitter and receiver also plays an important part. In this frequency range, time and space variations of received signal and interference ratios are best described statistically.

Within the last decade a number of methods and procedures have been developed for calculating field strength and its variability at VHF/UHF/SHF. The work discussed here follows procedures that have been used by the Institute for Telecommunication Sciences (ITS, formerly the Central Radio Propagation Laboratory) to predict statistically the effects of terrain and atmosphere on the variability of field strength, and on the performance of radio systems (Rice et al.,

1967; Johnson, 1967; Longley and Rice, 1968). It is also convenient to use the concept of transmission loss (Norton, 1953 and 1959), which is the ratio (usually expressed in decibels) of power radiated to the power that would be available at the receiving antenna terminals if there were no circuit losses other than those associated with the radiation resistance of the receiving antenna.

The primary purpose of this report is to illustrate the application to interference predictions for air traffic control (ATC) systems of (a) the available desired-to-undesired signal ratios (protection ratios) predicted by Gierhart (1967) for an ATC satellite, (b) the transmission loss atlas developed by Gierhart and Johnson (1969), (c) the required protection ratios derived from measurements made by Hubbard and Glen (1968), and O' Brien and Busch (1969), and (d) the analysis of modulation characteristics reported by Hubbard et al. (1970).

Basic service requirements in terms of required signal ratios associated with intermodulation, noise, and interference are discussed in section 2. Methods for the prediction of available signal ratios and the determination of required signal ratios are summarized in section 3 and 4, respectively. Illustrative examples of the application of these methods are given in section 5. Frequency sharing with an air traffic control satellite is analyzed in appendix A.

The use in frequency engineering of information such as that presented here has been discussed by Hawthorne and Dougherty (1965) and Frisbie et al. (1969); information on spectrum engineering for air navigation aids is given by JTAC (1968), the international Civil

Aviation Organization (1968), and the Federal Aviation Administration[1] (FAA, 1965a, 1965b, 1969a, 1969b).

2. SIGNAL RATIO REQUIREMENTS

Satisfactory service is provided by a communication link when the information transmitted is received with the required fidelity. Intermodulation, noise, and interference limit the fidelity that can be obtained over a particular link at a given time. In general, service requirements should specify the extent to which degradation caused by these factors may be tolerated. However, circumstances may be such that initial link design and/or installation can provide adequate preformance with respect to some of these factors so that they need not be considered further, e.g., links are frequently engineered so that intermodulation and interference effects are negligible compared with an estimated constant noise level, and performance predictions are based only upon the time variability and prediction uncertainty associated with transmission loss estimates for the desired propagation path.

We will assume that satisfactory service is obtained only when

$$(R_{IM})_a > (R_{IM})_r , \quad (1)$$

$$(S/N)_a > (S/N)_r , \quad (2)$$

and

$$(D/U)_a > (D/U)_r , \quad (3)$$

where

R_{IM} = signal power-to-intermodulation power ratio in dB,

[1] When the Federal Aviation Agency (FAA) became a part of the Department of Transportation in April 1967, it was given the new name Federal Aviation Administration (still FAA).

S/N = dimensionless signal power-to-noise power ratio (sec. 3.3.4),

D/U = desired signal power-to-undesired signal power ratio in dB.

and the subscripts a and r denote available and required ratios, respectively.

To allow unique values for these ratios, they can be determined for the case where the loss in fidelity associated with the other two ratios is negligible e.g., $(D/U)_r$ would be determined for the case where $(R_{IM})_a \gg (R_{IM})_r$ and $(S/N)_a \gg (S/N)_r$.

Though convenient, this method neglects whatever interdependence the required ratios may have, and levels of fidelity used to determine them would probably be somewhat larger than that actually obtained when the available ratios are all equal to their respective required ratios. An approximate compensation for this effect can be made by increasing the required ratios to account for the increase in apparent undesired power when more than one available ratio is important, e.g., by 5 dB ($\approx$10 log 3) if all available ratios are near their required values, or by increasing the two required ratios that are near their available ratios by 3 dB ($\approx$10 log 2) if one available ratio is very much greater than its required value (see sec. 3.3.2 and app. D).

The significance as well as the magnitude of these ratios depends upon the location of the measurement point within the receiving system to which they are referred. In this report the ratios will be understood to be available power ratios at the receiving antenna output; the problem of deriving these ratios from measurements made at other points in the receiving system is left to the user (sec. 3.3.2).

The distinguishing characteristic of intermodulation is that it cannot be reduced effectively by simply increasing the radiated power of the desired station; i.e., an increase in radiated power will increase the available desired power, but this increase will be accompanied by a corresponding increase in intermodulation power and $(R_{IM})_a$ will be unchanged. Actually, an attempt to increase $(R_{IM})_a$ by increasing radiated power would result in a decrease of fidelity because of increased equipment noise level if the power received is in excess of the receiver saturation level. Intermodulation may be caused by nonlinearities in the equipment, resulting from, for an example, a transmission line that is not properly matched across the frequency band required (Medhurst, 1959), or from propagation where it is primarily associated with multipath (Beckmann and Spizzichino, 1963, ch. 16; Dougherty, 1968; Sunde, 1969).

Propagation via tropospheric scatter is basically a multipath phenomenon (Beach and Trecker, 1963), and it is customary to limit path intermodulation by restricting the operating bandwidth used over such paths (Shaft, 1961; Sunde, 1964). Antenna directivity and/or an improvement in receiver capture ratio (sec. 4.5) can sometimes be used to reduce path intermodulation caused by scattering or reflection from terrain on line-of-sight or diffraction paths. Wideband microwave line-of-sight links may experience occasional path intermodulation (Gierhart et al., 1964) because of atmospheric multipath (Crawford and Jakes, 1952). The nature of these disturbances suggests that adaptive systems to sense and adjust the bandwidth in accordance with the capabilities of the path might be useful, but site relocation, alternate routing, or simply accepting short-time periods of inferior performance may be more practical.

Some of the methods mentioned above for combating path intermodulation can also be used to help alleviate the detrimental effects of phase interference fading when low signal level rather than path intermodulation is the basic problem. However, the diversity techniques frequently used to counter these low signal levels should not be expected to be effective in reducing $(R_{IM})_a$, except perhaps by sophisticated combiner circuits.

Intermodulation will not be discussed further here since a more comprehensive treatment is beyond the scope of this report. It has been mentioned primarily to alert the reader to the existence of a limitation to link performance that cannot be solved by increasing radiated power.

In this report, the noise power involved in S/N at the output terminals of the receiving antenna is taken to be the effective system noise power obtained from (40) in section 3.3.2. The undesired signal power involved in D/U is the power that would be available at the output terminals of the receiving antenna when noise is neglected and no power from the desired station is present. This power may result from one or many undesired signal transmissions and is not dependent upon the receiver bandpass characteristics.

The service requirements described above are based only on the fidelity required for satisfactory transmission and do not allow adequately for the uncertainties associated with the transmission characteristics of radio channels. These determine the time availability of satisfactory service that will be discussed in section 3.

Semi-empirical methods of predicting the time variability, location-to-location variability, and service probability of transmission loss for tropospheric communication circuits have been developed by Barsis et al. (1962), Rice et al. (1967), and Longley and Rice (1968). The prediction of available ratios as presented here

is in the context of these methods, and the reader is encouraged to become familiar with them.

A required grade of service g_s for desired signal in the presence of undesired signals will guarantee a corresponding degree of fidelity of the information delivered to the receiver output and is assumed to depend only upon whether a required desired-to-undesired signal ratio $R_r(g_s)$ is exceeded. If increasing values of available grades represent better grades of service, $R_r(g_s)$ must increase with g_s.

A communication link is assumed to provide satisfactory service of a given grade g_s if the available signal-to-noise ratio R_a exceeds the required protection ratio $R_r(g_s)$ for at least a fraction q_T of the time; i.e., satisfactory service exists if

$$R_a(q_T) > R_r(g_s). \qquad (4)$$

In this expression $R_a = (S/N)_a$, or $R_a = (D/U)_a$, or R_a is a suitable combination of $(S/N)_a$ and $(D/U)_a$, and $(R_{IM})_a \gg (R_{IM})_r$. Interference from unwanted signals is further discussed by Rice et al. (1967, ann. V).

More complex methods of defining satisfactory service in terms of time availability q_T, location availability q_L, and service probability Q have been developed (Longley and Rice, 1968, ann. 1) but are beyond the scope of this report. Variability of received signal level with location and orientation of an airborne terminal can be treated as "short-term" fading (Gierhart and Johnson, 1967). The relative importance of time availability and service probability is illustrated in section 5.1.

3. PREDICTION OF AVAILABLE SIGNAL RATIOS

Service requirements can be stated by specifying signal ratios (R_{IM}, and/or S/N, and/or D/U) along with a point in the receiving system to which they are referred), and time availability q_T (see sec. 2). As stated earlier, the limitations imposed by R_{IM} are neglected here; i.e., $(R_{IM})_a >> (R_{IM})_r$. A detailed analysis of the case where both S/N and D/U are important simultaneously is beyond the scope of this report. We will assume that an adequate allowance for S/N and D/U can be made by treating each separately. An approximate but simple way to treat cases where both $(S/N)_a \simeq (S/N)_r$ and $(D/U)_a \simeq (D/U)_r$ is to consider each separately but to increase each required value by 3 dB (see sec. 2).

In this discussion $D/U(q_T)$ will be used to designate the value of the available signal power ratio expressed in dB as a function of the time availability q_T at the receiving antenna terminals. It can be either $(D/U)_a$ or $(S/N)_a$. Hence,

$$D/U(q_T) = W_D(q_T) \ominus W_U(q_T) \text{ dB}, \tag{5}$$

where $W(q_T)$ is the hourly-median available power at the receiving antenna terminals in dBW that is exceeded a fraction q_T of the time, and the subscripts D and U are used to designate desired or undesired components, respectively. More precisely $W(q_T)$ is a quantile or percentile corresponding to the probability distribution function value $1 - q_T$. The operational symbol $\ominus$ is used to indicate the process by which the distribution of a random variable $z' = x - y$ is determined from the distribution of the random variables x and y. When x and y are statistically independent, a convolution operation can be used (see sec. A.2.3). If the distribution functions associated with

$W_D(q_T)$ and $W_U(q_T)$ are approximately normal, a simplified approximate method (if we assume statistical independence) given by Rice et al. (1967, sec. V.7) can be used to determine $D/U(q_T)$; i.e., (5) becomes

$$D/U(q_T) \simeq W_D(0.5) - W_U(0.5) + Y_T(q_T) \quad \text{dB}, \qquad (6)$$

where Y_T gives the variability of $D/U(q_T)$ about its median value, $D/U(0.5)$, and is obtained from

$$Y_T(q_T) \simeq \mp \sqrt{Y_D^2(q_T) + Y_U^2(1 - q_T)} \quad \text{dB}, \qquad (7)$$

where $\sqrt{\ }$ implies a positive square root and $\mp$ is negative only when $q_T \geq 0.5$. The variability of $W_D(q_T)$ and $W_U(q_T)$ about their median values are defined as $Y_D(q_T)$ and $Y_U(q_T)$, respectively. Values of $Y_U(1 - q_T)$ are obtained by evaluating $Y_U(q_T)$ at $1 - q_T$, i.e., if $q_T = 0.9$, then $Y_U(1 - q_T) = Y_U(0.1)$.

Estimates of long-term median value of basic transmission loss, L_{bm} in dB, values given by Gierhart and Johnson (1969) can be used to calculate long-term median available power at the terminals of an antenna, W_m in dBW, in terms of (a) the power delivered to the terminals of the transmitting antenna, W_t in dBW, (b) the path antenna power gain, G_{pp} in dB, and (c) a conditional adjustment A_Y in dB to L_{bm} based upon the variability $Y(q_T)$ of the available power about its long-term median W_m, i.e.,

$$W_m = W_t + G_{pp} - (L_{bm} + A_Y) \quad \text{dBW} \qquad (8)$$

where G_{pp} and A_Y can be obtained from (9) and (10).

Path antenna power gain includes the effect of losses (a) associated with the antenna's inability to radiate all the available power delivered to its terminals, and (b) the inability of the path to

realize the full free-space gain of the antennas; e.g., when the antenna beams do not intersect, and/or the antennas do not have the same polarization, and/or the propagation mechanism does not allow full gains to be realized (Rice et al., 1967, secs. 2.4, 5.2, 9.4; Longley and Rice, 1968, sec. 1-3). When the full free-space gains of the antenna are nearly realized, G_{pp} can be replaced by

$$G_{pp} \simeq G_t + G_r \quad \text{dB}, \tag{9}$$

where G_t and G_r are the maximum free-space gains of the transmitting and receiving antennas in dB greater than an isotropic radiator.

The term A_y is added to L_{bm} to prevent available signal powers from exceeding levels expected for free-space propagation by an unrealistic amount when L_{bm} is close to its free-space value L_{bf} and the variability $Y(q_T)$ is large, i.e.,

$$A_y = 0 \quad \text{for } (L_{bf} - 3) < (L_{bm} - Y(0.1)); \tag{10a}$$

otherwise,

$$A_y = L_{bf} + Y(0.1) - L_{bm} - 3 \quad \text{dB}. \tag{10b}$$

Such conditions can exist for line-of-sight links extending close to the radio horizon. The free-space basic transmission loss value, L_{bf}, is calculated from path distance d in nautical miles (nm) and frequency f in MHz from the expression

$$L_{bf} \simeq 37.8 + 20 \log f + 20 \log d \quad \text{dB}, \tag{11}$$

where d is used to approximate the free-space direct ray path between antennas. The modification of W_m by A_y in (8) can decrease W_m by as much as $\simeq$15 dB.

Available power variability $W(q_T)$ is the available power exceeded for a fraction q_T of the time, i.e.,

$$W(q_T) = W_m + Y(q_T) \quad \text{dBW.} \tag{12}$$

It is related to long-term basic transmission loss variability $L_b(q_T)$ by

$$L_b(q_T) = W_t + G_{pp} - W(q_T) \quad \text{dB,} \tag{13a}$$

which can be used with (8) and (12) to obtain

$$L_b(q_T) = L_{bm} + A_Y - Y(q_T) \quad \text{dB.} \tag{13b}$$

Note that $L_b(q_T)$ represents loss values that are not exceeded for a fraction q_T of the time, whereas $W(q_T)$ represents values of received power levels that are exceeded for a fraction q_T of the time.

Values of $Y(q_T)$ can be estimated by the methods given in section 3.1.

The use of these relationships will be illustrated by their application to cases where (a) there is interference from a single undesired source (sec. 3.1), (b) there is interference from multiple undesired sources (sec. 3.2), and (c) service is limited by noise (sec. 3.1). In these applications we will assume that (a) the expressions given in this section are valid, (b) L_{bm} values obtained from Gierhart and Johnson (1969) are applicable, and (c) signal level variabilities obtained with the long-term power fading model described by Rice et al. (1967, sec. 10) are suitable. Thus, these examples include only long-term variability; i.e., $Y(q_T)$ is the variability associated with "hourly medians", and the median levels are the medians of hourly medians or long-term medians as given in the transmission loss atlas developed by Gierhart and Johnson (1969). Information contained in the atlas may be used to estimate gross

transmission characteristics at frequencies of 125, 300, 1600, 5100, and 15,000 MHz. Curves of L_{bm} are given as a function of (1) path distance for antenna elevations of 0.025, 0.050, 0.1, 0.5, 1, 2, 5, 10, 15, 25, 30, 40, 60, 80, 100, and 150 thousand feet above ground, and (2) actual direct ray takeoff angle for the same values of antenna elevation, but with one terminal fixed at synchronous satellite altitude. The methods used to develop these curves and propagation considerations that may be important when applying the curves to specific problems are discussed in the atlas.

Longley and Rice (1968, ann. 1) assume that the effects of short-term or within-the-hour fading are allowed for by the required signal ratios, i.e., the $(D/U)_r$ for a particular link is the hourly median value required in the presence of whatever short-term fading (undesired transmissions included) is associated with the link. Methods are given by Rice et al. (1967, ann. V) for (a) determining $(D/U)_r$ in the presence of short-term fading from the ratio required without fading[2], and (b) estimating the "long-term cumulative distribution of instantaneous power". Hence, the allowance for short-term fading could be included in $(D/U)_r$, as required by the context here, or in $(D/U)_A$ if the methods summarized above for calculating $(D/U)_A$ were expanded accordingly[3].

---

[2] Rice et al. (1967, sec. V.2) describe short-term fading by the Nakagami-Rice distribution. To use this method an estimate of the ratio, K, in decibels between the steady component of the received power and the Rayleigh fading component must be made for the short-term fading expected on the link (Norton et al., 1955b; Janes, 1955).

[3] Gierhart and Johnson (1967) include an allowance for the short-term fading associated with phase-interference fading and aircraft antenna gain variability in their estimates of available signal ratios.

3.1 Interference From a Single Source

D/U(q_T = 0.9) calculations based on (5) through (13) for the single interfering source case will be illustrated in this section for the following configuration:

(a) An aircraft receiving terminal at a height, H_r, of 5,000 ft above the surface with an antenna directivity of 3 dB (greater than isotropic) toward the desired station and -1 dB toward the undesired terminal. Antenna efficiency and transmission line loss factors are assumed to be equal for both desired and undesired signals so that D/U(0.9) at the terminals of an ideal antenna (100% radiation efficiency) placed at the aircraft location would equal the D/U(0.9) at any point in the receiver predetection system. A $W_0(0.9) \geq -157$ dBW at the terminals of the ideal antenna is taken as the minimum power required for satisfactory service in the absence of interference. This power level is about 9 dB greater than the Johnson's noise level obtained from (28b) for a 6-kc noise bandwidth and corresponds to 20-dB less than 1 μV across 50 Ω.

(b) A ground-based desired transmitting terminal located at a distance, d, of 180 nm from the receiver with an antenna height, H_t, of 50 ft above the surface. Its antenna radiates 30 dBW at a frequency f of 125 MHz and has a gain of 10 dB toward the receiver.

(c) An airborne undesired transmitting terminal at an altitude, H_t, of 30,000 ft above the surface at a distance of 380 nm from the receiver. Its antenna radiates 14 dBW at about 125 MHz (either cochannel or adjacent channel) and has a 2-dB gain toward the receiver.

The geometry involved is illustrated in figure 1.

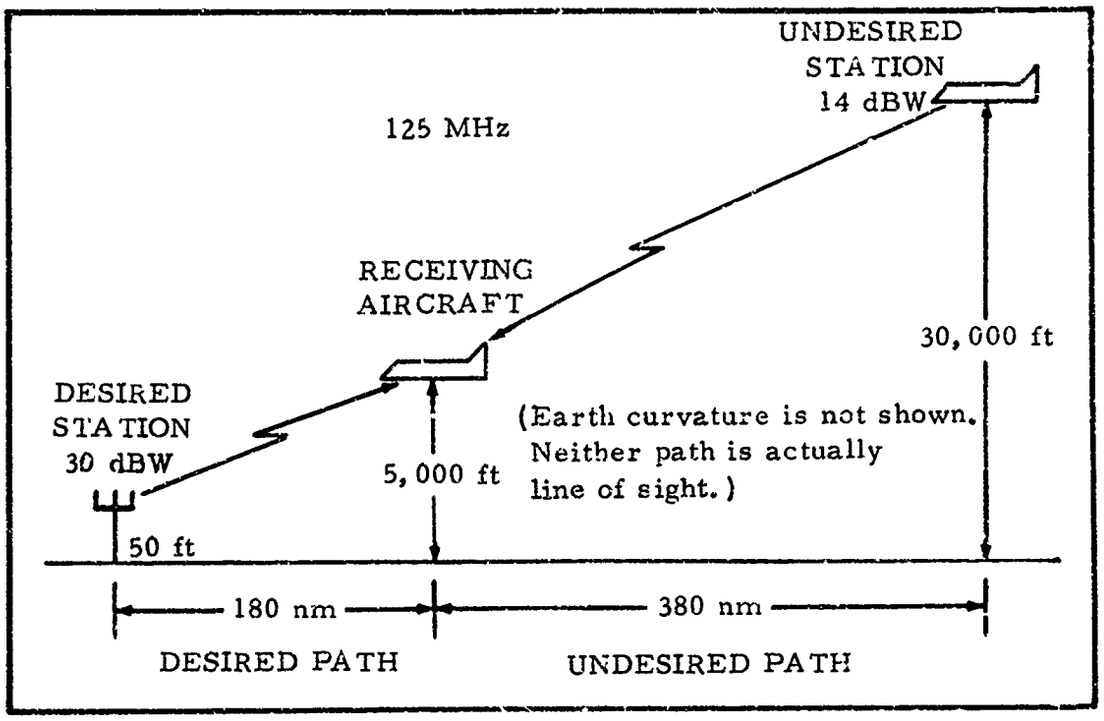

Figure 1. Geometry for example in sec. 3.1.

The effective distance d_e required to calculate $Y(q_T)$ with the Rice et al. (1967, ch. 10) model is defined as

$$d_e = 130\, d_K / (d_L + d_{s1})\ \text{km} \quad \text{when } d_K \le d_L + d_{s1}, \qquad (14a)$$

or

$$d_e = 130 + d_K - (d_L + d_{s1})\ \text{km} \quad \text{when } d_K > d_L + d_{s2}, \qquad (14b)$$

where

$$d_L = d_{L1} + d_{L2}\ \text{km}, \qquad (15)$$

and d_K is the great-circle path distance in kilometers (1 nm = 1.852 km) Smooth-earth terminal radio horizon distances d_{L1} and d_{L2} can be obtained from figure 2. The theoretical distance d_{s1} between the radio horizons, which corresponds to a path distance ($d_K = d_L + d_{s1}$) where diffraction and scatter fields are approximately equal over a smooth earth with an effective earth's radius of 9000 km, is given in figure 3

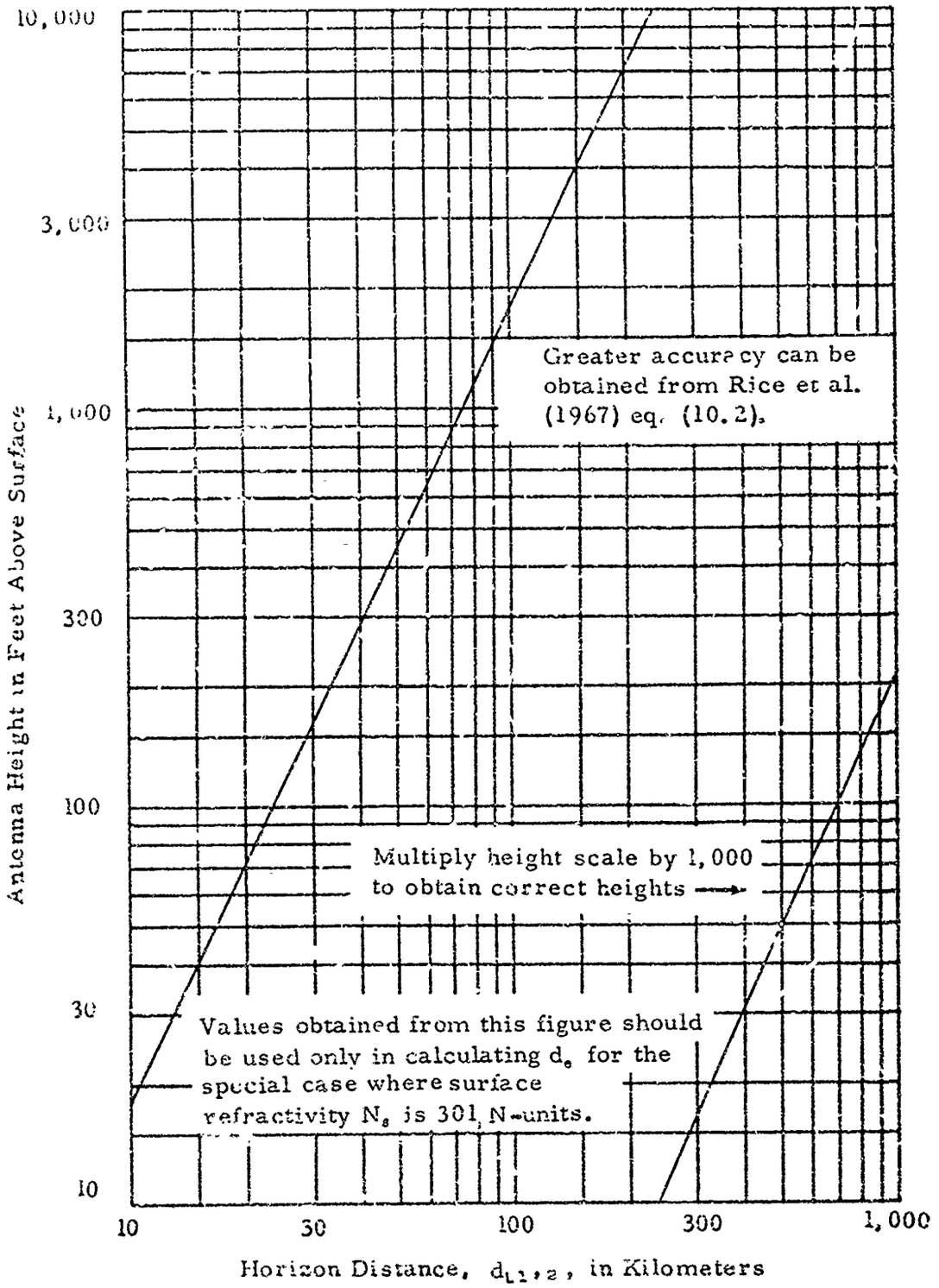

Figure 2. Antenna height vs. horizon distance, $d_{L1,2}$.
(After Gierhart and Johnson, 1969, fig. B.3.)

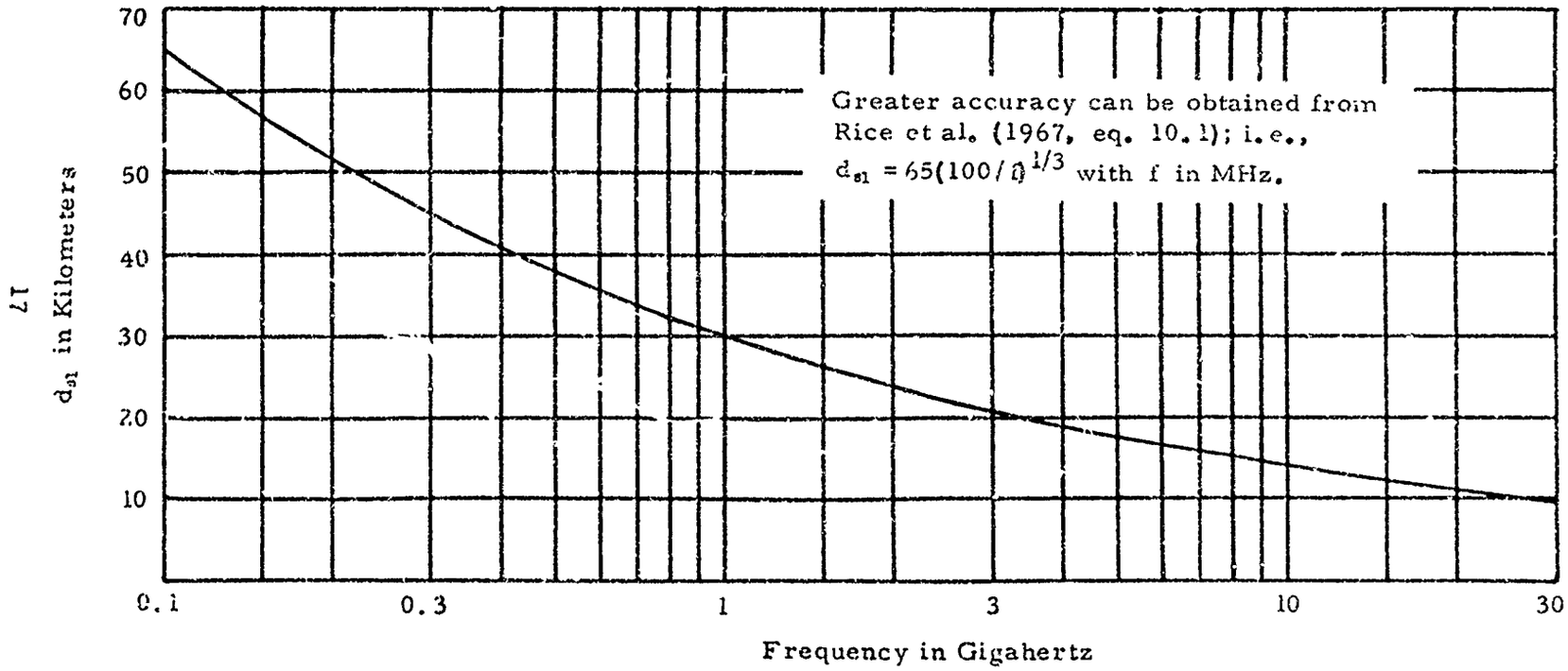

Figure 3. d_{s1} vs. frequency. (After Gierhart and Johnson, 1969, fig. E.4.)

as a function of frequency. Effective distance calculations that are applicable to this example can be summarized as follows:

Parameter		Desired Path	Undesired Path
H_t	ft	50	30,000
d_{L1}	km	16.6	395.1
H_r	ft	5,000	5,000
d_{L2}	km	165.4	165.4
$d_L = d_{L1} + d_{L2}$	km	182	560.5
f	MHz	125	~125
d_{s1}	km	60.3	60.3
$d_L + d_{s1}$	km	242.3	620.8
d	nm	180	380
$d_K = 1.852\ d$	km	333.4	703.8
d_e	km	221	213

Long-term variability $Y(q_T)$ of available power about its long-term median is a function of q_T, d_e and f, i.e.,

$$Y(0.1) = Y_o(0.1,\ d_e)\ g(0.9,\ f) \quad \text{dB}, \quad (16a)$$

$$Y(0.01) = \text{lesser of} \begin{cases} 2.00\ Y(0.1) \\ \quad \text{or} \\ L_{bn} + A_Y - L_{bf} + 5 \end{cases} \quad \text{dB}, \quad (16b)$$

$$Y(0.001) = \text{lesser of} \begin{cases} 2.73\ Y(0.1) \\ \quad \text{or} \\ L_{bn} + A_Y - L_{bf} + 5.8 \end{cases} \quad \text{dB}, \quad (16c)$$

$$Y(0.0001) = \text{lesser of} \begin{cases} 3.33\ Y(0.1) \\ \quad \text{or} \\ L_{bn} + A_Y - L_{bf} + 6 \end{cases} \quad \text{dB}, \quad (16d)$$

$$Y(0.9) = Y_o(0.9,\ d_e)\ g(0.9,\ f) \quad \text{dB}, \quad (16e)$$

$$Y(0.99) = 1.28\ Y(0.9) \quad \text{dB}, \quad (16f)$$

and

$$Y(0.999) = 2.41\ Y(0.9) \quad \text{dB}, \quad (16g)$$

$$Y(0.9999) = 2.90\ Y(0.9) \quad \text{dB}. \quad (16h)$$

The relationships involving L_{bf} have been included to prevent available signal powers from exceeding levels expected from free-space levels by unrealistic amounts.

Variabilities applicable to this example for all hours in a continental temperate climate[4] are calculated from (16), where the d_e values obtained above are used to obtain Y_o values from figure 4 and 125 MHz is used to obtain the frequency factor, $g(q_T, f)$ from figure 5, i.e.,

Parameter	Desired	Undesired
q_T	0.9	0.1 (1 - 0.9)
d_e km	221	213
Y_o dB	-8.0	9.45
g	1.085	1.095
Y dB	Y_D = -8.68	Y_U = 10.348
Y^2 dB^2	75.34	107.08

[4] Work in preparation by Barsis et al. (1970) indicates that the variability associated with air/ground propagation in a continental temperate climate for effective distances less than 200 km is not as great as that predicted by the Longley and Rice (1968, fig. 1.4) variability model. Therefore, the all-hours continental U. S. time block variability given by equations (III. 69) and (III. 70) with constants from tables III. 3 and III. 4 in the report by Rice et al. (1967) is recommended for use with the L_{bs} atlas (Gierhart and Johnson, 1969) when a continental climate (all-hours) is involved. Variabilities applicable to individual time blocks and other climate types can be obtained from Rice et al. (1967, ann. III, ch. 10). These variability models do not include attenuation caused by rain which can become a very important part of system design at frequencies above 6 GHz. Rice et al. (1967, sec. 3.3) and/or Skerjanec and Samson (1970) can be used to estimate rain attenuation.

Estimates of L_{bs} and variability for satellite links as a function of takeoff or look angle (fig. A. 1) can be made using Gierhart and Johnson (1969, sec. 4) and Rice et al. (1967, sec. I. 2), respectively.

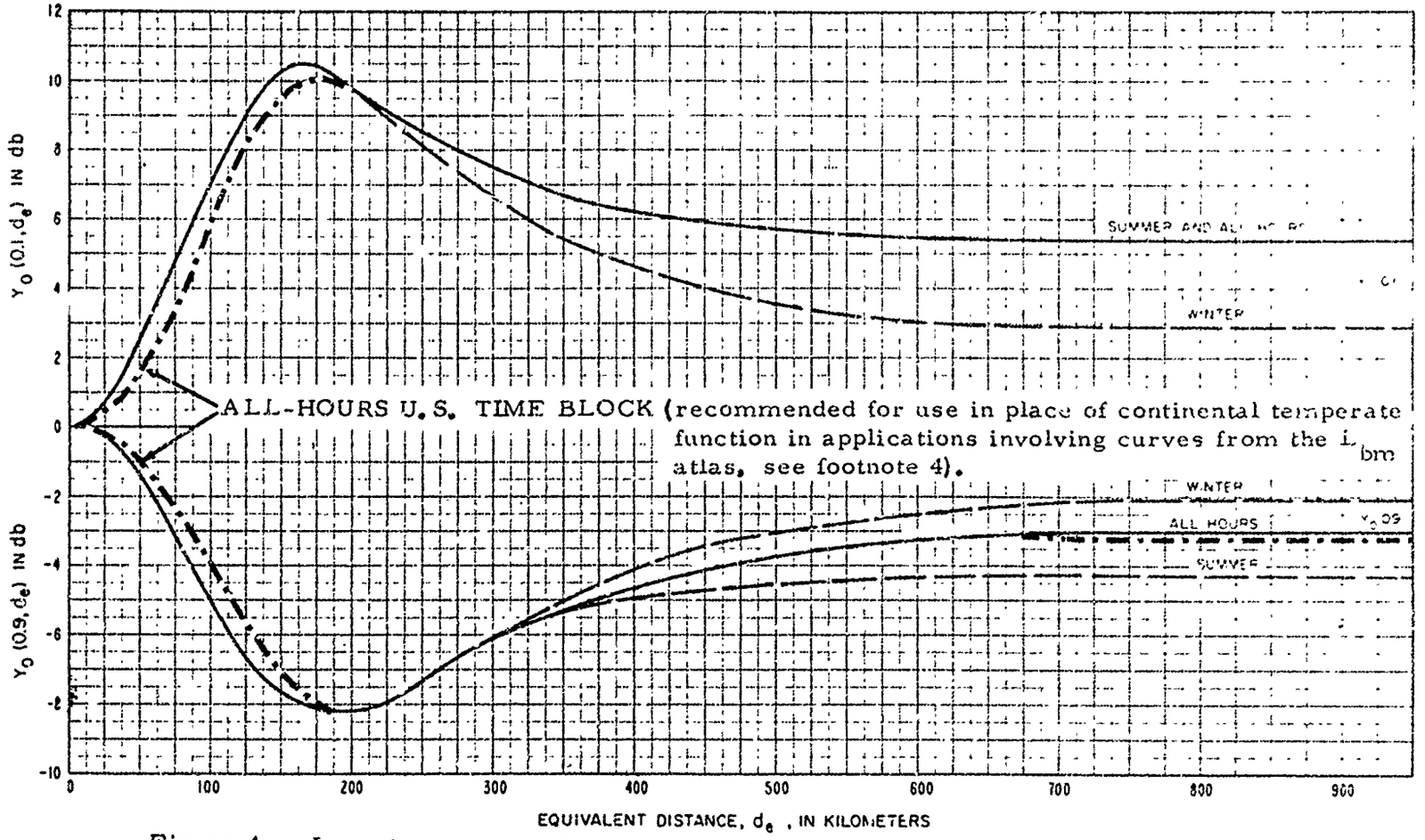

Figure 4. Long-term power-fading function $Y_0(q_T, d_e)$ for continental temperate climate. (After Longley and Rice, 1968, fig. 1.4.) Values for the all-hours U. S. time block function given by Rice et al. (1967, sec. III.7.1) are shown as dotted lines where they differ from those of the all-hours continental temperate climate function.

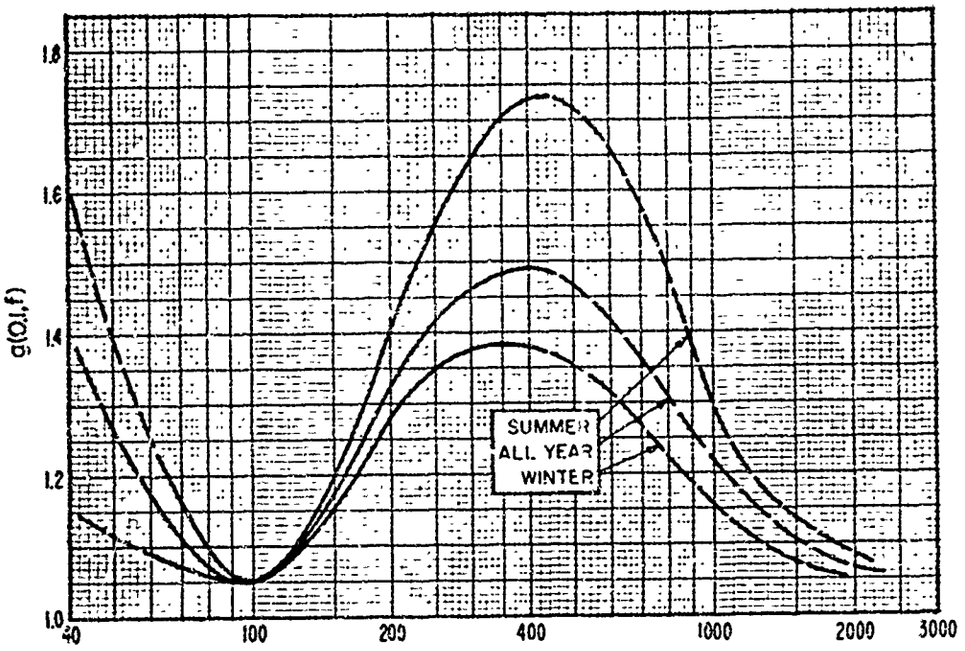

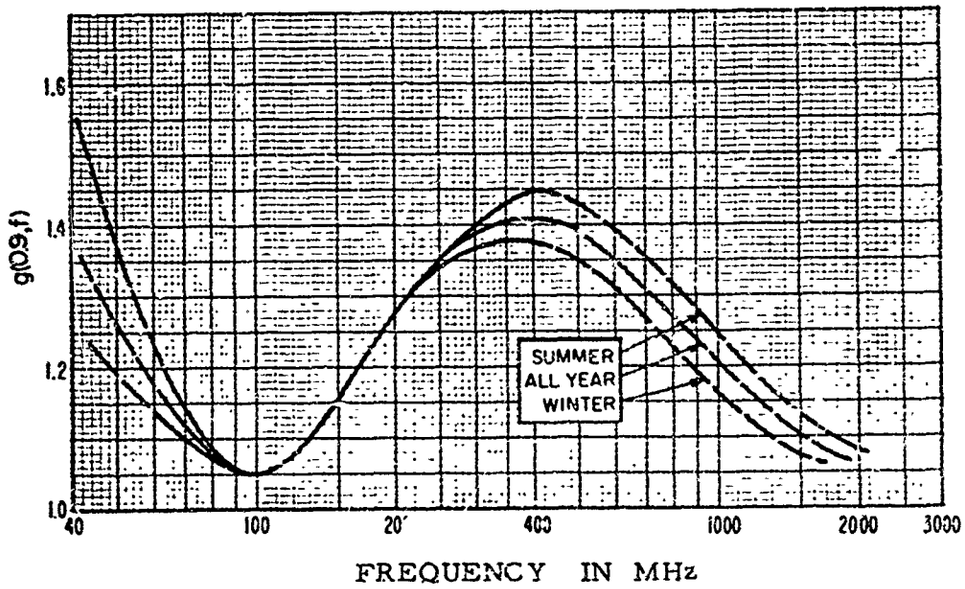

Figure 5. The frequency factor $g(q_T, f)$, based on U.S. overland data. (After Longley and Rice, 1968, fig. 1.5.)

Then Y_T is obtained from (7),

$$Y_T(0.9) = -\sqrt{Y_D^2(0.9) + Y_U^2(0.1)} = -\sqrt{182.42} = -13.5 \text{ dB}.$$

L_{bn} values from figures 6 and 7, variabilities, and (10) and (11) are used to determine A_Y values, i.e.,

Parameter		Desired	Undesired
$Y_o(0.1)$	dB	9.25	9.45
g		1.095	1.095
Y(0.1)	dB	10.1	10.3
f	MHz	125	~125
d	nm	180	380
L_{bf}	dB	124.9	131.4
H_r	ft	5,000	5,000
H_t	ft	50	30,000
L_{bs}	dB	176	175
A_Y	dB	0	0

Then, previously obtained parameter values are used with (8) to calculate $W_D(0.5)$ and $W_U(0.5)$, i.e.,

Parameter		Desired	Undesired
W_t	dBW	30	14
G_{pp}	dB	13 (10 + 3)	1 (2 - 1)
L_{bs}	dB	(-) 176	(-) 175
A_Y	dB	(-) 0	(-) 0
	dBW	-133 = $W_D(0.5)$	-160 = $W_U(0.5)$

Since $Y_T(0.5) = 0$, D/U(0.5) can be obtained from (6), i.e.,

$$D/U(0.5) = W_D(0.5) - W_U(0.5), \qquad (17)$$

and

$$D/U(0.5) = -133 + 160 = 27 \text{ dB}.$$

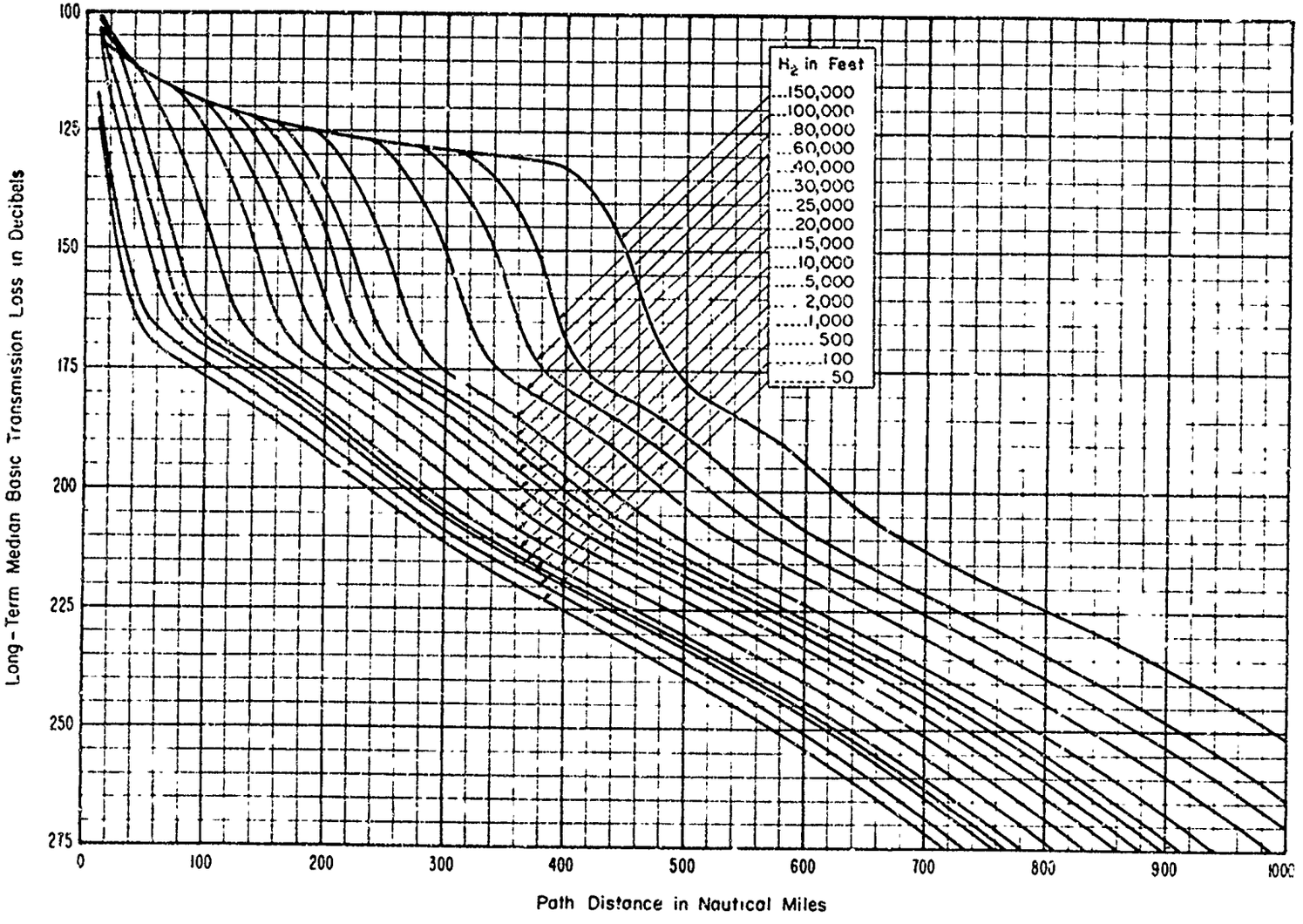

Figure 6. Basic transmission loss vs. distance; f = 125 MHz, H_1 = 50 ft. (After Cierhart and Johnson, 1969, fig. 2.)

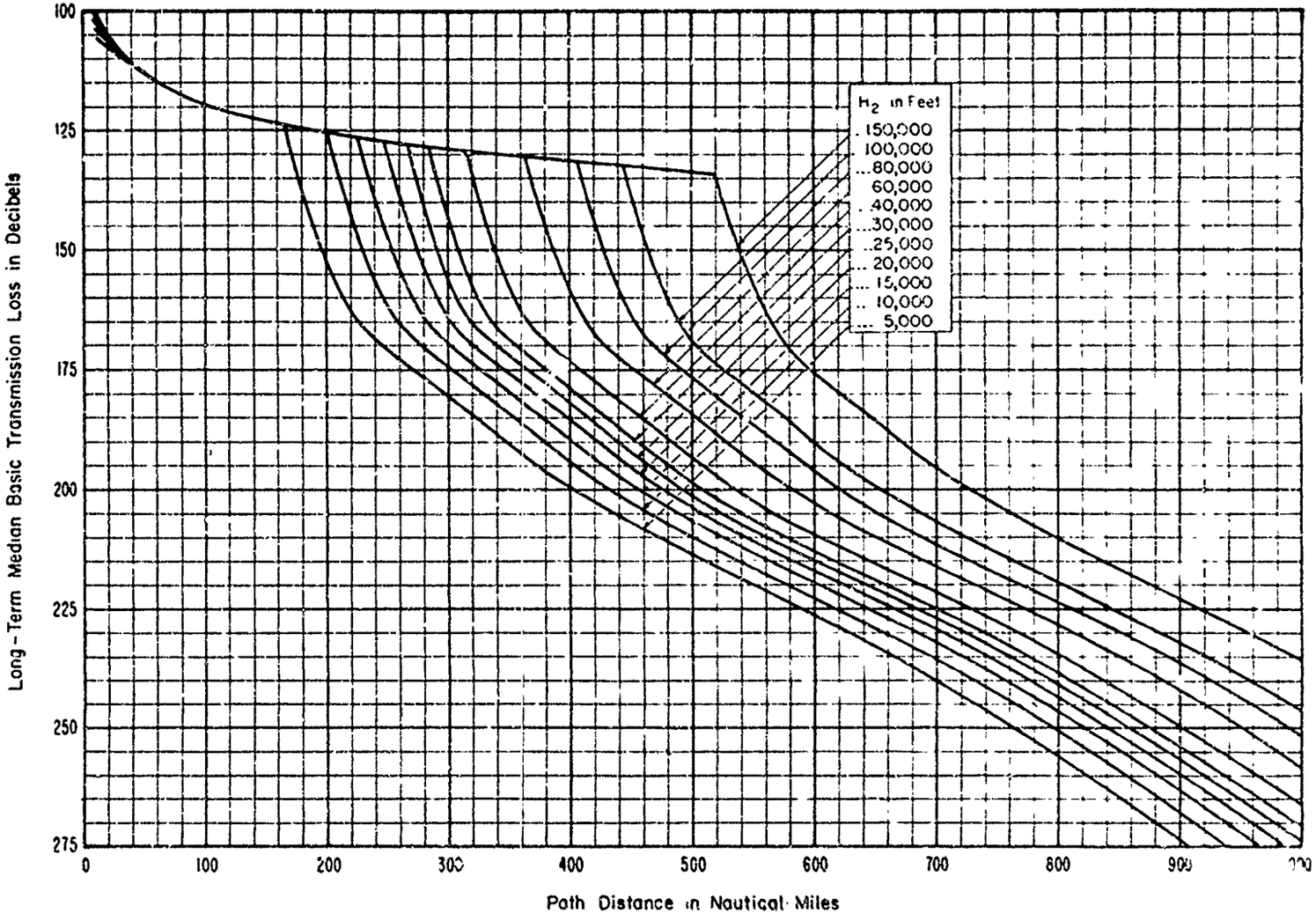

Figure 7. Basic transmission loss vs. distance; f = 125 MHz, H_1 = 5,000 ft. (After Gierhart and Johnson, 1969, fig. 7.)

Consequently, a signal ratio of 27 dB or greater would be available during 50% of the time. $D/U(0.9)$ calculated from (6) gives

$$D/U(0.9) = W_D(0.5) - W_U(0.5) + Y_T(0.9) = 27 - 13.5 = 13.5 \text{ dB}.$$

A more stringent service requirement of $q_T = 0.9999$ would result in an available signal ratio of $D/U(0.9999) = 27 - 42.7 = -15.7$ dB.

The availability of service without interference can be checked via (12), i.e.,

$$W_D(0.9) = W_D(0.5) + Y_D(0.9) \quad \text{dB},$$

i.e.,

$$W_D(0.9) = -133 - 8.7 = -141.7 \quad \text{dBW},$$

which is greater than the -157 dBW required.

Either (13a) or (13b) can be used to calculate $L_b(0.9)$ for the desired path; i.e., using (13a) gives

$$L_b(0.9) = W_t + G_{pp} - W_D(0.9) \quad \text{dB},$$

and

$$L_b(0.9) = 30 + 13 + 141.7 = 184.7 \text{ dB},$$

or from (13b),

$$L_b(0.9) = L_{bz} + A_v - Y_D(0.9) \quad \text{dB},$$

and

$$L_b(0.9) = 176 + 0 + 8.7 = 184.7 \text{ dB}.$$

Note that $L_b(0.9)$ is the loss value that is <u>not exceeded 90%</u> of the time or is <u>exceeded 10%</u> of the time.

In summary, satisfactory service for $q_T = 0.9$ exists (a) in the absence of undesired transmissions, since $W_D(0.9) > -157$ dBW, and (b) when the receiver noise level is neglected and the required system is probably operating above its noise threshold (W_D is 15 dB above -157 dBW for 90% of the time), the minimum acceptable $(D/U)_r$ should be about 13 dB (see sec. 2). In this case a 0.5-dB decrease in $(D/U)_r$ would probably be more than adequate to allow for the noise contribution,

since the sum of two powers is only about 0.2 dB greater than the larger power when the two levels are 15 dB apart (see app. D).

3.2 Interference From Multiple Sources

Equations (5) through (17) can be used to estimate $D/U(q_T)$ when the undesired power is made up of contributions from multiple sources. To accomplish this either the "power convolution" method[5] or the "log-normal" method[5] (Norton et al., 1952) can be applied to combine the undesired power statistics predicted for each undesired signal by using the methods discussed above for a single undesired signal. The "power convolution" method is more cumbersome but probably more accurate if the signal levels are statistically independent and can be applied in situations where intermittent transmissions are involved (see sec. A.2.3). Correlation between signal levels can be included if the "log-normal" method is used, but the assumption of statistical independence simplifies the method considerably. Median total power levels can be estimated by a "median power sum" method (Rice et al., 1967, sec. V.5) in which the median undesired power (in watts) is approximated by the sum of the median undesired signal powers (in watts), where the median noise power can be included, if desired.

$D/U(q_T = 0.9)$ calculations for multiple interfering sources by a simplified log-normal method will be illustrated in this section for the following configuration.

(a) An aircraft receiving terminal with characteristics identical to the one used in the example in section 3.1. However,

---

[5] Both of these methods are discussed and illustrated by application in sec. A.2.3.

three (two more) interfering stations are assumed, and the receiving antenna gains toward these stations is taken as -1, -1, and + 2 dB.

(b) A ground-based desired transmitting terminal with characteristics identical to the one used in the example in section 3.1.

(c) Three airborne undesired transmitting terminals, each with characteristics identical with those of the terminal used in the example in section 3.1. Although these aircraft are all at the same distance from the receiving aircraft, they are not at the same bearing.

The simplified log-normal discussed and used in section A.2.3 assumes n statistically independent undesired powers, each with a mean value of α W and a variance of μ W^2. However, undesired powers with unequal statistics can be considered if $n\alpha$ and $n\mu$ in (A-5) and (A-6) are taken to be the sum of individual means, $\sum_n \alpha_i$, and the sum of individual variances, $\sum_n \mu_i$, respectively; i.e., the mean[6] M_n and the variance σ_n^2 of the normally distributed (in dBW) total undesired power resulting from n statistically independent undesired signals are given by

$$M_n = c \left[\ln\left(\sum_n \alpha_i\right) - \frac{1}{2} \left(\frac{\sigma_n}{c}\right)^2 \right] \quad \text{dBW}, \tag{18}$$

and

$$\sigma_n^2 = c^2 \ln \left\{ 1 + \left[\sum_n \mu_i / \left(\sum_n \alpha_i\right)^2 \right] \right\} \quad \text{dB}^2, \tag{19}$$

where ln means natural logarithm and

$$c = 10 \log e = 4.34294, \tag{20}$$

with logarithm to base 10 indicated by log.

---

[6] M_n is also the median since the mean and median of a normally distributed random variable are equal.

Although (18) and (19) are exact when (a) the signal levels are statistically independent, and (b) the total undesired power is normally distributed in dBW, the process must be regarded as approximate, since these conditions will probably not be completely met in practice.

If the power in dBW received from the i^{th} station is normally distributed, (18) and (19) with n = 1 can be manipulated to obtain each a_i and u_i from the mean M_i and variance σ_i^2 of the normally distribution dBW levels, i.e.,

$$a_i = \exp\left\{\frac{1}{2}\left(\frac{\sigma_i}{c}\right)^2 + \frac{M_i}{c}\right\} \quad W, \tag{21}$$

and

$$u_i = a_i^2 \left\{\exp\left[\left(\frac{\sigma_i}{c}\right)^2\right] - 1\right\} \quad W^2. \tag{22}$$

For this special case (Crow et al., 1960, pp. 229-230),

$$\sigma_i^2 = Y_i^2 \,(q_T = 0.1587) \quad dB^2 \tag{23}$$

and

$$\sigma_i = Y_i \,(q_T = 0.1) \,/\, 1.282 \quad dB, \tag{24}$$

where Y_i is the long-term variability associated with the i^{th} signal.

Calculations of a_i's and u_i's for the three undesired stations from (21) through (24) and the values for $Y_U(0.1)$ and $W_U(0.5)$ obtained in section 3.1 are summarized below.

Parameter		Undesired Stations	
i		1 or 2	3
G_{pp}	dB	1 (2 - 1)	4 (2 + 2)
$W_U(0.5)$	dBW	-160	157
M_i	dBW	-160	-157
M_i / c		-36.841	-36.15
$Y_\cdot(0.1)$	dB	10.3	10.3
σ_i	dB	8.034	8.034
σ_i / c		1.850	1.850
$(\sigma_i / c)^2$		3.422	3.422
a_i	W	5.536×10^{-16}	1.104×10^{-15}
a_i^2	W^2	3.064×10^{-31}	1.220×10^{-30}
μ_i	W^2	9.083×10^{-30}	3.616×10^{-29}

Now $\sum_n \mu_i = 5.433 \times 10^{-29}\ W^2$ and $\sum_n a_i = 2.212 \times 10^{-15}$ W are used with (19), (24) and (18) to obtain $Y_U(0.1)$ and $W_U(0.5)$, i.e.,

$$\left(\frac{\sigma_n}{c}\right)^2 = \ln\left(1 + \frac{54.33}{4.891}\right) = 2.494,$$

$$\sigma_n = 4.343\ \sqrt{2.494} = 6.858\ \text{dB},$$

$$Y_U(0.1) = (1.282)(6.858) = 8.792\ \text{dB},$$

$$W_U(0.5) = M_n = \left[\ln (2.212 \times 10^{-15}) - \tfrac{1}{2}(2.494)\right](4.343),$$

and

$$W_U(0.5) = -152.0\ \text{dBW}.$$

Y_T and D/U(0.9) are obtained as before from (7) and (6):

$$Y_T(0.9) = -\sqrt{Y_0^2(0.9) + Y_U^2(0.1)} = -\sqrt{75.34 + 77.30} = -12.4\ \text{dB},$$

$$D/U(0.5) = W_0(0.5) - W_U(0.5) = 10.3\ \text{dB},$$

and

$$D/U(0.9) = D/U(0.5) + Y_T(0.9) = 10.3 - 12.4 = -2.1\ \text{dB}.$$

The "median power sum" method previously mentioned can be used to estimate $W_u(0.5)$, i.e.,

$$W_u(0.5) \simeq 10 \log \sum_a 10^{M_i/10} \text{ dBW} \qquad (25)$$

$$\simeq 10 \log \left[(1 + 1 + 2)\ 10^{-16} \right] = -154 \text{ dBW}.$$

This value does not agree with the -152-dBW value obtained by the "log-normal" method, because the "log-normal" method sums mean powers in watts rather than median levels. Since in the Longley and Rice (1968, ann. 1) variability model, $Y(q_T)$, segments of two normal distribution functions with standard deviations of about the same magnitude are used to describe variability for $q_T < 0.5$ and $q_T > 0.5$, values of $W_u(0.5)$ obtained by the "log-normal" method are probably more accurate. Both methods will yield similar results when the variabilities are low, e.g., $\alpha \simeq 10^{M_i/10}$ W to within 0.5 dB when $\sigma_i \leq 2$ dB. When the maximum value of $Y(0.1)$ obtainable from the long-term power fading model in section 3.1 of about 16 dB (fig. 30, d_e=160 km) is applicable, the "log-normal" method will yield $W_u(0.5)$ values that are larger than those obtained with the "median power sum" method by an amount that will not exceed 1 dB times the number of undesired sources involved. The $Y_u(0.1)$ resulting from use of the "log-normal" method will always be less than the largest $Y_i(0.1)$ involved.

3.3 Interference From Noise

3.3.1 Description of the Noise Environment

Adequate description of the noise environment in which a communication system operates must be known in order to predict system performance. Certain variations of atmospheric noise power

with time of day, season, frequency, and geographic location do have systematic trends. However, other variations, such as day-to-day levels of atmospheric noise within a given hour and the short-term distributions of man-made noise, do not follow well-defined trends and must be described statistically (Disney and Spaulding, 1968). No single parameter of the noise environment will provide a completely adequate description, but it is meaningful to select one parameter for use in predicting system performance. The average noise power density is generally the most helpful and convenient to use for this purpose and is used exclusively in this report to present both noise measurements and to compute system requirements.

Of primary importance in system design and evaluation is the available noise power density at a receiving terminal in the system. This power density is conveniently expressed as a noise factor, referred to the noise power density available at the terminals of a lossless antenna. This factor is defined as

$$f_a = \frac{p_n}{k T_o B_n} = \frac{T_a}{T_o} , \qquad (26)$$

where

p_n = noise power available from an equivalent lossless antenna in the bandwidth B_n in W,

k = Boltzman's constant = 1.38×10^{-23} joules/°K,

T_o = the reference temperature in °K, taken as 288°K (after Norton, 1953),

B_n = effective receiver noise bandwidth in Hz (footnote 10, sec. 4.2.3), and

T_a = antenna noise temperature in °K (in the presence of external noise).

From (26), it is apparent that f_a is easily related to either noise power in a given bandwidth or to antenna temperature due to external noise.

Note that both f_a and T_a are independent of bandwidth, since p_n is proportional to bandwidth, as is the reference power ($k T_o B_n$) in (26). The quantity $k T_o B_n$ is commonly known as Johnson noise power in W, in the bandwidth B_n. It can be expressed in terms of a power density as

$$p_J = k T_o = 1.38 \times 10^{-23} \times 288 \text{ °K}$$
$$= 397.44 \times 10^{-23} \text{ W/Hz}, \quad (27)$$

or in dB as

$$P_J = 10 \log p_J = -230 + 26$$
$$= -204 \text{ dB relative to 1 W/Hz}, \quad (28a)$$

or in terms of total Johnson noise power (reference power) as

$$P_r = P_J + 10 \log B_n$$
$$= -204 + 10 \log B_n \quad \text{dBW}, \quad (28b)$$

where B_n is the noise bandwidth in Hz.

The antenna noise factor of (26) can be similarly expressed in $dB/kT_o B_n$ as[7]

$$F_a = P_n - P_r$$
$$= P_n + 204 - 10 \log B_n \quad dB/kT_o B_n, \quad (29)$$

where

$$P_n = 10 \log p_n \quad \text{dBW}.$$

Measured values of the antenna noise figure F_a for various noise sources, both terrestrial and man-made, are shown in figures 8 and 9. The curves represent median values of the noise power and are currently the best available estimates of both atmospheric and man-made noise

---

[7] $dB/kT_o B_n$ is used to denote dB relative to $kT_o B_n$ throughout this report.

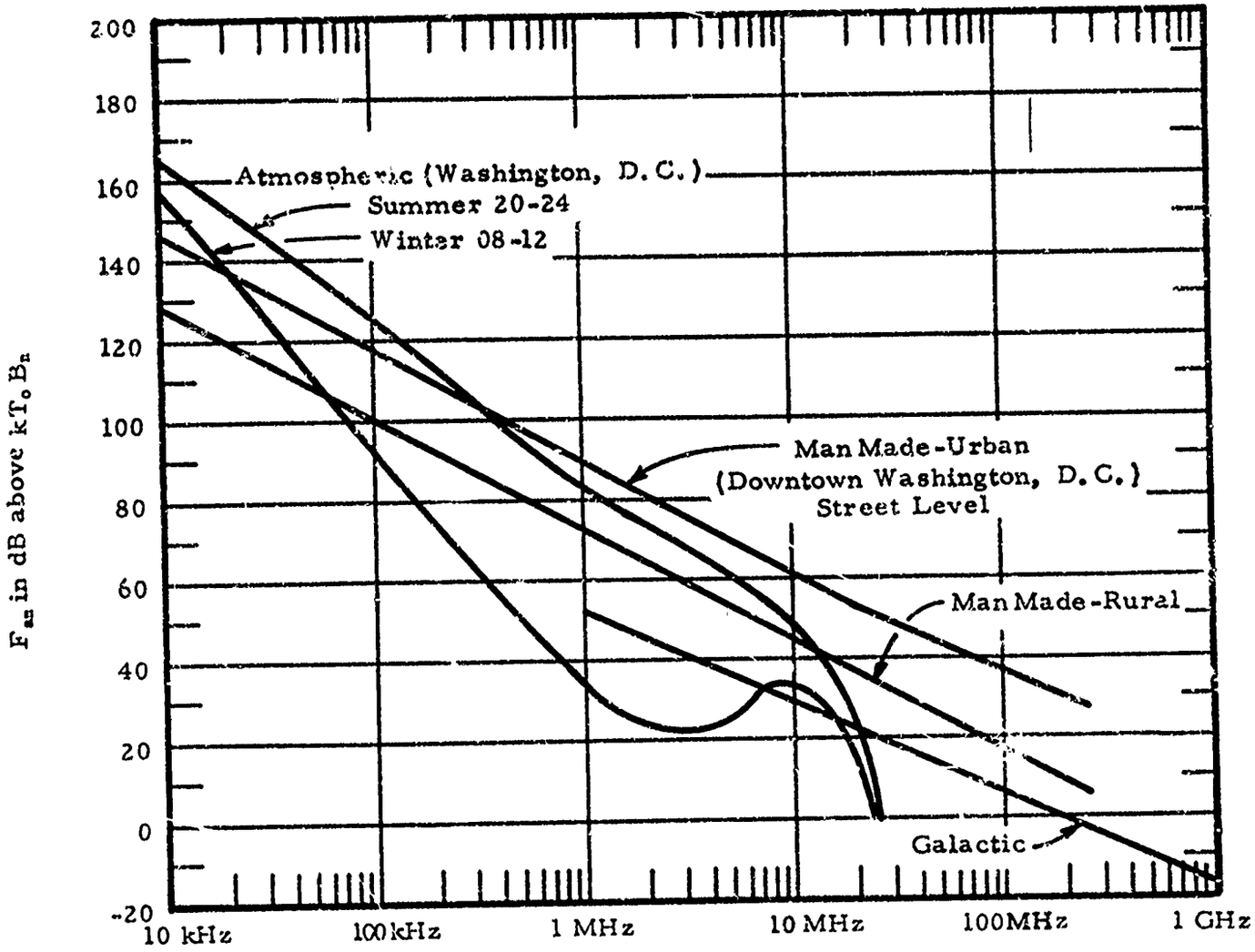

Figure 8. Median values of noise power expected from various sources, omni-directional antenna. (After Disney and Spaulding, 1970, fig. 55)

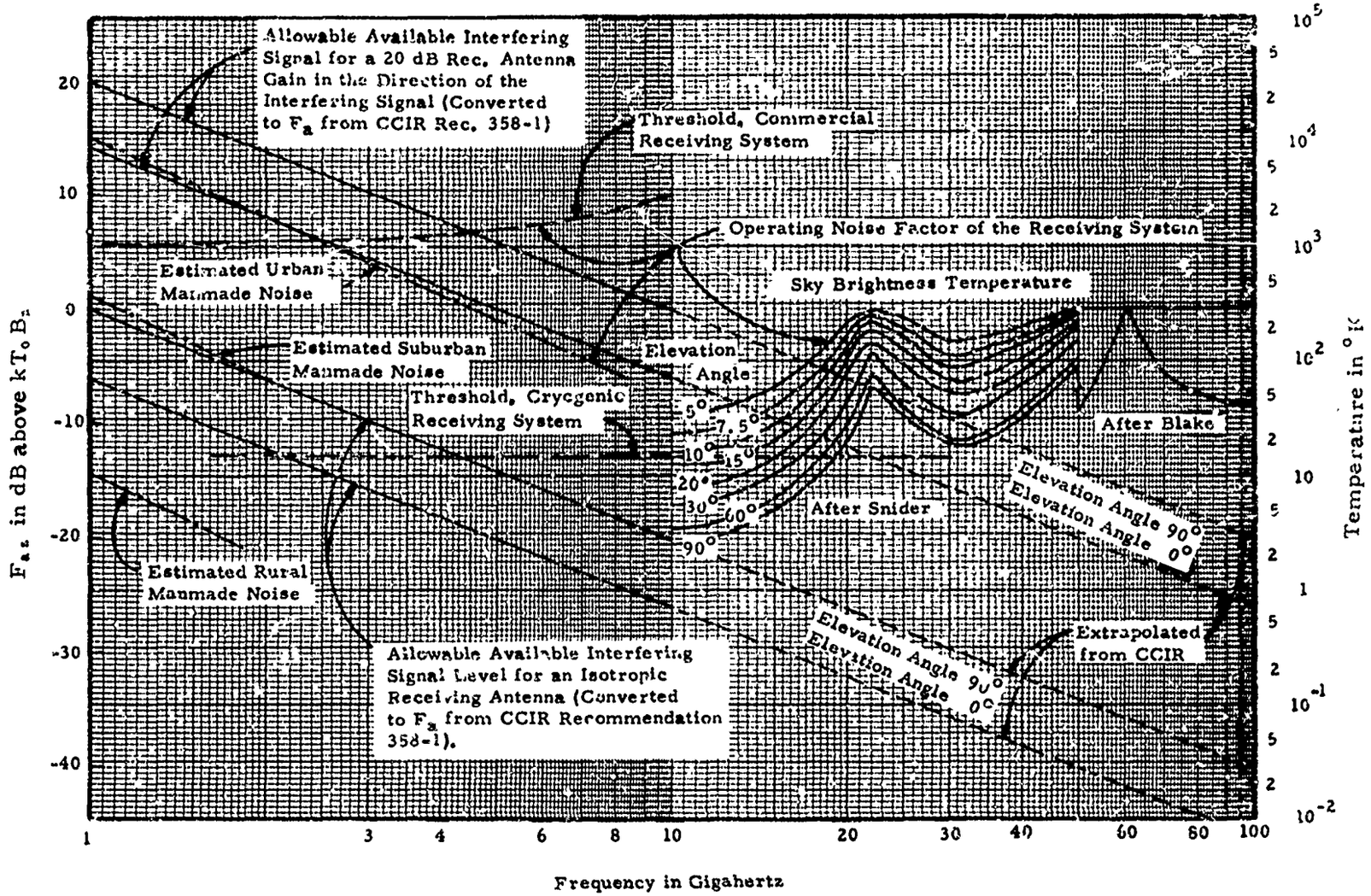

Figure 9. Median values of noise power and typical thresholds of receiving systems.

levels. They include recent measurements made by the Institute for Telecommunication Sciences (ITS). A more complete analysis of the distribution in amplitude and time of these noise sources is given by Disney and Spaulding (1970). The distribution of noise power density levels about the median values in figure 8 are given in the following table. Dispersion of the data at the higher frequencies in figure 9 is not available at this time.

Noise Classification	Freq. Range (MHz)	rms Deviation (dB)
Urban	1-10	± 3
	10-500	± 6
Suburban	1-10	± 4
	20-500	± 8
Rural	1-10	± 6
	20-500	± 2.5

It should be noted that the above deviations are for the average power values for each location and frequency, and not the instantaneous variations which would be much larger than the values shown.

The recommendations of CCIR for the maximum allowable interfering satellite signal at a terrestrial station have been plotted in figure 9 for both an isotropic antenna and one of 20-dB gain. The recommendation is made in power flux density units in a 4-kHz bandwidth, which has been converted to F_a in $dB/k\,T_o\,B_n$ for figure 9. (See sec. 3.3.3.) These recommended values are given for comparison with typical receiving system threshold and noise interference levels in the 1-to-10-GHz frequency range.

To determine the median noise power level (F_{am}) from figures 8 and 9, the highest noise curve appropriate to the system usually dominates. For example, in figure 9, a terrestrial radio relay receiving system operating at 4 GHz would correspond to the curve marked "Commercial Receiving System", (F_{am} = 6.5 $dB/k\,T_o\,B_n$),

whereas at 2 GHz in an urban environment man-made radio noise would be expected to dominate (F_{am} = 7.5 dB/$kT_o B_n$).

The following paragraph from JTAC (1968) summarizes the description of expected noise power from various sources.

"The predominant noise source varies with frequency. In areas relatively free from man-made noise, atmospheric noise dominates for a high percentage of time at frequencies below 20 MHz, and galactic sources dominate from 20 MHz to the frequency at which the noise within the receiver becomes important. This can be expected to occur between 100 and 500 MHz, depending upon the quality of the first stages of the receiver. In areas of high man-made noise, it is likely these unintended radiations will dominate over a large important segment of the usable frequency spectrum, e.g., 200 MHz to 1000 MHz. It is likely that the unintended radiations from electric power transmission and use will dominate below 10 MHz and radiations from motor vehicles will dominate above 20 MHz". In addition, at 10 GHz, the sky brightness temperature begins to dominate, particularly at antenna elevation angles below 10°.

The spectrum between 1 and 10 GHz is particularly attractive to the establishment of satellite communication frequencies, as a "noise window" exists between galactic noise (below 1 GHz) and sky brightness temperature (above 10 GHz). The noise at the upper limit varies with the elevation angle of the antenna above the earth's horizon and depends on atmospheric gases and precipitation within the antenna bandwidth.

Extensive studies have been made to determine the proliferation of unintended man-made noise. A survey of published and gathered data describing unintentionally generated man-made VHF/ UHF noise has been made by Skomal (1965). Measurements have been carried out at ground level, from aircraft, on and above rural and urban areas.

Of particular interest are those made by Buehler et al. (1968) above Seattle at 5000 ft, at 137 MHz. Figure 10 shows the increase in noise power level above the central area which agrees in general with those shown in figure 8 for "Man-Made Urban (Downtown Washington)". Figure 8 indicates a level of 30 dB at street level.

The increase of noise with altitude is illustrated in figures 11 and 12. Because of the larger number of noise sources visible with higher altitude, the noise level also increases. Typical results at altitudes above the 10,000 ft shown in figure 11 are indicated in figure 12. These curves were adapted from a noise contour figure (Buehler and Lunden, 1966) for 1 MHz above the land side of Seattle.

As shown, the noise level increases with higher altitude until 60,000 ft is reached. At 60,000 and 80,000 ft, at distances beyond 25 sm from the Seattle core area, it remains constant, while within 25 sm it decreases with increasing elevation. At 10 sm we see a drop in the noise level of 2 dB/$k T_o B_n$ when elevation is changed from 40,000 to 60,000 ft and an additional loss of 2.5 dB/$k T_o B_n$ between 60,000 and 80,000 ft.

The dotted line between 0 and 10 sm in figure 12 is taken from a figure given by Buehler and Lunden (1966) showing high noise levels within a 1-sm radius of the city core at 5000 ft. Another paper of interest is by Ploussious (1968), who made measurements at 226.2, 305.5, and 369.2 MHz over Boston, New York, Baltimore, Philadelphia, and Miami to determine the characteristics of city noise and its effect on UHF. The magnitude of power density above these cities was computed to be 3×10^{-18} to 1×10^{-18} W/m^2 -Hz (denoting power flux density per Hz). Using Spaulding's (1969) method, we converted these values to F_a (dB/$k T_o B_n$) where

$$P_D = \frac{E_n^2}{120\pi} = \frac{E_n^2}{377} \quad , \tag{30}$$

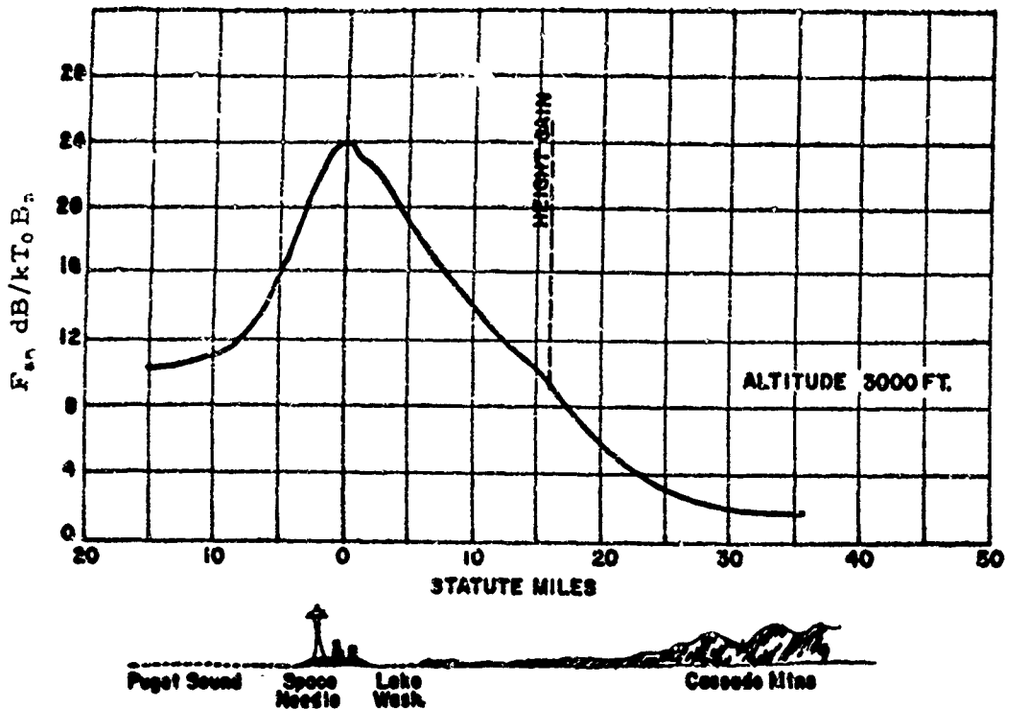

Figure 10. 137-MHz noise traverse across Seattle (Buehler et al., 1968).

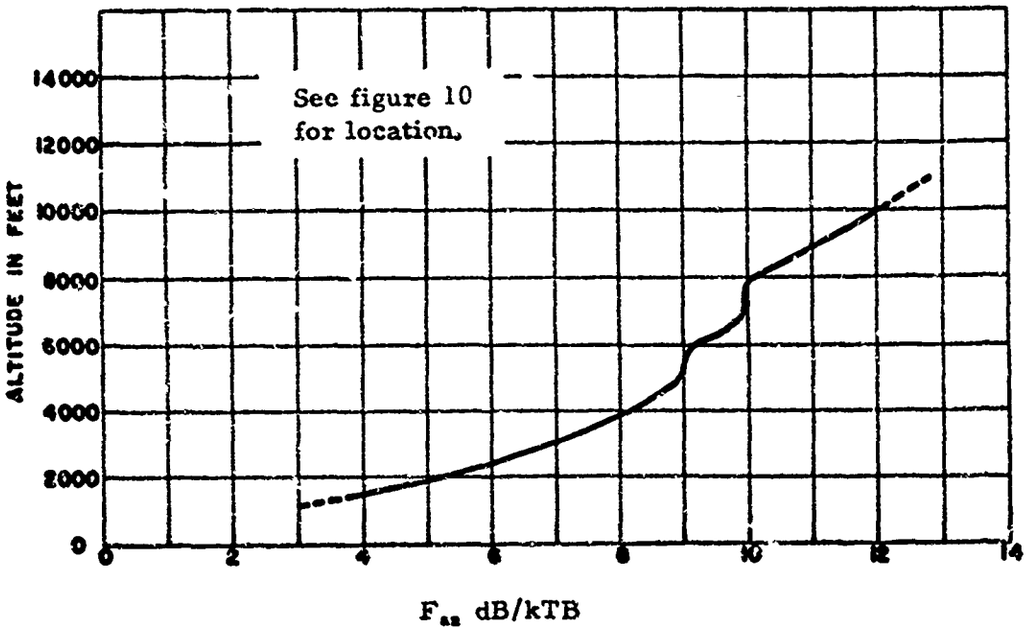

Figure 11. Height gain of 137-MHz city noise (Buehler et al., 1968).

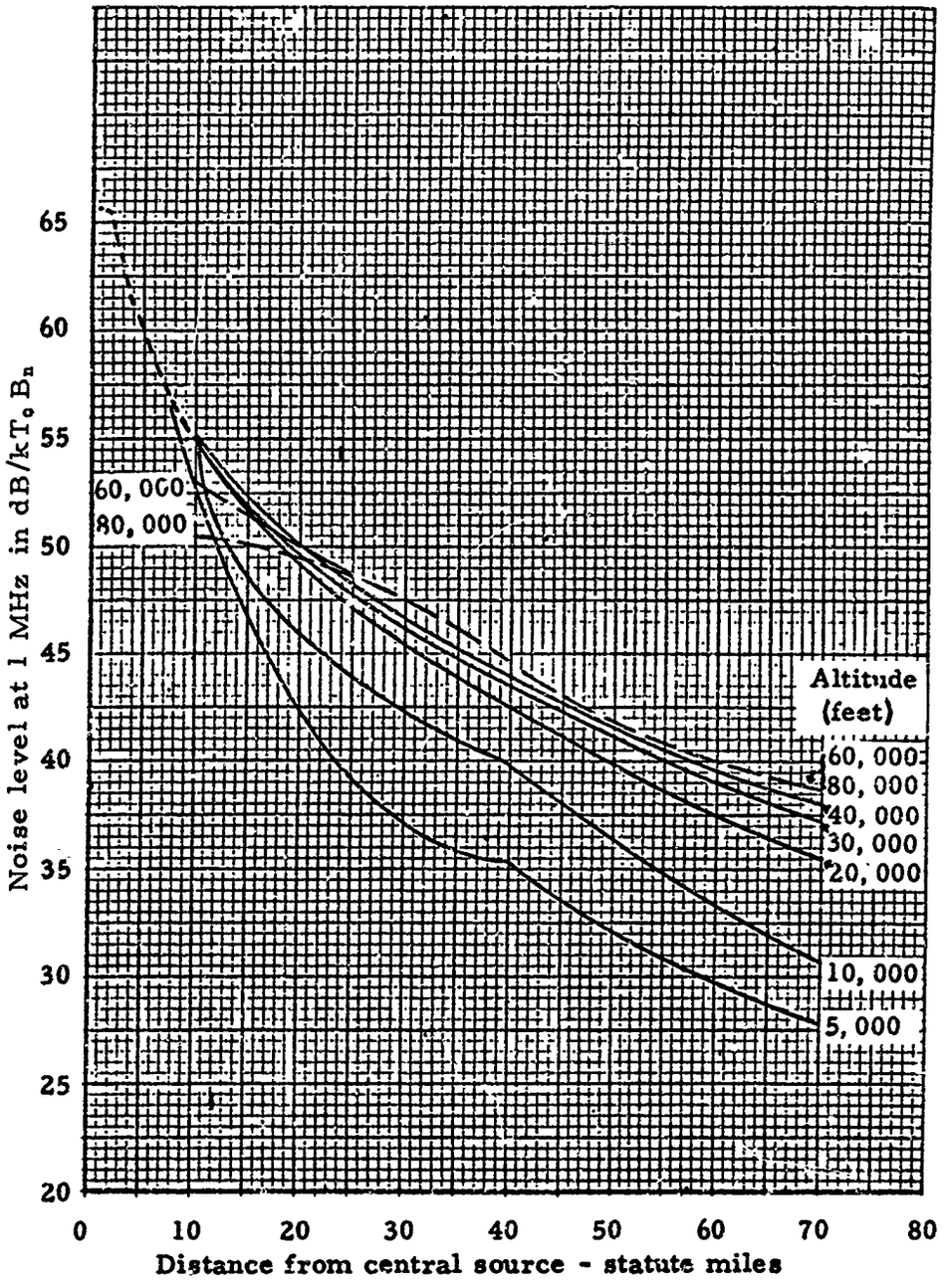

Figure 12. Man-made noise at various elevations above Seattle, Washington.

and

P_0 = power flux density in W/m^2 - Hz,

E_n = signal flux density in V/m - Hz.

Solving (30) for E_n, we have E_n in a range between 3.35 and 1.94 $\mu V/m$ - 10 kHz. Converting these values to F_a gives

$$F_a = E_{n_{dB}} - 20 \log f_{MHz} - 10 \log B_n + 95.5 , \qquad (31)$$

where $E_{n_{dB}}$ = rms field strength for a bandwidth B_n in dB above $\mu V/m$,

f_{MHz} = frequency in MHz,

B_n = effective noise bandwidth in Hz (10 kHz for this example),

and

$$F_a = 20 \log 1.94 - 20 \log 250 - 10 \log 10^4 + 95.5$$
$$= 20 (0.2871) - 20 (2.3974) - 10(4) + 95.5$$
$$= 13.3 \text{ dB}/kT_C B_n .$$

Converting 3×10^{-18} W/m^2 -Hz to F_a results in F_a = 18.05 dB/ $kT_o B_n$. This gives us an F_a range of 13.3 to 18.05 dB/$kT_o B_n$ as an estimate of noise encountered at 250 MHz over these cities. This estimate is based on measurements made at aircraft altitudes above 5000 ft. Below 5000 ft the identification of individual noise sources was sometimes possible.

It has become common practice in some of the literature to refer to external or antenna noise temperature rather than a noise factor. The relationship between these two terms is given by (26) and can be written

$$T_a = f_a T_o , \qquad (32)$$

where T_o is again the reference temperature, usually taken as 288 °K. A convenient logarithmic curve for converting f_a to F_a (in dB/$kT_o B_n$)

and either of the terms f_a or F_a to antenna temperature T_a is given in figure 13. Examples of the use of this curve are as follows:

(a) Given: $f_a = 100$. Desired: F_a.

Procedure: Enter the horizontal scale for $f_a = 10^2$ and read the vertical scale for $F_a = +20$ dB/KT_oB_n.

(b) Given: $F_a = -20$ dB. Desired: f_a.

Procedure: Enter the vertical scale for $F_a = -20$ dB and read the equivalent value of $f_a = 10^{-2} = 0.01$ on the horizontal.

(c) Given: $F_a = -20$ dB. Desired: T_a.

Procedure: Enter the vertical scale for $F_a = -20$ dB and read the corresponding value of T_a/T_o as 10^{-2}. Thus, $T_a = 10^{-2}\ T_o = 2.88°K$.

(d) Given: $f_a = 0.1$. Desired: T_a.

Procedure: Based on (32)

$T_a = f_a\ T_o = 0.1 \times 288°K = 28.8°K$.

3.3.2 Determination of System Operating Thresholds

For communication systems whose performance is noise limited, the operating system threshold can be estimated from the gross noise characteristics presented in the previous section and from the noise factors of the elements of the receiving system. The general definition of noise factor (Friis, 1944) is given as the ratio of the S/N ratio at the input to the S/N ratio at the output of a linear device. This factor can be written for any general network as

$$f_n = \frac{S_i/N_i}{S_o/N_o} = \frac{N_o}{kT_oB_nG_n}, \qquad (33)$$

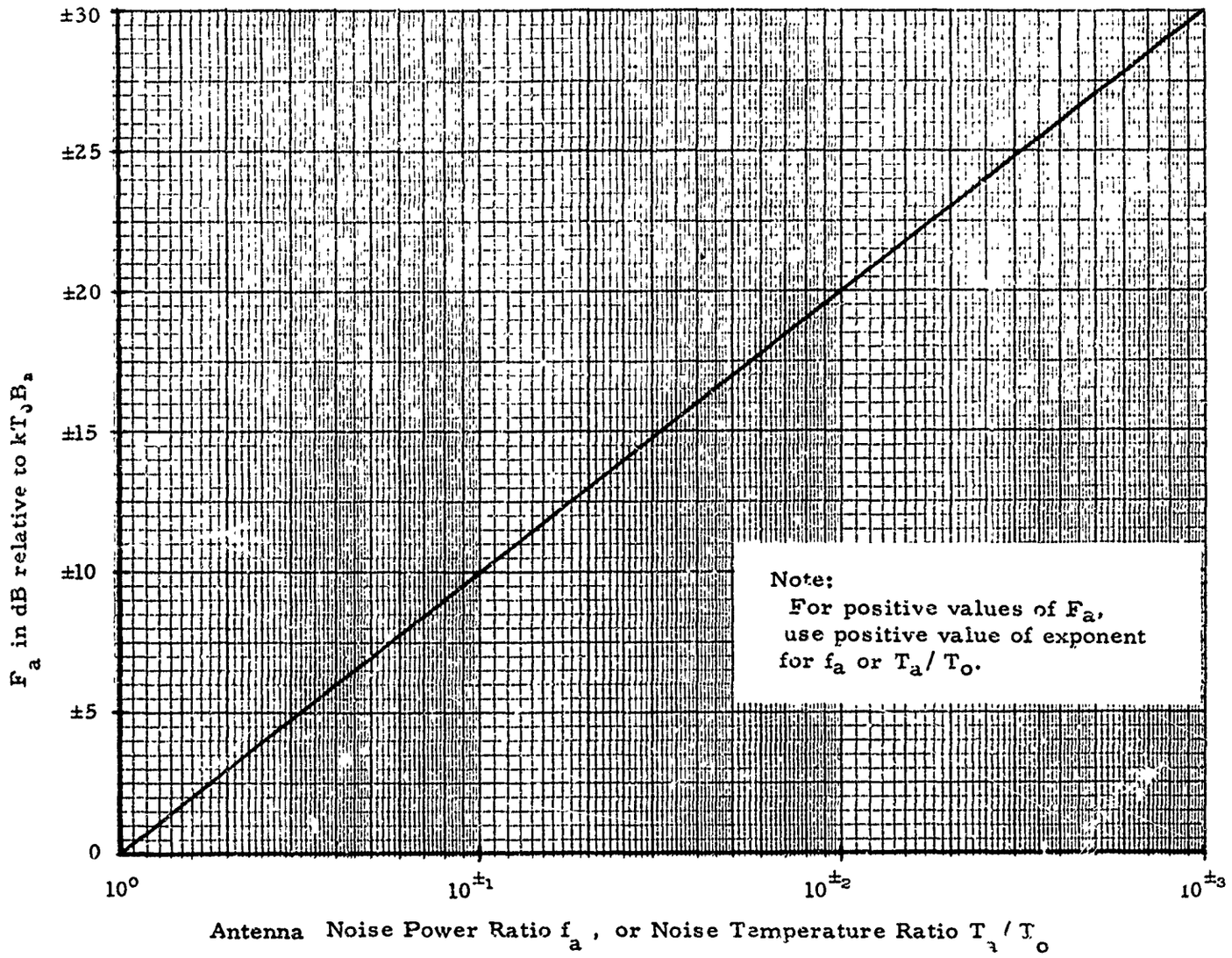

Figure 13. Conversion graph for antenna noise factor and/or temperature. ($T_o = 288^\circ K.$)

where S_i = available input signal power, N_i = available input noise power ($k T_o B_n$), S_o = available output signal power, N_o = available output noise power, G_n = gain of the device ($G_n = S_o / S_i$), and the factor $k T_o B_n$ is that defined previously for Johnson noise.

It is important to note here that "available power" refers to the power that would be delivered to a matched impedance. In other words, the above definitions do not account for an impedance mismatch effect that may exist between linear devices combined in tandem. This will be noted later in the discussion of system operating threshold.

From (33) we see that the noise factor is equivalently defined as the ratio of the noise power output of the device to the noise power that would be available if the device merely amplified the thermal noise of the source. This can be expressed as

$$f_n = \frac{kT_0B_nG_n + \Delta N}{kT_0B_nG_n} = 1 + \frac{\Delta N}{kT_0B_nG_n}, \qquad (34)$$

where ΔN is the internal noise introduced by the device or network. The internal noise can also be related directly to an effective noise temperature from (34) as

$$f_n = 1 + \frac{kT_eB_nG_n}{kT_0B_nG_n} = 1 + \frac{T_e}{T_0}, \qquad (35)$$

where T_e is defined as the effective noise temperature, or the temperature at the input of the device that would account for the internal noise ΔN. The effective noise temperature should not be confused with an actual physical noise temperature, as they are not necessarily the same. The effective temperature is more useful in engineering practice since it entails the loss or gain factors of the device by definition. Quite frequently, a receiver or other device is evaluated

in terms of effective noise temperature rather than a noise factor or figure[8]. Thus, from (35) we obtain for a device having self-noise the following relationship between noise factor and effective noise temperature:

$$T_e = (f_n - 1)\, T_c \,. \tag{36}$$

We see from (34) that an ideal device (one having no self-noise) is represented by an $f_n = 1$, or an equivalent effective noise temperature of $T_e = 0\,°K$ from (36). A noise figure (see footnote) for a linear device is given by

$$F_n = 10 \log f_n \quad \text{dB}, \tag{37}$$

and for the above ideal device, $F_n = 0$ dB. A noise figure for a receiver given as 6 dB would thus correspond to a noise factor of $f_r = 4$ and an effective noise temperature $T_e = (f-1)\, 288 = 864\,°K$.

A chart useful in converting from one to another of the above noise terms is shown in figure 14. The true conversion curve between noise factor and effective noise temperature is based on (36) in which the noise factor f appears. It is at times desirable to convert from noise figure in dB directly to effective temperature without the necessity of first converting back to a noise factor. An approximate method for this conversion has been given by McCurley and Blake (1961) as

$$T_e(\text{approx.}) = \frac{600\, F_n}{9 - F_n} \;°K\,, \tag{38}$$

---

[8] "Noise factor" and "noise figure" are not well defined or standardized in the literature. In this report the term "noise factor" will be used to denote a ratio quantity, and "noise figure" will denote the logarithmic conversion of a noise factor to dB.

where F_a is the noise figure in dB. A plot of this relationship is shown in the dotted curve in figure 14 and is seen to be valid for noise figures of 3 dB or less.

It is important to recognize in the above discussion a fundamental difference between the definition of antenna noise factor f_a in (26) and the later definition used for the noise factor of a linear device or network in (34) and (35). The antenna noise factor used in this report is based upon the consideration of the noise output from an equivalent lossless antenna in the presence of external noise only, and with no internal noise. This definition permits a direct relationship between the measured external noise powers in figures 8 and 9. Thus these external noise source levels are expressed directly in terms of the antenna noise figure F_a. In contrast, the definition of the noise factor for other networks or devices are based upon a consideration of the available input noise plus self-noise contributed by the network or device. This fundamental difference leads to the two separate relationships for equivalent noise temperature in figures 13 and 14. Note also that the two definitions are equivalent when the network or device under consideration has no self-noise ($f_n=1$).

These two basic definitions have been found most convenient to apply to system design and analysis problems. North (1942) originally defined an operating noise factor that characterizes the noise performance of an entire receiving system in contrast to the noise factor of a receiver alone. Norton (1953) gave a more general expression for this factor and designated it as an effective system noise factor, based upon the element noise factors defined above. The effective system noise factor concept makes appropriate allowance for the external noise received by the antenna as well as the receiver noise and accounts for the effects of losses in the antenna circuit and transmission line.

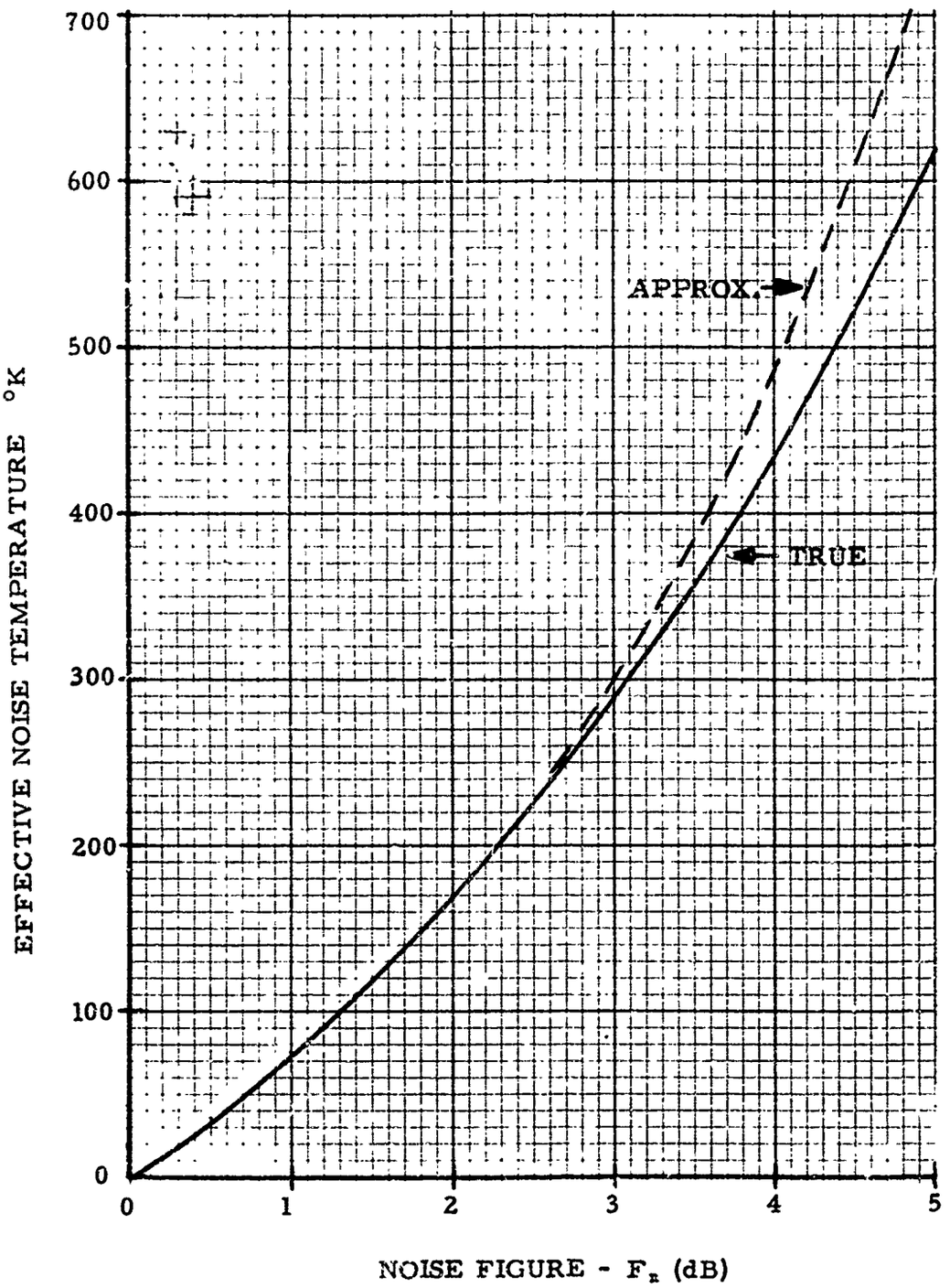

Figure 14. Conversion of noise figure to effective noise temperature for general networks.

As noted previously, the noise factor definitions given in this section are based upon "available" power or "effective" temperature considerations. Norton(1953, 1962) has shown that the noise figure for a network can also be written as

$$f_n = 1 + (\ell_n - 1)\,\frac{T_n}{T_o}\ , \qquad (39)$$

where ℓ_n = the loss factor for the network = $S_i / S_o \geq 1$, and T_n is the absolute temperature of the network or device. Applying (39) to the equation for several networks in tandem derived by Friis (1944), Norton gives the following general expression for an effective system noise factor:[9]

$$f_s = f_a + (\ell_c - 1)\,\frac{T_c}{T_o} + \ell_c\,(\ell_t - 1)\,\frac{T_t}{T_o} + \ell_c \ell_t\,(f_r - 1)\ . \qquad (40)$$

The parameters in this expression are as noted in the illustration of the network in figure 15. In this manner, the total receiving system noise factor is dependent upon the external noise described in the effective (lossless) antenna noise factor f_a, the receiver noise factor f_r, and the associated losses in the actual antenna circuit (ℓ_c) and the transmission line (ℓ_t). It can be shown that, if we assume the antenna circuit and transmission line temperatures to be the same and equal to the reference temperature, T_o, (40) can be simplified to

$$f_s = f_a - 1 + f_c f_t f_r\ , \qquad (41)$$

since from (39) we see that for $T_n = T_o$ the network factor $f_n = \ell_n$. The assumptions used to arrive at the simplified expression (41) under

---

[9] This expression is for a system containing a receiver with single response. For a more general expression applicable to a receiver with significant image or other responses, see Norton (1953).

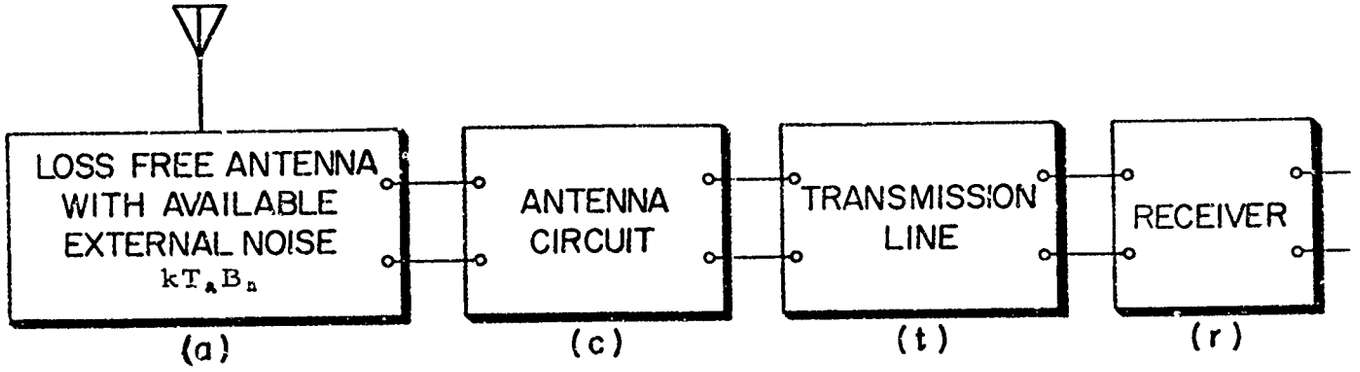

Figure 15. System illustration of (40).
(After Norton, 1962, fig. 2).

most operating conditions will cause less than 1-dB error (Disney and Spaulding, 1970). A complete development leading to (40) and (41) can also be found in a report by Barsis et al. (1961, app. III).

As an example of the application of the system noise factor concept, the following operating noise threshold calculation is made for a receiver operating in a rural environment:

(1) System parameters

Frequency: 125 MHz

Receiver bandwidth: 30 kHz

Antenna: isotropic ($G_r = 0$ dB)

Noise factor: $f_r = 3.16$ (5 dB)

Antenna circuit losses = 1 dB ($f_c = 1.26$)

Transmission line losses = 1 dB ($f_t = 1.26$)

(2) Johnson noise power per unit bandwidth

From (28a),

$$P_J = kT_o = -204 \text{ dB relative to } 1 \text{ W/Hz}$$

(3) System noise factor

From (41),

$$f_s = f_a - 1 + f_c f_t f_r ,$$

and from figure 8, we find that man-made rural median noise power at 125 MHz is approximately 15 dB above $kT_o B_n$. Converting this value to equivalent noise factor from figure 13, we have $f_a = 31.6$. Then,

$$f_s = 31.6 - 1 + (1.26 \times 1.26 \times 3.16)$$

$$= 31.6 - 1 + 5.02 = 35.62 .$$

Again, using figure 13, we obtain

$$F_s = 15.5 \text{ dB},$$

which is equivalent to a system noise temperature of

$$T_s = 35.62 \times 288°K = 10,259°K.$$

(4) System noise power density

Combining the result for F_s in step (3) with the Johnson noise power in step (2), we find the system noise power density to be

$$\begin{aligned} P_n &= P_j + F_s \\ &= -204 + 15.5 \\ &= -188 \text{ dB relative to 1 W/Hz}. \end{aligned}$$

(5) Total system noise power

In the receiver (with an equivalent noise power bandwidth of 30 kHz), the total system noise power is found from step (4) to be

$$\begin{aligned} P_T &= P_n + 10 \log B_n \\ &= -188.5 + 10 \log 30 \times 10^3 \\ &= -188.5 + 44.7 \\ &= -143.8 \text{ dBW in 30 kHz bandwidth.} \end{aligned}$$

The above value of P_T is the operating threshold for the system and represents the total available noise power in the receiver in the specified rural environment.

In such systems as the conventional ATC communication network, there will frequently be undesired signals, in addition to the noise power, at the receiver input terminals. These interfering signals can be accounted for in terms of additional undesired power combined

with the noise power to determine a new operating threshold. For example, assume a cochannel signal from a satellite FM emission at the terminals of the example terrestrial receiver above. If this

al is of the same power level as the noise threshold, the total noise plus interference power will result in a new threshold level:

$$P_T = -143.8 + 3 = -140.8 \text{ dBW in 30 kHz bandwidth .}$$

Note from figure D-1 in appendix D that two signals of equal power combine to a total power 3 dB higher than the level of either individual signal. Also from figure D-1, we see that if an interfering signal is at least 6 dB lower than the noise threshold, the threshold level will increase by less than 1 dB.

3.3.3 Noise and/or Signal Power Flux Density

Both noise and signal levels are sometimes expressed in units of flux density i.e., a power level per square meter of area. Thus, if desired, the above sample calculations can be converted to power flux density in the following manner:

$$\text{Power flux density} = \frac{P_s}{A_e} \text{ W/m}^2 \qquad (42)$$

where P_s is the total power in W and A_e is the effective area of the antenna in square meters given by

$$A_e = g_r \lambda^2 / 4\pi \text{ m}^2 , \qquad (43)$$

where g_r = the antenna gain relative to isotropic, and

λ = wavelength of operating frequency in meters.

Thus, P_{TF} (total system noise power flux density) for the example system in step (4) above becomes (in dB)

$$P_{TF} = P_T - 10 \log A_a$$

$$= -143.8 - (-3.4)$$

$$= -140.4 \text{ dB relative to 1 W/m}^2 \text{ in 30 kHz.}$$

It is generally more straightforward and less cumbersome in system analysis to work in basic power units and with the concept of transmission loss rather than in the flux density units. However, the latter are useful in the analysis of satellite systems because of a current CCIR (1967) recommendation. For example, CCIR Recommendation 358-1 specifies the maximum allowable satellite signal received on the earth's surface for microwave systems with directional antennas as

$$P_w = \left[-152 + \frac{\gamma}{15}\right] \text{ dB relative to 1 W/m}^2 \text{ in a 4-kHz bandwidth,} \quad (44)$$

where γ is the look angle of the terrestrial receiver antenna toward the satellite in degrees. Thus the factor $\gamma/15$ permits an increase in flux density of 6 dB directly under the satellite because of the directive antenna. In the terrestrial ATC network, the antennas are generally isotropic, and the allowance for directivity in this case is not practical. To illustrate computations where power flux density units are used, however, we shall for the sake of example take the basic nondirective value given in (44). The basic -152 dB power flux density level given for a 4-kHz bandwidth can be converted to a 30-kHz bandwidth power level as follows:

$$P_T = P_M + (-3.4) + 10 \log \left[\frac{30}{4}\right]$$

$$= -152 - 3.4 + 8.75$$

$$= -146.65 \text{ dBW in 30-kHz bandwidth.}$$

In this case, a satellite terminal in the ATC system that does not exceed the basic level of (44) would produce the above interfering signal level at the terrestrial receiver. From step (5) in section 3.3.2, the system noise threshold was found to be -143.8 dBW in the 30-kHz bandwidth. The difference between the noise threshold and the undesired satellite signal is 2.85 dBW. Entering this difference into figure D.1, we find a 1.8-dB increase in system threshold. Thus the new threshold becomes

$$P_T = -143.8 + 1.8 = -142 \text{ dBW in 30 kHz} .$$

This value can be used with an appropriate protection ratio to establish the required level for a desired signal into the example receiver with a 30-kHz bandwidth.

3.3.4 Signal-to-Noise Ratio Notations

In the literature, the definitions applied to S/N are quite varied, and it is often difficult to compare system performance characteristics directly because of these variations. In this section we shall comment briefly on a few of the more common notations and the relationship between them where applicable.

Perhaps the most prevalent definition is the straightforward ratio of total signal power to total noise power in a specified common bandwidth, where the mean or average power of the signal and noise fluctuations is usually implied. It is, however, sometimes more convenient to relate peak power values or peak envelope power (PEP). Such ratios should be clearly defined by the author and designated by appropriate use of subscripts or other distinguishing notation. It is also common practice to note carrier-to-noise ratios (C/N) and other quantities, such as D/U signal ratios. The signal and noise parameters involved in these ratios are clearly implied by the notation, but the actual power level (average, peak, etc.) is subject to the same variation as in S/N notations.

A common variation in notation is to designate a S/N density ratio, perhaps denoted as S/N_W, which is total signal power to noise power density N_W (noise power per Hz bandwidth). This particular notation is convenient for comparing performance characteristics of several different systems in which the required bandwidth may be quite different. For example, see the systems comparison in figure 27. For ratios specified in this manner, the total noise power is obtained by multiplying the noise density term N_W by the appropriate bandwidth B. Thus, S/N can be expressed as

$$\frac{S}{N} = \frac{S}{N_W B_n}, \tag{45}$$

and in dB form as

$$\left(\frac{S}{N}\right)_{dB} = \left(\frac{S}{N_W}\right)_{dB} - 10 \log B_n . \tag{46}$$

For example, if (S/N_W) dB = 50 dB for a system having a 10-kHz bandwidth, the equivalent $(S/N)_{dB}$ is

$$\left(\frac{S}{N}\right)_{dB} = 50 - 10 \log 10^4$$

$$= 50 - 40 = 10 \text{ dB}.$$

Another notation often used, particularly in multichannel voice communication systems, is one that specifies the noise or interference power in a 4-kHz bandwidth. Conversion of such ratios can be made in a similar manner as indicated above, or related to some other bandwidth with certain restrictions. If conversion is made to a wider bandwidth than that specified in the original ratio, a simple bandwidth-ratio conversion is usually made. A simple bandwidth conversion is strictly true under the assumption that the noise power is uniformly distributed over the bandwidth of interest.

As an example, let S/N_c denote an S/N where N_c is specified as the noise power in a channel of 4-kHz bandwidth (B_c = 4 kHz). Then

$$\frac{S}{N_H} = \frac{S}{N_c} \times 4000 , \tag{47}$$

or in dB

$$\left(\frac{S}{N_H}\right)_{dB} = \left(\frac{S}{N_c}\right)_{dB} + 10 \log (4 \times 10^3)$$

$$= \left(\frac{S}{N_c}\right)_{dB} + 36. \tag{48}$$

Also, S/N_c can be converted to S/N for some other bandwidth B as follows (under the assumption made above):

$$\frac{S}{N} = \left(\frac{S}{N_c} \times 4000\right) \times \frac{1}{B} , \tag{49}$$

or in dB

$$\left(\frac{S}{N}\right)_{dB} = \left(\frac{S}{N_c}\right)_{dB} + 36 - 10 \log B . \tag{50}$$

In dealing with multichannel systems, a number of noise and signal power level terms are encountered, which are however, beyond the scope of this report Many of them are referenced to a certain weighting term, such as FIA, C, or CCIF psophometric. When these weights are indicated - (usually by an appropriate notation with lower case letters a, c, and p respectively) - they refer to a particular weighting or spectral shaping function applied to the voice frequency spectrum. For illustration purposes, the characteristic shaps of these weighting functions are shown in figure 16 (Oliver, 1964).

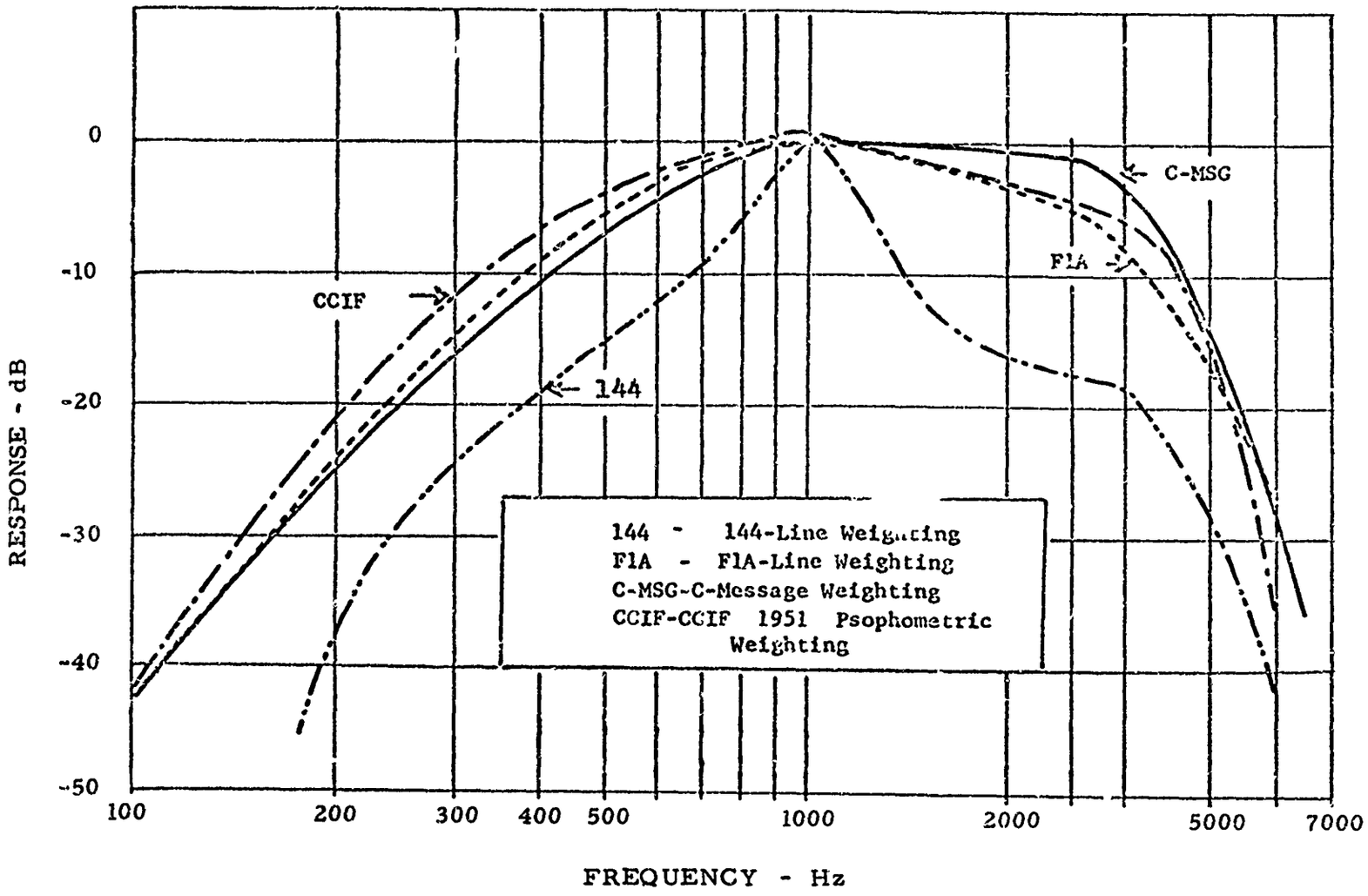

Figure 16. Line weighting for telephone circuits. (After Oliver, 1964).

4. DETERMINATION OF REQUIRED SIGNAL RATIOS

4.1 Discussion

As noted in section 2, the required signal power at the input terminals of a receiver in a communication system depends on the required grade-of-service (g_s) established for the system. In this section we shall discuss the methods of measuring the grade of service for a voice communication system and other forms of information transmission and to relate this parameter to the required signal ratios for satisfactory system performance. Emphasis will be placed on the grade of service required for voice communication circuits, since this is of prime concern to the present ATC communication system. However, digital modulation and transmission systems will be treated briefly, as they are also important to the ATC system. Determination of both the grade of service and required signal ratios is based on laboratory measurements, theoretical considerations, and overall system performance analysis.

Determining the required g_s in radio communications is generally not a simple or straightforward process, because it is dependent in turn on many other factors and system parameters. Also, grade of service should not be viewed as an absolute measure, since in an operating system it will be variable; at times the actual grade of service provided will perhaps exceed the one established as a minimum required for the system, and at other times, due to propagation anomalies and unexpected interference, it will fall short of the established minimum. Therefore, in system design or analysis, the most general procedure is to determine a minimum acceptable grade of service under static or median conditions and to allow for the expected propagation or interference in the specification of other system parameters, such as transmitter power. For example, if a required $D/U(g_s)$ has been

determined for a communication system based on median values of transmission loss in the propagation medium and it is known with some degree of certainty that the system will be subject to normal fading on the order of 6 dB about the median, the power budget can be increased by 6 dB to provide a compensating fade margin. The transmitter power can then be increased, the antenna system gain improved, the path length reduced, or a combination of such alternatives applied to alter the power budget appropriately. Examples of these design procedures are given in section 5 of this report.

The required grade of service for a voice communication system should ultimately be established in accordance with the requirements of the system user. In other words, the performance of these systems should be evaluated so that the measure used is indicative of the performance that would be ascribed by the system users in subjective performance tests. To counteract these arduous and time-consuming tests, a well-defined and reasonably well-established objective performance rating based on an articulation index (AI) has been devised (French and Steinberg, 1947; Kryter, 1962; Kryter and Ball, 1964), and found to be quite useful in voice system evaluations (Busch, 1969). The AI is a quantitative measure calculated from S/N averaged over 20 specified frequency bands in the voice spectrum and has been shown to be well correlated with subjective intelligibility ratings. The latter should perhaps be used as an absolute standard for voice circuit performance, based on established test procedures and word lists, such as the "modified rhyme test" (MRT), (House et al., 1963; House, 1965) phonetically balanced (PB) words, or messages typical of the system use. A secondary standard more readily applied for objective evaluation can be formulated from the AI performance technique.

The required grade of service for a digital transmission system is generally based upon the acceptable error performance of the system. There are two principal measures of error performance encountered in the literature, both of which are defined as error rates or percentage of error. One is based on bit (binary digit) errors (i.e., the straightforward errors in a binary bit stream) and the other on character errors. The latter refers generally to a coded system, in which a character is composed of a bit sequence that defines a unique code word or message. In these cases, the character error rate is more important than the bit error rate, as it is often possible with coding techniques (including error correcting codes) to correctly identify a character received with a number of bit errors occurring within the transmission. Error rates considered in this report are restricted to bit rates in an uncoded binary stream.

The theoretical performance analysis of communication systems is fundamentally based on such quantities as S/N or carrier-to-noise (S_c/N) power ratios at various points in the system. For example, the performance of various modulation detection processes are characterized in terms of their S/N output to S/N input properties in much the same manner that noise factors were defined in section 3. On the other hand, system performance measurements such as those presented later in this section and in appendix C have been based on D/U at the input terminals of the receiver. The balance of this section is devoted to determining the relationship between these characterizations, their dependence upon other system parameters, and the specification of the required D/U in the analysis of overall system performance. Both measured quantities and those calculated from theoretical aspects are used. Fundamental characteristics of the modulation processes are included when they are used in the examples. For a more complete

summary of these characteristics the reader is referred to appendix B and to Hubbard et al. (1970).

4.2 System Parameters

Many parameters in a radio communication system affect the performance of that system. Some of these are of course under the direct control of the system designer; others, such as propagation and interference anomolies, are not. In contending with the latter, the designer can only be as cognizant as possible of their probability of occurrence and to assess their degradation of the system performance. In this section, we shall consider the most important system parameters necessary for determining the required signal ratios.

4.2.1 Grade of Service for Voice Systems

Several studies have been devoted to intelligibility testing of voice communication systems to determine grades of service obtained with varying degrees of noise interference. The basic tests used have included those mentioned previously, such as MRT, PB words, and sentence. A summary of typical results is shown in figure 17, which indicates that a higher degree of intelligibility for sentence tests is obtained at a lower articulation index than for other test vocabularies. The primary reason for this is the redundancy of the language; the listener can usually properly receive the message in a sentence even if several words are missed or not understood. However, if the sentence contains detailed or specific information (such as a numerical value) that cannot be anticipated or associated with some other element of the sentence, intelligibility is significantly reduced when this information is lost. A comparison of the performance characteristics obtained when rhyme tests or nonsense syllables and sentence vocabulary tests are used is shown in figure 17. In the former there is

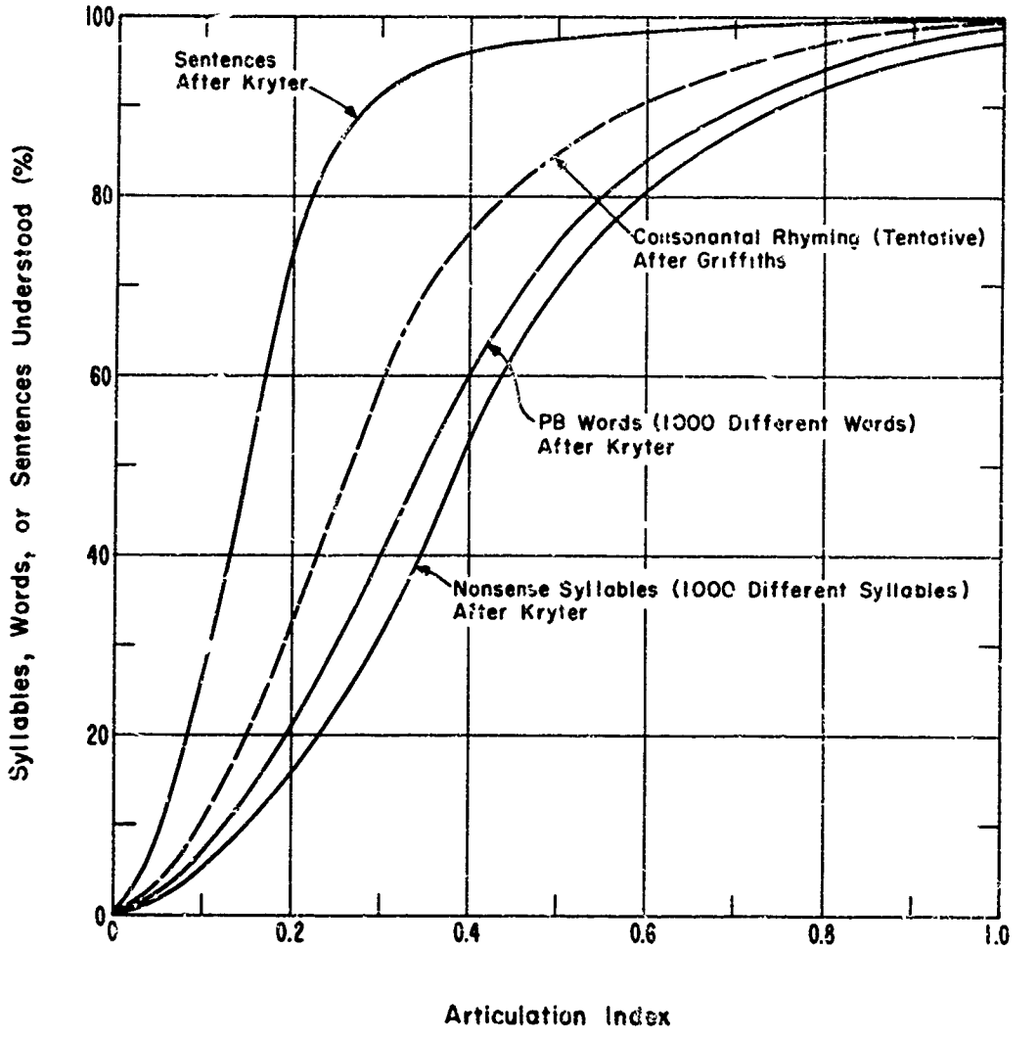

Figure 17. Approximate relations between articulation index and various measures of speech intelligibility. (After Kryter, 1962a; Griffiths, 1968.)

no message redundancy or word association to imply a missing message element.

Phonetically balanced words are a group of test words that have essentially the same number of phonetic sounds (phonemes) in each. In nonsense syllable tests (as in fig. 17), a test vocabulary of meaningless monosyllabic sounds composed of consonant-vowel-consonant form is used. Since they are meaningless sounds, the test listener is unable to guess the correct sound from either association or familiarity. In consonantal rhyming tests, a vocabulary of words that rhyme in either the final or initial consonat (such as meat - beat, or bat - back respectively) are used, generally composed of the consonant - vowel - consonant form. The MRT is of this type, but differs in test administration and evaluation procedures (House et al., 1963).

Intelligibility testing can result in wide variability. For example, Akima et al. (1969) have compared the results of a PB word test obtained in several investigations of AM/ DSB systems. These results are shown in figure 18, in which we see that the results are spread over a range as wide as 10 to 12 dB for a given articulation score. A number of variables can account for the spread in these data; the training and experience of both the talkers and the listening panel may be quite different, the modulation and level settings may vary, and the environmental conditions, such as ambient background noise, may differ greatly. If well-trained and well-chosen teams of talkers and listeners are used, results can be very reliable (Stuckey, 1963) when other conditions are well specified and controlled.

To provide some insight into both present and future ATC voice circuit requirements, a series of subjective and objective tests relevant to the ATC system have been performed (Hubbard and Glen,

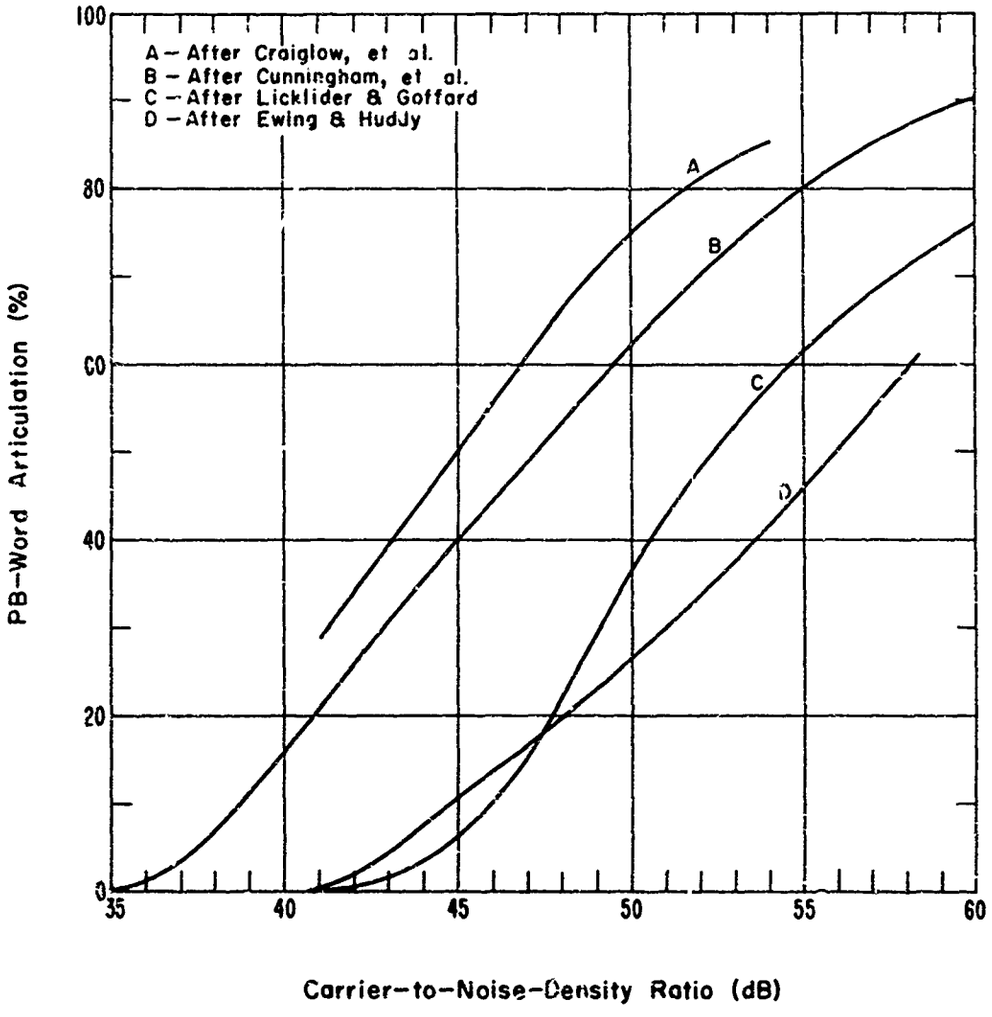

Figure 18. Relation between S_o / N_H and PB word articulation for DSB-AM signals and white Gaussian noise by different investigators. (S_o / N_H ratio is the ratio of carrier power to average noise power contained in a 1-Hz bandwidth.) (After Cunningham et al., 1947; Licklider and Goffard, 1947; Graiglow et al., 1961; Ewing and Huddy, 1966.)

1968). These tests were performed for both an AM-DSB and an FM VHF voice circuit in a laboratory system configuration under the following conditions:

	AM-DSB	FM
Receiver Type	TMR-5	TMR-5
	(Manufactured by Defense Electronics, Inc.)	
Noise figure	5 dB	5 dB
3 dB bandwidth	20 kHz	20 kHz
Modulation	100% (voice peak)	5-kHz peak deviation
Desired IF level	-33 dBm	-35 dBm
Equivalent RF level *	-107 dBm	-105 dBm
Test frequency	10 MHz IF	10 MHz IF
Output bandwidth	10 kHz	10 kHz
Undesired signal	Broadband Gaussian Noise	

*(see app. C, fig. C.35)

The analysis details of these tests are discussed in the above report, and will not be repeated here. A typical library of enroute ATC messages was used in one subjective test, and a more standard MRT word list was also used. An objective measurement under the same interference conditions was performed with the "speech communication index meter" (SCIM) (Kryter and Ball, 1964). The SCI is a measured index very closely related to the AI.

Thirty FAA controllers from the National Aviation Facilities Experimental Center (NAFEC) who are experienced in the ATC communication system were used as listeners. Evaluation of these data enabled us to measure grades of service as determined by system users and to relate them directly to a range of S/N values at the input

to the receiver. These tests were made under conditions of wideband noise interference to the desired signals, as this is anticipated to be the worst situation for noncoherent forms of interference. Additional objective tests presented in this report (app. C), and the reports by Hubbard and Glen (1968) and O' Brien and Busch (1969) largely verify this assumption for the cochannel tests. Some forms of coherent interference in the cochannel configuration can be more detrimental to performance; an example is the audible beat-frequency interference between channel carriers as shown in figure C. 19, appendix C.

Overall performance characteristics derived from wideband noise interference tests with MRT words and ATC messages are presented in figures 19 and 20. The MRT and ATC message evaluations and the SCI data from the associated objective tests are included. Figure 19 shows the results of the AM tests, and figure 20 shows similar data for FM tests. The curves in these figures are plotted for the sample means, and the calculated standard deviation for each data point is indicated. As the performance curves approach 100% intelligibility levels, the standard deviation becomes quite small, indicating more confidence in message interpretation with increasing S/N values. It is of interest that the MRT test for the AM system in figure 19 agrees quite well with the results obtained by Lick'ider and Goffard (1947), shown in figure 18, when S_c / N_W is converted to S/N for a 20-kHz bandwidth (see sec. 3.3.4).

The air traffic controller's ability to read typical ATC messages intelligibly with relatively high noise interference is evident from a comparison of the step-function character of the ATC performance curves with those derived from the standard MRT tests. Because of the small ATC vocabulary, interdependence of words,

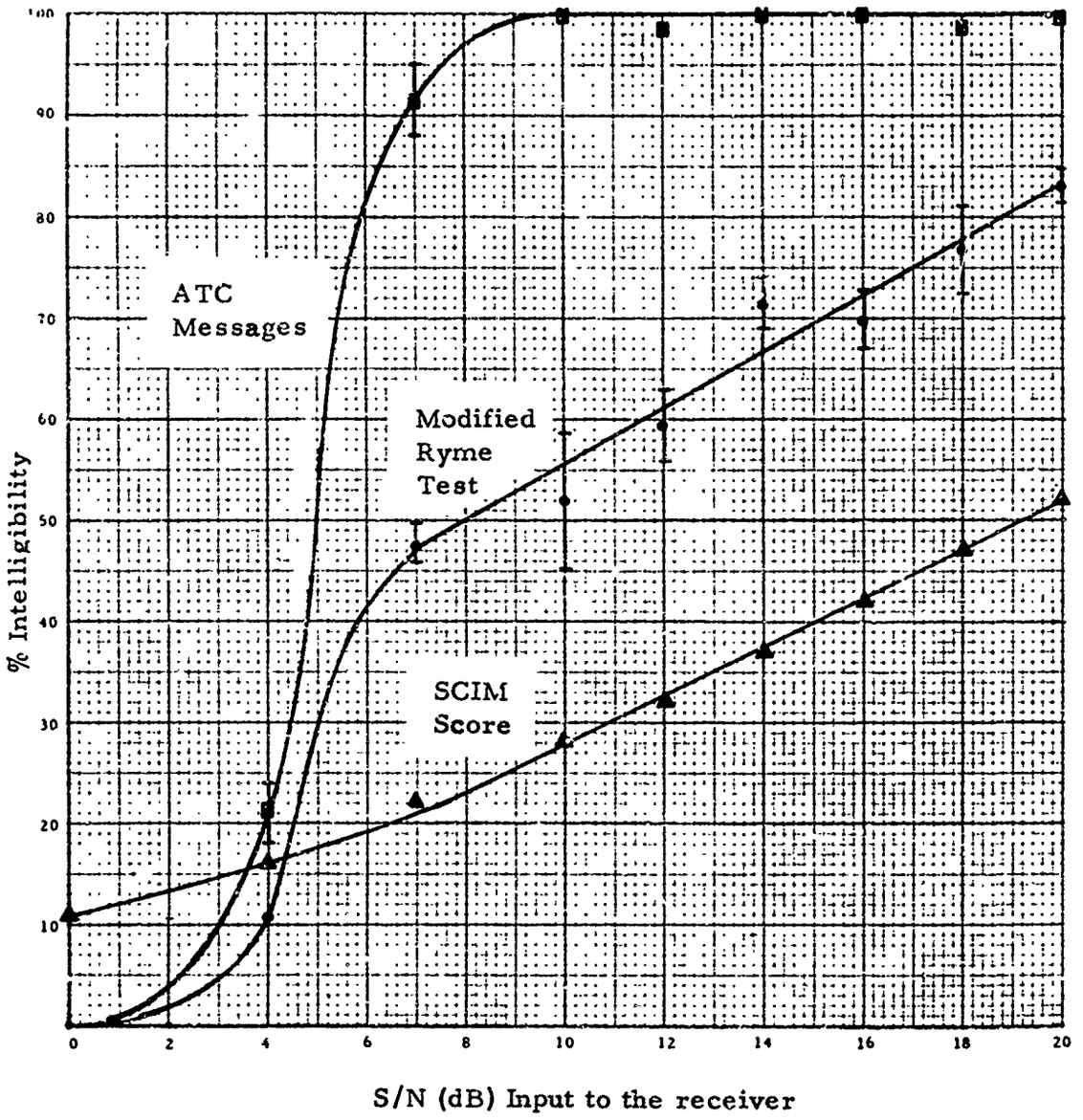

Figure 19. AM performance vs. wideband noise.

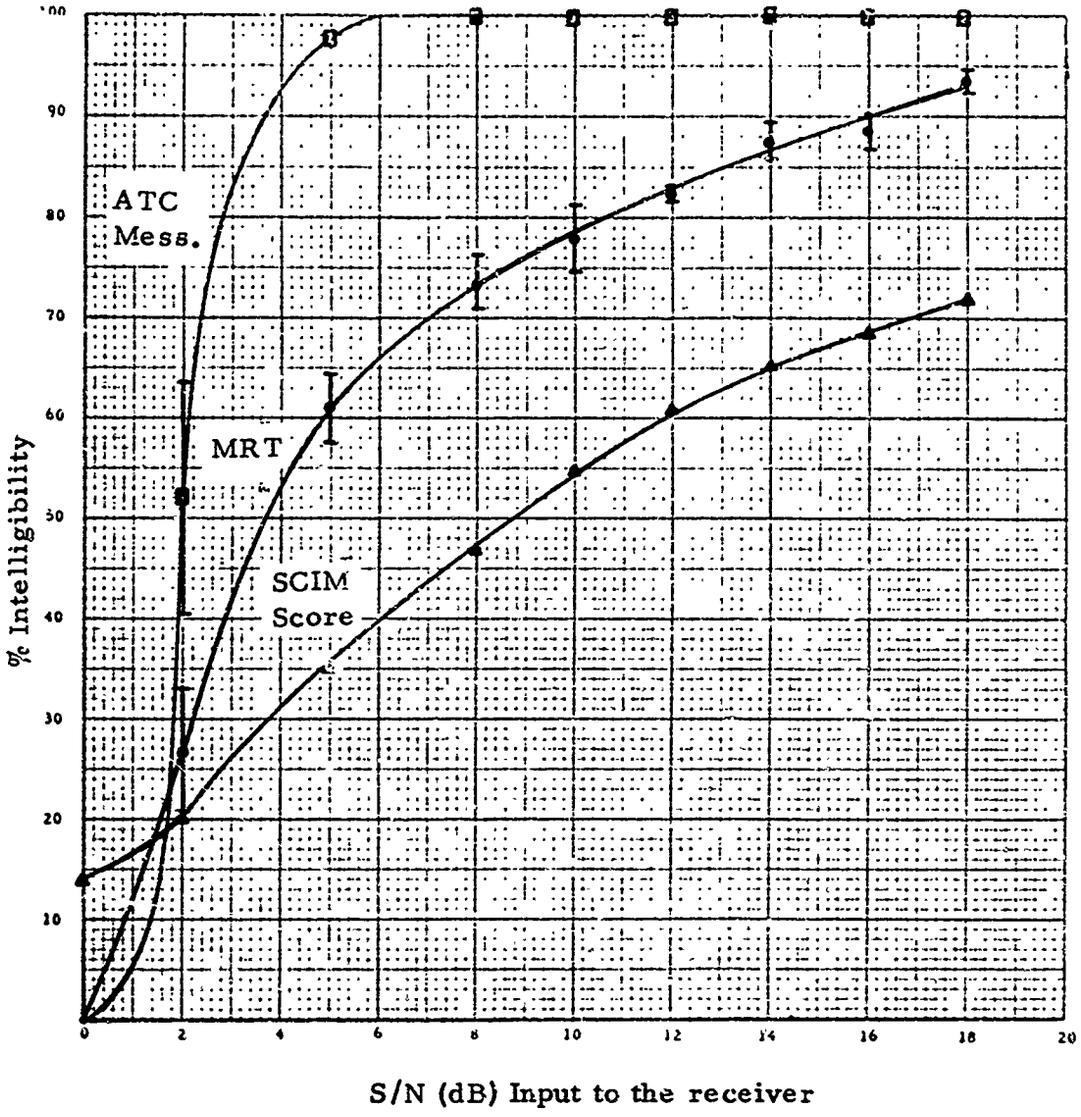

Figure 20. FM performance vs. wideband noise.

redundant message characteristics, context in which an ATC message may be given, and the controller's training, the evaluators were able to correctly identify the ATC messages more easily than the noninterdependent MRT words subjected to the same interference.

Kryter and Ball (1964) have shown the close realtionship between SCI scores and AI, which in turn is related to speech intelligibility, as indicated by the curves in figure 17.

Similar transfer relationships between the subjective ATC and MRT tests and the objective SCI have been derived from the data in figures 19 and 20. Figure 21 shows the intelligibility evaluated by the ATC controllers' panel versus the SCI scores for the AM system, and figure 22 presents similar characteristics for the FM system. Note that slightly higher subjective intelligibility was obtained at a given SCI value for AM than FM. The reason for this is unknown, but perhaps again indicates the controllers' experience in the conventional AM ATC system.

Because of the statistical uncertainty of the subjective data and the highly experienced listening panel used for deriving figures 21 and 22, care must be taken in application of these curves. They show, for example, that a SCI ≥ 0.4 will generally result in 100% ATC message intelligibility when the ATC personnel are experienced. However, the ATC communication system must accomodate less experienced personnel as well (such as the aircraft pilot in a noisy ambient environment), working in the commercial, military, and general aviation fields. The required grade of service for such personnel should not be directly inferred from the curves in figures 21 and 22. Their requirements may be more nearly those indicated by figure 17, or an SCI ≥ 0.85 for a high percentage of intelligibility as suggested by O'Brien and Busch (1969).

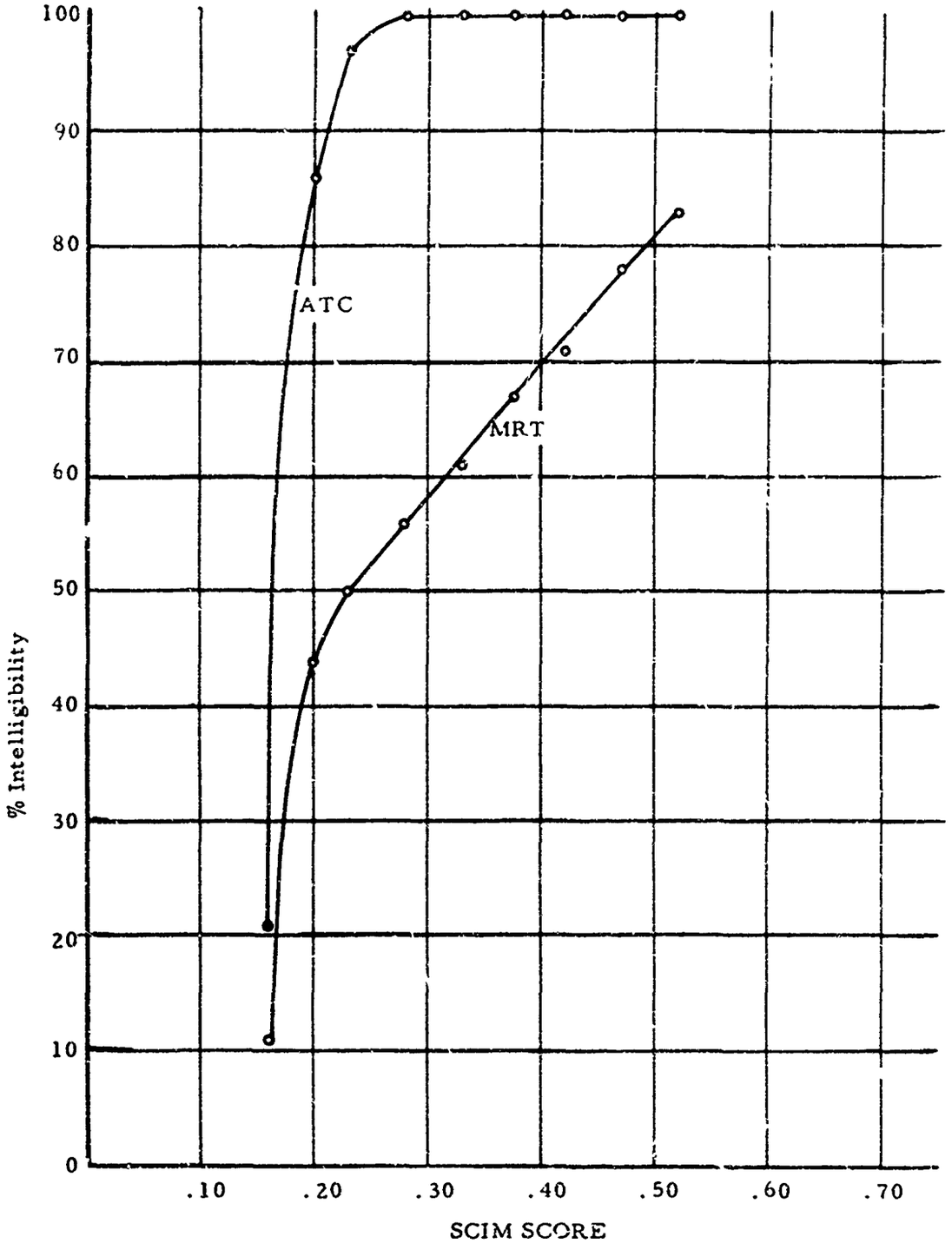

Figure 21. AM test - relation between SCI and measures of ATC message and MRT word intelligibility.

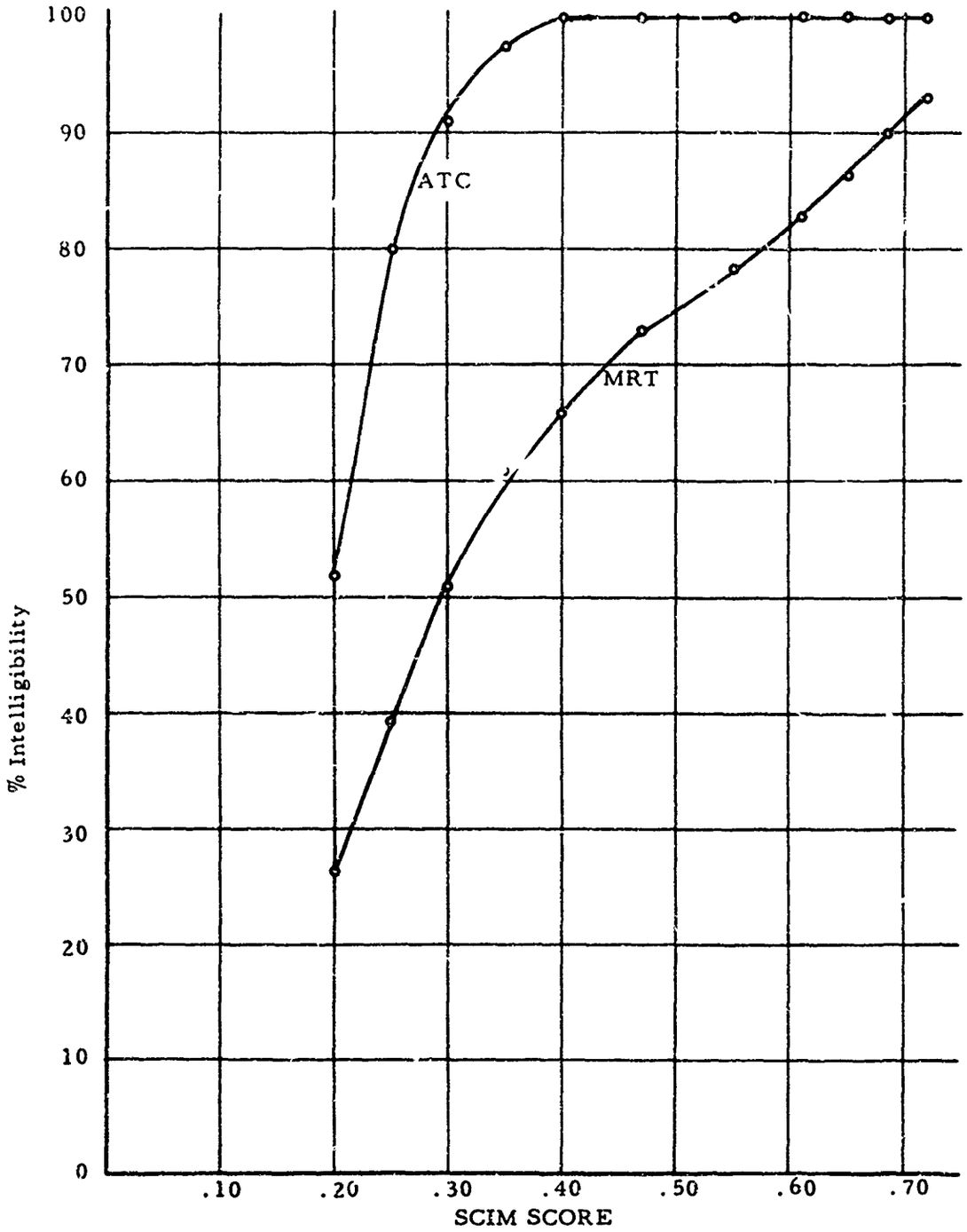

Figure 22. FM test - relation between SCI and measures of ATC message and MRT word intelligibility.

The characteristics presented in this section will form a basis for establishing the required grade of service in the ATC voice communication channel. They are used in later examples for determining the required signal ratios and in assessing the performance of several possible channel configurations for the ATC system.

4.2.2 Grade of Service for Digital Systems

Two aspects for grade of service in a digital communication system must be considered, depending upon the application of the system. If digital techniques are used for transmission of data signals and reception is in a digital mode, the grade of service is based entirely on the error performance as mentioned previously. When the digital system is used to transmit analog and/or voice signals, as in pulse code modulation (PCM) or delta modulation (DM) schemes, the grade of service will again be based upon S/N and/or intelligibility.

Only the binary error performance of frequency-shift keying (FSK) and phase-shift keying (PSK), the two most widely used digital transmission forms, will be considered. However, on-off amplitude shift keying (ASK) is also noted, as it may be of benefit to ATC systems. The fundamental error performance characteristics of these systems are illustrated in figure 23. The optimum threshold characteristics of the on-off ASK system can be shown to be the same as those for the noncoherent FSK system (Stein and Jones, 1967). The advantage of ASK is that, compared with FSK, a reduced transmission bandwidth is required. However, ASK on-off systems are threshold dependent and perform poorly in fading transmission channels. From figure 23, we see that the grade of service in terms of error performance depends on the type of transmission and detection used. For example, if system

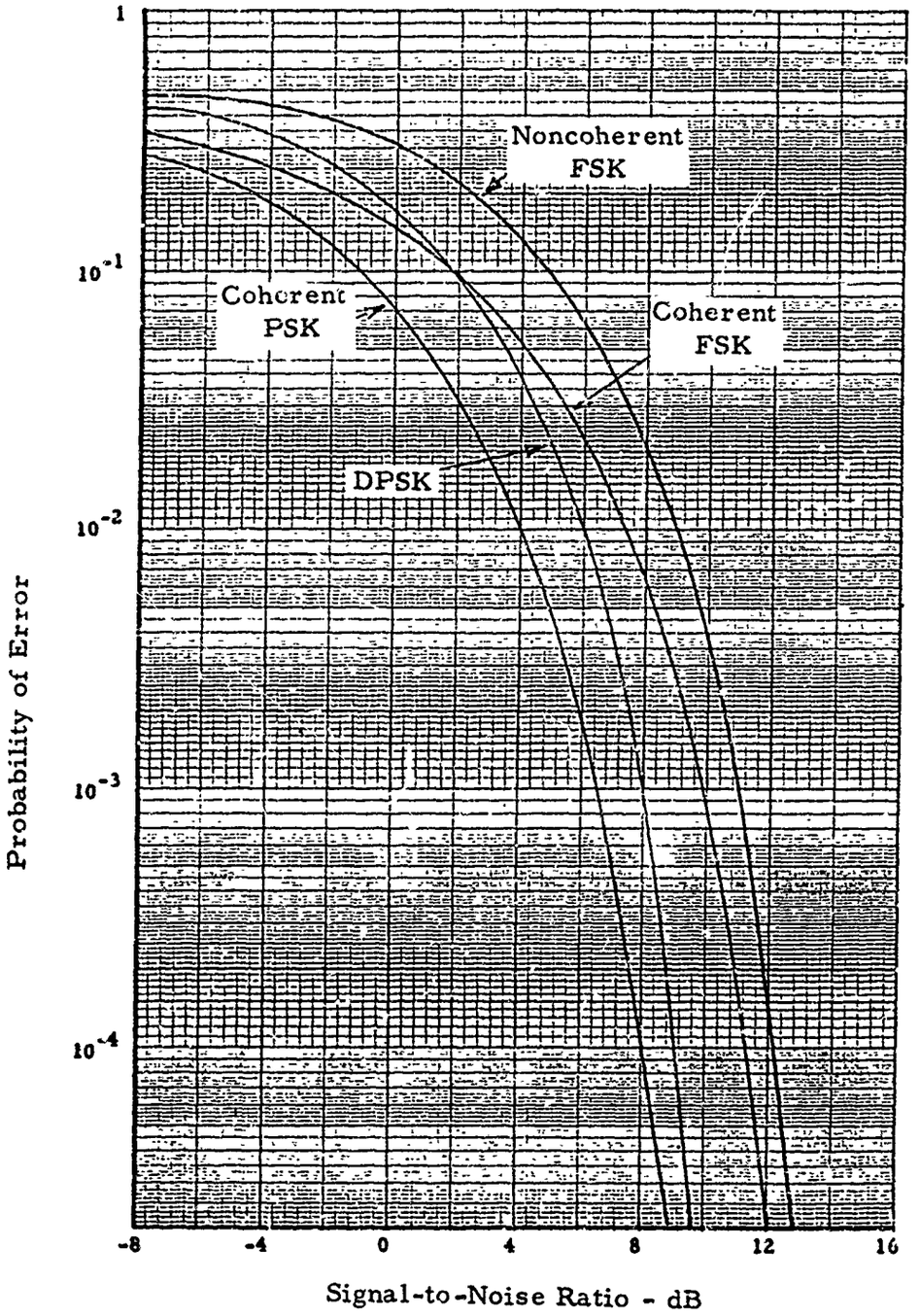

Figure 23. Error rates in binary systems.

performance requires a probability of error of 10^{-3} or less, a noncoherent FSK system will require approximately 4.5 dB higher S/N than for a coherent PSK.

The performance curves in figure 23 are based upon steady signal conditions and thus represent optimum expected performance. Fading conditions within the transmission channel must be taken into account to specify the required S/N to provide the required grade of service. An approximate degradation of performance can be given for the typical slow, Rayleigh fading channel (Schwartz et al., 1966). For this fading condition and $S/N \gg 1$, the probability of error (P_e) is found to be inversely proportional to S/N. It can be stated as follows:

$$P_e \approx 1/\rho \quad \text{for noncoherent FSK,} \tag{51a}$$

$$P_e \approx 1/2\rho \quad \text{for coherent FSK and DPSK,} \tag{51b}$$

and

$$P_e \approx 1/4\rho \quad \text{for PSK,} \tag{51c}$$

where ρ is the input S/N ratio. This characteristic for fading conditions results in the requirement that a 1-0 dB increase in S/N is required for every decade improvement in P_e as compared to an approximate 1-dB increase at high S/N for the nonfading conditions in figure 23. The characteristics of (51) are plotted in figure 24 for values of $S/N > 5$ dB.

It is important to note that in between the extreme performance characteristics indicated by figures 23 and 24, there is a large family of performance curves based upon diversity reception, combining and multilevel transmission techniques. It is beyond the scope of this report to consider these techniques, but an excellent reference on multiple FSK is Akima (1963) and on diversity techniques (among others) Schwartz et al. (1966, chs. 10 and 11). Required S/N_W for some diversity orders have been calculated for slow Rayleigh fading by Akima et al. (1969), and are given later in table 2.

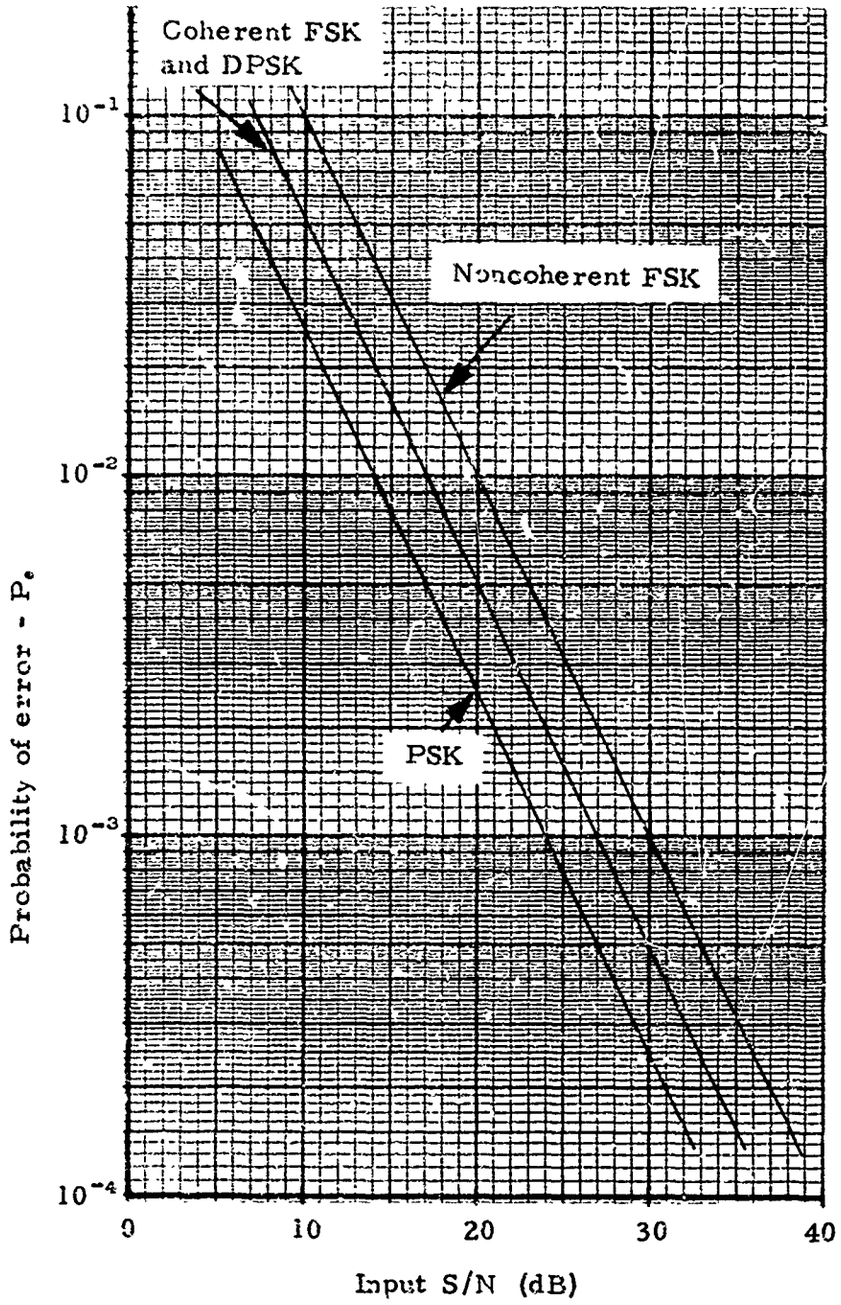

Figure 24. Approximate binary system performance in slow, Rayleigh fading.

For the transmission of voice or other analog signals in a digital system, the signal must be converted to a digital format. There are a number of methods either devised or proposed for this purpose (Proc. IEEE, 1967), but two such systems predominate: pulse code modulation (PCM) and delta modulation (DM), which will be the only techniques considered in this report. A more detailed discussion of these methods and their characteristics are included in appendix B.

Although the error performance of PCM and DM techniques is important, it is not the primary characteristic needed for establishing grades of service. Since these systems are used in the transmission of voice or analog information, their output S/N characteristics for the analog signal is of primary concern. Unfortunately, because there is no vast accumulation of either engineering experience or empirical data to assist in the evaluation of these systems, we must rely almost exclusively on theoretical analyses. Digital errors occurring in the system due to quantizing, coding, and detection result in a self-noise relative to the voice or analog signal outputs. For PCM, this noise has been calculated by Akima (1963) for a sinusoidal input signal sampled at the Nyquist rate. These calculations coupled with the prediction of errors caused by additive Gaussian noise in N-ary FSK transmission yield the theoretical S/N performance curves shown in figure 25 for binary transmission (N = 2). The parameter n in this figure is the number of elements used in the quantized signal. The limiting region of the curves is established by the quantizing noise level. Quantizing noise for a DM system has been computed by van de Weg (1953), and corrected for a 3-dB error by Hartman (Hubbard et al., 1970). The resulting threshold performance of DM is plotted from these results as the dashed lines in figure 25. Performance below threshold and the location of the knees of the DM performance

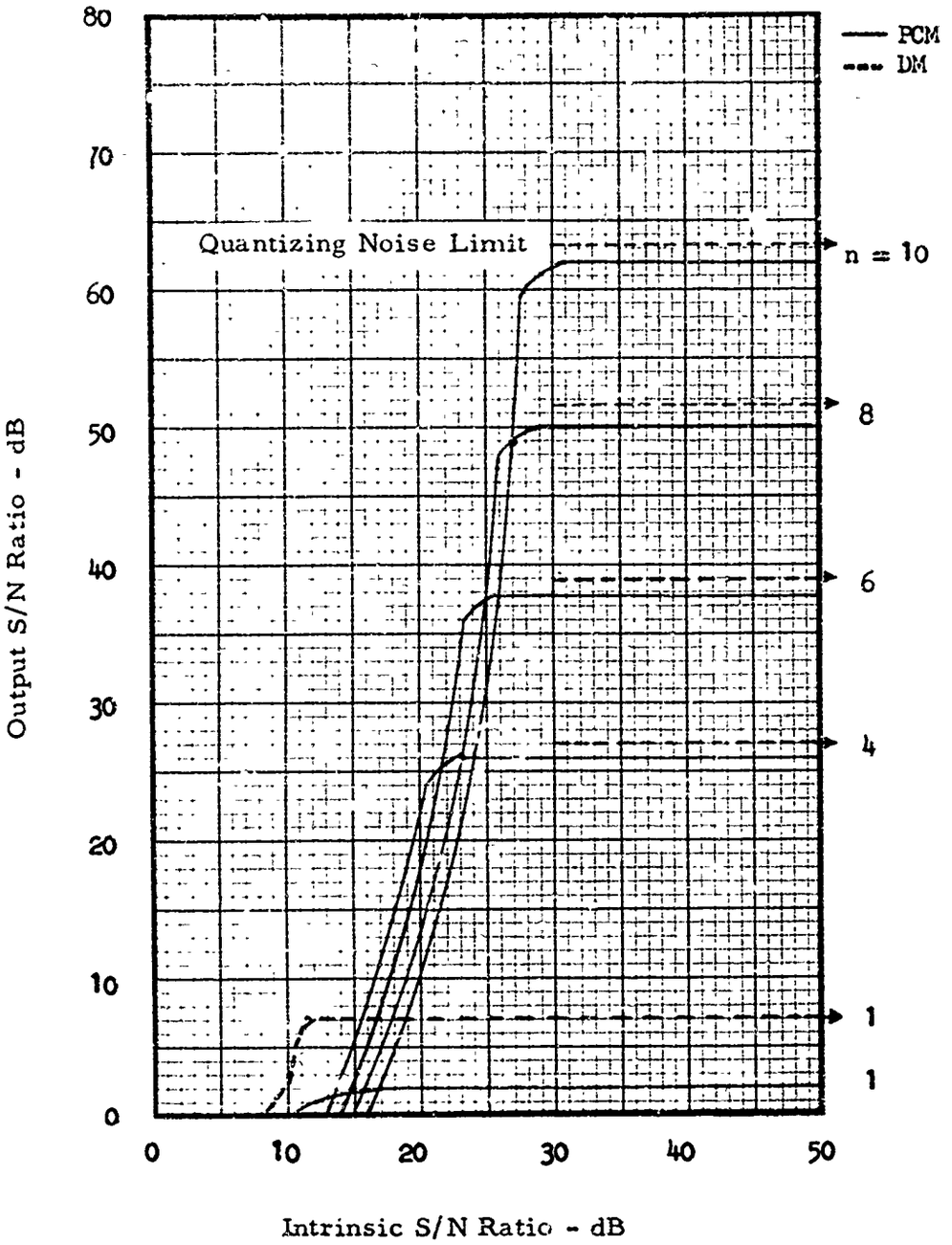

Figure 25. Signal-to-noise characteristics for PCM-FS and DM (N = 2).

curves are unknown. One curve for DM (n = 1) has been extrapolated to reflect a calculation by Wolf (1966) but its validity is questionable (see app. B). Figure 25 is useful, however, to establish at least a first order estimate of the S/N input required to achieve a given S/N output. The latter will then relate to a grade of service for a voice communication system as developed in subsequent sections.

4.2.3 Signal-to-Noise Power Ratio

In the preceding discussion we note that grade-of-service definitions are based in essence on one form or another of an S/N. For example, the subjective and SCIM performance measurements for a typical ATC voice circuit are presented in terms of an S/N at the input to the receiver (figs. 19 and 20). Error performance characteristics for the digital transmission systems are also dependent on S/N. Thus this ratio is an important parameter throughout the communication system, and certain values must be met or exceeded in the noise environment to provide the desired grade of service.

In the typical ATC circuits considered in the measurements presented above, the S/N associated with the required grade of service can be used directly to specify other system parameters. However, it is important to note that these measurements apply to a particular set of receiver characteristics (such as a 20-kHz IF bandwidth), and may not apply directly to other conditions. In this section, we will describe the manner in which the required $S/N(g_s)$ at the receiver input terminals can be estimated from theoretical values of S/N at other points in the circuit. Examples are presented for an AM and FM system, and the calculated estimates are compared directly with measured values in figures 19 and 20.

Using methods suggested by Kryter (1962a), Akima et al. (1969) have computed the relationship between AI and the speech S/N density

ratio at the audio frequencies. This characteristic is shown in figure 26. The theory for computing AI and a number of measurements in voice communication systems indicate that articulation depends primarily on the speech to noise power density ratio rather than S/N (Akima et al., 1969). As a result, the articulation varies only slightly with IF receiver bandwidth. This is illustrated by the PB word articulation test results shown in figure 27. Note that at 60% PB articulation, the spread of these data is approximately 3 dB for IF bandwidth ranging from 2.4 kHz to 52 kHz. This fact simplifies the theoretical determination of $S/N(g_s)$ in a voice communication system, as it permits a direct translation of a S/N value at the input to the detector to an equivalent value of S/N at the input to the receiver, almost independent of IF bandwidth. This characteristic is demonstrated only for the broadband noise interference case, and is probably not applicable to coherent forms of interference, which are discussed in later sections (4.3, 4.4, and 4.5) of this report.

The insensitivity of articulation scores to IF bandwidth shown by figure 27 should not be misinterpreted. Note that these data are plotted as a function of signal carrier to noise <u>density</u> ratio in which the noise power is defined in a 1-Hz bandwidth. The total noise in the receiver, of course, is a function of bandwidth, and the receiver threshold is thus very sensitive to bandwidth, as discussed in section 3.3.2. If the data in figure 27 were plotted for each case as a function of S/N (N = total noise power in the bandwidth) a wide variation of S/N values for a given articulation score would be evident, and consequently a wide range of required signal power would be noted in each case.

To illustrate the application of these data and characteristics, consider an AM-DSB voice system in which the receiver has a 20-kHz

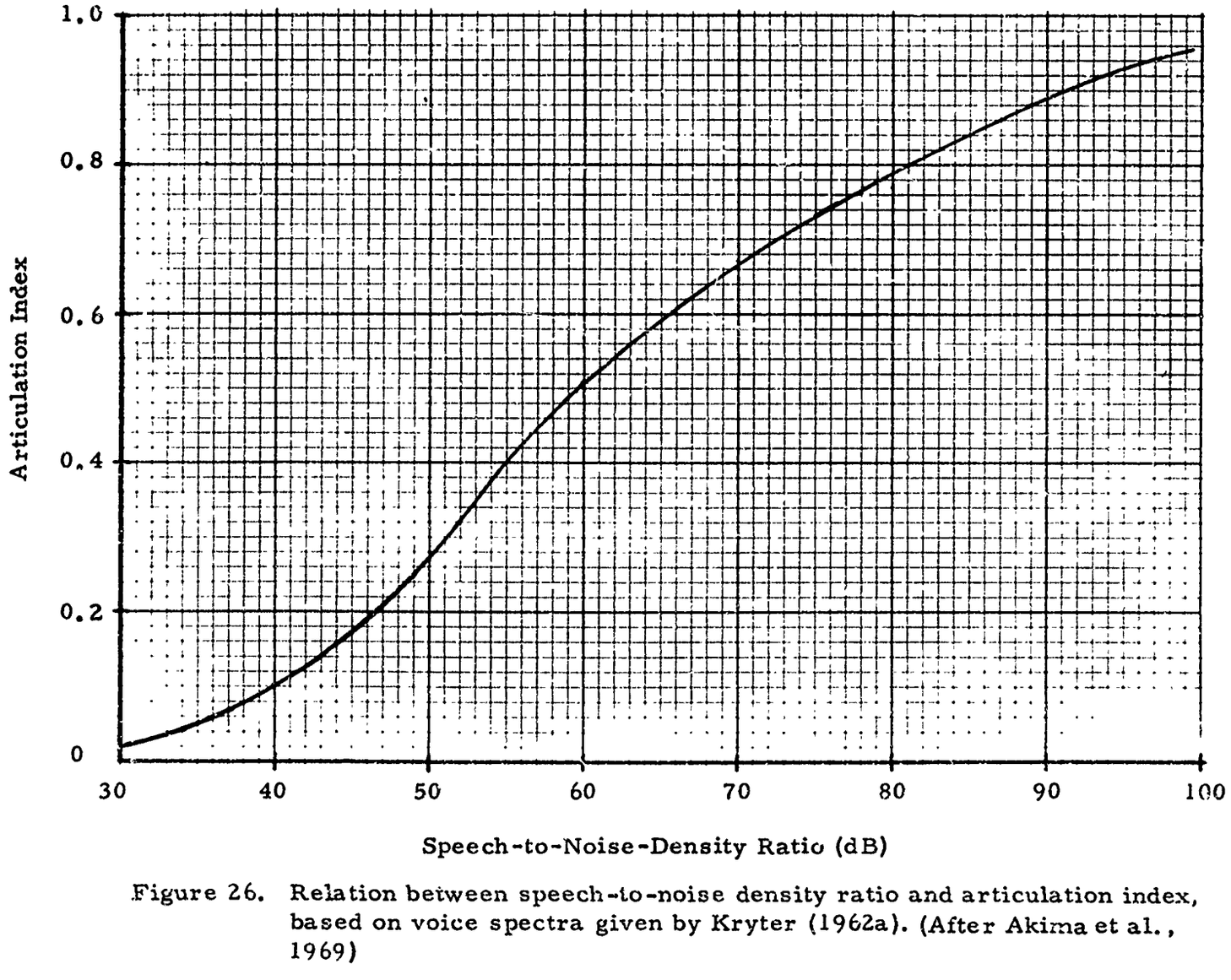

Figure 26. Relation between speech-to-noise density ratio and articulation index, based on voice spectra given by Kryter (1962a). (After Akima et al., 1969)

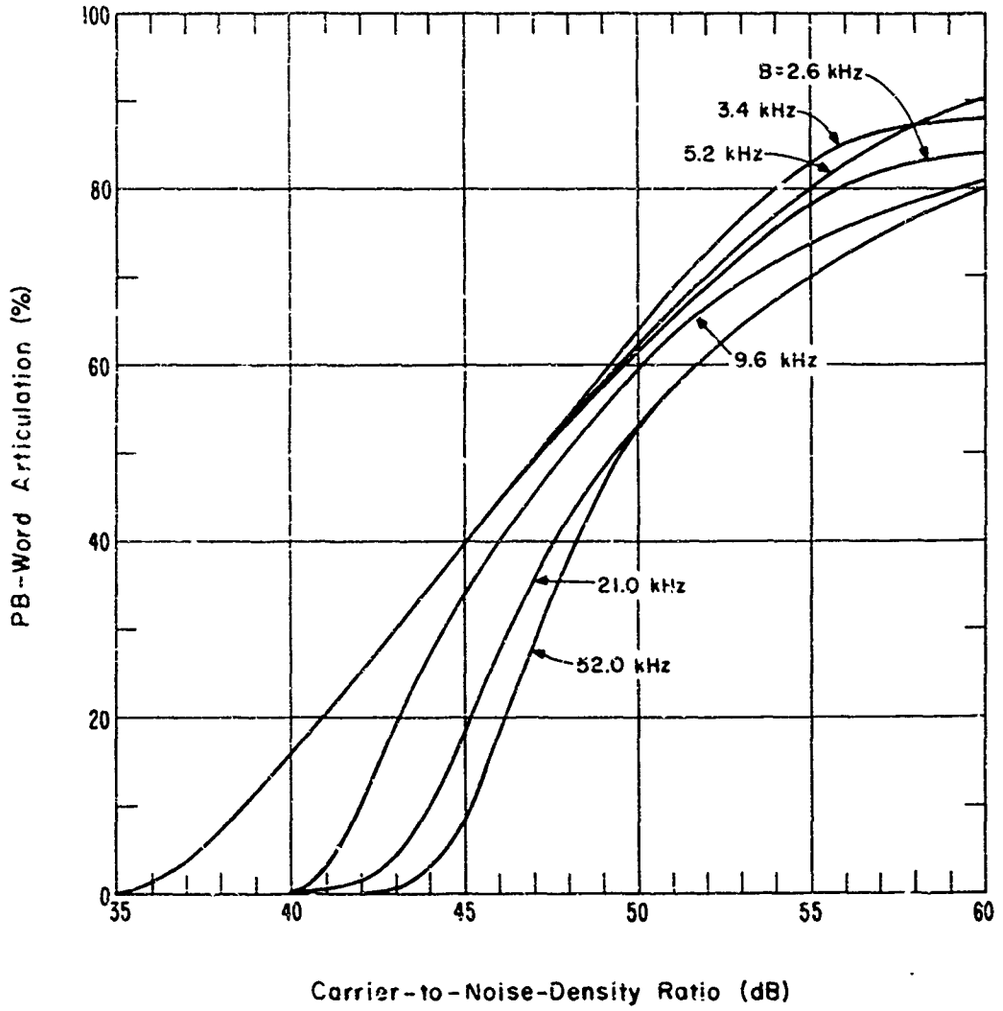

Figure 27. Relation between S_c / N_W and PB word articulation for DSB-AM signals and white Gaussian noise for different values of the IF bandwidth B. (S_c / N_W is the ratio of carrier power to average noise power contained in a 1-Hz bandwidth). (After Cunningham et al., 1947.)

IF bandwidth, and in which a linear amplitude detector with the characteristics shown in figure 28 is used. We shall assume that a grade of service is required that will assure approximately 100% ATC message intelligibility under stable conditions. The following procedure is used to estimate the required S/N at the receiver input terminals:

(1) From figure 21 we find the AI (or SCIM score) required for a g_s corresponding to 100% ATC message intelligibility to be

$$AI \geq 0.3 .$$

(2) From figure 26, for an AI = 0.3 we find the required S/N_W at the baseband or audio frequencies to be

$$S/N_W = 52 \text{ dB} ,$$

which is the value required at the output of the detector. Assuming an audio output filter bandwidth for the receiver as

$$B_o = 10 \text{ kHz} ,$$

we convert to S/N at the output of the detector-filter (see sec. 3.3.4)

$$(S/N)_o = S/N_W - 10 \log B_o$$

$$= 52 - 40 = 12 \text{ dB}.$$

(3) From figure 28, we find the carrier to noise power input ratio $(S_c/N)_i$ at the linear detector corresponding to $(S/N)_o$ = 12 dB to be

$$(S_c/N)_i = 9 \text{ dB} .$$

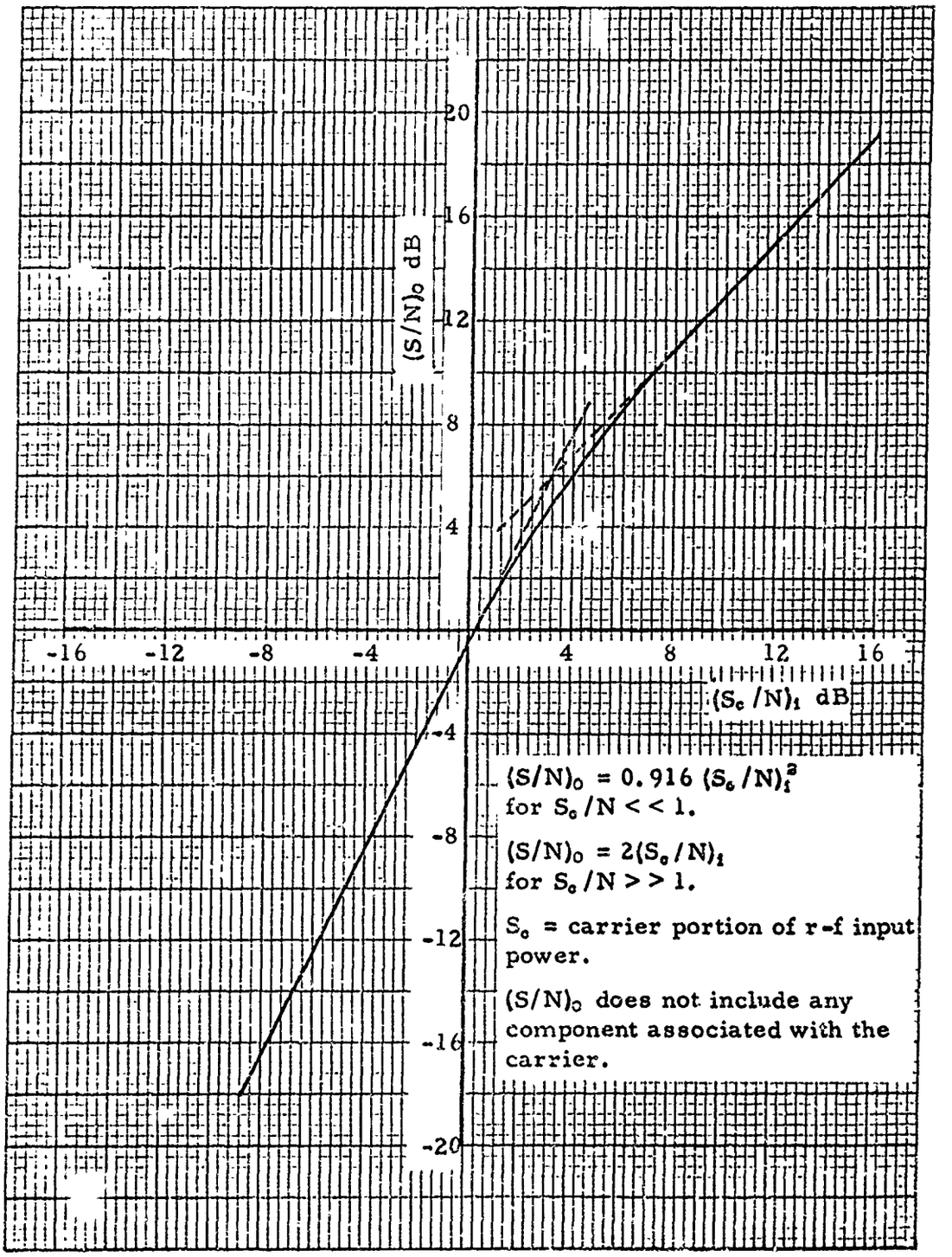

Figure 28. Performance characteristics of a linear amplitude detector.

Based on an earlier premise, the above S_c / N_W can be translated to the required $S_c/N(g_s)$ power ratio at the input to the receiver almost without regard to IF bandwidth. However, a correction for the effective noise bandwidth of the receiver[10] should be made. Skolnik (1962, p. 24) has computed the ratio of effective noise bandwidth to 3-dB bandwidth for several types of receivers. These are given in table 1. For the example chosen, we shall assume two stages of single-tuned amplifiers in the receiver IF strip. Thus, from table 1, the effective noise bandwidth is

$$\begin{aligned} B_n &= 1.22\ B_{3\ dB} \\ &= 1.22 \times 20\ \text{kHz} \\ &= 24.5\ \text{kHz}. \end{aligned}$$

The proportionality factor of 1.22 in this case will increase the effective noise power density in the receiver by 1.22 (or approximately 0.9 dB). Applying this correction, the approximation to the required $S_c/N(g_s)$ at the input to the receiver terminals for this example becomes

$$S_c/N(g_s = 100\%\ \text{ATC message intelligibility}) = 9.9\ \text{dB}.$$

The parameters selected for this example are those that apply to the measurements presented in figure 19, and the required S/N estimated above can be compared directly with the 10-dB measured value. The agreement is very good.

---

[10] Effective receiver noise bandwidth is defined as the bandwidth B_n of a rectangular filter, which will have the same total noise power at its output as the true filter response characteristic.

Table 1. Comparison of noise bandwidth and 3-dB bandwidth

Type of Receiver Coupling Circuit	No. of Stages	Ratio of Noise Bandwidth to 3-dB Bandwidth
Single-tuned	1	1.57
	2	1.22
	3	1.16
	4	1.14
	5	1.12
Double-tuned	1	1.11
	2	1.04
Staggered triple	1	1.048
Staggered quadruple	1	1.019
Staggered quintuple	1	1.01
Gaussian	1	1.065

A similar example in which we assume an FM system is presented as follows:

Required g_s = 100% ATC message intelligibility.

Receiver 3-dB bandwidth = 20 kHz.

AF output bandwidth B_o = 10 kHz.

Modulation index β_f = 1.2.

(f_m = 4.2 kHz, ΔF = 5 kHz).

(1) From figure 22 for the specified g_s, AI $\geq$ 0.4.

(2) From figure 26 at AI = 0.4, S/N_W = 55 dB

$(S/N)_o = S/N_W - 10 \log B_o$ = 15 dB.

(3) Figure 29 gives the typical performance characteristics for FM detectors. From the curves at $(S/N)_o$ = 15 dB, we estimate for β = 1.2

$(S_c/N)_i$ = 6 dB.

(4) Again making a correction of 0.9 dB for the effective noise bandwidth, we find

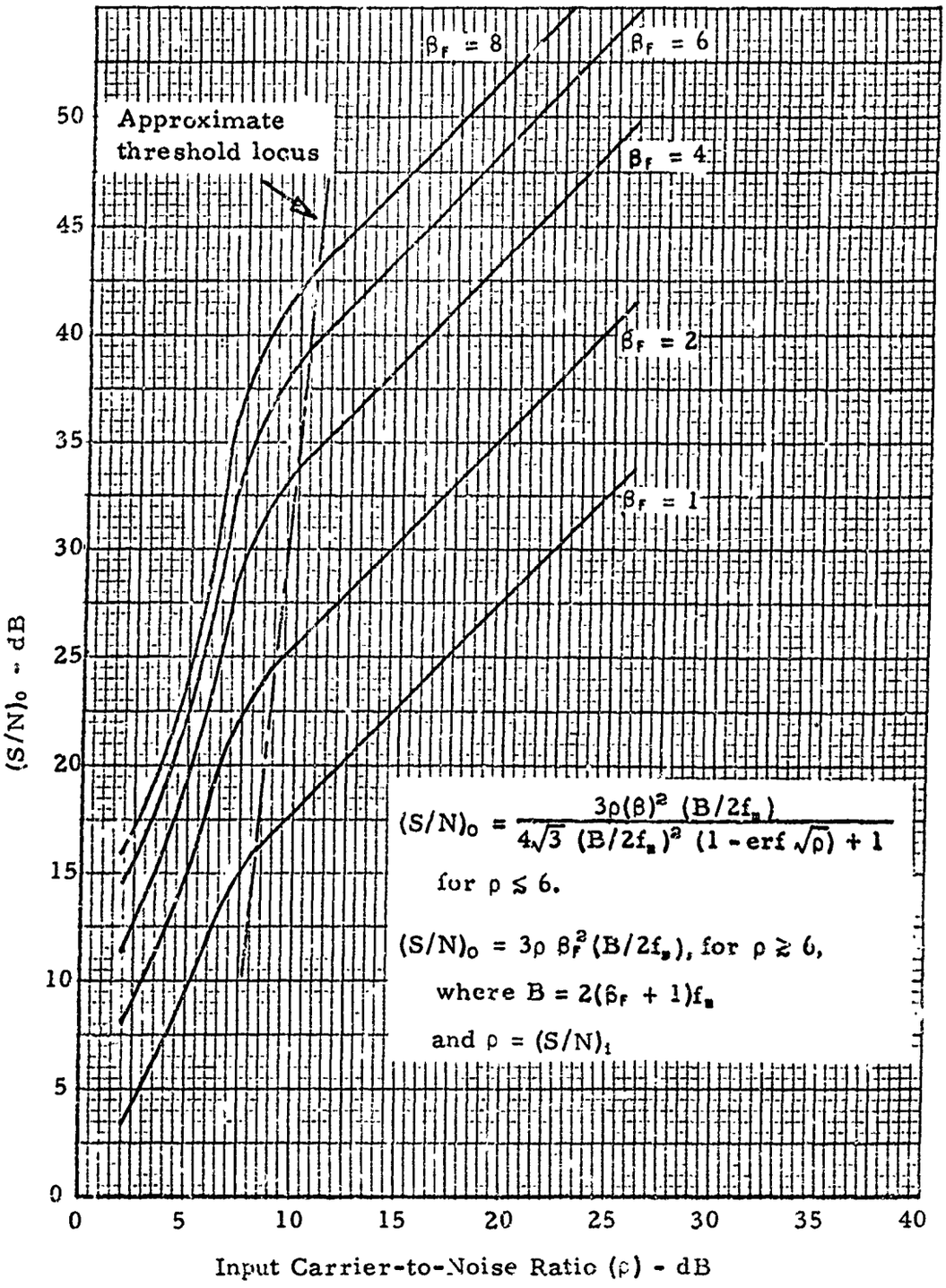

Figure 29. Performance characteristics of FM detectors, where $B = 2(\beta_F + 1)f_m$.

$S/N(g_s$ = 100% ATC message intelligibility) = 6.9 dB, which can be compared with the measured value of 6 dB in figure 20.

In the example above, note that the parameters selected show that the FM detector would be operating at near-threshold level. Thus a grade of service should perhaps be specified as AI = 0.6 or MRT score = 83% (fig. 20). This would require an S/N of approximately 12 dB and would assure operation above threshold level in the FM receiver.

It should be emphasized again that the required S/N calculated in this section are based on steady signal conditions and thus represent optimum values for a noise-limited service. Propagation anomalies must be accounted for by the techniques used for predicting the available signal ratios in section 3. The limiting noise power level can be computed as in section 3.3 and the required optimum signal power determined from the required $S/N(g_s)$ value as computed above.

For example, consider the noise-limited receiving system discussed in section 3.3.2. The limiting system noise power at the input to the system was found to be approximately

$$P_T = -144 \text{ dBW in a 30-kHz bandwidth.}$$

If an $S/N(g_s)$ of 10 dB has been determined necessary to provide the required grade of service, then the minimum signal power required is

$$S = P_T + 10 = -134 \text{ dBW.}$$

The EIRP from the transmitter must be sufficient to provide the above minimum signal power, together with the transmission loss and any required fade margin for the associated propagation path.

Based on the approximate grade-of-service transfer function given in figure 17 and using techniques similar to those described in this section, Akima et al. (1969) and Barghausen et al. (1969) have

computed the required S/N_W for some standard voice emission systems. These are shown in table 2 for two listed grades of service and include some estimates of ratios required in fading channels with and without diversity. The stable condition values agree well with those determined in this report. For example, consider the 6A3 value given for 90% intelligibility in this table:

$$S/N_W = 50 \text{ dB (6A3 emission).}$$

Reception of this signal in a receiver with an effective noise bandwidth of 20 kHz would result in

$$\begin{aligned} S/N &= S/N_W - 10 \log (20 \times 10^3) \\ &= 50 - 43 = 7 \text{ dB,} \end{aligned}$$

which agrees quite well with the AM-ATC curve of figure 19.

4.3 Cochannel and Adjacent Channel Protection Ratios

As stated previously, broadband noise interference is considered to be the worst case at a receiving terminal with the noted exception of cochannel beat-note interference. If the system is subject to interference from many like transmissions on adjacent channels and/or cochannels separated by long distances, the effect is a "noise-like" environment. If the system is subject to interference from only one or a few like transmissions, the interference is more coherent and is less similar to broadband noise. To determine the interference effect in the latter case, a number of laboratory tests have been performed on typical ATC equipment configurations to determine the required signal ratios for various grades of service. The desired-to-undesired signal power ratio D/U has been used in these tests to distinguish them from the noise-limited measurements. Data gathered in tests at ITS, ESSA (Hubbard and Glen, 1968) and at

Table 2. S/N_W required for satisfactory service in standard voice emission systems. (After Barghausen et al., 1969).

Radio Telephone Description	Required S/N_W in Occupied Bandwidth Relative to Noise in a 1-Hz Bandwidth (dB)					
	Grade of Service					
	S/N_W Operator-to-Operator [1]			Good Commercial Quality		
	Stable Condition	Fading Condition		Stable Condition	Fading Condition	
		No Diversity	Dual Diversity		No Diversity	Dual Diversity
6A3 Double sideband - AM	50	51	48	67	75	70
3A3 Single sideband - AM						
3A3a (reduced carrier)	48	49	46	65	73	68
3A3j (suppressed carrier)	47	48	45	64	72	67
6A3 Independent sideband - AM						
6A3b (2-voice channels)	49	50	47	66	74	69
9A3b (3-voice channels)	49	50	47	66	74	69
12A3b (4-voice channels)	50	51	48	67	75	70

[1] For 90% intelligibility of related words.

NAFEC (O' Brien and Busch, 1969) are compiled in tables 3, 4 and 5, and are discussed in appendix C. The wideband noise interference data for the SCI performance curves in figures 19 and 20 are also in appendix C, figures C.16 and C.17.

In all the tests reported, use has been made of the SCIM objective measurement technique discussed in section C.1. The SCI was measured either directly on the SCIM analyzer or indirectly through magnetic tape recordings of the SCIM output signals from each test configuration. The SCI values measured can be used to establish other grade-of-service specifications from figures 21 and 22 for the ATC controller, or from figure 17 for the inexperienced system user.

Tables 3 and 4 summarize two sets of ITS measurements. The curves from which required D/U ratios were determined are shown in the figures in appendix C. For the initial measurements (table 3), the SCIM signal was recorded on magnetic tape and sent to NAFEC for analysis on the SCIM analyzer. Without direct access to the SCIM analyzer in these tests, we could not predetermine whether the desired carrier signal was sufficient to overcome inherent receiver noise and achieve a SCI of 0.99.

Table 4 summarizes the tests where the SCIM generator and analyzer were available to ITS and it was possible to establish test carrier levels high enough to obtain 0.99 SCI readings. In this way, -87 dBm was chosen as a suitable desired carrier level to overcome inherent system noise. The earlier measurements were usually run at lower carrier levels (as shown in table 3) in comparison with the levels indicated in table 4.

The required D/U's contained in these tables have been determined on the basis of a SCI $\geq$ 0.4. This value of the SCI was

Table 3. Measured desired to undesired signal ratios required for a speech communication index equal to or greater than 0.4 (20-kHz IF bandwidth).

Figure No.	Receiver	Test Configuration	Test No.	Peak Modulation Level Desired	Peak Modulation Level Undesired (3)	Signal Level (dBm) (RF*) (Note 1)	Required D/U dB (2)
C.24	960	AM_D/AM Adj. (IF)	X-8	95%	95%	- 95*	-48.5
C.26	TMR-5	AM_D/FM Adj. (IF)	2	120%	10 kHz Dev.	-103*	- 6
C.25	960	AM_D/FM Adj. (IF)	X-7	60%	2.5 kHz Dev.	- 95*	-65
			X-7A	60%	4.5 kHz Dev.	- 95*	-63
			X-7B	60%	6.75 kHz Dev.	- 95*	-61
C.18	TR-711	FM_D/FM Co. (IF)	8-4	5 kHz Dev.	5 kHz Dev.	-106*	+ 5
C.19	TMR-5	AM_D/AM Co. (IF)	1A	120% (4)	30%	- 95*	+ 1
		AM_D/AM .6 kHz offset	1B	120%	30%	- 95*	+11
		AM_D/AM 5 kHz offset	1C	120%	30%	- 95*	+ 1
C.33	TR-711	FM_D/AM Adj. (RF)	X-13	3 kHz Dev.	95%	-101	-38
			X-13A	6 kHz Dev.	95%	-101	-41
			X-13B	9 kHz Dev.	95%	-101	-44
			X-16	3 kHz Dev.	95%	- 85	-36.5
			X-16A, 16B	6, 9 kHz Dev.	95%	- 85	-41
C.28	TMR-5	FM_D/AM Adj. (IF)	8-6	kHz Dev.	95%	-117*	-43
C.29	960		X-4B	1.9 kHz Dev.	95%	- 94*	-39.5
C.31	TR-711		X-9	3 kHz Dev.	95%	-125*	-32.5
C.27	TMR-5		5 (4) →	~40 kHz Dev.	30%	-130*	-47.5
C.30	960		X-5	1.25 kHz Dev.	95%	-110*	-42.5
C.30	960		X-6	1.25 kHz Dev.	95%	-120*	-35.0
C.22	TR-711	FM_D/AM Co. (RF)	X-14	3 kHz Dev.	95%	-101	+ 7
			X-14A	6 kHz Dev.	95%	-101	+ 4
			X-14B	9 kHz Dev.	95%	-101	+ 2
C.33			X-15	3 kHz Dev.	95%	- 85	+ 8
			X-15A	6 kHz Dev.	95%	- 85	+ 3
			X-15B	9 kHz Dev.	95%	- 85	+ 1
C.21	TR-711	FM_D/AM Co. (IF)	X-11	3 kHz Dev.	95%	-108*	+ 1
			X-11A	6 kHz Dev.	95%	-108*	+ 2
			X-11B	9 kHz Dev.	95%	-108*	+ 2
C.21	TR-711		X-12A	6 kHz Dev.	95%	-125*	+ 6.5
			X-12B	9 kHz Dev.	95%	-125*	+ 3
C.20	TMR-5		6 (4) →	~40 kHz Dev.	30%	- 80*	- 3

Notes: (1) (*) RF equivalent carrier level determined from RF-IF AGC Characteristic Voltage Curves.
(2) Based on a grade of service where SCI ≥ 0.4.
(3) All adjacent channel tests made with 25 kHz separation.
(4) These modulation levels are discussed in Appendix C.

(1) (*) RF equivalent carrier level determined from RF-IF AGC Characteristic Voltage Curves.
(2) All adjacent channel tests made with 25 kHz separation.
(3) These modulation levels are discussed in appendix C.

Table 4. Measured desired to undesired signal ratios required for speech communication indices equal to or greater than 0.4 and 0.85.

Figure No	Test Configuration[2]	Carrier Frequencies and Modulation Technique						IF Filter Bandwidth (kHz)	Required D/U[3] dB	
		Desired Freq. (MHz)	Modulation	Undesired Freq (MHz)	Modulation	Undesired Freq (MHz)	Modulation		SCI= .4	SCI= .85
C.4	FM_9/FM Adj.	135.000	FM	134.975	FM			20	-45	-43
		135.000	FM	134.975	FM			10	-54	-53
C.4	FM_9/FM Co.	135.000	FM	135.000	FM			20	+3	17
		135.000	FM	135.000	FM			10	0	+19
C.5	FM_9/FM/AM Adj.	135.000	FM	134.975	FM	134.950	AM	20	-39	-35
C.6	FM_9/AM/FM Adj.	135.000	FM	134.975	AM	134.950	FM	20	-38	-35
C.7	FM/FM_9/AM Adj.	135.000	FM	134.975	AM	135.025	FM	20	-43	-40
C.8	FM_9/AM Adj.	135.000	FM	134.975	AM			20	-41	-39
		135.000	FM	134.975	AM			10	-54	-40
C.8	FM_9/AM Co.	135.000	FM	135.000	AM			20	+1	+23
		135.000	FM	135.000	AM			10	11	+28
C.9	FM_9/AM Adj.	135.000	FM	135.025	AM			20	-63	-40
		135.000	FM	135.025	AM			10	-63	-51
C.10	AM/FM_9/AM Adj.	135.000	FM	134.975	AM	135.025	AM	20	-40	-38
		135.000	FM	134.975	AM	135.025	AM	10	-59	-50
C.11	AM_9/FM Adj.	135.000	AM	134.975	FM			20	-41	-34
		135.000	AM	134.975	FM			10	-55	-44
C.12	FM/AM_9/AM Adj.	135.000	AM	134.975	FM	135.025	AM	20	-34	-17
		135.000	AM	134.975	FM	135.025	AM	10	-53	-33
C.13	FM/AM_9/FM Adj.	135.000	AM	134.975	FM	135.025	FM	20	-28	-10
		135.000	AM	134.975	FM	135.025	FM	10	-43	3
C.14	AM_9/FM/FM Adj.	135.000	AM	134.975	FM	134.950	FM	20	-22	-11
		135.000	AM	134.975	FM	134.950	FM	10	-41	-20
		135.000	AM	134.975	FM			20	-35	-25
		135.000	AM	134.975	FM			10	-53	-35
		135.000	AM			134.950	FM	20		-54
		135.000	AM			134.950	FM	10		-54
C.15	AM_9/FM Adj.	135.000	AM	135.025	FM			20	-3	+40
		135.000	AM	135.025	FM			10	-59	

Notes: 1) Amplitude modulation = 90%, frequency modulation = 5 KHz peak deviation.
2) All tests were made at the VHF r-f frequency reported, on the type TR-711 receiver.
3) Desired carrier power level was -87 dBm except for figure C.11, which was -77 dBm.

Amplitude modulation = 90%; frequency modulation = 5-kHz peak deviation.
All tests were made at the VHF r-f frequency reported, on the type TR-711 receiver.
Desired carrier power level was -87 dBm, except for figure C.11, which was -77 dBm.

chosen arbitrarily from figures 21 and 22 as that required to provide esentially 100% ATC message intelligibility for the experienced controller, and approximately 70% intelligibility of MRT words in each case. Table 4 also shows a tabulation of required D/U ratios based on SCI = 0.85, which has been suggested as a grade of service more representative of that required for the inexperienced system user.

Additional measurements were made at NAFEC (O'Brien and Busch. 1969) for configurations with channel separations of 50 kHz. These are summarized in table 5.

Modulation levels, desired signal levels, and other parameters were changed in the various tests shown in tables 3 and 4. When determining required D/U ratios at a particular SCI, variables such as these must be taken into consideration. That is, we should compare protection ratios from tests that were performed under similar conditions. Table 6 is a summary of all measurements, with those made under similar conditions grouped together. They include those made by NAFEC (O'Brien and Busch, 1969) and ITS (Hubbard and Glen, 1968), including additional tests reported in appendix C of this report. The table presents the required D/U for SCI = 0.4 and 0.85, as determined from the arithmetic means of the measured values, rounded

Table 5. Summary of required D/U (dB) for 50 kHz channel separation.

	10-kHz IF Bandwidth		20-kHz IF Bandwidth		30-kHz IF Bandwidth	
	SCI=.4	SCI=.85	SCI=.4	SCI=.85	SCI=.4	SCI=.85
AM_D / AM	-62	-51	-63	-53	-61	-51
AM_D / FM	-64	-56	-65	-60	-60	-54
FM_D / AM	-60	-45	-64	-55	-50	-42
FM_D / FM	-64	-48	-65	-59	-52	-47

off to the nearest dB (except where the value is less than one). The standard deviation was not computed since the small number of samples tends to make it meaningless. Based on the mean D/U, the time available for specified service and the number of interfering facilities (n) that can be tolerated at a satellite terminal in the conventional AM network can be determined from procedures given in appendix A (fig. A.5).

In each test configuration in tables 4 and 5, the subscript D is used to indicate the desired carrier. For example, AM/FM_D/AM indicates the FM desired signal and two AM adjacent-channel interfering signals. Details can be determined from the tables.

The cochannel tests involving AM desired signals (AM_D) are based on a small number of samples to determine the mean required D/U. However, for FM desired (FM_D) there are more samples and, as a result, more faith can be placed in the mean required D/U. In either case, the required ratios appear reasonable, and perhaps conservative, as the average has been weighted by the high D/U values (28 and 23 dB values in table 6) in the FM_D tests for SCI = 0.85.

Table 6 shows that an AM_D signal requires a lower protection ratio than an FM_D for a cochannel case. When SCI = 0.4, the mean required D/U is ~5 dB higher for the FM_D than for the AM_D signal. As shown in figures B.30 and B.31 (app. B), there is a higher level of potential interfering power in the 95% amplitude-modulated signal than in the FM carrier with 5-kHz deviation, which could explain the greater degree of interference to the FM_D signal.

The greater number of measurements used to determine the mean required D/U for adjacent channels lends more confidence to the results than for the cochannel cases. The mean required D/U's in these tests appear reasonable when compared with results of similar test

Table 6. Summary of all measurements and mean required D/U ratios (20-kHz IF bandwidth).

Test Configuration	SCI = 0.4		SCI = 0.85	
Cochannel	Required D/U (dB)	Mean D/U (dB)	Required D/U (dB)	Mean D/U (dB)
AM_o / AM	+1, 0*		+10*	
AM_o / FM	+1, -2*		+10*	
FM_o / AM	+1, +2, +3, +4, +10*	+5	+23, +14*	+19
FM_o / FM	+3, +5, +9*	+5	+28, +17, +14*	+20
25 KHz Channel Separation				
AM_o / AM	-48, -50*	-49	-47*	-47*
AM_o / FM	-53, -35, -41, -43, -35*	-41	-25, -30, -32, -25*	-33
			-39, -43, -40	
FM_o / AM	-41, -41, -41, -43, -38*	-41	-39, 40, -31*	-36
FM_o / FM	-45, -38*	-42	-43, -31*	-37
Two Interfering Signals				
FM/ AM_o/ FM	-28	-28	-16	-15
FM/ AM_o/ AM	-34		-17	
AM_o/ FM/ FM	-22		-11	
AM/ FM_o/ AM	-40	-40	-38	-37
FM/ FM_o/ AM	-43		-39	
FM_o/ FM/ AM	-39		-35	
FM_o/ AM/ FM	-38		-35	

Notes: (1) *NAFEC measurements (O'Brien and Busch, 1969).
(2) Modulation levels: AM - 90 and 95%, FM - 5kHz and 6kHz peak deviation.
(3) All measurements were made with types TMR-5 and TR-711 receivers.

*NAFEC measurements (O'Brien and Busch, 1969).
Modulation levels: AM - 90 and 95%, FM - 5 kHz and 6 kHz peak deviation.
All measurements were made with types TMR-5 and TR-711 receivers.

configurations, in which different parameters, such as modulation index and carrier level (figs. C.31, C.32, and C.33, app. C), were used.

4.4 Multiple Interfering Signals

In this series of configurations (tables 4 and 6), the values reported for the FM_D tests agree very closely with those reported for the adjacent channel tests (FM_D) with one interfering source. For configurations with AM desired signals and two interfering sources, however, the results do not agree well with those of the simple adjacent channel tests and their validity is open to doubt. The problem of receiver front end saturation (desensitization) considered as contributing to these poor performance figures is discussed in appendix C, sec. C.1.

4.5 FM Capture Effect

Aircraft communication is affected by a large number of extraneous and multipath signals. Multipath fading is prominent at low receiving antenna elevation angles (Baghdady and Gutwein, 1965) and in air-to-air propagation (Ellington and Kirk, 1967). The FM detection of desired signals in the presence of cochannel or adjacent channel interference and fading can be improved by increasing the capture ability of the receiver.

The capture ability of an FM receiver is often judged on the basis of a performance index called the "capture ratio". The capture ratio of a conventional demodulator is defined "as the highest value of weaker-to-stronger signal amplitude ratio for which the FM demodulator output is essentially dependent (on the average) only

upon the frequency modulation of the stronger of the two input signals. Stated differently, the capture ratio is a measure of how closely the weaker signal could approach the stronger one in amplitude and still remain suppressible - it is a measure of the smallest amplitude difference that a given FM demodulator is able to resolve in suppressing the weaker signal under the prescribed interference conditions" (Baghdady and Gutwein, 1965).

For example, the capture ratio of the TR-711 receiver used by ITS in the SCIM tests reported in appendix C is 0.8 or 2 dB. High-fidelity receivers may have capture specifications of less than 1 dB (capture ratio greater than 0.9). Other commercial receivers may have a much poorer capture ratio specification.

Proper design of the limiter and discriminator will support a high capture ratio and limit multipath effects. The "widebanding" technique (Panter, 1965, p. 195) requires that (a) the limiter and discriminator accommodate amplitude and frequency variations as the level of the interfering signal approaches the desired signal and (b) the stages preceding the limiter have a flat frequency response over the frequency range occupied by the desired signal.

Other techniques to improve capture ratios have been proposed by Baghdady (1969). They are described as the dynamic trapping, the feedforward, the feedback, and cascading narrow-band limiter techniques. However, the performance based on the narrow-band limiter technique can be exceeded by either the feedback or feed-forward systems. Proper design and use of the feed-forward and dynamic-trapping systems can result in capture of a weaker desired signal.

5. ILLUSTRATIVE EXAMPLES

5.1 Time Availability and Service Probability

Semi-empirical methods of predicting the time variability, location-to-location variability, and prediction uncertainty of transmission loss for tropospheric communication circuits have been developed and incorporated in the concept of service probability (Barsis et al., 1962; Rice et al., 1967, ann. V; Longley and Rice, 1968, ann. 1). Although comprehensive discussion of these methods is beyond the scope of this report, a simple illustrative example (Gierhart and Johnson, 1969, sec. 5.1) involving service probability is given in this section.

Information given in section 3.1 can be used to calculate the effective distance parameter d_e used by Rice et al. (1967, ch. 10) to describe the time variability of hourly median transmission loss Y(q) in terms of the time variability q[11], where q is the fraction of time for which a given value of transmission loss is not exceeded. Figure 30 (Rice et al., 1967, fig. 10.20) shows Y(q) versus d_e for a frequency of 417 MHz.

Prediction errors or path-to-path variance, $\sigma_e^2(q)$, and service probability, Q, has been discussed by Rice et al. (1967, ann. V). The interpretation of service probability depends upon the criterion for service applicable to specific situations, e.g., satisfactory service may require that signal level, S/N or some other parameter exceed

---

[11] In this section q is used for time availability to be consistent with the notation used by Rice et al. (1967) and Gierhart and Johnson (1969), and q_T was used previously to be consistent with the notation used by Longley and Rice (1968), i.e., $q_T = q$ in this report.

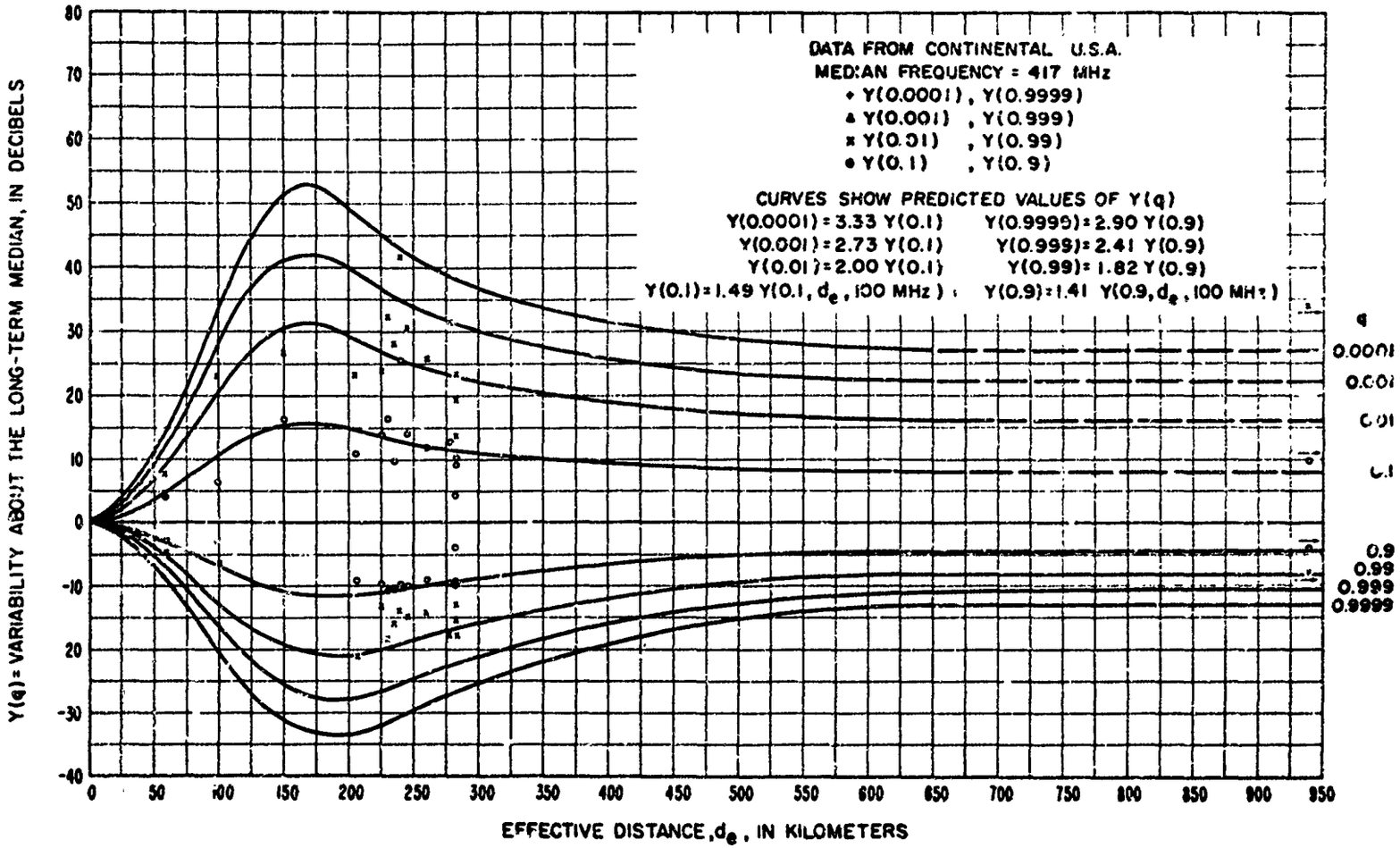

Figure 30. Long-term power fading for continental temperate climate, 250-to-450 MHz band with median frequency of 417 MHz (after Rice et al., 1967, fig. 10.20). Effective distance is discussed in sec. 3.1. $Y(q, d_e, 100\ MHz)$ as used by Rice et al. (1967) is identical with the $Y_o(q, d_e)$ used by Longley and Rice (1968) and in sec. 3.1.

a critical value for a specified time availability. A link designed so that the critical signal level is available when the transmission loss for the path corresponds to $L_{bs} + A_y$ (sec. 3) would have a time availability and service probability of 0.5, i.e., the probability that a particular link will provide a time availability of 0.5 is 0.5. Variation from this design may be interpreted as a change of time availability and/or service probability.

Where satisfactory service is defined in terms of critical hourly median signal level and the only uncertainty in the link performance estimate is associated with the transmission loss prediction, service probability is estimated from the path-to-path variance of Y(q). The extent in dB by which the actual received signal level would exceed the critical level when the basic transmission loss for the line is equal to the $L_{bs} + A_y$ level (q = 0.5 and Q = 0.5) can be defined as power margin. Levels of power margin required for various time availability and service probability values in a special case are shown in figure 31, e.g., a grade of service corresponding to q = 0.99 and Q = 0.5 would require a link designed with a power margin of about 20 dB. The frequency (417 MHz) and effective distance (175 km) used for this example were selected so that the time variability is close to the maximum obtainable for any combination or parameters when the long-term fading model is used.

Power margin levels ΔP shown in figure 31 were calculated from

$$\Delta P = -Y(q) + z_{so}\, \sigma_c(q) \text{ dB}, \qquad (52)$$

where Y(q) was obtained from figure 30, the standard normal deviate z_{so} is related to Q by figure 32 (Rice et al., 1967, fig. V.7), and $\sigma_c(q)$ was determined from Y(q) by (Rice et al., 1967, eq. (V.40)),

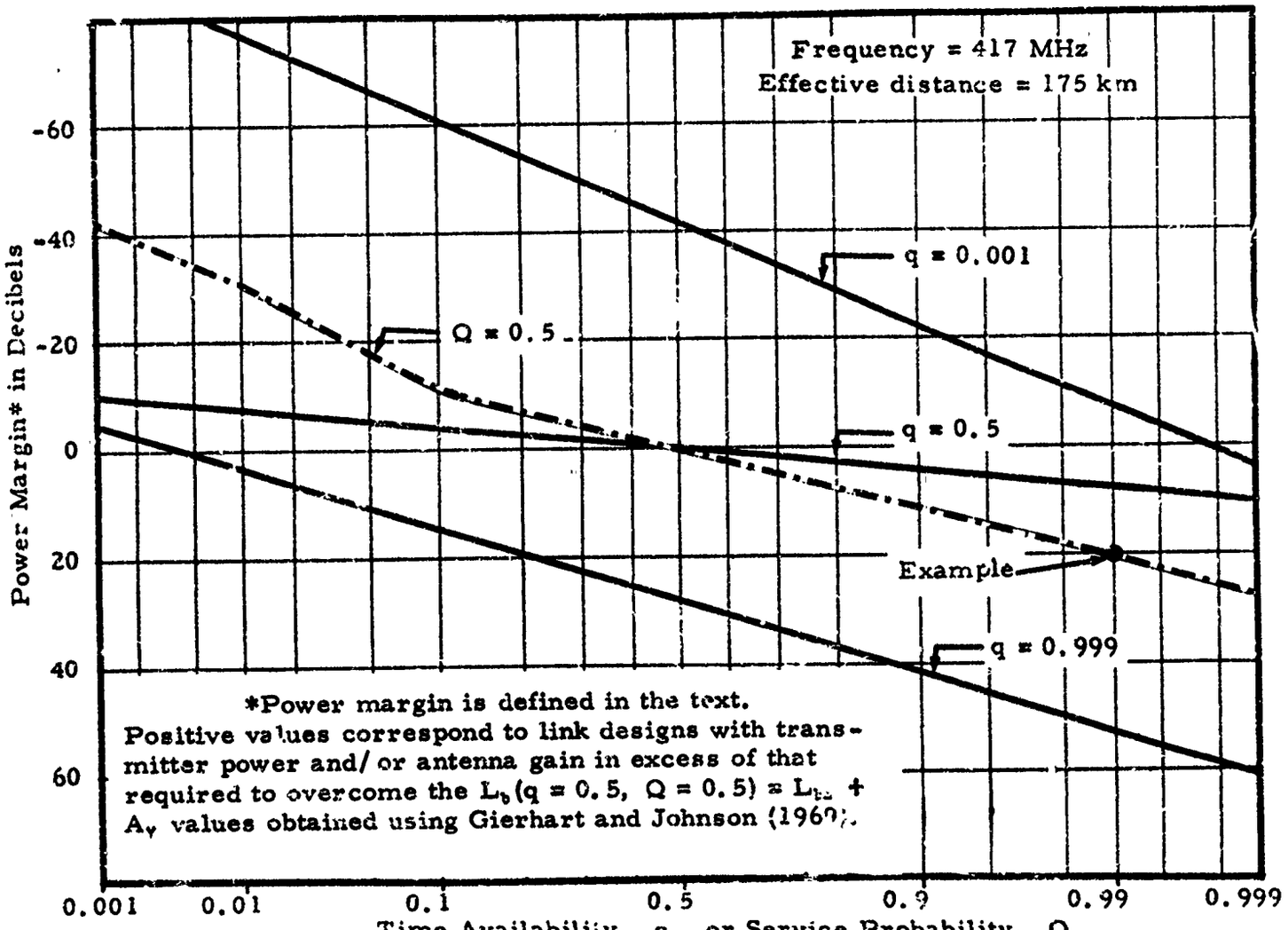

Figure 31. Power margin vs. q or Q.

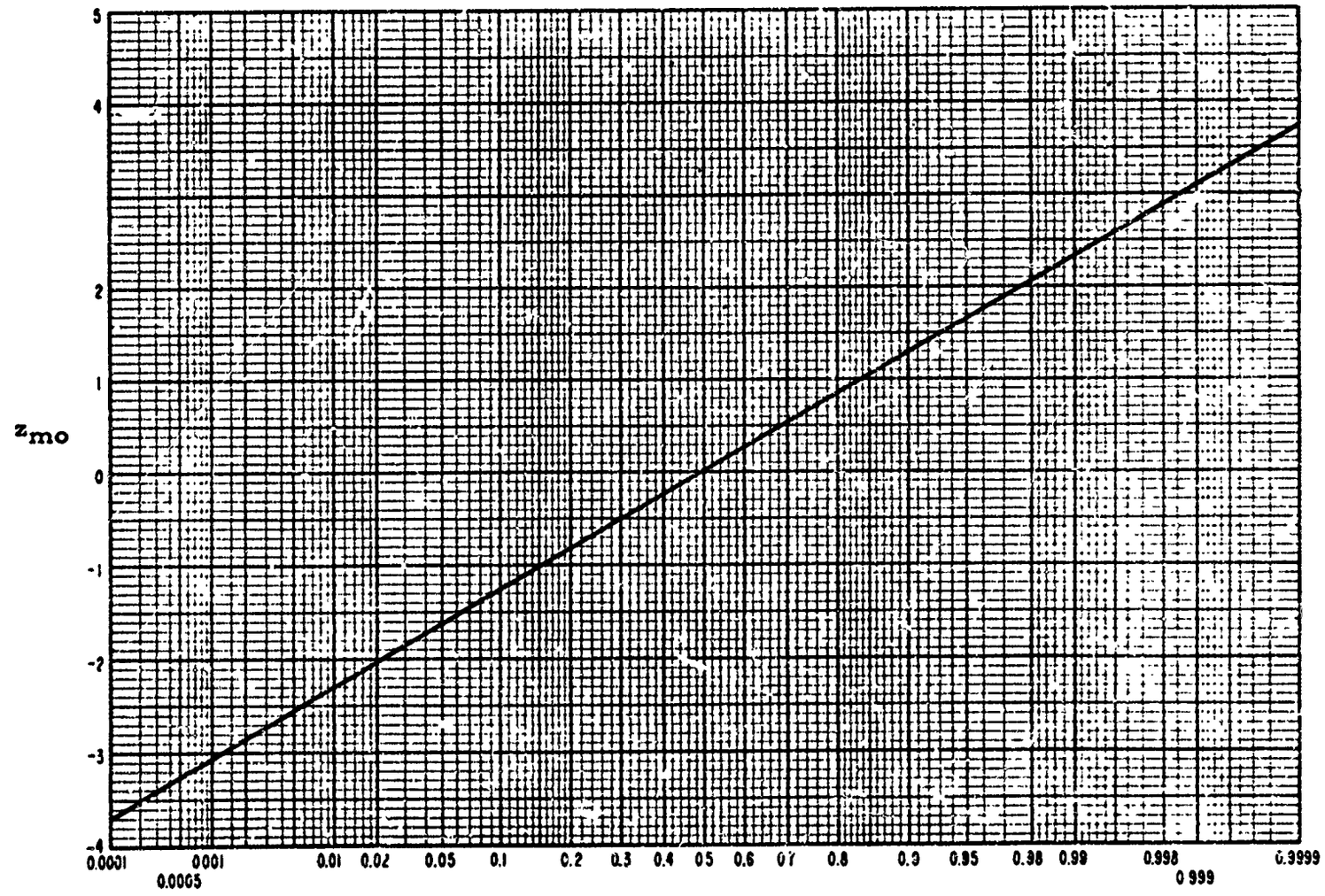

Figure 32. Standard normal deviate z_{mo} vs. service probability Q (after Rice et al., 1967, fig. V.7).

$$\sigma_o(q) = \sqrt{12.73 + 0.12Y^2(q)} \text{ dB.} \qquad (53)$$

For example, $Y(0.001) = 42$ dB for $d_o = 175$ km in figure 30 used with (53) gives $\sigma_o(0.001) = \sqrt{12.73 + 211.68} = 15$ dB. $Q = 0.999$ in figure 32 corresponds to $z_{so} = 3.1$, and these values used in (52) result in $\Delta P = -42 + (3.1)(15) = 4.5$ dB for $q = 0.001$ and $Q = 0.999$, which is as plotted in figure 31. When $Q = 0.5$, $z_{so} = 0$, so that $\Delta P = -Y(q)$ and values can be obtained directly from figure 30.

High service probability requirements can be used to minimize the probability of accepting an unsatisfactory system. Service probability is also useful as a weighting factor in cost-benefit studies. However, the probability of overdesign (excessive power, etc.) will increase with increasing Q, and the number of links that can be operated in a given area on a particular frequency band will decrease with increasing Q.

5.2 Service Restrictions Near an Undesired Station

Figure 33 shows a typical configuration of an aircraft (representing the receiving terminal), a desired transmitting facility, and an undesired transmitting facility. All three are aligned along a great-circle path, and for simplicity assumed to be above a smooth surface. In the example drawn, the aircraft is within the radio horizon of the desired facility, but beyond the radio horizon of the interfering station. The distances along the great-circle path from a point vertically below the aircraft to the desired and the undesired station are denoted by d_ϕ and d_ψ, respectively. The aircraft is at a height H_2 above the earth. The angle ξ between the horizon rays from the aircraft and the interfering station is an important parameter in the

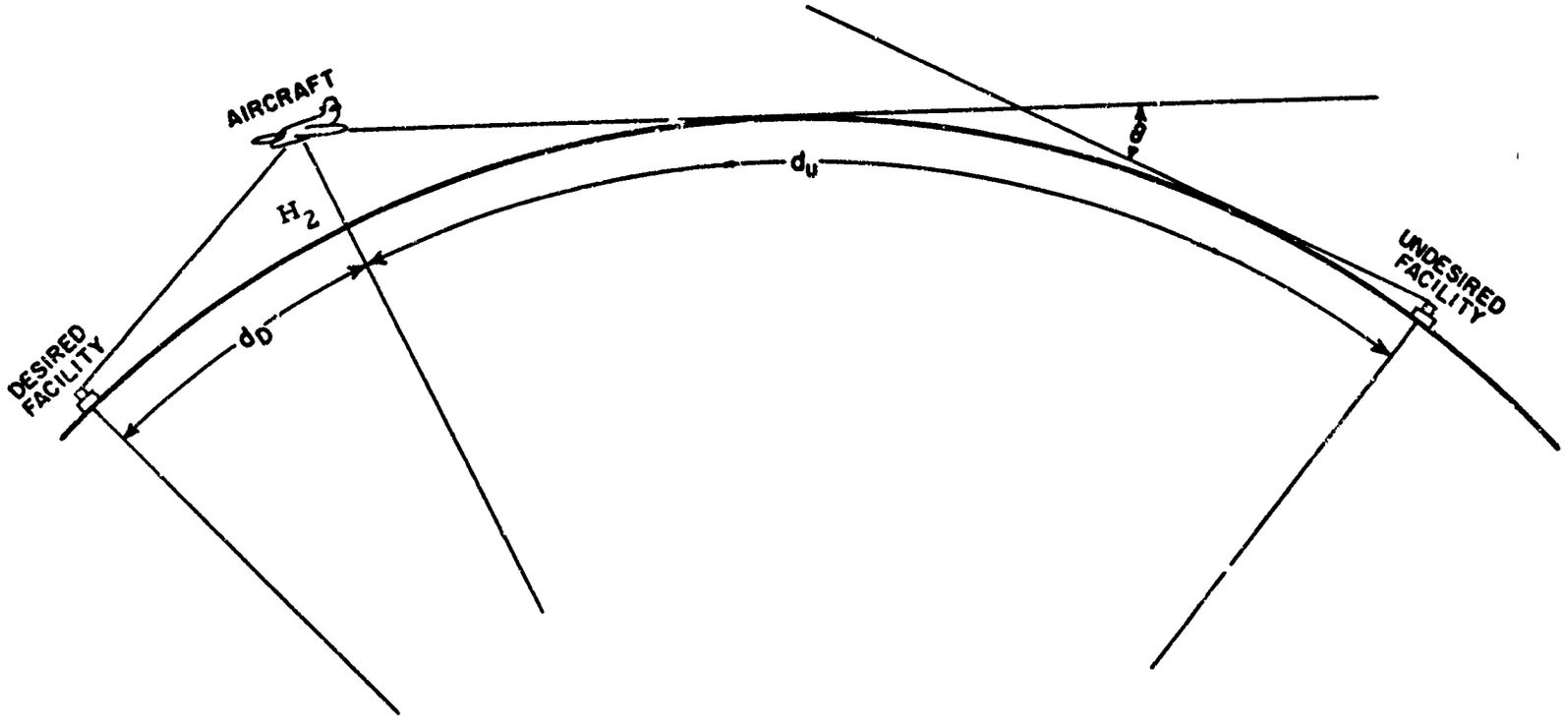

Figure 33. Relative positions of aircraft and facilities over a smooth earth.

calculation of transmission loss for beyond-the-horizon paths (Norton et al., 1955a). Figure 33 is oversimplified because radio rays can only be drawn as straight lines under special conditions, one of which is that H_2 must be less than 5000 ft (Rice et al., 1967, fig. 6.7).

A sample of the signal ratio curves developed by Gierhart and Johnson (1967, sec. 5.5) for the VHF omnirange (VOR)[12] is shown in figure 34. D/U in the neighborhood of an adjacent-channel undesired station are given for an aircraft altitude of 15,000 ft, e.g., the intersection of the D/U = -20 dB line at a distance of 34 nm with the curve for S = 40 nm means that at 15,000 ft the undesired signal exceeds the desired signal by 20 dB for 5% (100-95) of the time at a distance of 6 nm (40-34) from the undesired station. If, in an application to an adjacent-channel interference problem, the undesired signal causes trouble only when it is greater than the desired signal by 20 dB, service is available at least 95% of the time when the D/U curve for the station separation and aircraft altitude involved does not become more negative than -20 dB.

These curves do not show the effect of interference beyond the undesired station or at locations off the great-circle path connecting the stations, i.e., the distance d_0 shown on the abscissa scales locates the aircraft on the great-circle path between the desired and the undesired station. However, a method of approximating the locus of a constant interference ratio, $D/U(q_T)$, as a circle enclosing the

---

[12] The VOR is a navigation aid, and the signal ratio curves obtained for it are probably not applicable in a quantitative sense to communication systems. They are included here only to illustrate the application of a type of D/U presentation. Readers interested in a detailed description of the method used to obtain these curves are referred to Gierhart and Johnson (1967).

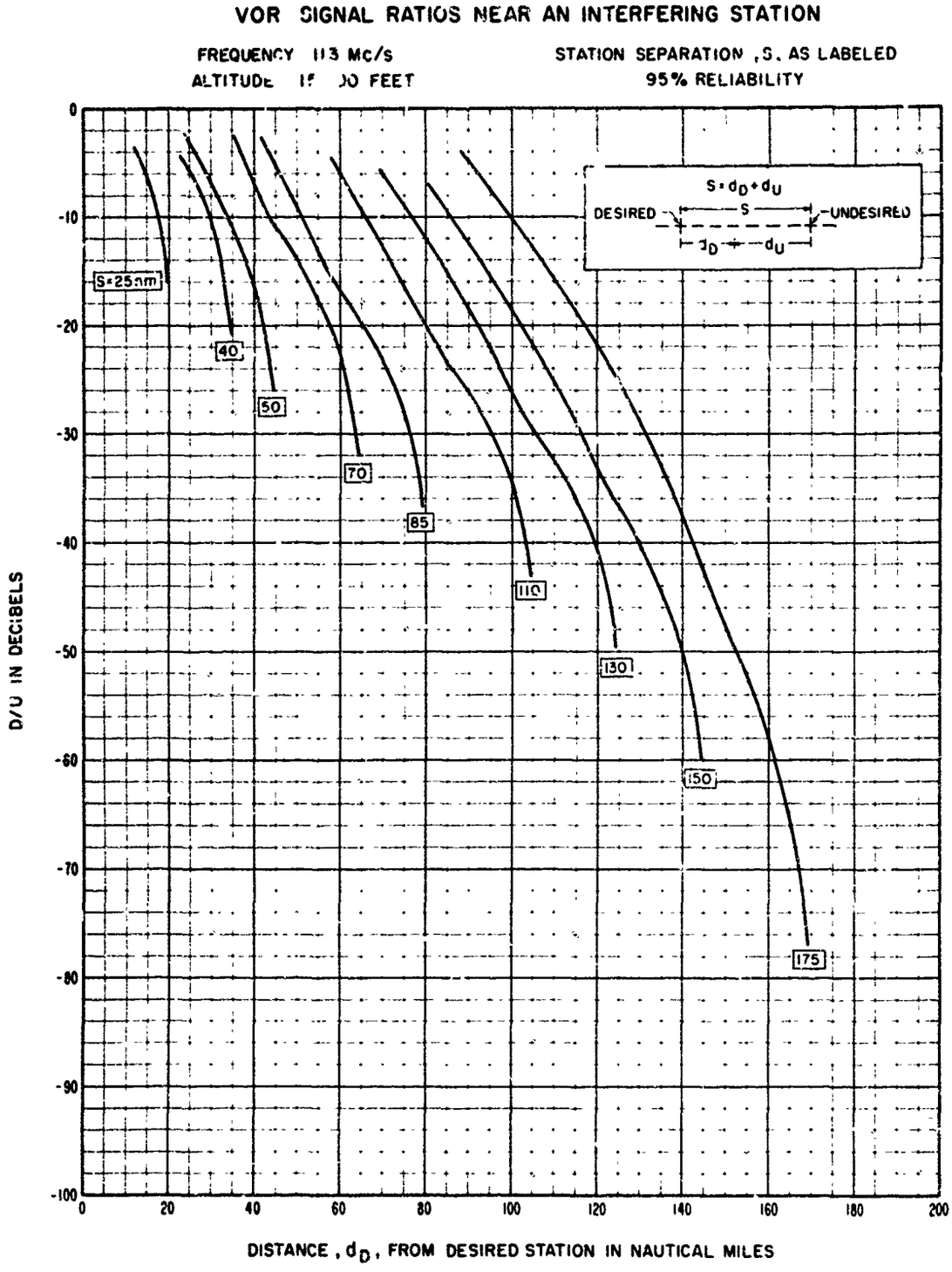

Figure 34. VOR signal ratios for 15,000 ft. (After Gierhart and Johnson, 1967, fig. 41.)

undesired station has been developed. For a given aircraft altitude, this circle is centered on an extension of the line connecting the ground stations concerned, but on the "far" side of the undesired station. The pertinent geometry is shown by a top and a side view in figure 35. Generally, service can be regarded as being unsatisfactory within this circle, even though some locations having satisfactory service may exist above the undesired station because of the vertical pattern of its antenna.

Two basic assumptions must be made as follows:

(a) The geometry represented by figure 35 is treated as plane geometry, i.e., the earth is assumed to be flat, and slant range projections, d_U and d_D, onto the horizontal plane are approximately equal to the actual ranges, r_U and r_D.

(b) The interference ratio, $D/U(q_T)$, is assumed to be proportional to the logarithm of the ratio of the ranges, r_D / r_U, i.e., $D/U(q_T) = M \log (r_D / r_U)$, where M is a constant.

Assumption (a) is reasonable if $d_D > d_U \geq$ (aircraft altitude/1600), where the distances, d_D and d_U, are in nautical miles and the aircraft altitude is in feet. Hence, the problem of finding the locus of r_D / r_U = constant can be solved through plane geometry. This locus is found to be a circle with radius R, whose center is set off from the path center by a distance C. The equations required to calculate C and R are given in figure 35.

As an example, consider the S = 150 nm curve in figure 34, (VOR; 15,000 ft). For $D/U(0.95) = -40$ dB, which may very well constitute the adjacent-channel interference threshold in a practical case, the distance, d_D = 130 nm, from the desired station (d_U = 20 nm)

$$B = d_D/d_U = (S - d_U) / d_U \cong r_D/r_U ,$$

$$C = \frac{S(B^2 + 1)}{2(B^2 - 1)} ,$$

$$R = \frac{SB}{B^2 - 1}$$

All distances are in identical units, e.g., nautical miles.

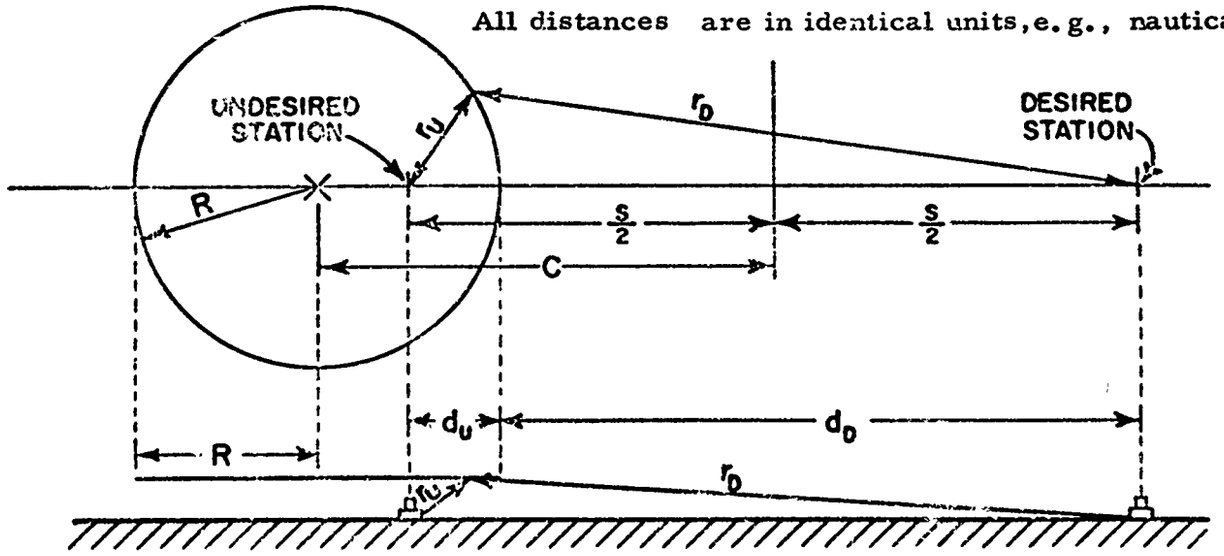

Figure 35. Locus of $D/U(q_T)$ = constant for an adjacent-channel undesired station. (After Gierhart and Johnson, 1967, fig. 64.)

is read from figure 34. B, C, and R are calculated from figure 35, i.e.,

$$B = \frac{130}{20} = 6.5,$$

$$C = 75(43/41) = 79 \text{ nm, and}$$

$$R = 975/41 = 24 \text{ nm.}$$

Thus, inside a circle with a radius of 24 nm, centered at a point 4 nm beyond the undesired station, VOR service at 15,000 ft aircraft altitude would be expected to be substandard.

This method is only approximate. The second assumption, (b), is violated by lobing in the transmission loss versus distance curve, which may occur at any constant altitude because of ground reflections or the ground antenna pattern. Assumption (b) is also violated by a change in the slope of the transmission loss versus distance curve which, as an example, occurs in the vicinity of the radio horizon. However, the use of the smallest d_0 corresponding to a particular station spacing and a particular signal ratio from Gierhart and Johnson (1967, sec. 5.5) avoids the ambiguity due to lobing. Furthermore, in most applications service is limited by noise rather than by interference if ranges beyond the radio horizon of the desired station are encountered (Vergara et al., 1962).

5.3 Satellite ATC System

The examples in this section illustrate the application of the methods mentioned in this report to a VHF synchronous satellite air traffic control system. Although most of the parameter values used

in these examples were recommended by Mr. Garth Kanen of the FAA in informal communications, they should be regarded only as reasonable estimates and not as "optimum" or officially sanctioned values. In fact, it is not certain that VHF frequencies will be used for satellite ATC systems (Haydon, 1970).

5.3.1 Interference at Satellite

Interference at a VHF satellite due to transmissions from a multitude of conventional ATC networks with amplitude modulation is analyzed in appendix A, some interference prediction examples are given in section A.2.5, and the frequency-sharing implications are summarized in section A.4. A network consists of a single ground-based facility and the aircraft it serves.

Even if the lowest required cochannel protection ratio for a 0.4 SCI given in table 6 (-2 dB) is used to read figure A.5, service free of cochannel interference would not even be available 15% of the time when interference from a single conventional network is encountered. Thus, a clear channel would probably be required for the satellite system.

The number of adjacent-channel conventional AM networks allowable can be estimated by using a -45-dB protection ratio (table 4, SCI = 0.4, AM/FM_0/AM) to read figure A.5. This indicates that more than 1000 undesired adjacent-channel conventional networks could be tolerated within line of sight of the satellite even if very high (>99.99%) time availability requirements were imposed. However, the allowed number of networks includes those for both adjacent channels.

5.3.2 Interference at Satellite Facility from Aircraft

Adjacent channel interference at a satellite facility communicating with a satellite in a 15F3 mode (emission bandwidth B_R = 15 kHz, FM, maximum modulating frequency f_m = 3 kHz) can be experienced from an aircraft communicating with a conventional ATC facility in a 6A3 mode (emission B_R = 6 kHz, AM, f_m = 3 kHz) when the separation between the two channel centers is 25 kHz. Required ground-facility separations are shown in figure 36 These curves were developed from the transmission loss curves given by Gierhart and Johnson (1967) with the A_y discussed in section 3 neglected. Time availability and service probability are both 0.5. The conditions assumed for calculating a single point in figure 36 and sample calculations are given below.

Conditions

Satellite (15F3) transmission (desired).

Satellite EIRP is assumed sufficient to produce an available power of -140 dBW at the antenna terminals of the satellite ground facility.

Frequency	= 125 MHz = ±25 kHz.
Airborne (6A3) transmitter (undesired).	
EIRP	= 14 dBW.
Distance from 6A3 facility (d_ϕ)	= 25 nm.
Altitude ($h_s = H_2$)	= 5,000 ft.
Frequency	= 125 MHz.
Ground-based receiving facility for satellite.	
Antenna gain toward 6A3 aircraft	= 10 dB.
Antenna height	= 50 ft.

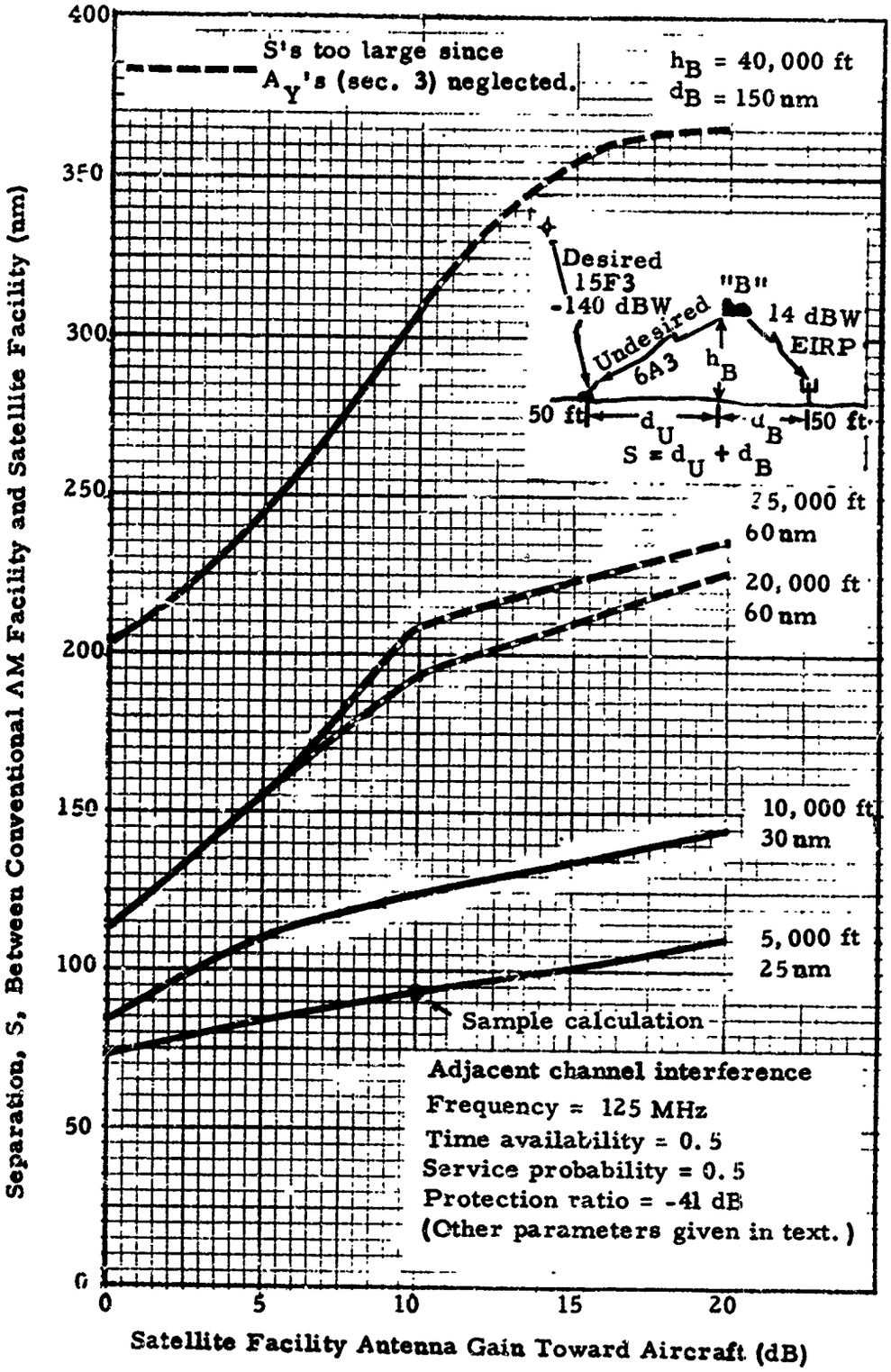

Figure 36. Interference at satellite ground station from aircraft using conventional AM facility.

IF bandwidth	= 20 kHz.
Channel spacing	= 25 kHz.
Required protection ratio from table 3 (AI ≃ SCI = 0.4)	= -41 dB.

Example of computation

(a) Compute the minimum allowable transmission loss for the aircraft to satellite facility (undesired) path when the facility antenna gain in the direction of the aircraft is assumed to be 10 dB.

-140 dBW	Desired signal level.
(-) -41 dB	Required protection ratio.
-99 dBW	Maximum allowable undesired signal level.
14 dBW	Undesired (6A3) aircraft EIRP.
10 dBi	Facility gain toward undesired aircraft.
(-)-99 dBW	Maximum allowable undesired signal level.
123 dB	Minimum allowable transmission loss.

(b) Compute the minimum station separation required to achieve a 123-dB minimum allowable transmission loss.

68 nm	15F3 facility to aircraft distance (fig. 6; H_1 = 50 ft; H_2 = 5,000 ft; L_{bm} = 123 dB).
25 nm	6A3 facility to aircraft distance d_0.
93 nm	Minimum station separation S.

5.3.3 Interference at Aircraft "A" Using Satellite from Aircraft "B"

An aircraft "B" using a conventional (6A3) facility can cause adjacent channel interference to the reception of a desired (15F3) satellite transmission at an aircraft "A". Required ground-facility separations for this case are shown in figure 37. These curves were

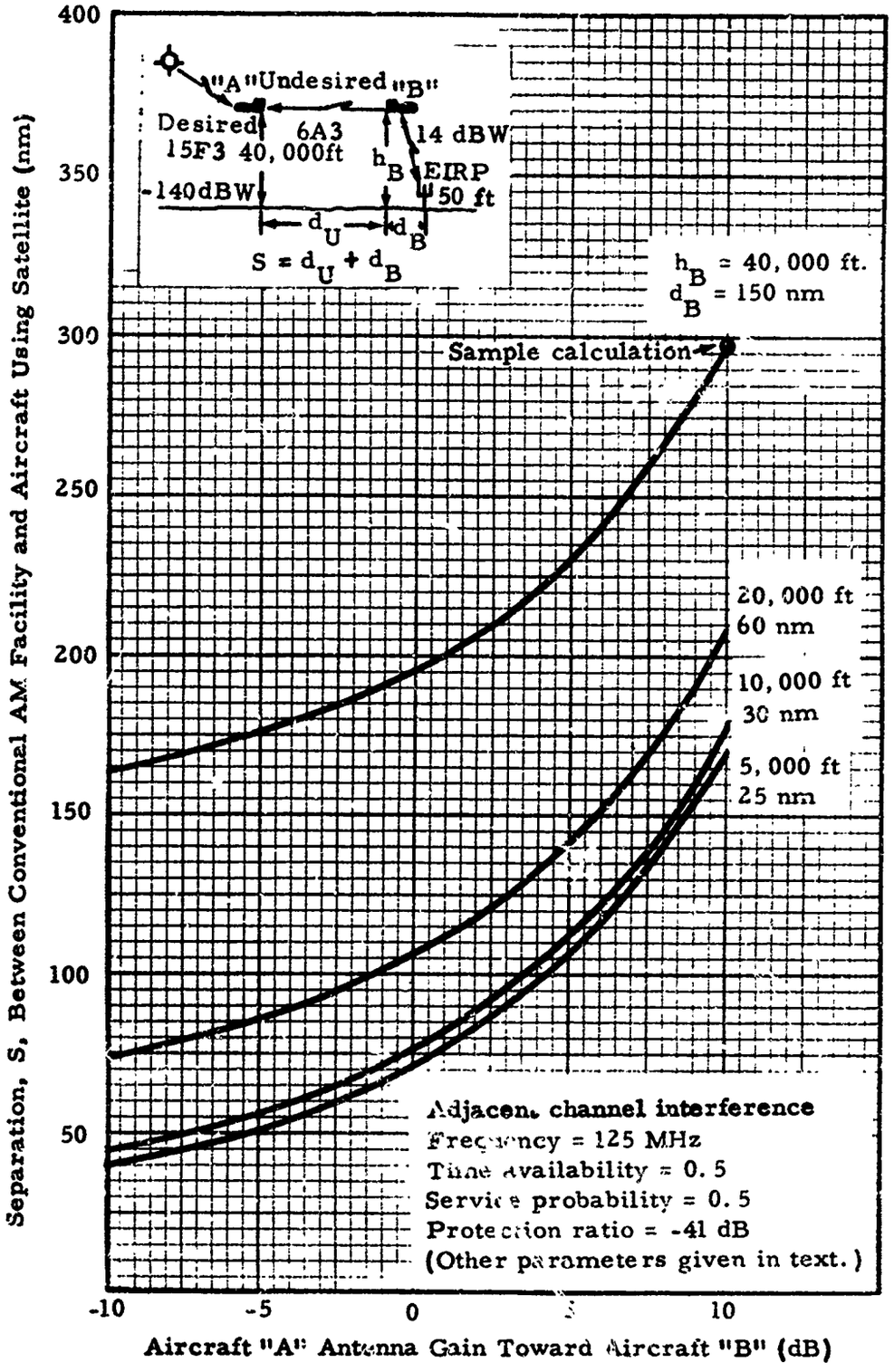

Figure 37. Interference at aircraft "A", using satellite, from aircraft "B", using conventional AM facility.

developed from the transmission loss curves given by Gierhart and Johnson (1967) with the A_γ discussed in section 3 neglected. Time availability and service probability are both 0.5. The conditions assumed for calculating a single point on figure 37 along with sample calculations are given below.

Conditions

Satellite (15F3) transmission (desired).

Satellite EIRP is assumed sufficient to produce an available power of -140 dBW at the terminal of aircraft "A" using the satellite.

Frequency	= 125 MHz = ±25 kHz.

Airborne (6A3) transmitter (undesired).

EIRP	= 14 dB.
Distance from 6A3 facility (d_s)	= 150 nm.
Altitude ($h_s = H_2$)	= 40,000 ft.
Frequency	= 125 MHz.

Airborne (15F3) receiving aircraft "A".

Antenna gain toward aircraft "B"	= 10 dB.
Altitude ($h_A = H_1$)	= 40,000 ft.
IF bandwidth	= 20 kHz.
Channel spacing	
Required protection ratio from table 3 (AI ≃ SCI = 0.4)	= -41 dB.

Example of computation

(a) Compute the minimum allowable transmission loss (123 dB) for the "B"-to-"A" (undesired) path as in section 5.3.2.

(b) Compute the minimum station separation required to achieve a 123 dB minimum allowable transmission loss.

148 nm	"B"-to-"A" path distance (fig. 38; H_1 = 40,000 ft; H_2 = 40,000 ft; L_{bm} = 123 dB).
150 nm	6A3 facility to "B" distance d_B.
298 nm	

5.3.4 Interference at Aircraft Not Using Satellite

5.3.4.1 Interference From Satellite. Interference to conventional AM networks from satellite transmission is discussed in section A.3. Figure A.7 shows the maximum service range reduction required to overcome interference versus normal facility service range for several required protection ratios. It is apparent that for the conditions assumed to develop figure A.7, the protection ratios listed in table 3 for cochannel and adjacent-channel operations would result in negligible service range reductions.

5.3.4.2 Interference From Satellite Ground Station. Adjacent channel FM transmissions from a satellite ground facility using 15F3 can cause interference to a conventional AM network using 6A3. It is assumed that adequate protection for the conventional facility from these transmissions is achieved if the satellite ground station is sufficiently separated from the aircraft using 6A3 when conditions are such that maximum undesired and minimum desired signal levels are available at the aircraft. These conditions are taken as the highest allowable aircraft altitude, minimum allowable satellite facility-to-aircraft distance, maximum allowable aircraft-to-desired AM facility distance, and the maximum applicable value of path antenna gain for the undesired signal path. Required ground-facility separations are shown in figure 39. These curves were developed from the transmission loss curves given by Gierhart and Johnson (1969) with the A_γ discussed in section 3

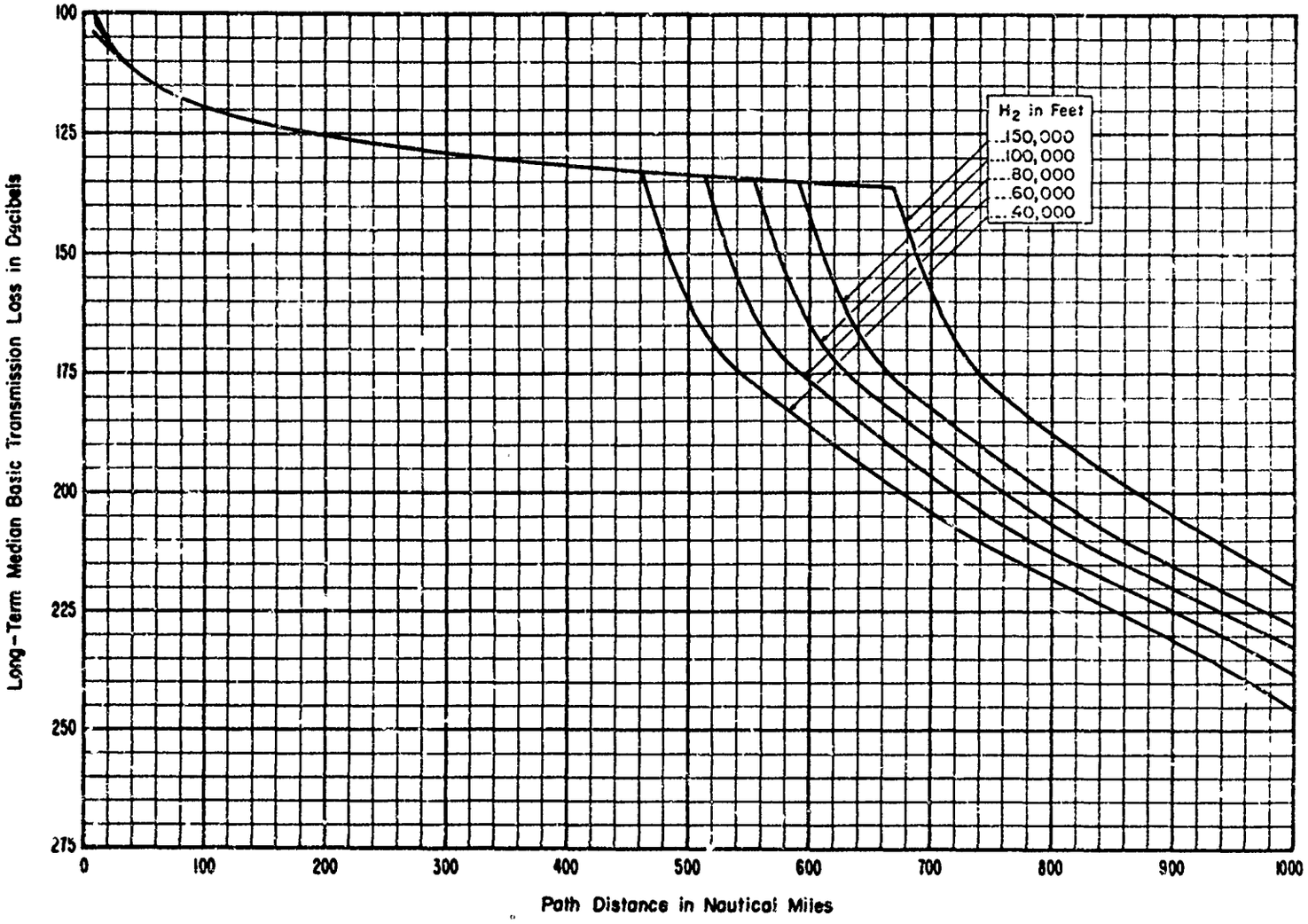

Figure 38. Basic transmission loss vs. distance; f = 125 MHz, H_1 = 10,000 ft. (After Gierhart and Johnson, 1969, fig. 13.)

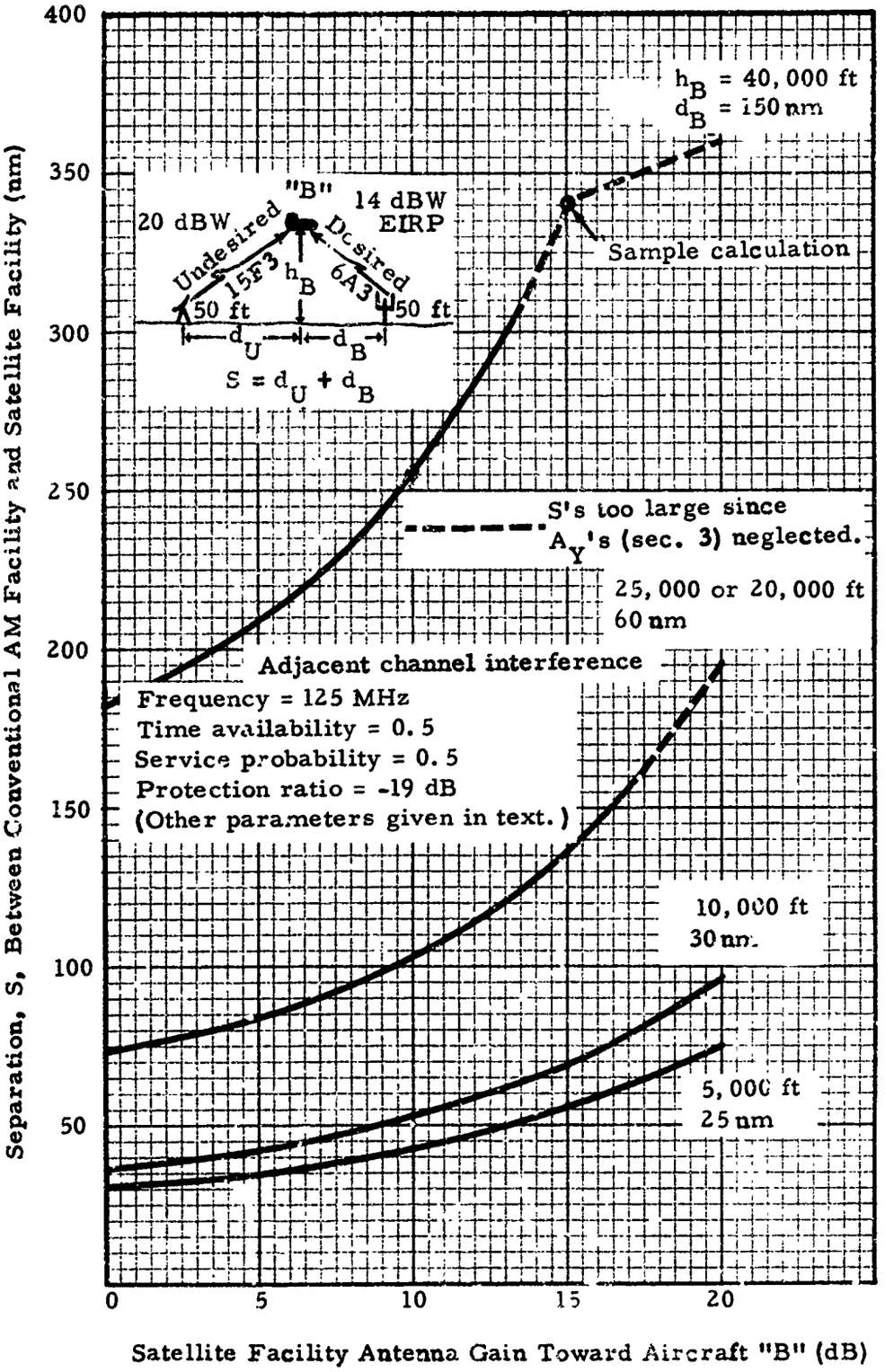

Figure 39. Interference from satellite facility at aircraft "B" using conventional AM facility.

neglected. Time availability and service probability are both 0.5. The conditions assumed for calculating a single point on figure 39 along with sample calculations are given below.

Conditions

Conventional (6A3) ground facility (desired).

EIRP	= 14 dBW.
Antenna height (H_1)	= 50 ft.
Frequency	= 125 MHz.

Satellite (15F3) ground station (undesired).

Radiated power (power into lossless antenna)	= 20 dBW.
Antenna gain toward aircraft	= 15 dB.
Height of transmitting antenna (H_1)	= 50 ft.
Frequency	= 125 MHz = ±25 kHz.

Airborne receiving terminal.

Altitude (h_8)	= 40,000 ft.
Distance from desired station (d_8)	= 150 nm.
Antenna gain	= 0 dB.
IF bandwidth	= 30 kHz.
Channel spacing	= 25 kHz.
Articulation index	= 0.4.
Required protection ratio from figure 40 (O' Brien and Busch, 1969, fig. 16)	= -19 dB.

Example of computation

(a) Compute desired signal level at terminals of aircraft antenna

14 dBW	EIRP.
(-)123 dB	Transmission loss (fig. 6, 150 nm, 40,000 ft).
0 dB	Aircraft antenna gain.
- 109 dBW	Desired signal level.

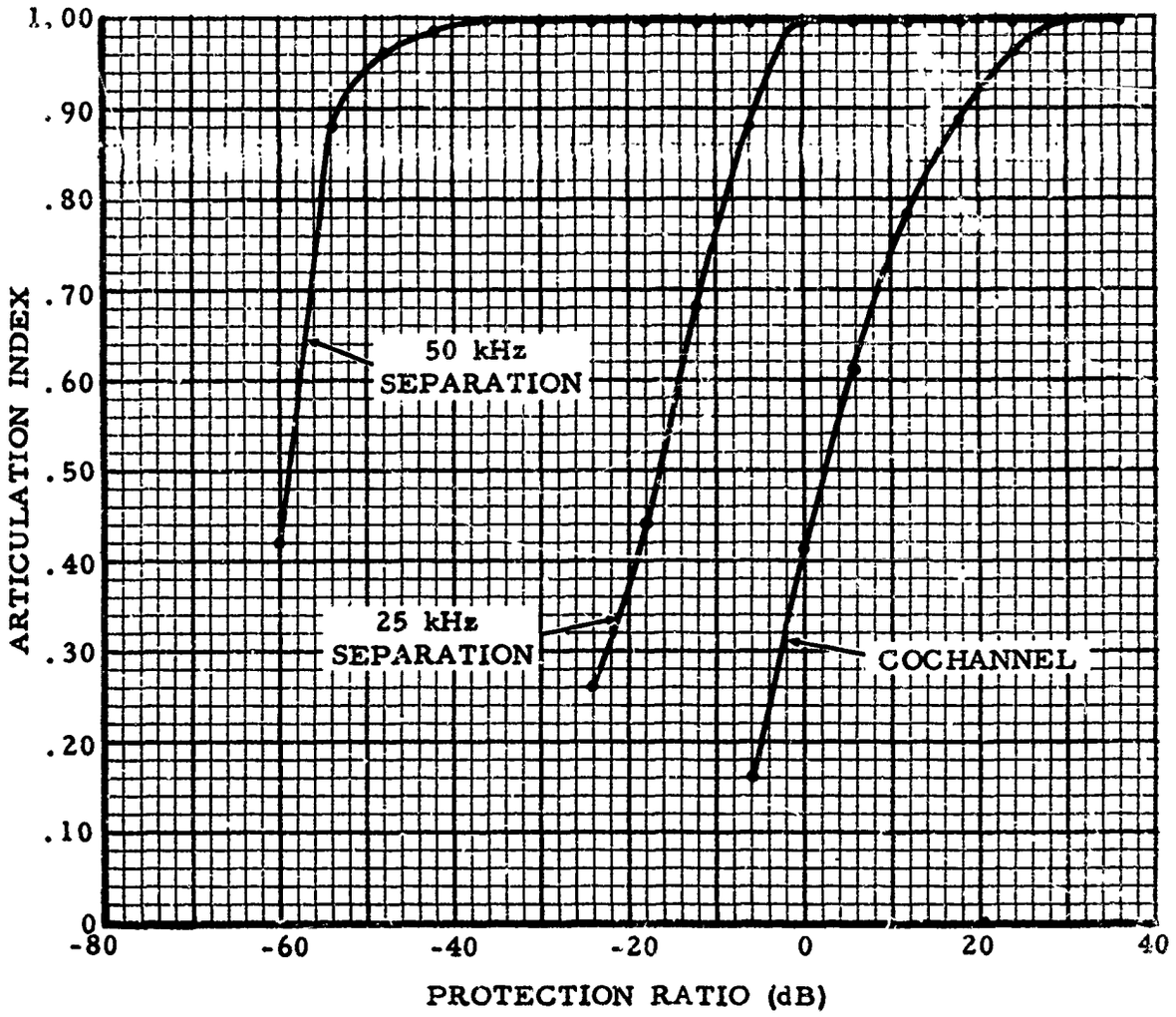

Figure 40. Values of articulation index vs. protection ratio, AM desired/ FM undesired - 30 kHz bandwidth. (After O'Brien and Busch, 1969, fig. 16).

(b) Compute the minimum allowable transmission loss for the satellite facility-to-aircraft (undesired) path when the gain of the facility antenna in the direction of the aircraft is assumed to be 10 dB.

-109 dBW	Desired signal level.
(-) - 19 dB	Required protection ratio.
- 90 dBW	Maximum allowable undesired signal level.
20 dBW	Undesired radiated power.
15 dB	Applicable gain, undesired station.
0 dB	Aircraft antenna gain.
(-) -90 dBW	Maximum allowable undesired signal level.
125 dB	Minimum allowable transmission loss.

(c) Compute the minimum station separation required to achieve a 120-dB minimum allowable transmission loss.

190 nm	Undesired distance (fig. 6; 40,000 ft; 120 dB).
150 nm	Desired distance (initial conditions).
340 nm	Minimum station separation.

5.3.4.3 Interference From Aircraft Using Satellite. Adjacent channel transmissions from an aircraft using 15F3 intended for a satellite relay can cause interference to a conventional facility using 6A3. It is assumed that adequate protection for the conventional facility from these transmissions is achieved if the aircraft "A" transmitting 15F3 is sufficiently separated from the aircraft "B" using 6A3 when conditions are such that maximum undesired and minimum desired signal levels are available at aircraft "B". These conditions are taken as highest allowable distance from aircraft "B" to its desired ground station, and the maximum applicable value of path antenna gain for the aircraft "A"-to-aircraft "B" path. Required ground station separations are shown in figure 41.

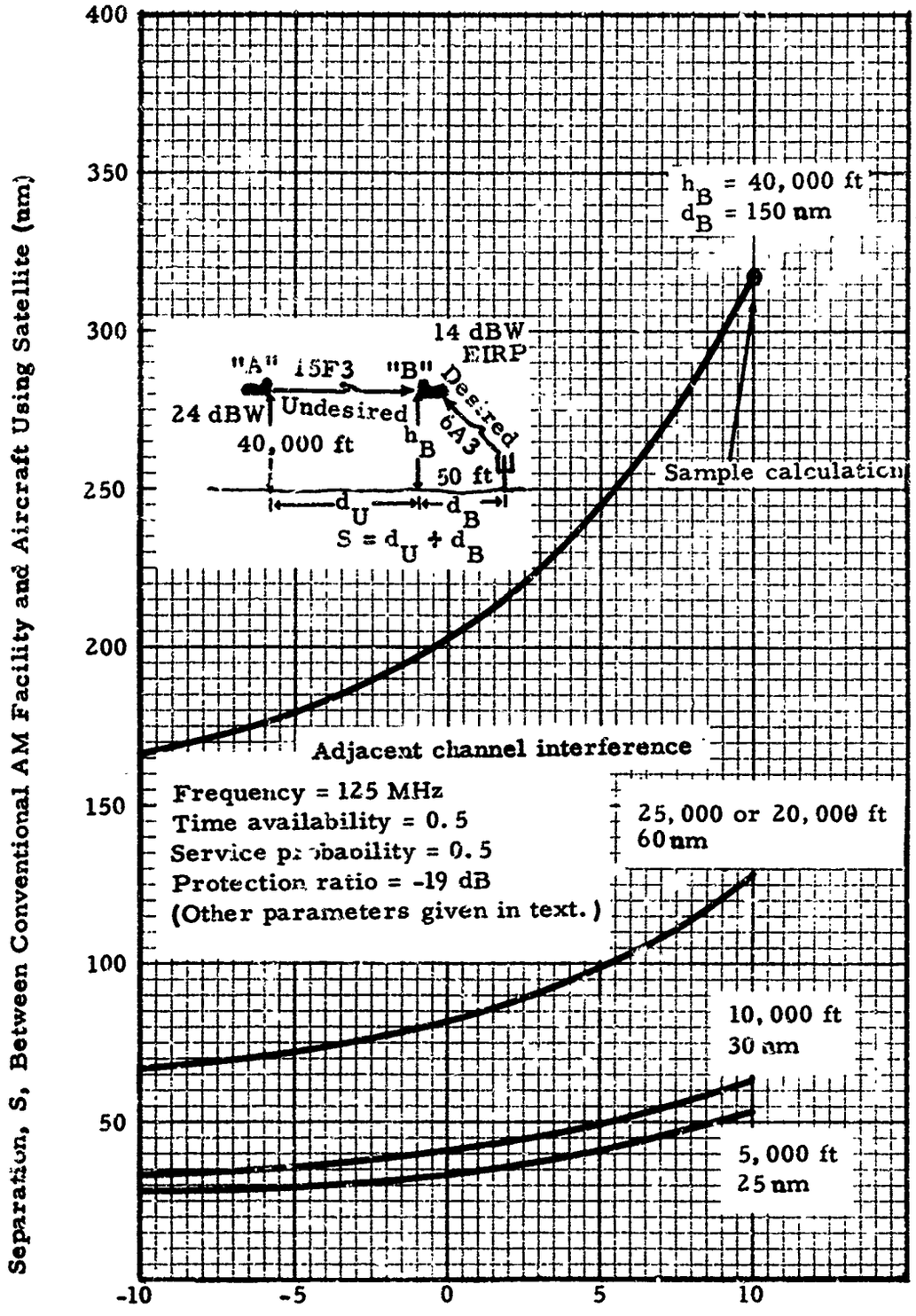

Figure 41. Interference from satellite facility at aircraft using conventional AM facility.

Conditions

Conventional (6A3) facility (desired).

Same as in section 5.3.4.2.

Aircraft "A" (15F3, undesired).

Radiated power	= 24 dBW.
Antenna gain toward "B"	= 10 dB.
Altitude (h_A)	= 40,000 ft.
Frequency	= 125 MHz = ±25 kHz.

Other parameters including those for the airborne receiving terminal, "B", are the same as those given in section 5.3.4.2.

Example of computation

(a) Compute the desired signal level at the terminals of aircraft "B" as in section 5.3.4.2.

(b) Compute the minimum allowable transmission for aircraft "A"-to-aircraft "B" (undesired) path when the gain of the aircraft "A" antenna in the direction of aircraft "B" is assumed to be 10 dB.

-90 dBW	Maximum allowable undesired signal level (calculated as in sec. 5.3.4.2).
24 dBW	Undesired radiated power.
10 dB	Aircraft "A" antenna gain.
0 dB	Aircraft "B" antenna gain
(-)-90 dBW	Maximum allowable undesired signal level.
124 dB	Minimum allowable transmission loss.

(c) Compute the station separation required to achieve a 124-dB minimum allowable transmission using figure 38 (Gierhart and Johnson, 1969, fig. 13).

168 nm Undesired distance (fig. 38; 40,000 ft; 124 dB).

150 nm Desired distance (initial conditions).

318 nm Minimum station separation.

Many of the points needed to draw the curves shown in figure 36, 37, 39, and 41 require d_U's for L_{bs}'s that cannot be accurately obtained from Gierhart and Johnson's (1969) atlas becuase of the short distances (or low L_{bs}'s) involved. However, in these cases an adequate estimate of d_U can be obtained by equating L_{bs} to the free-space basic transmission loss L_{bf}, i.e.,

$$L_{bs} = L_{bf} = 37.8 + 20 \log f + 20 \log d_U \quad \text{dB}, \qquad (54)$$

or

$$20 \log d_U = L_{bf} - 37.8 - 20 \log f = C_U \quad \text{dB}, \qquad (55)$$

and

$$d_U = 10^{C_U / 20} \text{ nm}, \qquad (56)$$

where f is frequency in MHz. For example, these equations yield a d_U = 166 nm for L_{bs} = 124 dB, which is nearly equal to the 168 value just obtained, i.e.,

$$C_U = 124 - 37.8 - 20 \log 125 = 86.2 - 41.9 = 44.3 \text{ dB},$$

and

$$d_U = 10^{44.3/20} = 10^{2.22} = 166 \text{ nm}.$$

The adjustment factor A_y discussed in section 3 was not used in developing these figures, but the range of parameters considered is such that the resulting station separations are correct or somewhat too large. This occurs because (1) A_y's for the desired transmissions are not significant for the conditions considered, (2) A_y's for the undesired transmission would cause the undesired signal levels to decrease if they were included, and (3) a decrease in undesired signal levels would result in smaller station separations.

5.4 System Hardware Engineering Examples

There are a number of practical constraints imposed by equipment limitations that must be considered in overall system planning. Each of these will have an impact on the system design, such as on frequency channel allocations and on electromagnetic compatibility problems. The two most important constraints as far as band-planning is concerned are the frequency tolerances for the system and the frequency stabilities that are maintained. A third important parameter to consider is the peak-power requirements and/or radiation produced in various modulation processes. These three engineering constraints are discussed in this section.

In planning the use of a band of frequencies allocated for a specific communication service, where system users are assigned contiguous channels, the frequency tolerance of the channel carrier becomes important. The channel bandwidth permitted must be sufficiently wide to accommodate the signal emission bandwidth, and the adjacent-channel separation must be adequate to prevent adverse interference to a desired channel. Frequency tolerances and stabilities of both the transmitter and the local oscillators in the receivers combine to increase both the required channel frequency separation and the required system bandwidth respectively. These effects will be noted in following examples.

Frequency tolerance is defined as the allowable frequency departure of the center frequency of any emission signal from the assigned carrier frequency. In general, allowable tolerances are established on a worldwide basis for various frequency bands and station categories by the International Telecommunication Union (ITU). In the United States, more restrictive requirements may be imposed by other regulatory agencies, such as the Federal

Communications Commission (FCC). For the convenience of the reader, the following table contains an abstract of tolerances specified by the ITU for several types of radio services in the frequency bands of interest in this report (ITT, 1969).

As an example, consider an aeronautical station assignment in the VHF band at 125 MHz. Table 7 specifies the transmitter tolerance as $\pm 50 \times 10^{-6}$ (.005%) or better. Thus, at 125 MHz, the carrier offset frequency of the transmitter can be

$$\pm f_d = 125 \times 10^6 \times 50 \times 10^{-6} = 6.25 \text{ kHz}.$$

An adjacent-channel assignment in the same service could have a tolerance of the same magnitude. Taking the extreme condition, assume that the displacements of two contiguous channels are of opposite signs so that the actual carrier frequencies are closer together than the specified channel separation by an amount

Table 7. ITU frequency tolerances.

Frequency Band	Type of Service	Tolerance (Parts per 10^6)
118 - 136 MHz	Fixed station > 50 W	20
	Aeronautical	50
	Aircraft	50
1540 - 1660 MHz	Fixed station > 100 W	100
	Land based	300
	Mobile	300
	Radio determination	500
5000 - 5250 MHz	Fixed station > 100 W	100
	Land based	300
	Mobile	300
	Radio determination	2000
15,400 - 15,700 MHz	Fixed station	500
	Radio determination	7500

$$2 f_d = 12.5 \text{ kHz}.$$

To fully protect the service in either channel from the adjacent channel, the minimum required channel spacing must be increased, i.e., an additional 12.5 kHz between the channels is required in this example. Because added frequency spacing for channel protection wastes spectrum space, spectrum use is enhanced whenever frequency tolerances can be made smaller. In the above example, for instance, if the nominal channel separation is to be 50 kHz, the additional separation above would account for 25% of the available band, leading to a loss of a possible 5 channels in every 20 assigned for use.

In some services, it is possible to alleviate the protection requirements if actual channel assignments can be made on a geographic basis. In other words, if an adjacent channel is assigned only in a geographic location remote from the service area of the desired channel, the added spacing between the channels is not necessary and the spectrum space is conserved. This type of channel assignment is generally possible in the ATC environment. Frequency tolerances as listed in table 7 are considerably greater in the higher frequency bands, and thus for the same emission service as considered in the VHF example above the protection requirements would waste more spectrum space. Geographic assignment of channels should be used, or the ITU tolerances significantly improved, in these bands.

Frequency instability is defined as the drift from the nominal frequency as a function of time. It is usually measured or specified as an rms value over a specific interval of time. For example, the frequency stability of a crystal or other highly stable oscillator is specified as short-term and long-term, such as the following:

Short-term stability: 8×10^{-10} averaged over 1 ms.

1.5×10^{-10} averaged over 10 ms.

Long-term stability: $< 5 \times 10^{-10}$ averaged over 24 hr.

The rms value of frequency drift of an oscillator does not convey the peak deviation unless the distribution of the drift is known. However, since the fluctuations in the short-term interval are generally quite rapid, the rms drift is indicative of performance. Long-term drifts are generally much smaller in rms value than the short-term and consequently are not as important in band-planning as the short-term drifts.

Oscillators applicable to mobile and/or aeronautical terminals are generally of the quartz-crystal type, stabilized for temperature drift through the use of controlled ovens. Much more stable oscillators, such as rubidium and atomic standards, may be considered for fixed and/or ground stations in the aeronautical service. The frequency instability of the transmitter and local oscillators require additional bandwidth in the system design. The worst case as far as band-planning is concerned is perhaps the drift between oscillators in airborne equipments, and thus the air/air channel is the most critical for determining the additional bandwidth required. Figure 42 illustrates the requirement. The solid spectral line at f_o in the RF range of the sketch represents the assigned carrier frequency for a particular channel. We assume in figure 42 that the transmitter frequency has drifted by a value of Δf_o below the assigned frequency in (a) and above this frequency in (b). The channel or transmission bandwidth B_c is illustrated by the rectangular spectral function around the actual carrier frequency f_o'. As a worst case, we also assume that the local-oscillator frequency in the receiver has drifted in the opposite direction from the transmitter drift. The results of

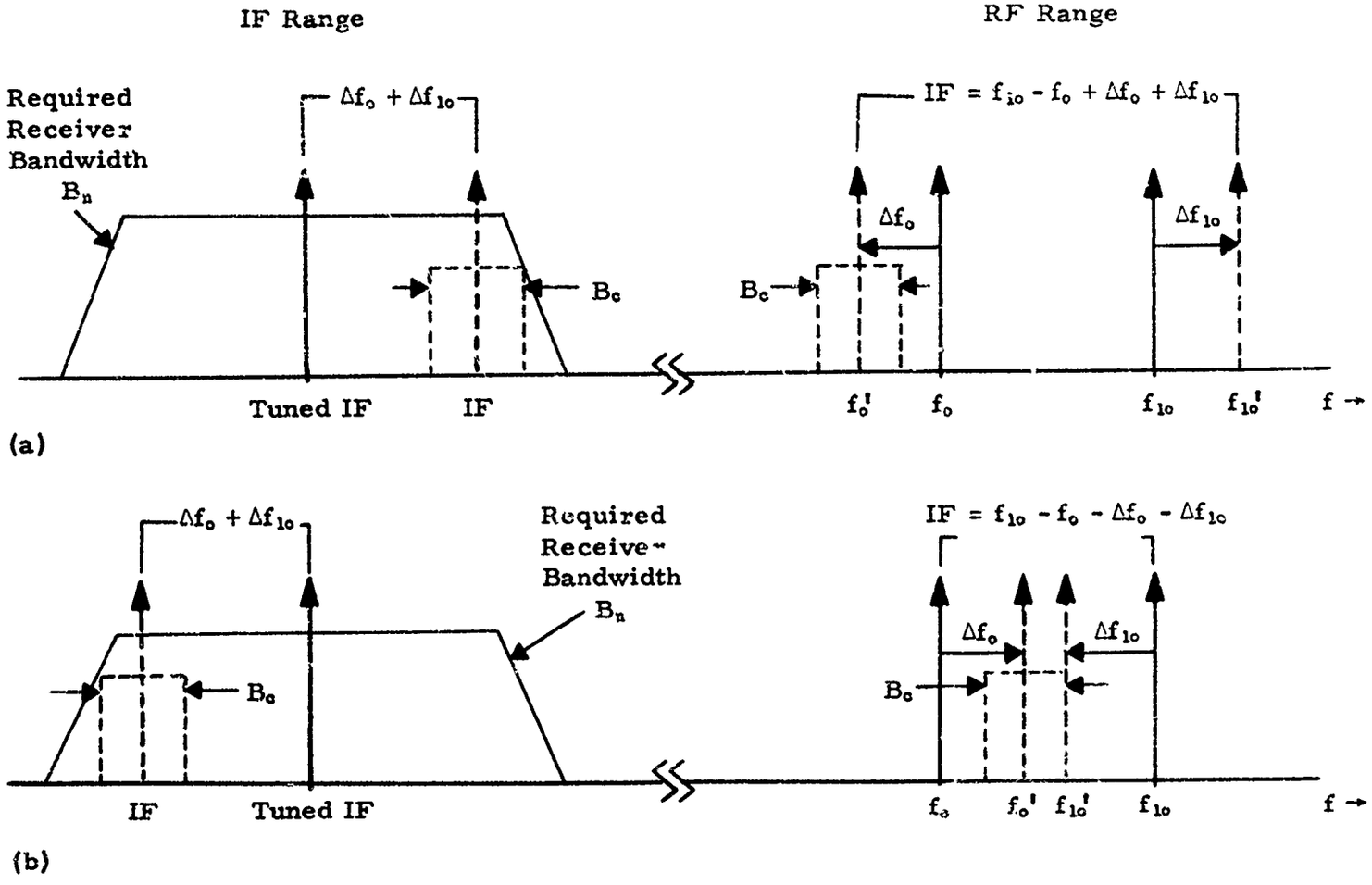

Figure 42. Receiver bandwidth required for equal and opposite drifts in transmitter and receiver local-oscillator frequencies.

these drifts at the IF of the receiver are illustrated on the left in figure 42. The actual IF is seen to move respectively both above and below the tuned IF by an amount

$$\Delta IF = \Delta f_o + \Delta f_{lo} , \tag{57}$$

which is the compound or total frequency drift. The actual operating IF is determined from the expressions given in figure 42 for each case. Note that the tuned IF remains fixed in spectral position, as this is the frequency at which the IF amplifier strip in a super-heterodyne type receiver is fix-tuned.

The additional receiver bandwidth required to accommodate the compound frequency drift has been exaggerated in figure 42 for illustrative purposes. However, this factor can be significant in comparison with the transmission bandwidth, depending upon the magnitude of the frequency drifts. The total increased IF bandwidth is

$$2\Delta IF = 2(|\Delta f_o| + |\Delta f_{lo}|) . \tag{58}$$

As seen in figure 42, if the receiver is to pass the transmission or message bandwidth B_c without distortion, the total IF bandwidth of the receiver must be at least twice as wide as the compound drift plus the transmission bandwidth, i.e.,

$$\begin{aligned} B_n &= 2(|\Delta f_o| + |\Delta f_{lo}|) + B_c \\ &= 2\Delta IF + B_c \end{aligned} \tag{59}$$

The increased IF bandwidth requirement of (58) (if we assume equal transmitter and local-oscillator drifts) is plotted in figure 43 for each of the four frequency bands of interest in this report. A single frequency within each band has been selected (near bandcenter) for illustrative purposes. The bandwidth increase is plotted versus frequency stability. A line for the emission bandwidths of two typical

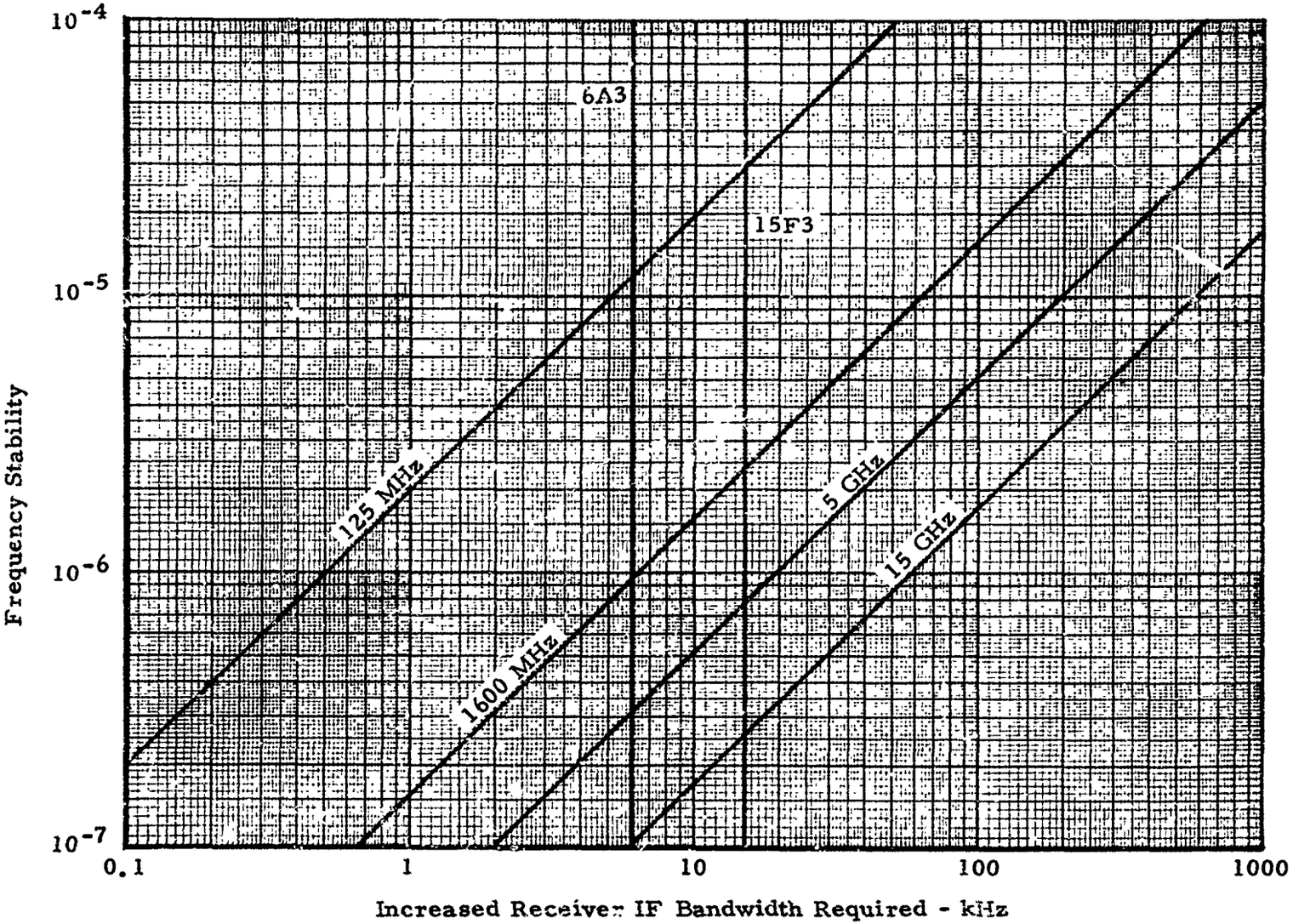

Figure 43. Increased receiver IF bandwidth required to accomodate the compound frequency drifts in the transmitter and local oscillator for various bands.

systems (6A3 and 15F3) (ITT, 1969) are plotted in the figure. The intersection of these lines with the curves represents the point at which the added bandwidths required to accomodate the frequency instabilities are equal to the emission bandwidths. In other words, at these points of intersection the receiver bandwidth must be doubled over the emission bandwidth requirement.

The effect of increasing the receiver bandwidth is to increase the overall system noise threshold (see sec. 3.3.2) at the receiver, and to increase its susceptability to other interfering signals. Thus for the points of intersection in figure 43, the system noise threshold would be increased by 3 dB. This can be considered a practical limit in system planning, and thus only the region to the left of the emission bandwidth lines in figure 43 would be considered practical for single-channel service configurations. Other emission lines may be added to this figure, or other threshold lines for more restrictive added bandwidth requirements may be considered by the reader. Note for example that the frequency stability for a 6A3 channel in the 15.5-GHz band must be better than ± 1 part in 10^7 to limit the added bandwidth requirement to the transmission bandwidth or less.

Using the above concepts, Frisbie et al. (1969) have computed the number of possible channel frequency assignments per MHz of band space as a function of frequency stability for several contiguous channel configurations. Their computations include an additional term for Doppler frequency shifts between a satellite terminal and a moving aircraft. For the two lower bands (VHF and C-band), however, the Doppler shift is less than 1 kHz at aircraft velocities below about 500 nm/hr. The results of some of these computations are presented in figure 44. The channel spacing factors used in the

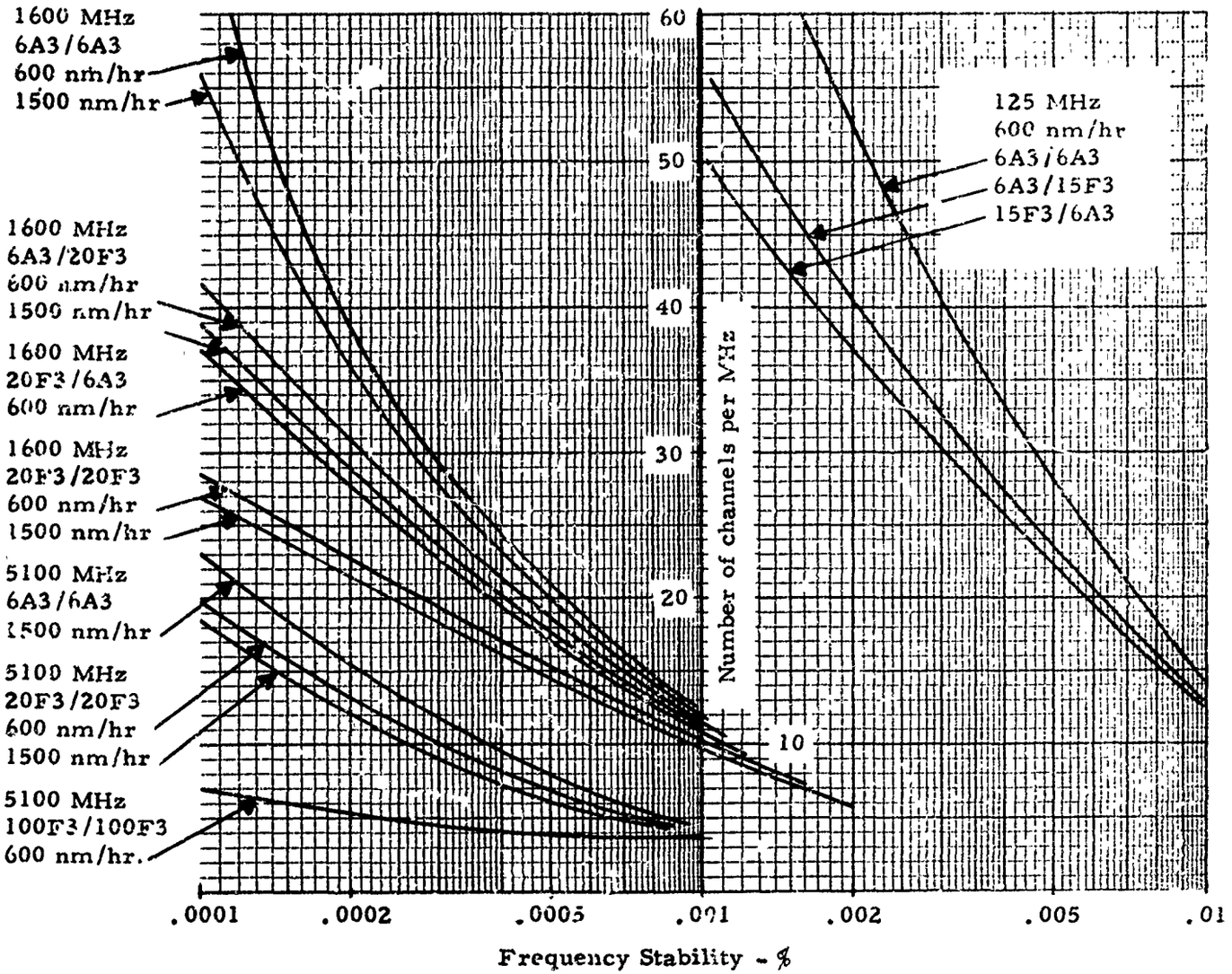

Figure 44. Number of contiguous channel assignments per MHz of band as a function of frequency stability (after Frisbie et al., 1969).

development of this figure are based upon the following criteria:

1) The receiver IF bandwidth characteristic is assumed to have a shape factor (SF) as

$$SF = B_{60_{dB}} / B_n = 1.5 \qquad (60)$$

where $B_{60_{dB}}$ = the receiver bandwidth at the -60 dB level,

B_n = required receiver bandwidth (fig. 42).

2) The minimum channel spacing is computed on the basis that an adjacent channel emission bandwidth is allowed to overlap the desired-channel receiver characteristic at the -60 dB, and no higher, level. The computation is then made from

$$\text{Min. } |(f_o)_a - (f_o)_d| = \left(\frac{B_n}{2} \times 1.5\right) + \left(\frac{B_c}{2}\right)_a + |\Delta f_o|_d + |\Delta f_o|_a \qquad (61)$$

where B_c = the channel or emission bandwidth in Hz

Δf_o = total carrier frequency drift in Hz including the Doppler shift f_D given by

$$f_D = \frac{v f_o}{3 \times 10^8} \quad , \qquad (62)$$

where v = rate of change in path length (m/s).

The subscripts a and d indicate the adjacent and desired channels respectively. These factors are illustrated in figure 45.

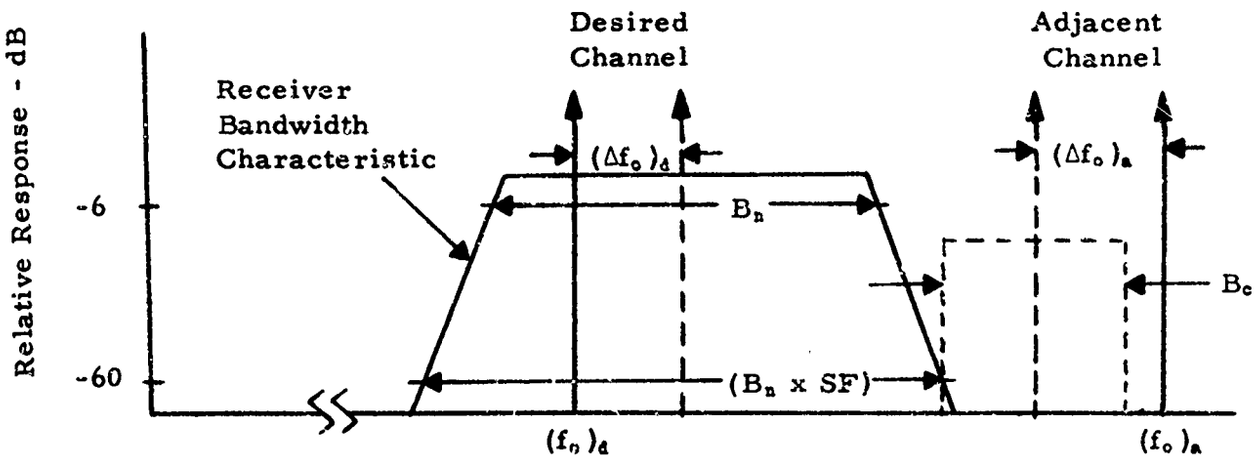

Figure 45. Channel spacing factors used in the development of figure 44.

The last equipment constraint we wish to consider is the peak-power requirements for various transmission signals. In appendix B, table B.3, we list the peak-to-average power ratios for several modulated signals. In all cases except for PM and FM, the modulated signal ratios (Λ_M) are a function of the peak-to-average power ratio of the baseband signal (Λ_B), which are given in figure B.32. Table B.3 shows that for PM and FM, the peak-power handling capacity for a transmitting power amplifier stage or the receiving amplifiers must be twice that of the nominal carrier power. Thus for example, if the transmitter power is to be a nominal 1 kW, the power amplifier must be capable of 2-kW peak to avoid distortion of the modulated signal.

For AM and AM-DSB/SC, the values of Λ_B and Λ_M have been computed in table B.4, for $\alpha = 10^{-4}$ and $M = 0.8$. For example, if a speech signal (Laplace in table B.4) is used in the baseband we find respectively:

$$\Lambda_M = 8.1 \text{ dB} \qquad \text{(AM)},$$

and

$$\Lambda_M = 19.2 \text{ dB} \qquad \text{(AM-DSB/SC)}.$$

Thus in these particular cases, the peak power requirement $\hat{P}$ for a 1-kW transmission are respectively (without speech clipping):

$$\hat{P} = 6.45 \times 1 = 6.45 \text{ kW} \qquad \text{(AM)},$$

and

$$\hat{P} = 83 \times 1 = 83 \text{ kW} \qquad \text{(AM-DSB/SC)}.$$

The latter is a rather formidable requirement, and emphasizes the advantage that may be gained from signal-processing techniques applied to the baseband signal, such as speech clipping. The peak-power advantage of AM is also evident from this example.

6. ACKNOWLEDGMENTS

The authors wish to thank Dr. E.L. Crow, Dr. W.J. Hartman, Mrs. M. Laughrun and Messrs. G.W. Haydon, G.M. Kanen and J.J. Tary for review of the manuscript and many helpful suggestions. We are also grateful to Messrs. B.C. Willmarth, J.B. Wood, H.A. Erickson, J.V. Cateora, and Mrs. N.R. Holmberg for the laboratory tests, SCIM analysis, and computer programming.

7. REFERENCES

Abramson, N. (1963), Bandwidth and spectra of phase and frequency modulated waves, IEEE Trans. Commun. Systems, CS-11, No. 4, 407.

Abramowitz, M. and I.A. Stegum (1964), Handbook of Mathematical Functions. NBS Applied Mathematics Series 5-5 ($6.50)[4].

Akima, Hiroshi (1963), The error rates in multiple FSK systems and the signal-to-noise characteristics of FM and PCM-FS systems, NBS Tech. Note 167 ($0.40)[4].

Akima, H., G.G. Ax, and W.M. Beery (1969), Required signal-to-noise ratios for HF communication systems, ESSA Tech. Rept. ERL 131-ITS 92 ($0.60)[4].

Baghdady, E.J. (1961), Lectures on Communication System Theory. (McGraw-Hill, New York, N.Y.).

Baghdady, E.J. and J.M. Gutwein (1965), FM capture performance: characterization and measurement, International Telemetering Conference Proc. 291, International Foundation for Telemetering, Washington, D.C.

Baghdady, E.J. (1966), Communication theory and techniques (unpublished notes).

Baghdady, E.J. (1969), Signal design for spectrum sharing, Lecture No. IX-12, CU/ESSA Electromagnetic Propagation Course, Boulder, Colorado.

Balakrishnan, A.V. (1963), Space Communications (McGraw-Hill, New York, N.Y.).

Barghausen, A.F., J.W. Finney, L.L. Proctor, and L.D. Schultz (1969), Predicting long-term operational parameters of high-frequency sky-wave telecommunication systems, ESSA Tech. Rept. ERL 110-ITS 78 ($2.25)[4].

Barsis, A.P., K.A. Norton, P.L. Rice, and P.A. Elder (1961), Performance predictions for single tropospheric communication links and for several links in tandem, NBS Tech. Note No. 102 ($3.00)[4].

Barsis, A.P., K.A. Norton, and P.L. Rice (1962), Predicting the performance of tropospheric communication links, singly and in tandem, IRE Trans. Commun. Systems CS-10, No. 1, 2-22.

Barsis, A.P., G.D. Gierhart, F.M. Capps, and E.M. Gray (1970), Air-ground radio wave propagation measurements in the 820-to 850-MHz frequency range, (to be published).

Beach, C.D. and J.M. Trecker (1963), A method for predicting interchannel modulation due to multipath in FM and PM tropospheric radio systems, Bell System Tech. J. 42, No. 1, 1-36.

Bean, B.R. and E.J. Dutton (1966), Radio Meteorology, NBS Monograph No. 92 ($2.15)[4].

Beckmann, P. (1967), Probability in Communication Engineering (Harcourt, Brace and World, Inc., New York, N.Y.).

Beckmann, P. and A. Spizzichino (1963), The scattering of electromagnetic waves from rough surfaces, International Series of Monographs on Electromagnetic Waves 4 (Pergamon Press, New York, N.Y.).

Bedrosian, E. (1962), The analytic signal representation of modulated waveforms, Proc. IRE 50, 2071-2076.

Bennett, W.R. (1948), Spectra of quantized signals, Bell System Tech. J. 27, 446-472.

Bergemann, G.T. and H.L. Kucera (1969), Signal characteristics of a very-high-frequency satellite-to-aircraft communication link, IEEE Trans. Commun. Technol. COM-17, No. 6, 677-685.

Blackband, W.T. (1967), Propagation Factors in Space Communications (CIRCA Publications, Inc., New York, N.Y. 10803).

Booker, H.G. and C.G. Little (1965), Atmospheric research and electromagnetic telecommunication, IEEE Spectrum 2, two parts, August and September.

Buehler, W.E., G.H. King, and C.D. Lunden (1968), VHF city noise, IEEE Electromagnetic Compatibility Symp. Record, IEEE 68C12-ECMC.

Buehler, W.E. and C.D. Lunden (1966), Signature of man-made high-frequency radio noise, IEEE Trans. Electromagnetic Compatibility EMC-8, No. 3.

Busch, A.C. (1969), How do we get from theory to practice? NAFEC Working Paper, Presented at IEEE International Conference Man/Machine Systems, St. John's College, Cambridge, England, (September).

CCIR (1967), Maximum allowable values of power flux-density at the surface of the earth produced by communication satellites, Recommendation 358-1, Documents of the XIth Plenary Assembly ITU, Geneva, Vol. IV, p. 212.

Commerce Technical Advisory Board (1966), Electromagnetic spectrum utilization - the silent crisis ($0.50)*.

Craiglow, R.L., N.R. Getzin, and R.A. Swanson (1961), Power requirements for speech communication systems, IRE Trans. Audio AU-9, 186-190.

Crawford, A.B. and W.C. Jakes, Jr. (1952), Selective fading of microwaves, Bell System Tech. J. 31, No. 1, 68-90.

Crow, E.L., F.A. Davis, and M.W. Maxfield (1960), Statistics Manual (Dover Publications, Inc., New York, N.Y.).

Cunningham, W.J., S.J. Goffard, and J.C.R. Licklider (1947), The influence of amplitude limiting and frequency selectivity upon the performance of radio receivers in noise, Proc. IRE 35, 1021-1025.

Davenport, W.B. (1952), An experimental study of speech wave probability distributions, J. Acoust. Soc. of Am. 24, 390-398.

Davenport, W.F., Jr. and W.L. Root (1958), Random Signals and Noise (McGraw-Hill, New York, N.Y.).

de Jager, F. (1952), Deltamodulation, a method of PCM transmission using the one-unit code, Philips Research Rept. 7, 442-466.

DeZoute, O.J. (1964), Long distance VHF communications system test at Barnstable, Massachusetts, FAA Rept. No. RD-64-139[2].

DeZoute, O.J. (1965), Future satellite communication subsystem investigation, Unpublished[1] FAA Interim Rept. No. RD-65-77[2].

Disney, R.T. and A.D. Spaulding (1968), Interference measurements and analysis, Item 19 CDRL Final Rept., Unpublished[1] ESSA Res. Labs. Rept. in Support of Hard Rock Silo Development, Program 125B[5].

Disney, R.T. and A.D. Spaulding (1970), Amplitude and time statistics of atmospheric and man-made radio noise, ESSA Tech. Rept. ERL 150-ITS 98 ($1.25)[4].

Dougherty, H.T. (1968), A survey of microwave fading mechanisms, remedies and applications, ESSA Tech. Rept. ERL 69-WPL 4 ($0.50)[4].

Dudzinsky, S.J., Jr. (1969), Polarization discrimination for satellite communication, Proc. IEEE 57, No. 12, 2179-2180.

Ellington, T.D. and K.W. Kirk (1967), Fading characteristics on air-to-air communication links, Electronic Commun., Sept./Oct.

Ewing, G.D. and N.W. Huddy, Jr. (1966), RF clipping and filtering to improve the intelligibility of speech in noise, IEEE Trans. Audio Electroacoustics AU-14, 184-186.

FAA (1963), Antenna, VHF, circularly polarized, FAA Specification No. FAA-E-2019[2].

FAA (1965a), VHF/UHF Air/Ground Communications Frequency Engineering Handbook, FAA Handbook[3] No. 6050, 4A.

FAA (1965b), Radio Frequency Management Principles and Practices; General, Organization and Functions, FAA Handbook[3] No. 6050, 8.

FAA (1969a), Frequency Management Engineering Principles; Geographical Separation Criteria for VOR, DME, TACAN, ILS, and VOT Frequency Assignments, FAA Handbook 6050, 5A[3].

FAA (1969b), Frequency Management Principles Spectrum Engineering Measurements, FAA Handbook 6050.23[3].

French, N.R. and J.C. Steinberg (1947), Factors governing the intelligibility of speech sounds, J. Acoust. Soc. of AM. 19, 90-119.

Friis, H. T. (1944), Noise figures of radio receivers, Proc. IRE 32, No. 7, 419-422.

Frisbie, F. L., D. J. Hamilton, C. D. Innes, F. S. Kadi, and G. M. Kanen (1969), A comparative analysis of selected technical characteristics for several frequency bands available to aeronautical satellite services, Unpublished[1] FAA report[2].

Gierhart, G. D. (1967), Frequency sharing with air traffic control satellites, Unpublished ESSA Tech. Memo. IERTM-ITSA 26[2], FAA Contract No. FA 66-WAI 112.

Gierhart, G. D. and M. E. Johnson (1967), Interference predictions for VHF/UHF air navigation aids, ESSA Tech. Rept. IER 26-ITSA 26 (AD 654924)[3], FAA Contract No. FA 64-WAI 69.

Gierhart, G. D. and M. E. Johnson (1969), Transmission loss atlas for select aeronautical service bands from 0.125 and 15.5 GHz, ESSA Tech. Rept. ERL 111-ITS 79 ($1.25)[4], FAA Contract No. FA 69-WAI 134.

Gierhart, G. D., C. A. Samson, and R. W. Krinks (1964), Comparison of 9293 and 9430 Mc/s propagation data taken over long line-of-sight paths, Unpublished NBS report[5]

Glasser, J. R. (1967), Adjacent channel interference in FM communications systems, IEEE Conf. Rec. 1967 Annual Conf. IEEE Vehicular Tech. Group.

Golden, T. S. (1970), A note on correlation distance of VHF fading from irregularities in the equatorial ionosphere, Radio Science 5, No. 6, 943-947.

Grann, O. T. (1965), FAA high gain air/ground VHF/UHF troposcatter system, FAA Rept. No. RD-65-40[2].

Griffiths, J. I. (1968), Optimum linear filter for speech transmission J. Acoust. Soc. of Am. 43, 81-86.

Hawthorne, W. B. and L. C. Dougherty (1965), VOR/DME/TACAN frequency technology, IEEE Trans. Aerospace Nav. Electron. ANE-12, No. 1, 11-14.

Haydon, G. W. (1970), Analysis of VHF and UHF aviation satellite systems, (to be printed).[1,2]

Higgins, W.T. (1968), Bandpass filtering and matching circuits at VHF, Electronic Commun. 15.

Hinchman, W.R. (1969), Use and management of the electrospace: a new concept of the radio resource, IEEE Conf. Rec. of 1969 International Conf. on Commun., 13-1 to 13-5.

Holbrook, B.D. and J.T. Dixon (1939), Load rating theory for multichannel amplifiers, Bell System Tech. J. 14, No. 1, 2-7.

Hollingworth, R.G. (1967), The power density spectra of certain frequency modulated waves, Tech. Rept. 67079, Royal Aircraft Establishment, London, England.

House, A.S., C. Williams, M.H.L. Hecker, and K.D. Dryter (1963), Psychoacoustic speech tests: a modified rhyme test, USAF Tech. Doc. Rept. No. ESD-TDR-63-403.

House, A.S. (1965), Articulation-testing methods: consonantal differentiation with a closed response set, J. Acoust. Soc. of Am. 37, 158-166.

Hubbard, R.W. and D.V. Glen (1968), Required frequency protection ratios for an FAA satellite air traffic control communication system, Unpublished[1] ESSA Tech. Memo. ERLTM-ITS 140[2], FAA Contract No. FA 67-WAI 130.

Hubbard, R.W., D.V. Glen, and W.J. Hartman (1970), Modulation characteristics critical to frequency planning for the aeronautical services, ESSA Tech. Memo. ERLTM-ITS 232[2], FAA Contract No. FA 67-WAI 134.

International Civil Aviation Organization (1968), International Standards and Recommended Practices Aeronautical Telecommunications, Annex 10 I (International Civil Aviation Organization; Montreal 3, Quebec, Canada).

IEEE (1970), Special issue on air traffic control, Proc. IEEE 58, No. 3.

ITT (1969), Reference Data for Radio Engineers, 5th ed. (Howard W. Sams & Co., Inc., New York, N.Y.).

Janes, H.B. (1955), An analysis of within-the-hour fading in the 100- to 1000-Mc transmission, J. Res. NBS 54, No. 4, 231-250.

Jasik, H. (1961), Antenna Engineering Handbook (McGraw-Hill, New York, N.Y.).

Johnson, M.E. (1967), Computer programs for tropospheric transmission loss calculations, ESSA Tech. Rept. IER 45-ITSA 45 ($1.00)[4].

JTAC (1961), Frequency Allocations for Space Communications (Joint Technical Advisory Committee, New York, N.Y. 10017).

JTAC (1964), Radio Spectrum Utilization (Joint Technical Advisory Committee, New York, N.Y. 10017).

JTAC (1968), Spectrum Engineering - The Key to Progress (Joint Technical Advisory Committee, New York, N.Y. 10017).

Kerr, D.E. (1964), Propagation of Short Radio Waves, MIT Radiation Laboratory Series 13, (Boston Technical Publishers, Inc., Lexington, Mass.).

Kirby, R.S., J.W. Herbstreit, and K.A. Norton (1952), Service range for air-to-ground and air-to-air communications at frequencies above 50 Mc, Proc. IRE 40, No. 5, 525-536.

Kryter, K.D. (1962a), Methods for the calculation and use of the articulation index, J. Acoust. Soc. of Am. 34, 1689-1697.

Kryter, K.D. (1962b), Validation of the articulation index, J. Acoust. Soc. of Am. 34, 1698-1702.

Kryter, K.D. and J.H. Ball (1964), A meter for measuring the performance of speech communication systems, Tech. Doc. Rept. No. FSD-TDR-64-674, Electronic Systems Div., Air Force System Command, L.G. Hanscom Field, Bedford, Mass.

Kuegler, G.K. (1969), Equatorial scintillations experienced during Apollo 11 support July 12 to July 24, GSFC Doc. X-460-69-534, Goddard Space Flight Center, Greenbelt, Maryland.

Lawrence, R.S., C.G. Little, and H.J.A. Chivers (1964), A survey of ionospheric effects upon earth-space radio propagation, Proc. IEEE 52, No. 1, 4-27.

Licklider, J.C.R. (1946), Effects of amplitude distortion upon the intelligibility of speech, J. Acoust. Soc. of Am. 18, 429-434.

Licklider, J.C.R. and S.J. Goffard (1947), Effects of impulsive interference upon AM voice communication, J. Acoust. Soc. of Am. 19, 653-663.

Longley, A.G. and P.L. Rice (1968), Prediction of tropospheric radio transmission loss over irregular terrain, a computer method - 1968, ESSA Tech. Rept. ERL 79-ITS 67 ($0.70)[4].

McClure, G.W. and J.C. Dute (1964), Survey and analysis of long-distance communications techniques, FAA Rept. No. RD-64-7[a].

McCurley, E.P. and C. Blake (1961), A simple approximate expression for converting directly from noise figures in dB to noise temperatures, Microwave J. IV, No. 4, 19.

Medhurst, R.G. (1959), Echo-distortion in frequency-modulation, frequency-division-multiplex trunk radio systems, Electron. Radio Engr. 36, No. 7, 253-259.

Miller, B. (1965), Satellites offer wide use by airlines, Aviation Week Space Technol. 83, No. 17, 86.

Moore, R.K. and C.S. Williams, Jr. (1957), Radar terrain return at near-vertical incidence, Proc. IRE 45, No. 2, 228-238.

NATO (1969), A survey of scintillation data and its relationship to satellite communications, AGARD Rept. 571[3].

Nesenbergs, M. (1967), Error probability for multipath fading - the "slow and flat" idealization, IEEE Trans. Commun. Technol. COM-15, No. 6, 797-805.

North, D.O. (1942), The absolute sensitivity of radio receivers, RCA Rev. 6, 332-343.

Norton,, K.A. (1953), Transmission loss in radio propagation, Proc. IRE 41, No. 1, 146-152.

Norton, K.A. (1959), System loss in radio-wave propagation, Proc. IRE 47, No. 9, 1661.

Norton, K.A. (1962), Efficient use of the radio spectrum, NBS Tech. Note 158 ($0.45)[4].

Norton, K.A., H. Staras, and M. Blum (1952), A statistical approach to the problem of multiple radio interference to FM and television service, IRE Trans. Ant. Prop. PGAP-1, 43-49.

Norton, K.A., P.L. Rice, and L.E. Vogler (1955a), The use of angular distance in estimating transmission loss and fading range for propagation through a turbulent atmosphere over irregular terrain, Proc. IRE 43, No. 10, 1488-1526.

Norton, K.A., L.E. Vogler, W.V. Mansfield, and P.J. Short (1955b), The probability distribution of the amplitude of a constant vector plus a Rayleigh-distributed vector, Proc. IRE 43, No. 10, 1354-1361.

O' Brien, P. J. and A. C Busch (1969), Effects of selective system parameters on co..munications intelligibility, FAA Rept. No. NA-69-21 (RD-68-59)[2], National Aviation Facilities Experimental Center 08405.

Oliver, W. (1964), White noise loading of multi-channel communications systems, Marconi Instruments Co., Englewood, N.J.

Panter, P.F. (1965), Modulation, Noise, and Spectral Analysis (McGraw-Hill, New York, N.Y.).

Ploussious, G. (1968), City noise and its effect upon airborne antenna noise temperatures at UHF, IEEE Trans. Aerospace and Electron. Systems AES-4, No. 1, 41-51.

Proc. IEEE (1967), Special Issue on Redundancy Reduction 55, No. 3.

Reed, H.R. and C.M. Russell (1964), Ultra High Frequency Propagation (Boston Technical Publishers, Lexington, Mass.).

Reinhart, E.E. (1966), Multiple access techniques for communications satellites: analog modulation, frequency-division multiplexing, and related signal processing methods, Memo. RM-5117-NASA, Rand Corp., Santa Monica, Calif.

Rice, P.L., A.G. Longley, K.A. Norton, and A.P. Barsis (1967), Transmission loss predictions for tropospheric communication circuits, NBS Tech. Note 101, Vols. I and II (AD 687 820 and AD 687 821)[3].

Schwartz, M , W.R. Bennett, and S. Stein (1966), Communication Systems and Techniques (McGraw-Hill Book Co., New York, N.Y.).

Shaft, P.D. (1961), Information bandwidth of tropospheric scatter systems, IRE Trans. Commun. Systems CS-9, No. 3, 280-287.

Skerjanec, R.E. and C.A. Samson (1970), Rain attenuation study for 15-GHz relay design, FAA Rept. No. FAA-RD-70-21, FAA Contract No. FA 65-WAI 86 (AD 709 348)[3].

Skolnik, M.I. (1962), Introduction to Radar Systems (McGraw-Hill Book Co., New York, N.Y.).

Skomal, E.N. (1965), Man-made VHF/UHF noise, IEEE Trans. Electromagnetic Compatibility, EMC-7, No. 3, p. 263.

Spaulding, A. D. (1969), Characterization of additive disturbances, Lecture presented at joint University of Colorado/ Environmental Science Services Administration Summer Course on Communication Systems and Time-Variant Electromagnetic Propagation Media, Boulder, Colorado, June 16-July 3, 1969.

Spence, R. E. (1966), Future role of satellites in air traffic control, IEEE Spectrum 3, No. 7, 112-115.

Stein, S. and J. J. Jones (1967), Modern Communication Principles (McGraw-Hill Book Co., New York, N. Y.).

Stuckey, C. W. (1963), Investigation of the precision of an articulation-testing program, J. Acoust. Soc. of Am. 35, 1782-1787.

Sunde, E. D. (1964), Intermodulation distortion in analog FM tropo-scatter systems, Bell System Tech. J. 43, No. 1, 399-435,

Sunde, E. D. (1969), Communication Systems Engineering Theory (John Wiley and Sons, Inc., New York, N. Y.).

Takahashi, K. (1969), Diversity effect on VHF space communications, IEEE Trans. Ant. Prop. AP-17, No. 3, 331-337.

Trott, R. C. (1966), Interference rejection through the use of "notch" filters, presented before IEEE Vehicular Communications Group, Dallas Chapter (copies of this paper and an Inter-modulation Product Chart--151 MHz to 161 MHz are available from Decibel Products, Inc., 3184 Quebec Street, Dallas, Texas 75247).

van de Weg, H. (1953), Quantizing noise of a single integration delta modulation system with an N-digit code, Philips Research Rept. 8, 367-382.

Vegard, W. C., J. L. Levatich, and T. J. Carroll (1962), VHF air-ground propagation far beyond the horizon and tropospheric stability, IRE Trans. Ant. Prop. AP-10, No. 5, 608-621.

Wolf, Jack K. (1966), Effects of channel error on delta modulation, IEEE Trans. Commun. Technol. 14, No. 1, 2-7.

Woodward, P. (1952), The spectrum of random phase modulation, Memo. No. 642, Telecommunications Research Establishment, Great Malvern, Worcestershire, England.

Zetterburg, L. (1955), A comparison between delta and pulse code modulation, Ericsson Tech. 2, 95-154.

---

[1] These documents are in the public domain since they were issued as official government writing. However, they are considered unpublished since they were not printed for wide public distribution.

[2] Requests for copies of these documents should be addressed to FAA Systems Research & Dev. Services, Spectrum Plans and Programs Branch RD-510, Washington, D.C. 20553.

[3] Copies of these reports are sold for $3.00 each (microfiche, $0.65) by the Clearinghouse for Federal Scientific and Technical Information, Springfield, Va. 22151. Order by indicated accession number.

[4] Copies of these reports are sold for the indicated price by the Superintendent of Documents, U.S. Government Printing Office, Washington, D.C. 20402.

[5] Available from the author(s), Institute for Telecommunication Sciences, Boulder, Colorado 80302.

APPENDIX A
Frequency Sharing With an ATC Satellite

This appendix is intended to provide the FAA with technical information relevant to the solution of frequency-sharing problems in the VHF band that are associated with the use of VHF for the aircraft/satellite link of a synchronous satellite air traffic control (ATC) system. Specifically, this appendix deals with the estimation of (a) RF D/U available at the satellite when interference from a multitude of conventional ATC networks is considered, and, (b) the extent to which the service range of a conventional ATC facility can be reduced because of interference caused by transmissions from a satellite.

The results are applicable to either cochannel or adjacent-channel interference problems, and can be easily modified to accommodate a variety of system parameter changes. Specific examples of several such modifications have been included. However, an estimate of the D/U required for satisfactory service (protection ratios) must be made by the user in order to apply these results to interference problems, as they are expressed in terms of the signal power ratios available under various conditions. The results of an experimental program to determine protection ratios for some of the system combinations that might be encountered in developing a satellite ATC system are discussed in section 4.

A.1 System Parameters

The system parameters used in this study were selected on the basis of information contained in the technical literature, discussions with FAA personnel, and the authors' analysis of the

systems involved. All nonsatellite stations considered here are assumed to require, for satellite observation, a look angle that is greater than 0.5° relative to a horizontal plane located at the point of observation, i.e., these stations are within ≈5000 nm of the subsatellite point (a point on the earth's surface directly below the satellite). The minimum look angle for the aircraft using the satellite is 12° or greater: ≈4000 nm from the subsatellite point. A wide variety of parameters of this type could be considered, but because of the urgent need for some specific results a very restricted set of parameters was selected. However, the results can be easily modified to allow for changes in some of the noncritical parameters, such as the EIRP of the aircraft using the satellite (see sec. A.2.5).

A.1.1 Satellite ATC System

The restricted nature of this study limits the requirements for satellite ATC system parameters to those involved in the VHF satellite/aircraft link. A specific set of parameters, listed in table A.1, had to be selected for this study even though the parameters to be used in the final system design are unknown. In fact, it is not certain that VHF frequencies will be used for the satellite system (Haydon, 1970).

Literature dealing directly with satellite ATC systems (DeZoute, 1965; McClure and Dute, 1964; Miller, 1965; and Spence, 1966) was used as a guide in selecting parameters. Although some consideration was given to the associated practical and theoretical problems, the equipment configuration implied should be regarded simply as a reasonable illustration of a possible system and not as an "optimum" one.

The IF bandwidth was chosen to fit comfortably in a 25-kHz channel and still pass the third pair of sidebands associated with a

Table A.1. Satellite ATC system parameters.

Item	Common Parameters
Frequency, f	130 MHz
Median basic transmission loss L_{bs}	166.3 dB
L_{bs} from fig. A.1 for 35° + 20 log (130/125)	
Fading margin, M.	1.2 dB
Receiver IF noise bandwidth	20 kHz
Johnson's noise P_J	-161 dBW
(sec. 3.3.1)	
Modulation	FM-voice
Peak deviation	5 kHz
Effective S/N at antenna*	7 dB
(SCI = -.4, fig. C.17)	
Receiver noise factor, f_r	2.51
or figure $F_r = 10 \log f_r$	4 dB
Line loss factor, ℓ_t	1.259
or loss $L_t = 10 \log \ell_t$	1 dB
Line temperature T_t	288°K = T_o
Line noise factor, f_t	1.259
(fig. 15, sec. 3.3.2)	
Antenna circuit loss factor, ℓ_c	1.122
or loss $L_c = 10 \log \ell_c$	0.5 dB
Antenna circuit temperature T_c	288°K = T_o
Antenna circuit noise factor, f_c	1.122
(fig. 15, sec. 3.3.2)	

Table A.1 (continued)

Item	Parameters Not Common	
	Aircraft Terminal	Satellite Terminal
Antenna noise factor, f_a***	2	1
or figure $F_a = 10 \log f_a$ (dB)	3	0
(fig. 8, sec. 3.3.1)	galactic	$T_a = 288°K$
System noise factor, f_s	4.55	3.55
(eq. (40), sec. 3.3.2)		
System noise figure F_s (dB)	6.6	5.5
$F_s = 10 \log f_s$		
Total system noise power P_T (dBW)	-154.4	-155.5
$F_s + P_{fl}$, sec. 3.3.1		
Antenna elevation angle (deg)	35	-90
above horizontal		
Antenna beamwidth (deg)	65 vertical	17
	90 horizontal	17
Antenna gain G (dB)	4**	21**
above isotropic antenna	3*	20*
of same polarization	5***	22***
Polarization	vertical	left-hand circular
Polarization loss L_p (dB)	3	0
Signal power at antenna* W (dBW)	-147.4	-148.5
$P_T + (S/N)_{dB}$ at antenna* = $P_T + 7$		
Transmitter power W_t (dBW)	-1	0.1
$W + L_t + L_c$'s $+ L_p$'s $+ M_f + L_{bs} - G$'s $= W + 147.5$		
where G's are median values and W is for receiving terminal.		
EIRP (dBW)	2.5	20.6
$W_t - L_t - L_c + G_t = W_t - 1.5 + G_t$ where G_t is the maximum value.		

* minimum value
** median value
*** maximum value

3-kHz audio frequency. These are the only "significant" sidebands (Panter, 1965, p. 252; Abramowitz and Stegum, 1964, p. 398) for the 3-kHz tone when the modulation index is 1.4.

Noise figure calculations are based on information given in section 3.3. Antenna, transmission line and receiver noise factors are included. The only important contribution to the satellite antenna noise factor is taken to be the noise temperature of the earth, 288°K.

Satellite antenna beamwidth provides earth coverage only, and its gain corresponds to that of a helical antenna (Jasik, 1961, sec. 7.1). The left-hand circular polarization used will result in some rejection of right-handed elliptically polarized transmissions from conventional ATC facilities (Dudzinsky, 1969) and avoid fading caused by Faraday rotation (Blackband, 1967, pp. 37-43). However, a polarization loss of 3 dB is associated with the aircraft antenna since it is not circularly polarized.

The fading margin used to calculate required transmitter powers is sufficient to provide satisfactory service 99% of the time when a small desired signal level variability is assumed; i.e., a variability that is normally distributed in decibels about its median with a standard deviation of 0.5 dB (see fig. A.4). This variability is associated with the variation of transmission loss with look angle (fig. A.1) and failure to realize full antenna gain because of antenna orientation, but does not allow for multipath fading caused by reflections from the earth or scintillations due to the ionosphere. Fading due to these mechanisms will be discussed in section A.2.5.

Maximum power flux-density at the earth's surface due to a satellite at synchronous altitude (3.59×10^7m) with its antenna directed toward the earth in dBW for 1 m^2 (dBW/m^2) is 10 log (4 π) + 20 log (3.59×10^7) = 162.1 dB less than the satellite EIRP in dBW

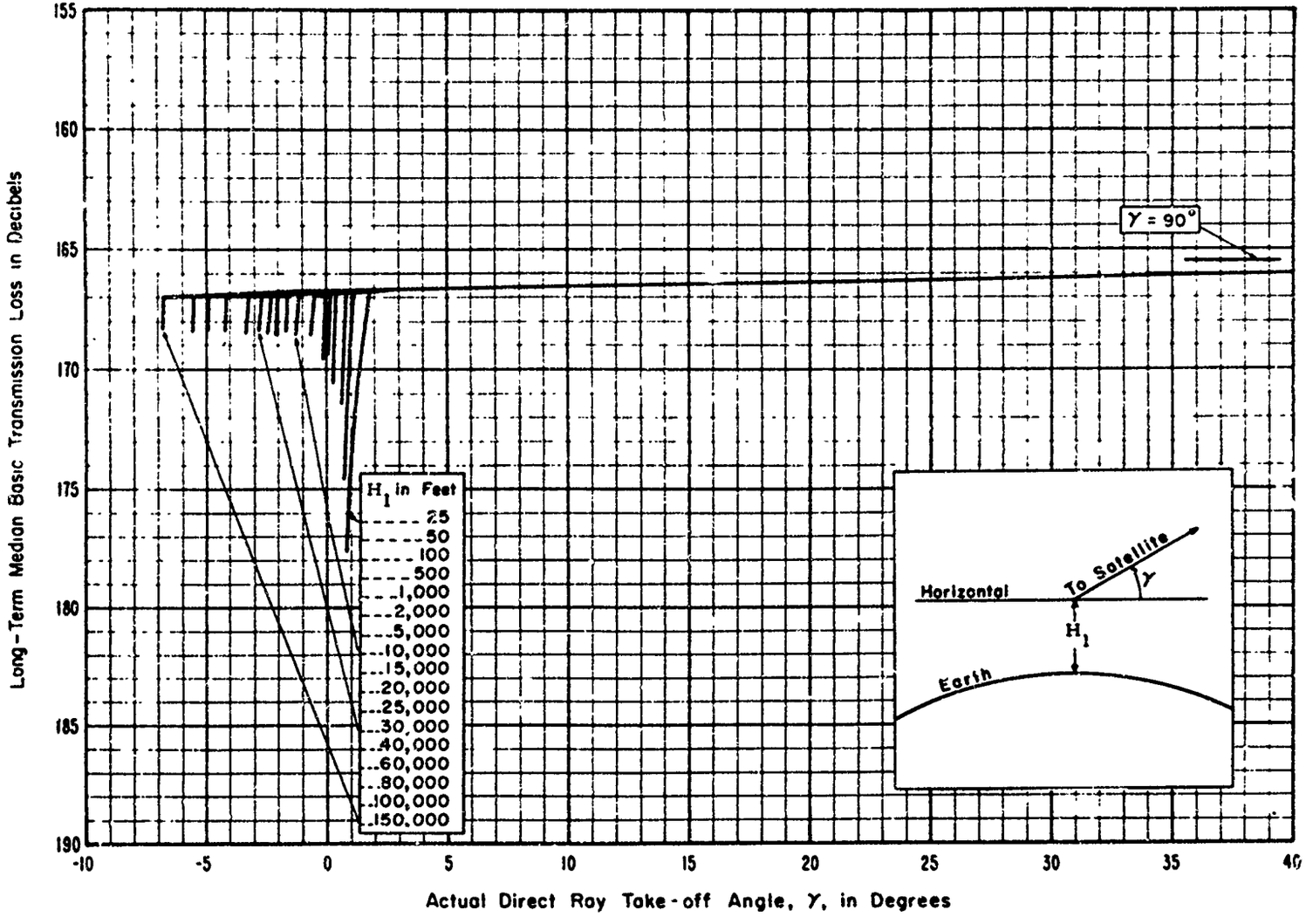

Figure A. 1. Basic transmission loss vs. angle; f = 125 MHz, H_2 = synchronous altitude. (After Gierhart and Johnson, 1969, fig. 86.)

when free-space propagation is assumed and reflections from the earth are neglected. The EIRP given in table A. 1 would result in a maximum power flux-density of -141.5 dBW/ m^2.

A. 1. 2 Conventional ATC Network

Conventional Aeronautical Mobile/ VHF ATC networks using amplitude modulation (AM) are considered as the source of interference to the aircraft/ satellite link of the satellite ATC system in this study. Such AM networks consist of a ground facility and the aircraft it serves. The need to consider interference caused by a large number of AM networks, and the difficulties that would be involved in an exact description of any one particular AM network during a specific interval of time have dictated the "typical network" approach. For this study all AM networks are assumed to have characteristics identical to those of a "typical" network. The system parameters assumed for the "typical" AM network are tablulated in table A. 2.

Table A. 2. Typical AM network system parameters.

Item	Aircraft Terminal	Ground Facility
Frequency	~130 MHz	~130 MHz
Modulation	AM voice	AM voice
IF bandwidth (receiver)	40 kHz	40 kHz
Audio bandwidth	3 kHz	3 kHz
Line loss	3 dB	2 dB
Antenna gain	(see fig. A. 2)	0 dB
Antenna polarization (transmit)	Vertical	Right-hand elliptical
Transmitter power	14 dBW	17 dBW

Documents dealing directly with conventional AM networks (FAA 1963, 1965a, and 1965b) were used as a guide in selecting these parameters. Exact values for them would be expected to depend on the particular facility and the aircraft types involved during a particular time period. The parameters selected are intended to provide an estimate of average or typical conditions. Because some of the initial calculations discussed here are more easily performed with discrete distributions, discrete random variables are used to describe the typical AM network.

The discrete distribution assumed for gain of the aircraft antenna is shown in figure A.2. It is based on an analysis of gain data for a number of aircraft antenna configurations. Several of the gain data distributions for which the final distribution is representative are also shown in the figure.

A.2. Interference at Satellite

The methods used for predicting distributions of D/U available at the satellite are outlined in this section. Also included are the resulting distributions and a discussion of methods to modify these results to account for changes in system parameters.

Distribution of D/U in decibels for n undesired AM networks will be denoted by D/U(p, n), where p represents the percent of time for which D/U equals or exceeds particular values.

To determine D/U(p, n) the following steps are necessary:

(1) Determine the distribution of desired FM signal power levels at the satellite on the assumption of continuous transmission from a single aircraft using the satellite.

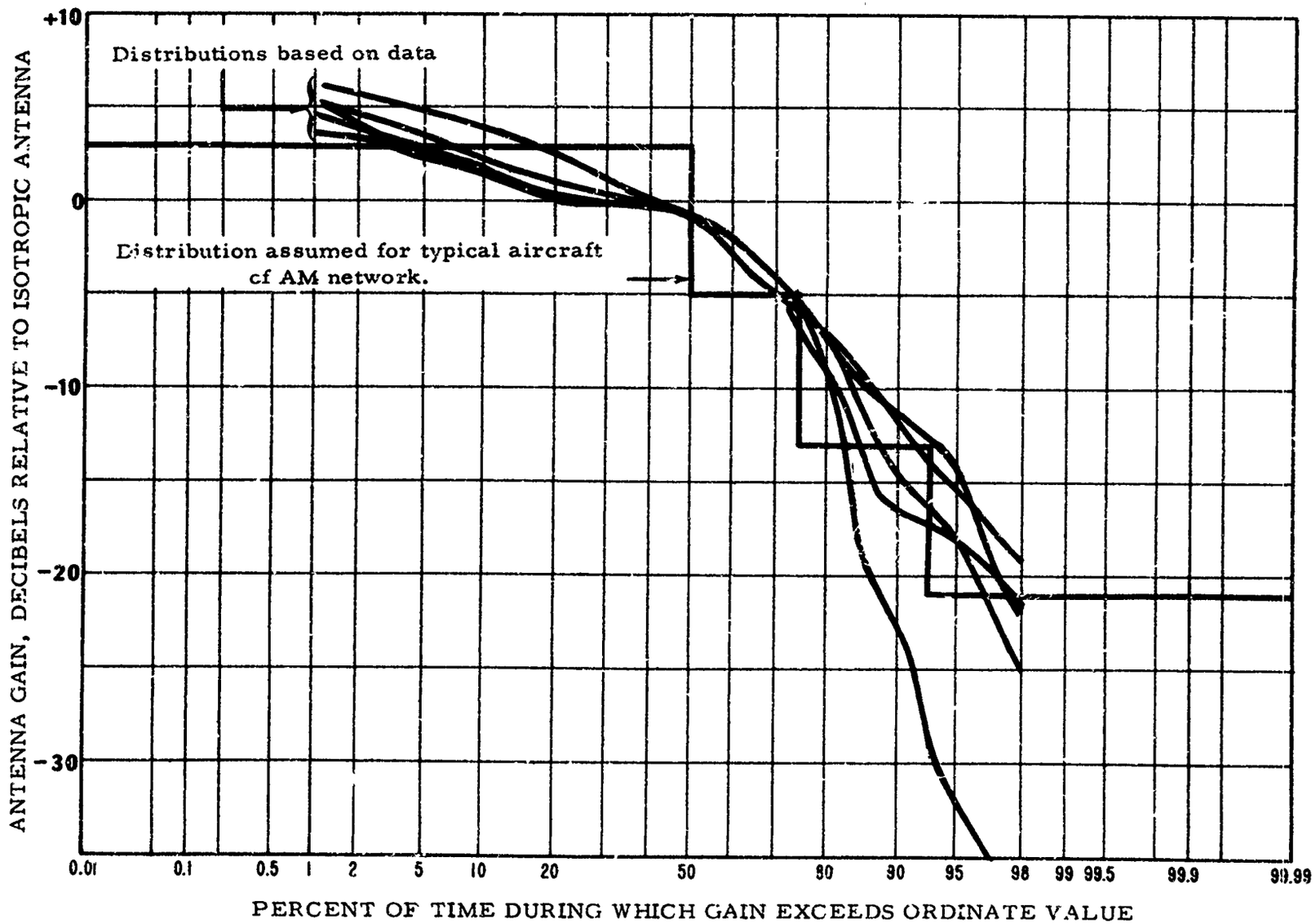

Figure A.2. Distribution of aircraft antenna gain.

(2) Determine the distribution of undesired signal power levels at the satellite that is caused by a single, typical AM network.

(3) Determine the distribution of undesired signal power levels at the satellite caused by n typical AM networks.

(4) Combine the distributions of desired and undesired signal levels to obtain D/U(p, n).

Distributions of D/U(p, n) are independent of system parameters common to both the desired and undesired signals. In this analysis, satellite antenna gain, satellite line loss, and median basic transmission loss can be treated as common to both signals. The calculated values of desired and undesired signal power normalized in the sense that the common parameters mentioned above are not included in calculating them.

A.2.1 Desired FM Signal Power at the Satellite

Circular polarization for the satellite antenna was selected so that fading caused by Faraday rotation could be neglected. Because the aircraft is located above the first kilometer of the earth's atmosphere and the takeoff angle for an aircraft-to-satellite ray is always greater than 12° relative to a horizontal reference at the aircraft, it is possible to neglect losses associated with the troposphere (JTAC, 1961). However, some consideration is given to ionospheric absorption variations (Balakrishnan, 1963; Lawrence et al., 1964), the change in basic transmission loss as the aircraft-to-satellite distance changes, and the failure to realize the full gain of the aircraft antenna at all aircraft locations. The loss associated with these factors is assumed to be normally distributed in decibels, with a standard deviation of 0.5 dB about a median of 0 dB. Even though the aircraft-to-satellite distance may vary from ≈19,400 to

≈22,300 nm, the difference in transmission loss caused by this distance change is only about 1 dB. Multipath fading caused by ground reflections and scintillations due to the ionosphere are neglected in the initial analysis, but will be discussed in section A.2.5.

Thus, the "normalized" desired signal power will be normally distributed in decibels with a standard deviation of 0.5 dB and a median value of -1.5 dBW. The median was calculated based on values for the aircraft terminal from table A.1 as follows:

Transmitter power	(+)-1.0 dBW.
Polarization loss	(-) 3.0 dB.
Line loss	(-) 1.0 dB.
Antenna circuit loss	(-) 0.5 dB.
Antenna gain	(+) 4.0 dB.
Median normalized power for aircraft (desired)/satellite link	-1.5 dBW.

Calculated values of desired and undesired signal power are normalized in the sense that items common to both systems are not included. Specifically, median satellite antenna gain and circuit loss, and median basic transmission loss are not included in normalized power calculations; i.e., available power at the terminals of the satellite antenna is 145.8 dB less than given normalized power levels.

A.2.2 Undesired AM Signal Power From a Single Network

The distribution of normalized signal power at the satellite from the typical AM network (sec. A.1.2) is developed by combining normalized power developed for a typical airborne terminal and a typical ground facility. Combining is performed by calculating the probability of obtaining certain discrete power levels when it is assumed that (a) the ground facility and airborne terminal do not

transmit at the same time, (b) the time during which transmission occurs is equally divided between the two, and (c) no transmissions occur during 5% of the time. Discrete distributions of the power available from each type of terminal and the discrete distribution resulting from the combination process are shown in figure A. 3. The mean and variance of the power distribution for a typical facility are 11. 52 W and 196. 27 W^2, respectively.

Statistics for power received from the undesired AM airborne terminal are developed on the assumption that, (a) the aircraft antenna gain effective for a direct ray to the satellite is statistically independent of the gain effective for a ray reaching the satellite via ground reflection, (b) the gain statistics shown in figure A. 2 are applicable to both rays, (c) the phase angle between the two signals is uniformly distributed between 0 and 2π (Norton et al., 1955b), and (d) the reflection coefficient of the earth is unity. To obtain the proper values of normalized power, the distribution developed based on these considerations was modified by the addition of 9 dB. This constant was calculated from values in table A. 2 for the aircraft terminal as follows:

Transmitter power	(+) 14 dBW.
Power increase due to modulation	(+) 1 dB.
Line loss	(-) 3 dB.
Polarization loss	(-) 3 dB.
Normalization constant for undesired AM aircraft transmissions	9 dBW.

Normalized power statistics for the ground facility were developed by using the "standard propagation curves for earth-space

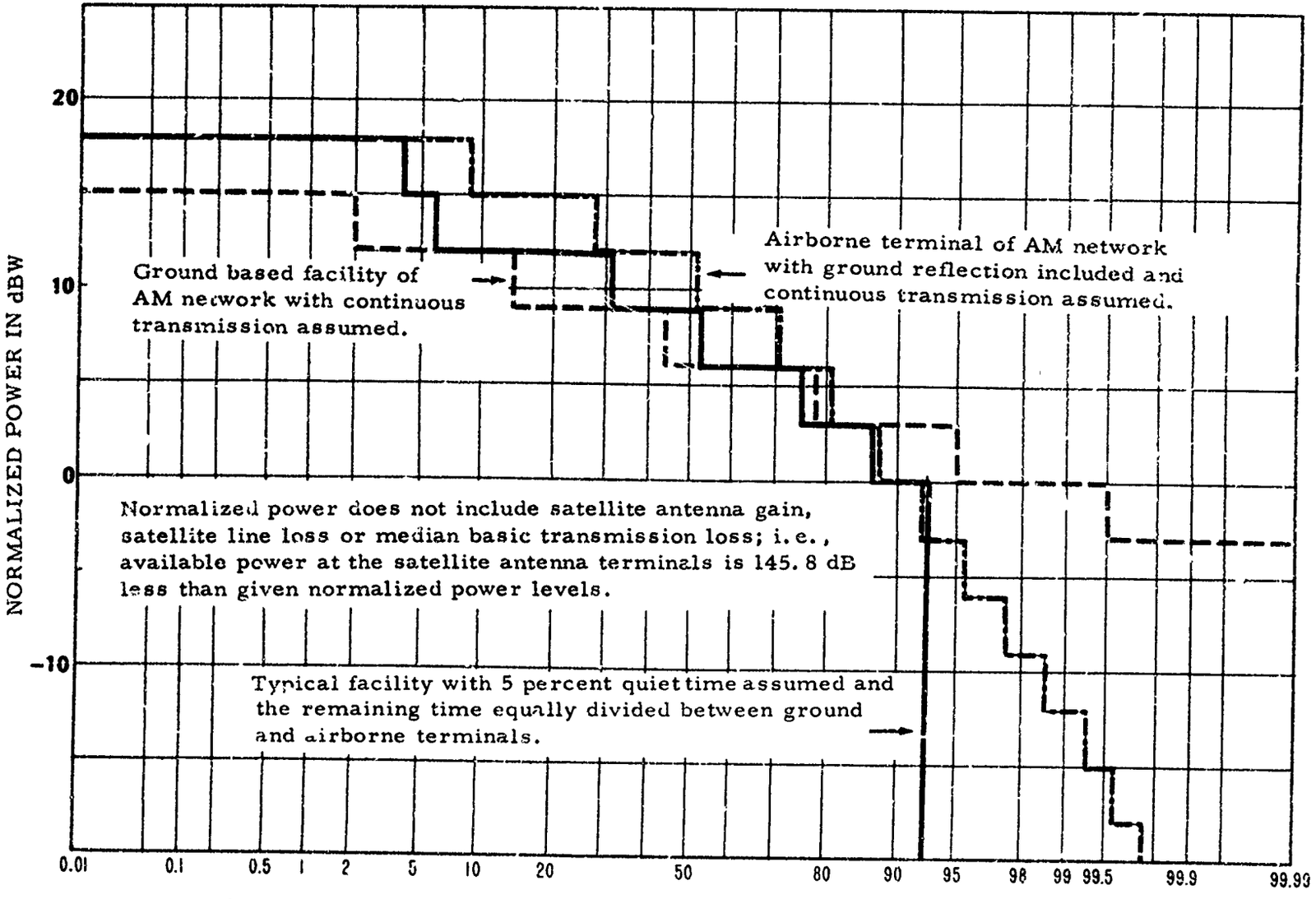

Figure A.3. Development of power distribution for typical facility.

links" given by Rice et al. (1967, fig. I-24, $\theta_o = 0.03$, 2 GHz), and making a minor adjustment (Rice et al., 1967, fig. 10.15) to account for the lower frequency (130 MHz) being considered in this study. A factor of 8 dBW was used to make the conversion to normalized power; it was calculated from values in table A.2 for the ground facility as follows:

Transmitter power	(+) 17 dBW.
Power increase due to modulation	(+) 1 dB.
Line loss	(-) 2 dB.
Polarization loss	(-) 10 dB.
Gain due to ground reflection	(+) 2 dB.
Antenna gain	(+) 0 dB.
Normalization constant for undesired AM ground facility transmissions	8 dBW.

For communicating with circularly polarized antennas (Reed and Russell, 1964, Ch. 8; Dudzinsky, 1969) the antennas must have the same polarization sense (right-handed or left-handed). The loss due to a polarization mismatch between the ground facility antenna (right-hand elliptical) and the satellite antenna (left-hand circular) is estimated to be 10 dB.

A.2.3 Undesired AM Signal Power From Multiple Networks

Distributions of normalized signal power at the satellite due to n typical AM networks are developed by combining the powers expected from the various networks by statistical means. The "power convolution" and "log-normal" methods of combining distributions are used. It is assumed that the average power received from a number of networks at any particular time is simply the sum of the average powers received from each individual station, and that

these powers are statistically independent random variables. The time period used to determine average powers must be long enough to assure that contributions to the resultant average power from terms that involve relative RF phase differences between the various signals received are negligible (Moore and Williams, 1957).

For a small number of networks the "power convolution" method is used to calculate distribution of resultant power levels. In this method successive convolutions of power (watts) distributions for groups of stations are performed to obtain the resultant power (watts) distribution for n networks. The operational aspects of this method are summarized by the following equations where the operational symbol $\oplus$ denotes the statistical convolution process, and U(p, n) represents the distribution of power, measured in watts, resulting from n undesired networks.

$$U(p, 2) = U(p, 1) \oplus U(p, 1), \qquad \text{(A-1a)}$$

$$U(p, 4) = U(p, 2) \oplus U(p, 2), \qquad \text{(A-1b)}$$

and

$$U(p, n) = U(p, \tfrac{n}{2}) \oplus U(p, \tfrac{n}{2}), \text{ for } n = 2^N, \qquad \text{(A-1c)}$$

where N is a positive integer. Successive convolutions by pairs are performed to minimize the number of operations required to find U(p, n).

If random variables x and y are statistically independent their distributions can be convoluted (Davenport and Root, 1958, pp. 36, 37, and 55), and the distribution of either the variable $z = x + y$, or the variable $z = x - y$ can be obtained, depending on the result required. The distribution of z can be obtained by selecting a number of equally spaced percentage values from the individual distributions, characterizing the levels in particular percentage

ranges by a specific x_i or y_j value, calculating all possible sums $z_k = x_i + y_j$, and forming a distribution of all values of z_k obtained in this manner (Rice et al., 1967, sec. 10.8). A distribution for z' can be obtained in a similar fashion.

If the uncorrelated random variables x and y are normally distributed (Panter, 1965, sec. 4.2) with means and variances of m_x, σ_x^2 and m_y, σ_y^2 respectively, then the distributions of z and z' will be normally distributed with means and variances that can be calculated as follows:

$$m_z = m_x + m_y \ , \qquad \text{(A-2)}$$

$$m_z' = m_x - m_y \ , \qquad \text{(A-3)}$$

and

$$\sigma_z^2 = \sigma_{z'}^2 = \sigma_x^2 + \sigma_y^2 \ . \qquad \text{(A-4)}$$

However, the power (watts) distribution for a typical AM network is not approximated very well by a normal distribution and this simple procedure should not be used.

A simplified version of the log-normal method given by Norton et al. (1952) was used for values of n greater than 16. This simplification results from the assumptions that the same distribution describes the power radiated by each undesired network and that the power levels received from the various networks are statistically independent. Because the log-normal method carries the assumption that the power (watts) resulting from one or several stations is log-normally distributed, it could not be used for small values of n. The relationships used to calculate the mean, M_n, and variance, σ_n^2, of the normally distributed dBW resulting from n stations by using the mean, α, in W, and variance, μ, in W^2, of a typical AM network are given below:

$$M_n = \left[\ln(n\alpha) - \frac{1}{2} \left(\frac{\sigma_n}{c} \right)^2 \right] c \quad \text{dBW}, \tag{A-5}$$

$$\sigma_n^2 = c^2 \ln \left[1 + \frac{n\mu}{(n\alpha)^2} \right] \quad \text{dB}^2, \tag{A-6}$$

where c is 10 log e as in (20). In this report "ln" is used for natural logarithm and "log" is used for common logarithm.

Values of M_n and σ_n calculated for several values of n and the corresponding values of $n\mu$, $n\alpha$, and 10 log $n\alpha$ are tabulated in table A.3.

It can be shown that M_n approaches 10 log $n\alpha$ and σ_n approaches zero as n approaches infinity. The values in table A.3 indicate that M_n can be taken as 10 log $n\alpha$ for n larger than 8 and that σ_n can be taken as 0 for n larger than 10^2. This means that power

Table A.3. Results of log-normal calculations.

n	$n\mu$ W^2	$n\alpha$ W	10 log $n\alpha$ dBW	M_n dBW	σ_n dB
1	196.27	11.52	10.6	8.7	4.13
2	392.54	23.04	13.6	12.4	3.23
4	785.08	46.08	16.6	16.0	2.44
8	1,570.16	92.16	19.7	19.3	1.79
16	3,140.32	184.32	22.7	22.5	1.29
32	6,280.64	368.64	25.7	25.6	0.92
10^2	1.9627×10^4	1.152×10^3	30.6	30.6	0.53
10^3	1.9627×10^5	1.152×10^4	40.6	40.6	0.17
10^4	1.9627×10^6	1.152×10^5	50.6	50.6	0.05
10^5	1.9627×10^7	1.152×10^6	60.6	60.6	0.00

received from n networks, where n is larger than 10^2, can be assumed to have a constant level given by

$$M_n = A + N \text{ dBW}, \tag{A-7}$$

where

$$A = 10 \log n \text{ dBW}, \tag{A-8}$$

and

$$N = 10 \log n \text{ dB}. \tag{A-9}$$

Distributions of undesired power $U_{dBW}(p, n)$, developed by the methods just discussed are shown in figure A.4 for several values of n, along with the distribution of power received from the desired station. This figure illustrates five points:

(1) The period of time for which no undesired power is transmitted diminishes rapidly as n increases.

(2) Although the log-normal method should not be used for small values of n, it yields results that are close to those obtained by the power convolution method for values of n as small as 16.

(3) The variation of undesired power about its median level decreases significantly as n increases.

(4) The power received from a single undesired network is greater than that received from the desired station a significant part of the time.

(5) The time variability associated with the desired station is much smaller than that associated with the undesired networks when their number is small.

A.2.4 Desired-to-Undesired Signal Ratios

The distribution of D/U(p, n) in decibels, for n undesired networks is calculated by the convolution procedure when both the desired power and undesired power are expressed in dBW. However,

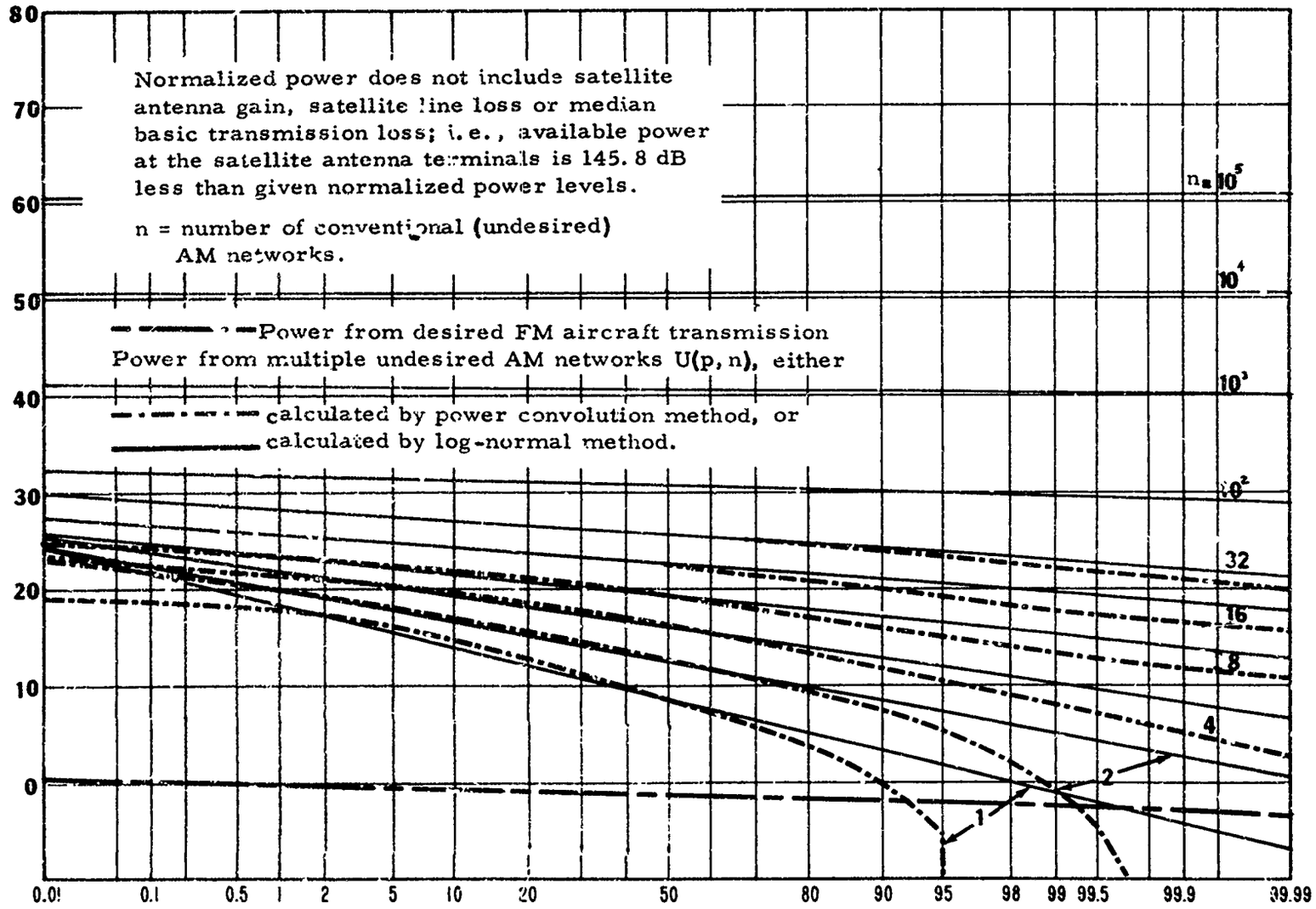

Figure A.4. Normalized power at satellite terminal.

the procedure required is somewhat different from the one called for in (A-1) in that the difference between the random variables is needed. This corresponds to the $z' = x - y$ case discussed in section A.2.3. With $D_{dBW}(p)$ and $U_{dBW}(p, n)$ used to represent the distributions of desired and undesired dBW, respectively, the required calculation can be expressed as

$$D/U(p, n) = D_{dBW}(p) \ominus U_{dBW}(p, n) \text{ dB}, \qquad \text{(A-10)}$$

where $\ominus$ indicates the required convolution procedure.

Three techniques can be used to perform the convolution indicated in (A-10); the technique depends on the value of n.

For $n \leq 32$, the variance associated with the power from the desired station is much smaller than that associated with the power from the undesired networks, and the desired power level is assumed to be constant and its mean level. Points for particular $D/U(p, n)$ can then be obtained by (a) reading U_{dBW} levels from U_{dBW} from (p, n) distributions (fig. A.4) corresponding to percentage values of 100-p, where p is the p of $D/U(p, n)$; (b) subtracting the resulting U_{dBW} levels from -1.5 dBW, which is the median "normalized" desired signal power level from section A.2.1; and (c) plotting the results as a function of p to obtain distributions of $D/U(p, n)$ in decibels.

For $n > 16$ the distributions of $U_{dBW}(p, n)$ are assumed to be normal. Distributions for $D/U(p, n)$, in decibels, are then normal with the mean, $D/U(50, n)$, and variance, $\sigma_{D/U}^2{}_n$, given by

$$D/U(50, n) = -1.5 - U_{dBW}(50, n) \text{ dB} \qquad \text{(A-11)}$$

$$\sigma_{D/U}^2{}_n = (0.5)^2 + \sigma_n^2 \text{ dB}^2 . \qquad \text{(A-12)}$$

For $n > 10^4$, the variance of $U_{dBW}(p, n)$ can be neglected in contrast to that of $D_{dBW}(p)$, 0.25 dB^2. Distributions of $D/U(p, n)$, in decibels, are then normal with a mean given by (A-11) and a variance of

$$\sigma_{p,n}^2 = (0.5)^2 \text{ dB}^2 \qquad \text{(A-13)}$$

The above discussion indicates that two techniques were used to obtain D/ U(p, n) distributions for n = 16 and n = 32. The results obtained, and the other D/ U(p, n) distributions determined for this study are shown in figure A. 5. Dashed lines show distributions resulting from the use of the technique discussed above for n ≤ 32.

Figure A. 5 is particularly useful when satisfactory service for the satellite is defined in terms of D/ U (protection ratio) that must be available or exceeded. For example, if a cochannel protection ratio >0 dB is required, then the time for which satisfactory service would be expected is <10% when interference from a single AM facility is considered. As another example, suppose that a signal ratio of -43 dB could be tolerated for adjacent-channel interference and that service is desired 99% of the time, then interference from 1000 adjacent-channel AM networks could be tolerated.

A. 2. 5 Modifications Required for Parameter Changes

The D/ U(p, n) distributions shown in figure A. 5 are dependent upon the specific parameters outlined in section A. 1. However, some parameters, such as satellite antenna gain (provided the beam is not made sufficiently narrow to discriminate against some undesired facilities), are noncritical in that a change will affect both the desired and undesired power equally, and the D/ U(p, n) distributions would remain valid. Other noncritical parameters are line loss at the satellite and free-space basic transmission loss between the earth and the satellite.

Modification of the parameters used in calculating the constant required for conversion to normalized desired signal power in section A 2. 1 would necessitate a similar modification of theD/ U(p, n)

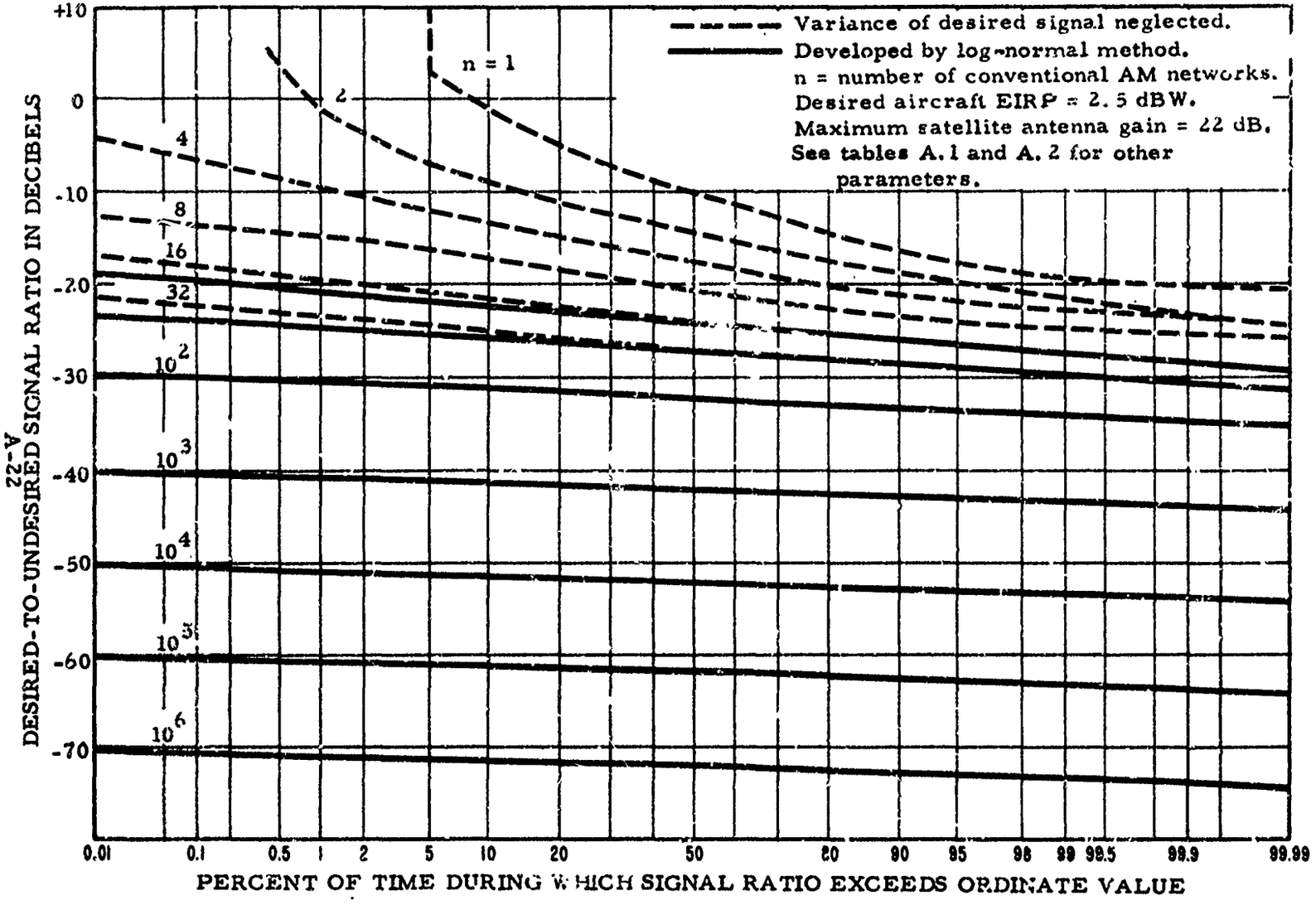

Figure A. 5. D/ U(p, n) at satellite terminal.

distributions, i.e., an increase of 3 dB in aircraft (desired) transmitter power would require that D/U values read from figure A.5 also be increased by 3 dB. For example, if (a) a D/U of 15 dB is required for satisfactory service, (b) service is required 95% of the time, and (c) frequency-sharing with 8 AM networks is desired then the -24 dB read from figure A.5 at the 95% level for n = 8 can be interpreted as meaning that the normalized desired station signal power must be increased by 39 dB (15 + 24) in order to achieve the desired frequency-sharing. The aircraft transmitting desired FM to the satellite could be modified to meet this objective by use of a circularly polarized antenna (3-dB increase) and an increase in the aircraft transmitter power by 36 dB to 35 dBW (~2 kW).

Figure A.5 can be used to estimate interference conditions caused by VHF extended range facilities (DeZoute, 1964; Grann, 1965) if we assume that the distributions for undesired power at the satellite remain unchanged in shape even though the levels involved may change. This requires that the constants used for conversion to normalized power for the airborne and ground stations differ from those of the AM network (sec. A.2.2), by about the same amount. An estimate of these constants for an extended range facility can be made as follows:

	Ground Station	Airborne Station
Transmitter power	(+) 33 dBW	(+) 27 dBW
Line loss	(-) 2 dB	(-) 1 dB
Polarization loss	(-) 3 dB	(-) 3 dB
Additional gain (reflection)	(+) 2 dB	0 dB
Antenna gain	(+) -4 dB (side-lobe)	(+) 4 dB
Extended range constants	26 dBW	27 dBW

Because these constants are 18 dB greater than those in section A.2.2, the D/U values read from figure A.5 should be decreased by 18 dB when this analysis is considered reasonable for extended range facilities.

In selecting parameters for the aircraft/satellite link and estimating the desired signal variability at the aircraft, we neglected the effects of reflection from the earth and ionospheric scintillation. Figure A. 5 can be used to estimate directly the number of AM networks tolerable when an allowance for these factors is included in the system design, if we assume that (a) the EIRP of the desired aircraft-to-satellite transmission is increased just enough to compensate for the additional signal attenuation at the encountered required time availability when service is not interference limited and (b) the number of tolerable AM networks is determined when the desired signal at the satellite is at its lowest acceptable level, e.g., an increase of 10 dB in desired transmission level required to overcome 10 dB of additional attenuation will provide the D/U in figure A. 5 when this attenuation is encountered (at required time availability).

Desired signal level distributions for the VHF satellite-to-aircraft link caused by earth reflection multipath or ionospheric scintillations are shown in figure A. 6. The point (-6 dB at 98. 6%) taken from NATO (1969, p. 42) is applicable to " . . . an aircraft flying over the North Atlantic somewhere between the southern tip of Greenland and Iceland. This flight path is at the edge of the region of maximum auroral disturbance, say at 60° N. geomagnetic latitude." It represents night hours and would be expected to be about half (3 dB) for daytime hours. Distributions "A" and "B" were taken from NATO (1969, p. 11), and Bergemann and Kucera (1969, fig. 3) respectively, and are based on experimental data. Distribution "C" is a Nakagami-Rice distribution (Rice et al., 1967, fig. VI, K = 4 dB) used to estimate a signal level distribution for the 7-to-15 dB equatorial scintillations reported by Kuegler (1969, p. 4). Although this distribution probably does not represent the worst equatorial scintillations possible, since

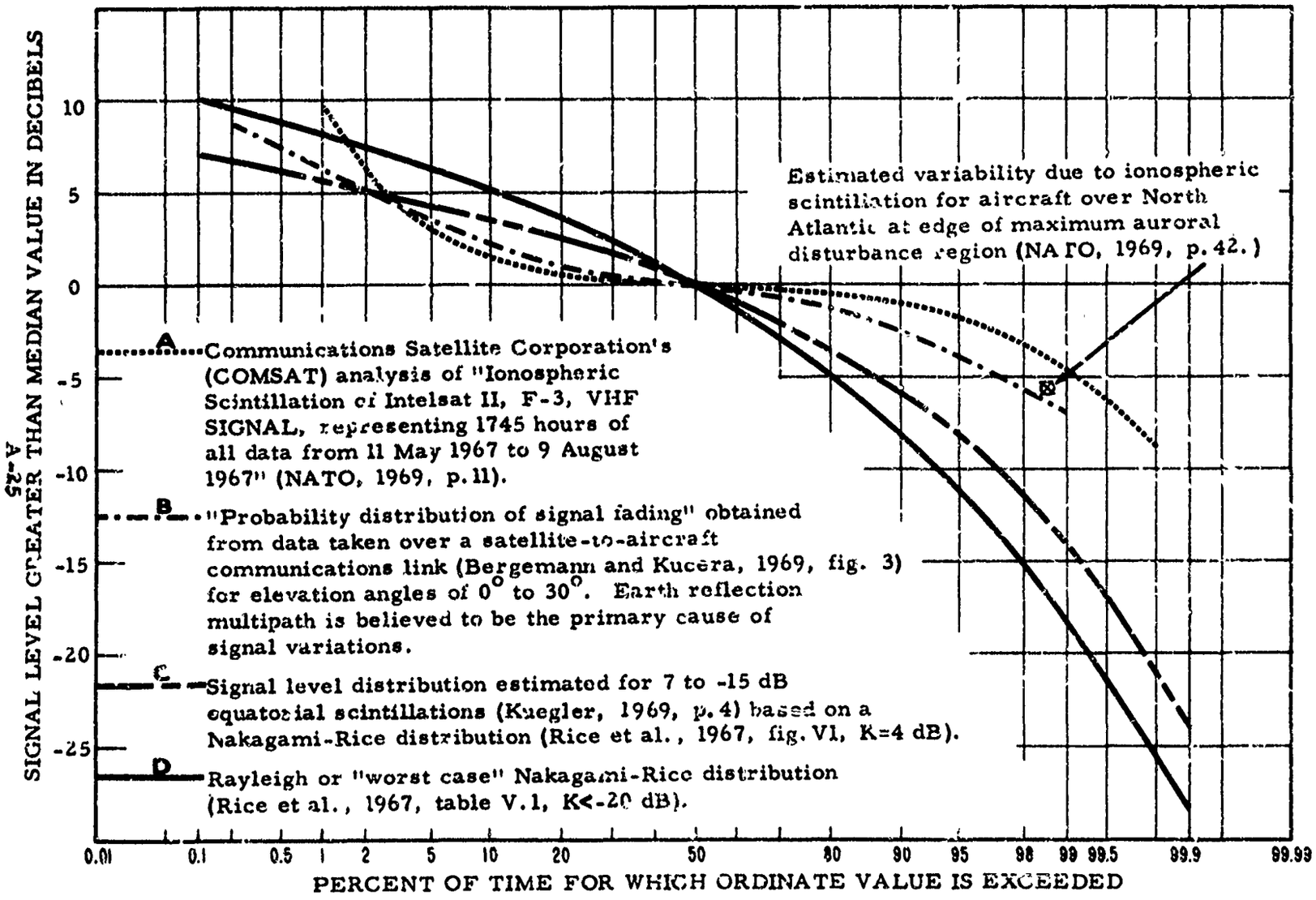

Figure A.6. Distributions of desired signal levels for VHF satellite-to-aircraft link.

the data were collected during July and maximum activity is expected during September (NATO, 1969, p. 65), it is applicable only to a period during which the fading occurs ("The evidence is that during periods of high sunspot number the extent of the high scintillation region near midnight is plus and minus 10°-15° from the geometric equator . . .," NATO, 1969, p. 57), and a distribution that includes the periods when less disturbed conditions are present would show less variability. A "worst case" Nakagami-Rice (Rice et al., 1967, table V.1, K < -20 dB) or Rayleigh distribution is shown as distribution "D" (Nesenbergs, 1967).

Figure A.6 implies that an increase in desired signal transmission level sufficient to achieve a 99% reliability during disturbed periods would be (a) 10 dB when the aircraft is at the edge of the maximum auroral disturbance region, and (b) 15 to 20 dB when strong equatorial scintillations are encountered. The requirement for such large increases in signal transmission level could be reduced by (a) compensation for poor propagation conditions in the areas and during the time for which it is expected by reducing the air traffic density so that a lower communication reliability could be safely tolerated, (b) use of polarization diversity, and (c) use of a higher frequency that would be less effected by the ionosphere.

Takahashi's (1969) analysis suggests that polarization diversity may be useful in combating ionospheric scintillations. This is not in accord with information given by NATO (1969, p.43) and Golden (1970) which indicates that polarization diversity (also frequency and space diversity) would be ineffective for aircraft use. However, polarization diversity would be expected to be effective in reducing earth reflection multipath when the transmitted wave is circularly polarized and the aircraft-to-satellite look angle is greater than about 12°. For these

look angles, the phase lag associated with a specular reflection for horizontal polarization differs by about 180° from that for vertical polarization (Rice et al., 1967, figs. III. 1 to III. 8).

Detrimental ionospheric effects decrease with increasing frequency (Little et al., 1964), and operation at 1, 500 MHz instead of 130 MHz would be expected to eliminate ionospheric scintillation or at least reduce it considerably. But, the use of circular polarization and/ or polarization diversity to combat Faraday rotation and earth reflection multipath would still be desirable. Systems more complex than the single-channel FM-voice system assumed here, such as those with a direct navigation and/ or surveillance function, may encounter problems at VHF with transmission through the ionosphere, such as angle-of-arrival fluctuations that cannot be solved simply by increasing transmitter powers. Such systems may benefit more from operation at a higher frequency than the voice system considered here (Haydon, 1970).

The curves in figure A. 5 can also be used to estimate interference conditions that might exist if the 1, 540 to 1, 570-MHz band were used for the aircraft/ satellite link, if various assumptions are made. One possible set of such assumptions is as follows:

(1) The distributions for desired and undesired power at the satellite terminal would remain unchanged in shape even though the levels might change.

(2) The transmitter powers for AM network service are increased by 22 dB in order to overcome the increase in free-space basic transmission loss caused by the increase in frequency.

(3) The 22-dB increase in free-space basic transmission loss for the desired aircraft-to-satellite link is overcome by

use of a circularly polarized aircraft antenna (3-dB gain), increasing the aircraft transmitter power by 19 dB (18 dBW total), and increasing the power of the satellite transmitter by 19 dB (19 dBW total).

This set of assumptions would allow the D/U values in figure A.5 to be used directly. If an increase of AM network powers of only 12 dB is assumed (instead of 22 dB), the D/U values in figure A.5 would be too low by 10 dB.

The modifications discussed above were included to illustrate how the curves shown in figure A.5 can be used to estimate interference conditions when system parameters differ from those assumed in developing the curves. Various assumptions are required to make these estimates, and their validity may be somewhat questionable in some cases. For example, the side-lobe antenna gains assumed in the discussion of extended range could be in error by several decibels. Better estimates can be made for situations in which the system parameters differ from those assumed for this analysis by repeating the analysis for the specific parameters of interest.

A.3. Interference to Conventional AM Networks

This section deals with the effect of satellite transmissions on the service range of AM networks that are directly illuminated by the satellite. A "worst case" approach is taken to this problem and curves are given that show the maximum service range reduction that could be required to overcome interference from the satellite versus normal AM network service range for various levels of desired-to-undesired signal ratios. AM networks are assumed to be most sensitive to interference at airborne receiving stations.

The distribution of undesired power available from the satellite at the terminals of an airborne receiving station of an AM network from the satellite can be obtained from the distribution labeled "airborne terminal . . ." in figure A. 3 by adding -157.2 dB to the indicated power levels. This conversion constant is determined by adding the difference (-12. 9 dB) in satellite-radiated power (0. 1 - 1 = -0. 9 dBW, table A. 1) and total AM aircraft-radiated power (14 + 1 - 3 = 12 dBW, sec. A. 2. 2) to the denormalization constant (-145. 8) given in figure A. 3, then adding 1. 5 dB to compensate for the fact that the lowest free-space transmission loss was not used in calculating the -145. 8 dB. If we assume that the satellite transmits continuously, the distribution shown in figure A. 3 (for airborne terminal) can be used directly as an estimate of the undesired power received from the satellite by an aircraft using a conventional AM ground ATC facility, provided the level adjustment just discussed is made. For example, an estimate of the maximum interfering power can be made by reading the highest level on the figure A. 3 distribution (18 dBW) and adding -157. 2 to it, i. e., 18 - 157. 2 ≃ -139 dBW.

For analysis of the AM network maximum service range reduction that could be required to overcome interference from the satellite, the normal service range of AM network is defined as the range at which the desired (from the ground AM facility) power available at the terminals of the aircraft antenna is -120 dBW (with 3-dB line loss, 5 uV across 50 Ω at receiver input), and the maximum undesired (from satellite) power available at the aircraft antenna terminals is taken as -139 dBW. Under these conditions the minimum D/ U, D/ U(min), at the normal service range is 19 dB.

To estimate the maximum reduction in service range required to assure D/ U(min) levels greater than 19 dB, we assumed that the

desired signal will increase as the distance (altitude fixed) to the ground facility is decreased and that the lowest increase, ΔD, in desired power for a decrease in distance from the normal range, R_N nm, to a reduced range, R_R nm, is given by

$$\Delta D = 20 \log \frac{R_N}{R_R} \quad \text{dB} . \qquad \text{(A-14)}$$

The distance dependence in (A-14) is the same as that associated with transmission loss in free space. The equation can be rearranged to give the range reduction, ΔR, required to achieve ΔD, i.e.,

$$\Delta R = R_N - R_R = R_N \left(1 - 10^{-\frac{\Delta D}{20}}\right) \text{ nm}, \; R_R \leq R_N . \qquad \text{(A-15)}$$

Values of D/ U(min) are related to ΔD by

$$D/U(\text{min}) = 19 + \Delta D \text{ dB}, \; R_R \leq R_N . \qquad \text{(A-16)}$$

The relationship between R_N, ΔR, and D/ U(min) is shown in figure A. 7. For example, if a D/ U(min) of 19 dB or less is sufficient to assure satisfactory service for the AM network, then no reduction in the normal range would be caused by interference from the satellite. If, on the other hand, a D/ U(min) of 25 dB is required and the normal service range of 200 nm, the maximum reduction of operating range expected because of interference from the satellite is 100 nm, and the operating range would be reduced from 200 to 100 nm.

If the normal service range is near or beyond the radio horizon, then the service range reduction indicated by figure A. 7 would be expected to be more than sufficient to assure satisfactory service for distances equal to or less than the normal service range reduced by the indicated amount, i.e., the range reduction indicated

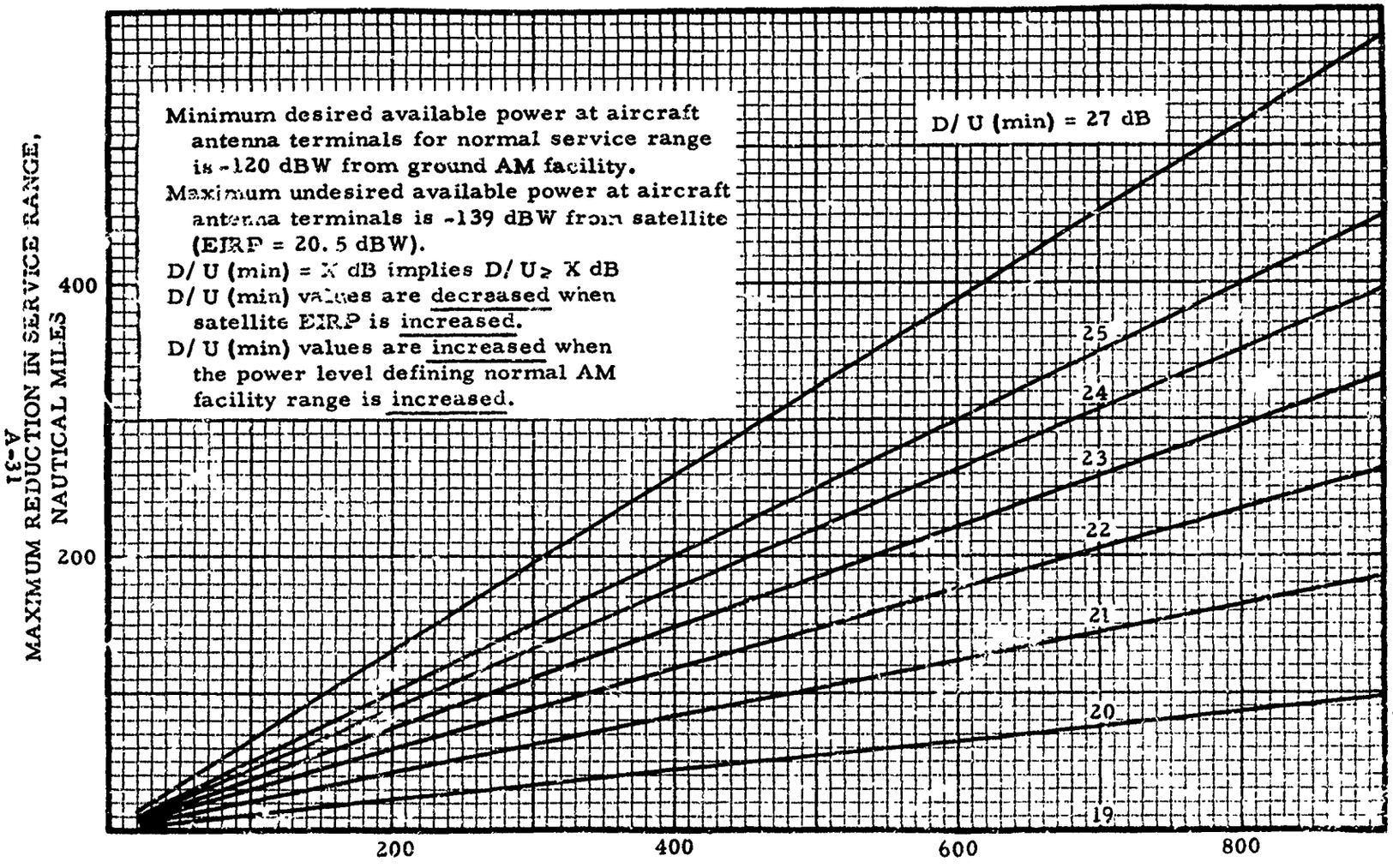

Figure A.7. Conventional AM network service range reduction caused by interference from satellite.

for these cases is expected to be too large by an amount that will be dependent upon the propagation parameters (terrain profile, terminal heights, etc.) involved in specific cases. When the desired signal does not increase with decreasing range (lobing) in the vicinity of the normal service range, the range reduction indicated may not be sufficient to assure satisfactory service. However, this is not considered to be a serious restriction, because the normal service range is most likely to be near or beyond the radio horizon.

Values of D/U(min) given in figure A.7 can be modified to account for parameter changes. For example, if the gain of the satellite antenna (satellite power unchanged) is decreased by several decibels, then the D/U(min) values should be increased by a similar amount. Application to an extended range facility might require that the power level used to define the normal service range be decreased by several decibels; then the D/U(min) values should be decreased by a similar amount.

As mentioned previously, the analysis used in developing figure A.7 is of the "worst-case" type, and range reductions determined from it (with system parameter changes properly considered) will be sufficient for "almost all" situations likely to occur. Better estimates can be made for particular situations if such information as terrain profiles, and antenna elevations is used, but the number of such special cases could easily become so large as to become unmanageable.

A.4. Frequency Sharing Implications

Estimates are shown in figure A.5 of the RF D/U available at the satellite when interference from a multitude of AM networks is considered. The methods used to make these estimates and

modifications that can be made to account for changes in system parameters are discussed in section A.2.5. Estimates of the extent to which the service range of AM networks can be reduced because of interference caused by satellite transmissions are shown in figure A.7. The development and possible modifications of these estimates were discussed in section A.3. Protection ratio values required to interpret the curves shown are discussed in section 4.

The following observations concerning interference can be made:

(1) To allow cochannel operation of the satellite system with a small (4) number of conventional facilities, the satellite receiver would have to be capable of providing satisfactory performance when the desired signal is 25 dB below the undesired signal; i.e., the required protection ratio must be -25 dB or lower. Thus, it is likely that a clear channel will be required for the satellite system.

(2) Significant service range reductions will be encountered for conventional facilities when they are operated cochannel with the satellite system if a protection ratio higher than 19 dB is required. This may provide another reason for a clear channel assignment to the satellite system.

(3) A required adjacent-channel protection ratio at the satellite as high as -45 dB would allow adjacent-channel operation with a significant number (10^3) of conventional facilities. However, the allowed number of stations must be divided between two channels since there are two adjacent channels.

(4) A service range reduction for conventional facilities because of adjacent-channel interference from the satellite would not be expected, because a required protection ratio as high as 19 dB could be tolerated.

These observations might have to be changed to some extent as changes in system parameters are considered. In this analysis we have assumed that all stations are within the horizon of the satellite, and frequency-sharing on a cochannel basis between a satellite system and AM networks should be possible if the AM networks are located sufficiently distant beyond the horizon of the satellite.

APPENDIX B
Modulation Characteristics

This appendix summarizes the fundamental characteristics of the basic analog and digital modulation methods for the ATC system and describes the salient features of the signal in a communication system. Emphasis is given to certain parameters of greater importance than others in relation to the systems and frequency bands considered, which are presented as practical considerations and constraints in system design and band planning. We concentrate on the information signal (which in this report we shall consistently refer to as the baseband signal) and its effect on the description of the modulated waveforms. The material has been condensed from a report by Hubbard et al. (1970).

The process of modifying carrier signals by an information signal is viewed in the classical sense of modulation as the operation of the baseband signal on the carrier. This process can be divided into two subclasses for analog modulation: linear and exponential. Each of these has a counterpart in digital schemes, as will be noted in section B.2.

Modulation can also be considered as a process operating directly on the baseband signal, rather than on the carrier as in the classical approach (Bedrosian, 1962). Both of these concepts are used here to describe analog modulation schemes. The classical concept is perhaps more useful in considering the actual physical or practical process of developing a modulated signal for transmission, while the more recent approach, based on signal-product concpets, is more useful in directly describing the spectral characteristics of the modulated signal. This is especially true for single-sideband (SSB) signals.

B. 1. Summary of Analog Modulation Methods

In analog modulation, the carrier waveform is assumed to be sinusoidal with constant amplitude A_0, constant angular frequency ω_0, and initial phase θ_0 and is expressed as

$$E_0(t) = A_C \cos(\omega_0 t + \theta_0) , \tag{B-1}$$

where $(\omega_0 t + \theta_0)$ is the total phase and can be written as

$$\varphi_0(t) = \omega_0 t + \theta_0 . \tag{B-2}$$

The time derivative of this expression is the angular frequency ω_0:

$$\dot{\varphi}_0(t) = \omega_0 = 2\pi f_0 . \tag{B-3}$$

Three separate parameters of the carrier waveform can be varied to modulate this signal in accordance with a baseband signal. These are the amplitude, frequency, and phase, each of which may become a function of time. Thus the modulated carrier can be expressed in general as

$$E_M(t) = A(t) \cos \varphi(t) , \tag{B-4}$$

where A(t) is the instantaneous amplitude, and $\varphi(t)$ is the instantaneous phase of the modulated carrier. The analog modulation techniques can be described as amplitude modulation (AM), phase modulation (PM), and frequency modulation (FM). In AM the instantaneous amplitude A(t) is made to vary with the baseband signal. In PM and FM, the angular frequency is caused to vary by modulating $\varphi(t)$ in accordance with the baseband signal. Each of these techniques can be considered by writing

the time variant parameters in terms of the unmodulated carrier as follows:

$$A(t) = a(t)\, A_0 \qquad \text{AM},$$

and

$$\omega(t) = \theta(t) + \omega_0 \qquad \text{PM},$$

$$\dot{\omega}(t) = \dot{\theta}(t) + \omega_0 \qquad \text{FM}.$$

Based on these relationships, we can write the modulated carrier waveform as

$$E_M(t) = a(t)\, A_0 \cos\left[\omega_0 t + \vartheta_0 + \theta(t)\right] . \qquad \text{(B-5)}$$

This expression can be used to define all the analog modulation methods by specifying how the carrier parameters depend upon the baseband signal $E_B(t)$. For example, to describe AM, we must specify the manner in which $a(t)$ depends on $E_B(t)$. In PM the phase $\theta(t)$ is caused to vary directly with $E_B(t)$, and in FM $\dot{\theta}(t)$ is proportional to $E_B(t)$. However, before discussing the individual features of these forms of modulation, we will use a normalized form of the modulated carrier in (B-5) to simplify later notation.

If we make certain assumptions about the total communication system between the modulator and the input to the receiver detector, a normalized expression for the modulated waveform will be useful at all intervening points of the system. The two necessary assumptions are that all intervening stages of the system are time-invariant and cause no appreciable distortion to the signal. Thus, if we normalize the expression (B-5) by the amplitude of the unmodulated carrier A_0, we can define

$$e_M(t) = \frac{E_M(t)}{A_0} = a(t) \cos\left[\omega_0 t + \theta(t)\right] , \qquad \text{(B-6)}$$

where the arbitrary phase angle θ_0 has been ignored without loss of generality. It follows that if we wish to write an expression for the

modulated waveform at any point in the system between the modulator and detector, we need only multiply (B-6) by the appropriate equivalent carrier amplitude at the desired point. This value can be determined from knowledge of the total gain and/or loss parameters from point to point in the system.

Similarly, we can write for convenience a normalized expression for the baseband signal $E_B(t)$. Normalization is made with respect to the peak value of the signal $\hat{E}_B$ and becomes

$$e_B(t) = \frac{E_B(t)}{\hat{E}_B} \tag{B-7}$$

In the classical description of modulation, we apply the modulating or baseband signal $e_B(t)$ directly to one of the time parameters of the unmodulated carrier wave of (B-6). Forexample, linear AM is accomplished by letting

$$a(t) = 1 + M\, e_B(t)\,, \tag{B-8}$$

where M is the modulation index, and we write the modulated waveform as

$$\begin{aligned} e_M(t) &= [1 + M\, e_B(t)]\ \cos[\omega_0 t + \theta(t)] \\ &= \cos[\omega_0 t + \theta(t)]\ + M\, e_B(t)[\cos\ \omega_0 t + \theta(t)]\ . \end{aligned} \tag{B-9}$$

This expression is composed of a pure carrier component of constant amplitude and a modulated component that has a particular spectrum. Other forms of linear and exponential modulation can be considered similarly; for example, if $a(t) = M\, e_B(t)$ in (B-8), then the resultant modulation is AM double sideband suppressed carrier (AM-DSB/SC).

In the transmission of such signals, we are concerned with their spectral characteristics, i.e., their bandwidth occupancy and power density. The two linear forms above are relatively simple to visualize

in spectrum. However, other forms, such as SSB and exponential modulation, are more difficult. Description of these forms is more straightforward if we use the signal-product concept mentioned earlier.

To describe modulation processes in signal-product form, we use analytic signal notation (summarized below), and from this notation we can readily develop the spectra for these signals. The Fourier operator is used frequently for the transform of signals between the time and frequency domains, which is defined by the transform pair as

$$F[x(t)] = X(\omega) = \int_{-\infty}^{\infty} x(t)\, e^{-j\omega t}\, dt, \qquad \text{(B-10a)}$$

and

$$x(t) = \frac{1}{2\pi} \int_{-\infty}^{\infty} X(\omega)\, e^{j\omega t}\, d\omega, \qquad \text{(B-10b)}$$

where F[ ] denotes the Fourier transform operator and X(ω) is the spectral function of the real signal x(t).

A complex function of time can be written

$$g(t) = x(t) + jy(t) = |g(t)|\, \exp j\theta(t), \qquad \text{(B-11)}$$

where x(t), y(t), $|g(t)|$, and θ(t) are all real-time functions that have the following relationships:

$$|g(t)|^2 = x^2(t) + y^2(t), \qquad \text{(B-12)}$$

$$\theta(t) = \tan^{-1}[y(t)/x(t)], \qquad \text{(B-13)}$$

and

$$x(t) = \text{Re } g(t) \qquad y(t) = \text{Im } g(t), \qquad \text{(B-14)}$$

where Re = real part and Im = imaginary part.

We also introduce the notation $g^*(t)$, where * indicates the complex conjugate

$$g^*(t) = x(t) - jy(t) . \qquad \text{(B-15)}$$

Analytic signal notation makes use of the fact that the mathematical analysis of real-time functions is often simplified by replacing the real signal with a complex function, such as g(t) in (B-11) (Bedrosian, 1962). If we apply this technique, the real signal of interest is taken as Re g(t) or $\frac{1}{2}[g(t) + g^*(t)]$. The imaginary part of the complex signal can be selected almost arbitrarily (Baghdady, 1961), but many authors have demonstrated that the most convenient function to select for the imaginary part of the representation is the Hilbert transform of the real part x(t). In this report the use of a Hilbert transform pair is made an integral part of the definition of an analytic signal. With this definition, (B-11) becomes

$$\underline{g}(t) = x(t) + j\overset{\vee}{x}(t) , \qquad \text{(B-16)}$$

where $\underline{g}(t)$ is used to denote the analytic signal. The imaginary part of $\underline{g}(t)$ in (B-16) is the Hilbert transform of x(t) described mathematically as the operation H[x(t)] and is written as

$$\overset{\vee}{x}(t) = H[x(t)] = \frac{1}{\pi} \int_{-\infty}^{\infty} \frac{x(\tau)}{t - \tau} \, d\tau , \qquad \text{(B-17)}$$

where $\int$ indicates the Cauchy principle value.

We see from the definition of the convolution integral (Stein and Jones, 1967) that (B-17) can also be written as

$$\overset{\vee}{x}(t) = x(t) \otimes \frac{1}{\pi t} , \qquad \text{(B-18)}$$

where the symbol $\otimes$ is used to denote the convolution process defined as

$$x(t) \otimes y(t) = \int_{-\infty}^{\infty} x(t)\, y(t-\tau)\, d\tau \,. \qquad \text{(B-19)}$$

By applying the following transform identity (Baghdady, 1961)

$$F[x(t) \otimes y(t)] = X(\omega) \cdot Y(\omega) \,, \qquad \text{(B-20)}$$

the transform of (B-18) yields

$$\overset{\vee}{X}(\omega) = j[\delta_{-1}(-\omega) - \delta_{-1}(\omega)]\; X(\omega) \,, \qquad \text{(B-21)}$$

where $\delta_{-1}(\omega)$ is the unit step function and is defined as

$$\delta_{-1}(\omega) = \int_{-\infty}^{\omega} \delta_0(x)\, dx \,, \qquad \text{(B-22)}$$

and $\delta_0(x)$ is the unit impulse function. From (B-21), we note that the Hilbert transform has had the following effects on the spectrum $X(\omega)$:

(a) The spectrum on the $\omega > 0$ axis has been phase shifted by $-j$ or $-90°$.

(b) The $\omega < 0$ portion of the spectrum has been phase shifted by $+j$ or $+90°$.

This can be written in terms of a transfer function for the Hilbert transform as

$$H_H(\omega) = -j\, \mathrm{sgn}(\omega) \,,$$

where

$$\mathrm{sgn}(\omega) = \begin{cases} +1, & \omega > 0 \\ 0, & \omega = 0 \,. \\ -1, & \omega < 0 \end{cases} \qquad \text{(B-23)}$$

The equivalent expression for (B-21) is then

$$\overset{\vee}{X}(\omega) = -j\, \mathrm{sgn}(\omega) \cdot X(\omega) \,. \qquad \text{(B-24)}$$

This spectral property of the Hilbert transform has special significance when applied to an analytic signal. To see this significance we shall find the spectrum of the signal in (B-16). Taking Fourier transforms of both sides of that expression and using (B-24), we obtain

$$\begin{aligned} \underline{G}(\omega) &= X(\omega) + j \overset{\vee}{X}(\omega) \\ &= X(\omega) + j[-j\,\mathrm{sgn}(\omega)]\; X(\omega) \\ &= [1 + \mathrm{sgn}(\omega)]\; X(\omega) . \end{aligned} \tag{B-25}$$

Applying the definition of sgn(ω) in (B-23), we see that

$$\underline{G}(\omega) = \begin{cases} 2\,X(\omega), & \omega > 0 \\ X(0), & \omega = 0 \\ 0, & \omega < 0 \end{cases} , \tag{B-26}$$

which has no spectrum on the $\omega < 0$ axis. Thus, (B-26) shows that the spectrum of an analytic signal is single sided, and this property is very useful in describing SSB modulation forms.

The two transforms (Fourier and Hilbert) discussed above and the analytic signal notation are used to describe the spectral properties of several signal notations. These are summarized in table B.1. Signal-product notation for modulated signals is based upon a modulation function m(t) and an exponential carrier function

$$e_0(t) = \exp j\,\omega_0 t . \tag{B-27}$$

Repeating an earlier premise that modulation is a process of multiplying two functions, such as m(t) and the carrier of (B-27), we obtain the modulated waveform

$$e_M(t) = m(t) \exp j\,\omega_0 t . \tag{B-28}$$

Taking Fourier transforms of (B-28) and using the results in table B.1, we find the general spectrum of the modulated wave to be

Table B.1. Time and spectral functions.

Time Function	Description of Time Function	Spectral Function	Description of Spectral Function	Special Characteristics
$x(t)$	Real time function	$X(\omega)$	Complex, two-sided, containing spectral components for $\omega > 0$ and $\omega < 0$	$X(-\omega) = X^*(\omega)$
$g(t)$	$g(t) = x(t) + j\,y(t)$ Complex time function with arbitrary imaginary part, $x(t)$ and $y(t)$ both real	$G(\omega)$	Complex, two-sided function with no general symmetry	$G(\omega) = X(\omega) + j\,Y(\omega)$ $G(-\omega) = X(-\omega) + j\,Y(-\omega)$ $= X^*(\omega) + j\,Y^*(\omega)$ $G^*(\omega) = X^*(\omega) - j\,Y^*(\omega)$
$g^*(t)$	$g^*(t) = x(t) - j\,y(t)$ Complex conjugate of $g(t)$ above	$F[g^*(t)] = G^*(-\omega)$ Folded conjugate of $G(\omega)$	Complex, two-sided function with no general symmetry	$G^*(-\omega) = X(\omega) - j\,Y(\omega)$
$\overset{\vee}{x}(t)$	$\overset{\vee}{x}(t) = x(t) * \frac{1}{\pi t}$ Hilbert transform of a real function $x(t)$	$\overset{\vee}{X}(\omega) = -j\,\mathrm{sgn}(\omega)\,X(\omega)$ Where $\mathrm{sgn}(\omega) = \begin{cases} +1, & \omega>0 \\ 0, & \omega=0 \\ -1, & \omega<0 \end{cases}$	Complex, two-sided function derived from $x(\omega)$ as follows: $\omega > 0$, $X(\omega)$ shifted -90°; $\omega < 0$, $X(\omega)$ shifted $+90^\circ$	$\overset{\vee}{X}(\omega) = \begin{cases} -j\,X(\omega), & \omega > 0 \\ +j\,X(\omega), & \omega < 0 \end{cases}$
$\underline{g}(t)$	$\underline{g}(t) = x(t) + j\overset{\vee}{x}(t)$ Complex, analytic function, $x(t)$ a real function	$\underline{G}(\omega) = X(\omega) + j\overset{\vee}{X}(\omega)$ $= [1 + \mathrm{sgn}(\omega)]\,X(\omega)$	Complex function, single-sided with no negative frequency spectrum	$G(\omega) = \begin{cases} 2\,X(\omega), & \omega > 0 \\ X(0), & \omega = 0 \\ 0, & \omega < 0 \end{cases}$
$\underline{g}^*(t)$	$\underline{g}^*(t) = x(t) - j\overset{\vee}{x}(t)$ Complex conjugate of analytic function $\underline{g}(t)$	$\underline{G}^*(-\omega) = X(\omega) - j\overset{\vee}{X}(\omega)$ $= [1 - \mathrm{sgn}(\omega)]\,X(\omega)$ $= F[\underline{g}^*(t)]$	Complex function, single-sided with no positive frequency spectrum	$\underline{G}^*(-\omega) = \begin{cases} 0, & \omega > 0 \\ X(0), & \omega = 0 \\ 2\,X(\omega), & \omega < 0 \end{cases}$
$e_o(t)$	$e_o(t) = \exp j\omega_o t$ A complex function represented by a rotating unit vector. Also an analytic signal.	$\Phi(\omega) = 2\pi\,\delta_o(\omega - \omega_o)$	A unit impulse located on the $\omega > 0$ axis at $\omega = \omega_o$	$\Phi^*(\omega) = \Phi(-\omega)$ $= 2\pi\,\delta_o(\omega + \omega_o)$
$x(t) \cdot y(t)$	The product of two arbitrary time functions. $x(t)$ and $y(t)$ may be real or complex.	$F[x(t) \cdot y(t)]$ $= \frac{1}{2\pi}[X(\omega) \circledast Y(\omega)]$	Convolution of the spectra $X(\omega)$ and $Y(\omega)$	Conversely: $F[x(t) \circledast y(t)] = X(\omega) \cdot Y(\omega)$

$$\Phi_M(\omega) = M(\omega - \omega_0) \; , \tag{B-29}$$

where $M(\omega)$ is the spectrum of the modulation function $m(t)$.

Equation (B-29) states that the spectrum of the modulated waveform will be precisely that of the modulation function, relocated from a reference of $\omega = 0$ to $\omega = \omega_0$ (the carrier frequency). Since (B-29) is obtained from an analytic signal, this general result does not represent the spectrum of a real modulated signal. The latter, however, can easily be obtained.

We recall that the real carrier signal can be written as $\frac{1}{2}[e_0(t) + e_0^*(t)]$, and, using table B.1 for the spectrum of analytic signals, we write the spectrum of the real carrier as

$$\begin{aligned} F[\text{Re } e_0(t)] &= F\{\tfrac{1}{2}[e_0(t) + e_0^*(t)]\} \\ &= \pi[\delta(\omega - \omega_0) + \delta(\omega + \omega_0)] \; , \end{aligned} \tag{B-30}$$

from which we note that, in terms of a real carrier, the spectrum of the modulation function will be translated to the region of the carrier frequency on both the positive and negative frequency axis. The complete modulated wave spectrum for a real carrier can then be written in the general form

$$\Phi_M(\omega) = \tfrac{1}{2}[M(\omega - \omega_0) + M^*(-\omega - \omega_0)] \; . \tag{B-31}$$

This equation can be used to evaluate the modulated waveform spectra for a variety of modulation functions.

B.1.1 The Modulated Signal

The modulating signal in the signal-product notation is considered as the modulation function $m(t)$, which is related in a prescribed manner to a function we shall call the baseband function $b(\tau)$. The latter is in turn related to the information signal $e_s(t)$ that is to be transmitted. These relationships for the analog modulation methods are tabulated in

table B. 2, in which the normalized modulated signal is given. Also, based on entries in table B. 1 and on (B-31), the spectral expressions for the modulation function and the modulated carrier signal are given for the linear forms. Note that these spectral functions are written in terms of the spectra of the baseband functions $\Phi_B(\omega)$. In all of the linear forms we note that the modulated signal spectra are either SSB or DSB signals that contain replicas of the baseband spectra in the region of the carrier frequency. The spectra of the baseband signals are discussed in section B. 1. 3. The factors β_f and β_p in table B. 2 are the modulation indicies for the exponential forms, FM and PM respectively.

Because of the nonlinear nature of the modulation function in the exponential forms, the spectra for these modulated waves cannot be derived simply. Estimates of their shape and spectral extent can be made, however. Two principal papers on this subject are those by Abramson (1963) and Hollingworth (1967). Their results are summarized in a report by Hubbard et al. (1970, sec. 2. 6. 1) for a general baseband function. For a single sinusoidal modulating signal, the modulated spectra can be estimated on the basis of Bessel functions. Curves useful for this purpose are shown in figure B. 1, where the Bessel function $J_n(\beta)$ of the first kind and order n is plotted versus the parameter n/β (Baghdady, 1961). Actually these are not continuous curves when n is taken in discrete values, but they are useful in estimating both the shape and extent of the modulated spectra when plotted as continuous functions. For example, consider an FM system with a peak deviation $\Delta F = 5$ kHz modulated with a 1-kHz sinusoid (f_s). Then,

$$\beta_f = \frac{\Delta F}{f_s} = 5 .$$

The total number of sideband components considered important to the signal estimate is usually based on an assumption that components

Table B.2. Analog modulation characteristics.

Class	Modulation Designation	Modulation Function $m(t)$	Normalized Baseband Function $b(t)$	Normalized Modulated Carrier $e_m(t)=\mathrm{Re}\left[m(t)\exp j\omega_o t\right]$	Spectrum of Modulation Function $M(\omega)$	Spectrum of Modulated Carrier $\Phi_M(\omega)$
LINEAR	AM-DSB/SC	$b(t)$	$Ne_B(t)$	$Ne_B(t)\cos\omega_o t$	$N\Phi_B(\omega)$	$\frac{N}{2}\left[\Phi_B(\omega-\omega_o)+\Phi_B(\omega+\omega_o)\right]$
	AM	$b(t)$	$1+Ne_B(t)$	$\left[1+Ne_B(t)\right]\cos\omega_o t$	$\delta(\omega)+N\Phi_B(\omega)$	$\frac{1}{2}\left[\delta(\omega-\omega_o)+\delta(\omega+\omega_o)\right]$ $+\frac{N}{2}\left[\Phi_B(\omega-\omega_o)+\Phi_B(\omega+\omega_o)\right]$
	AM-SSB/U	$\underline{b}(t)$	$N\left\{e_B(t)+j\check{e}_B(t)\right\}$	$N\left[e_B(t)\cos\omega_o t - \check{e}_B(t)\sin\omega_o t\right]$	$N\left[1+\mathrm{sgn}(\omega)\right]\Phi_B(\omega)$	$\frac{N}{2}\left\{\left[1+\mathrm{sgn}(\omega-\omega_o)\right]\Phi_B(\omega-\omega_o)\right.$ $\left.+\left[1-\mathrm{sgn}(\omega+\omega_o)\right]\Phi_B(\omega+\omega_o)\right\}$
	AM-SSB/L	$\underline{b}^*(t)$	$N\left[e_B(t)-j\check{e}_B(t)\right]$	$N\left[e_B(t)\cos\omega_o t + \check{e}_B(t)\sin\omega_o t\right]$	$N\left[1-\mathrm{sgn}(\omega)\right]\Phi_B(\omega)$	$\frac{N}{2}\left\{\left[1-\mathrm{sgn}(\omega-\omega_o)\right]\Phi_B(\omega-\omega_o)\right.$ $\left.+\left[1+\mathrm{sgn}(\omega+\omega_o)\right]\Phi_B(\omega+\omega_o)\right\}$
EXPONENTIAL	PM	$\exp jb(t)$	$\beta_p e_B(t)$	$\cos\left[\omega_o t+\beta_p e_B(t)\right]$		
	FM	$\exp jb(t)$	$\beta_f\int e_B(t)dt$	$\cos\left[\omega_o t+\beta_f\int e_B(t)dt\right]$		
	PM-SSB/U PM-SSB/L	$\exp j\underline{b}(t)$ $\exp j\underline{b}^*(t)$	$\beta_p\underline{e}_B(t)$	$\exp\mp\beta_p\check{e}_B(t)$ $\cos\left[\omega_o t+\beta_p e_B(t)\right]$		
	FM-SSB/U FM-SSB/L	$\exp j\underline{b}(t)$ $\exp j\underline{b}^*(t)$	$\beta_f\int\underline{e}_B(t)dt$	$\exp\mp\beta_f\int\check{e}_B(t)dt$ $\cos\left[\omega_o t+\beta_f\int e_B(t)dt\right]$		

Note: See text for spectral estimates of the exponential modulation forms.

below a certain value are insignificant. Thus, assume that those components below 0.1 times the unmodulated carrier can be ignored. In figure B.1 from the curve $\beta = 5$, we read a value of n/β at $J_n(\beta) < 0.1$ as

$$\frac{n}{\beta} \simeq 1.3$$

or

$$n = 1.3\,\beta = 6.5 .$$

In this case it is only necessary to consider the first six or seven orders of Bessel functions to describe the modulated waveform. Also, since $\beta_f = \Delta F / f_m$, we can write

$$\frac{n}{\beta_f}\Delta F = n f_m ,$$

and we recognize $n f_m$ as the maximum frequency in the modulated signal. Thus, the approximate bandwidth of the modulated spectrum is given by

$$B_m = 2\,\frac{n}{\beta_f}\Delta F = 2\,n f_m = 2 \times 6.5 \times 1 = 13\ \text{kHz} ,$$

where the factor 2 accounts for both sidebands, and the general shape of the upper sideband spectrum ($\omega > \omega_0$) is that of the $\beta = 5$ curve in figure B.1. If several sinusoids are used to modulate the carrier, each can be treated as above, and the total spectrum will become the sum of several curves similar to those in figure B.1. This procedure becomes cumbersome with more complicated baseband signals, and the methods referenced previously are suggested for these cases (Abramson, 1963; Hollingworth, 1967).

The spectral estimate for the single sinuosidal case above is similar to the familiar Carson's rule, which can be used to estimate the modulated signal bandwidth for a general baseband signal. It gives no estimate,

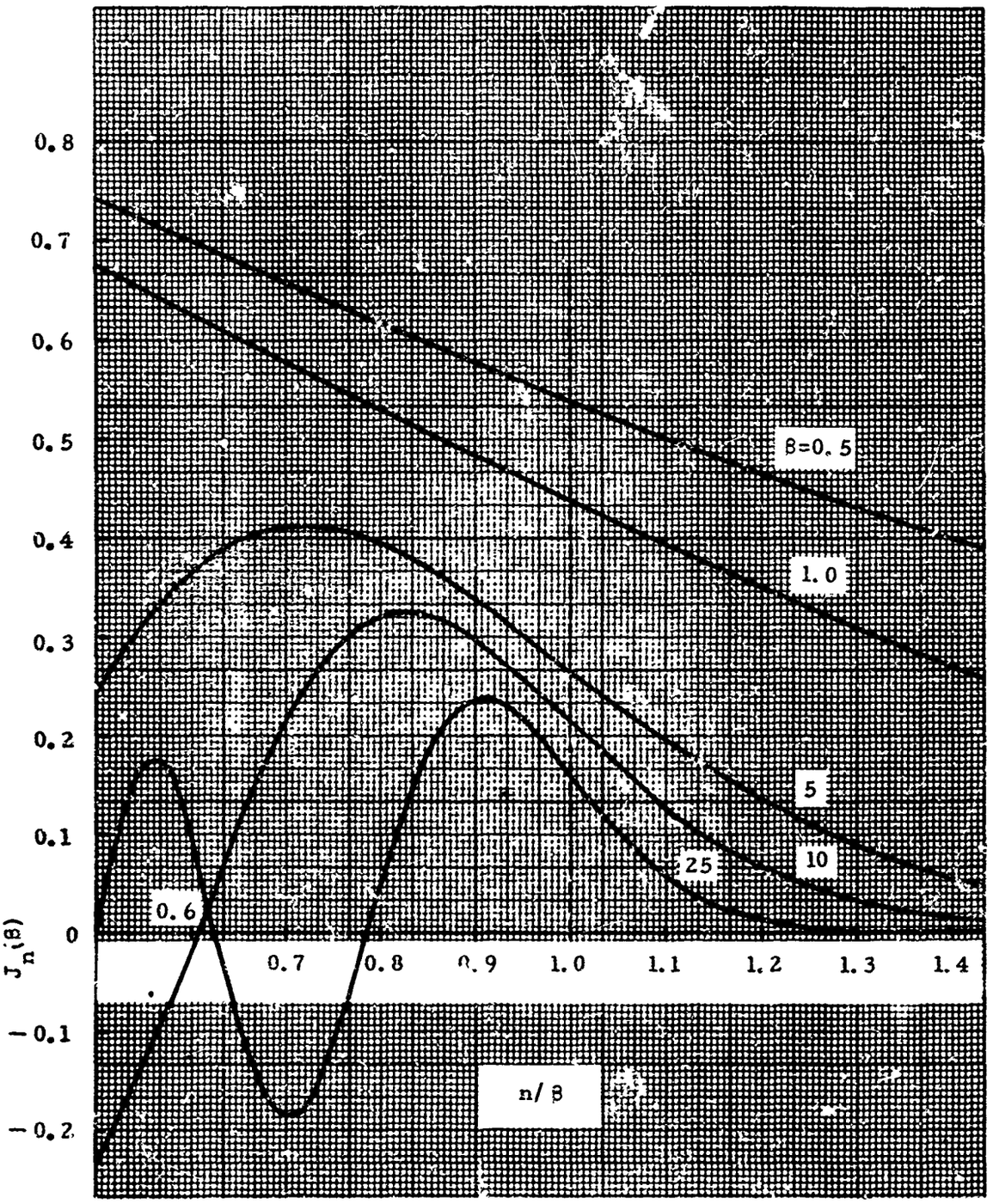

Figure B.1. Variation of $J_n(\beta)$ with n/β for values of n/β near unity. (After Baghdady, 1966)

however, of the modulated spectrum shape. Carson's rule for the bandwidth of the modulated signal for FM is

$$B_R \simeq 2(\beta_F + 1)\, f_m \,, \qquad \text{(B-32)}$$

where f_m is defined as the maximum frequency in the baseband signal. This expression is actually dependent upon the fraction (α) of the power in the modulated signal that is ignored in the estimate. It has been plotted in figure B.2with α as a parameter.

For a Gaussian amplitude signal, Reinhart (1966) has shown that the spectra for FM or PM can be analytically described, if we assume a particular tractable power density function. The general development is reviewed by Hubbard et al. (1970), in which the tractable power density function used by Reinhart (1966) is shown to be a reasonable "bracketing" function for a speech spectrum. The Gaussian statistics are not a good model for speech distributions (Hubbard et al., 1970). However, the results have been compared favorably with the FM spectral slope found by Glasser (1967) and the spectral signatures of figures B.27 and B.28. Figure B.3 presents the results of this development, in which the baseband spectral density function is given. The parameters in figure B.3 are as follows:

β_F = modulation index,

B_B = bandwidth of the baseband signal,

Λ_B = peak-to-average power ratio of the baseband signal (see sec. B.1.3),

f_p = frequency at which the baseband spectral density function $[S_{e_B}(f)]$ peaks, and

$f_d = \beta_F B_B \Lambda^{-\frac{1}{2}}$ = rms frequency deviation.

In summary, there is no general expression that will precisely determine the modulated signal spectrum and bandwidth for the exponential

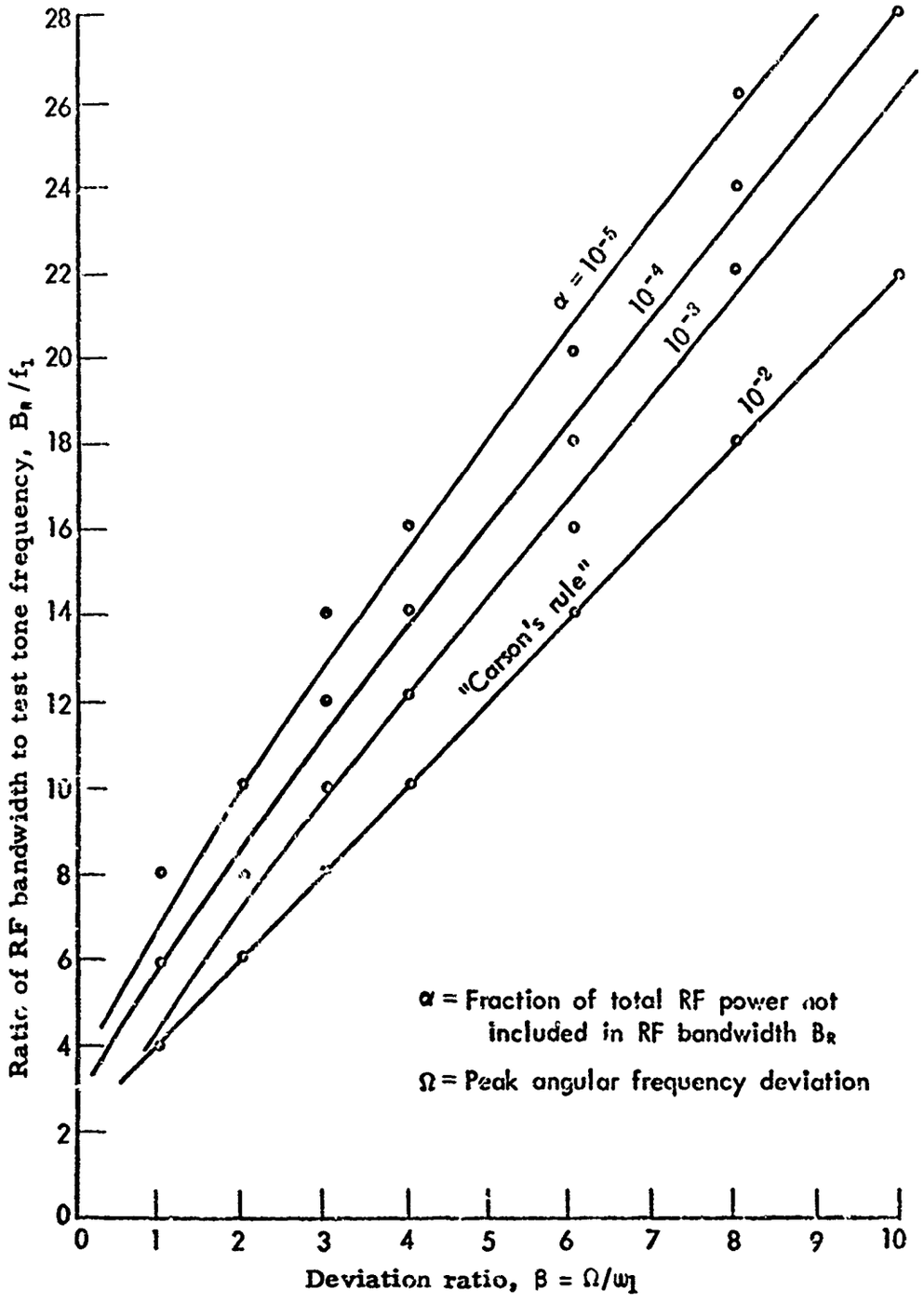

Figure B.2. RF bandwidth for FM by a sinusoidal test tone at frequency f_1 (after Reinhart, 1966).

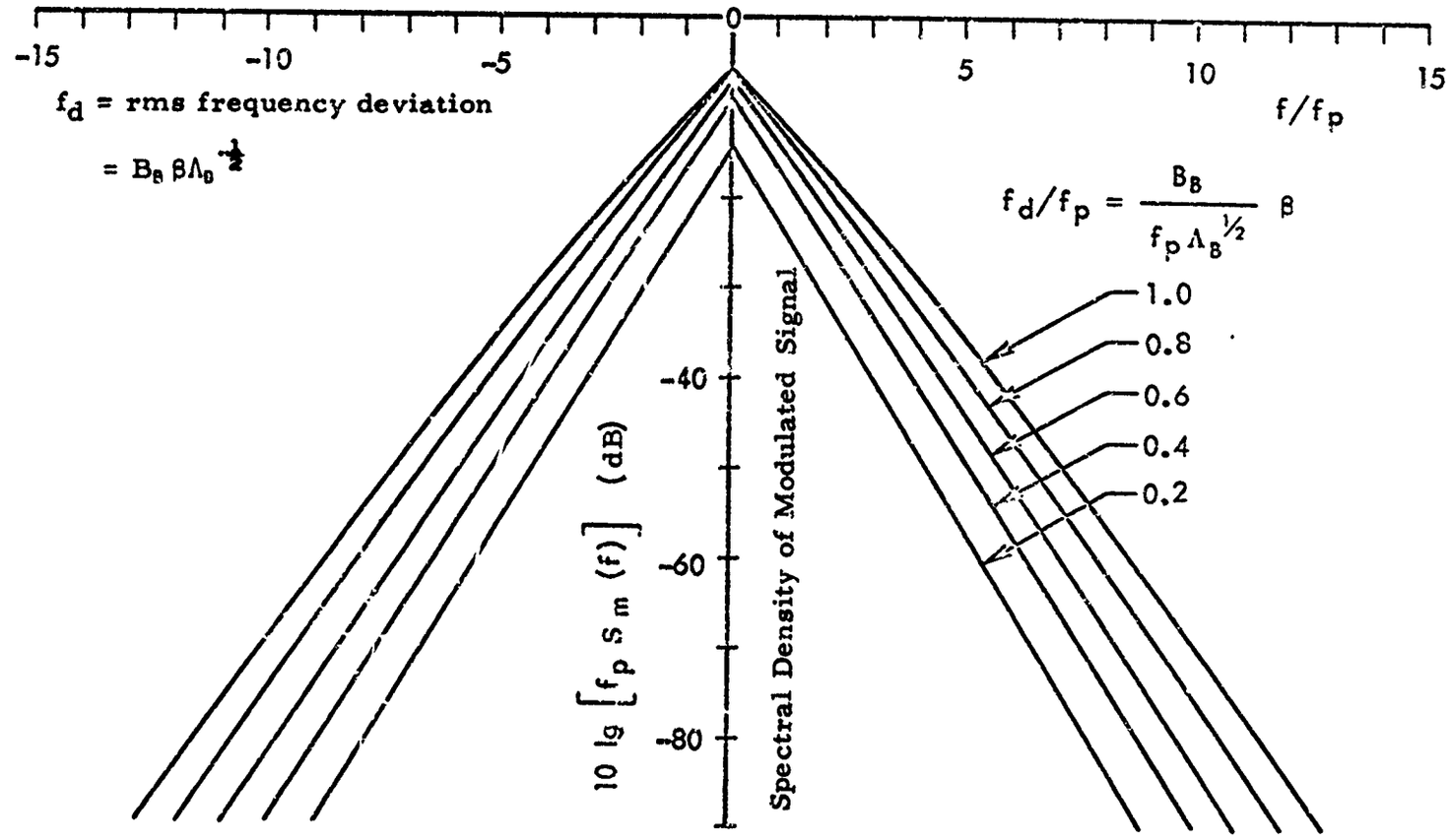

Figure B.3. Power spectra for FM by a Gaussian baseband with power spectrum

$$S_{e_B}(f) = \frac{2}{f_p \Lambda_B} \left(\frac{f}{f_p}\right)^2 e^{-2|f|/f_p}.$$ **(After Reinhart, 1966).**

forms. The methods presented here are presently the best known for estimating these modulation parameters. Examples of the complexity of these modulated spectra are illustrated in figures B.10 and B.11.

B.1.2 Spectrum Signatures of Modulated Signals

To aid in the evaluating of system performance tests reported in section 4 and appendix C, several spectrum signatures and output waveforms were recorded. These are shown in figures B.4 through B.31. Some tests noted in table 3 (sec. 4) were inadvertently performed with overmodulated signals. The modulation levels were adjusted by use of a 1-kHz tone in the SCIM signal, but the speech-shaped noise peaks in this signal are 12 dB higher in amplitude. The resultant spectra of the modulated signal and the distortion for FM are shown in figures B.10, B.11 and B.12. Other spectra signatures of interest are shown in the remaining figures, where each caption is self-explanatory.

B.1.3 The Modulating Signal

Three baseband signals are of primary interest in analog modulation processes: Gaussian noise, which is representative of analog data or multiplexed baseband signals; the sinusoid that is used as a test or pilot signal; and speech. These signals are described statistically (even though the sinusoid is a deterministic signal) and their properties are important for two reasons:

(1) The modulated signal spectrum shape and bandwidth are dependent upon the baseband signal (sec. B.1.1).

(2) The power relationships of the modulated signal are dependent upon the same properties of the baseband signal.

Modulating signal = 1000 Hz
Carrier = -33 dBm at 10 MHz FM
Deviation = 5 kHz on signal generator and receiver meters
IF bandwidth = 20 kHz
Input at playback input jack of TR-711 receiver
Output at video output jack of receiver

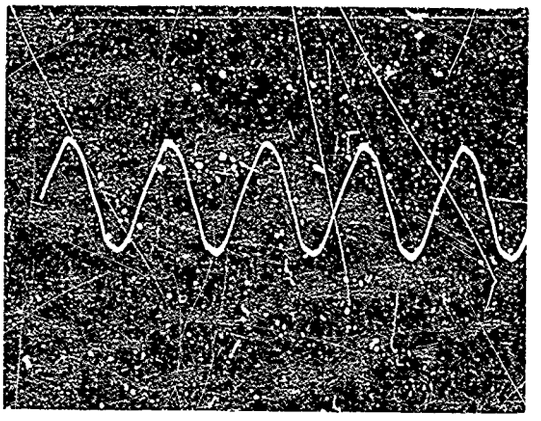

Figure B.4. FM receiver video output for sinusoidal signal with normal modulation.

Conditions are the same except the peak amplitude of the 1000-Hz modulating tone has been doubled.

Deviation = 9 kHz on receiver meter and 27.5 kHz on FM signal generator.

Figure B.5. FM receiver video output for sinusoidal signal with overmodulation.

Conditions are the same as in fig. B.4, except the peak amplitude of the 1000-Hz tone has now been quadrupled.

Deviation = 11.5 kHz on receiver meter and 27.5 kHz on FM signal generator.

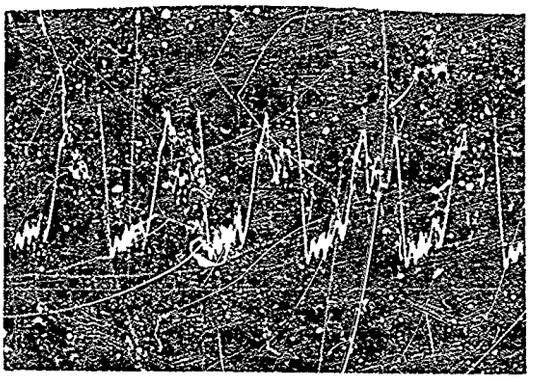

Figure B.6. FM receiver video output for sinusoidal signal with overmodulation.

Spectrum analysis for conditions in fig. B.4.

Calibration of the spectrum analyzer is:
Vertical calibration = 10 dB per division
Sweep calibration = 2 kHz per division; 20 kHz on left, 0 kHz on right.

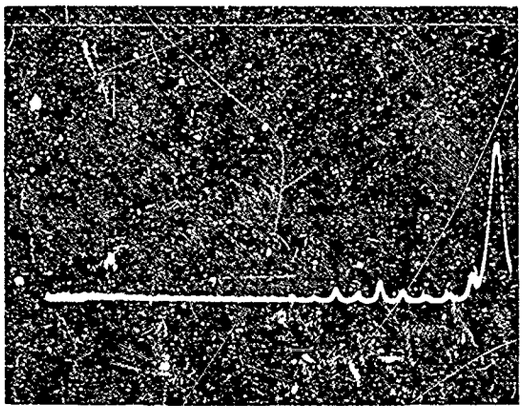

Figure B.7. Spectrum of FM receiver video output for sinusoidal signal with normal modulation.

Spectrum analysis for conditions in fig. B.5.

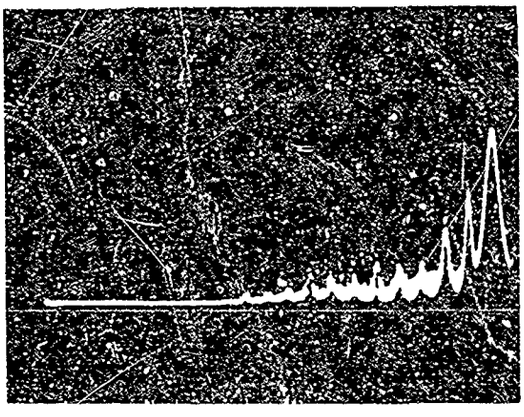

Figure B.8. Spectrum of FM receiver video output for sinusoidal signal with overmodulation.

Spectrum analysis for conditions in fig. B.6.

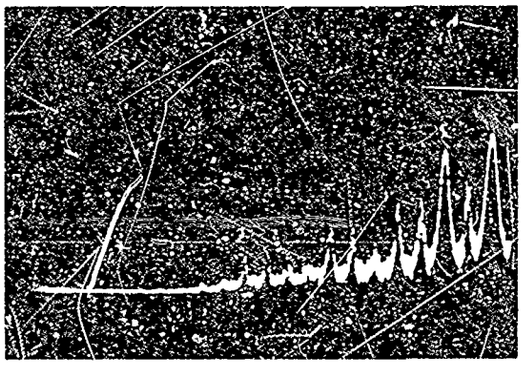

Figure B.9. Spectrum of FM receiver video output for sinusoidal signal with overmodulation.

Spectrum analysis of 80% amplitude modulated 1000 Hz.

Calibration of the spectrum analyzer is: Vertical calibration = 10 dB per division Sweep = 2 k Hz per division, 20 kHz on left, 0 kHz on right.

Carrier = -33 dBm at 10 MHz AM.

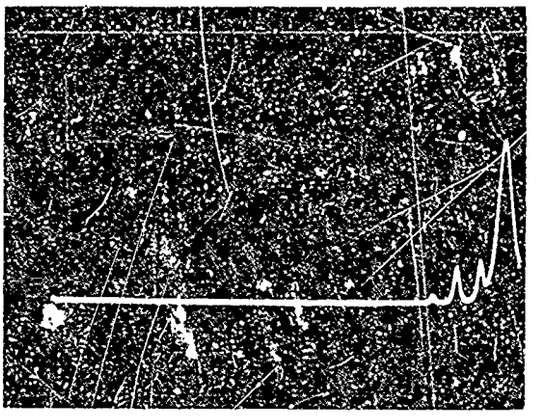

Figure B.10. Spectrum of AM receiver video output for sinusoidal signal with nominal modulation.

Shows the increasing wideband power when the peak amplitude of the modulation signal is doubled.

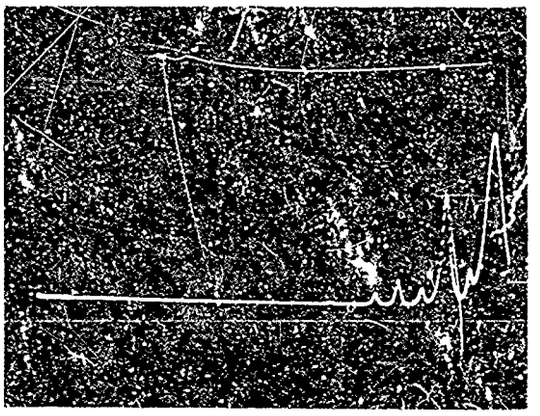

Figure B.11. Spectrum of AM receiver video output for sinusoidal signal with overmodulation.

The conditions are still the same as in fig. B.10, except the peak amplitude of the modulation signal is quadrupled.

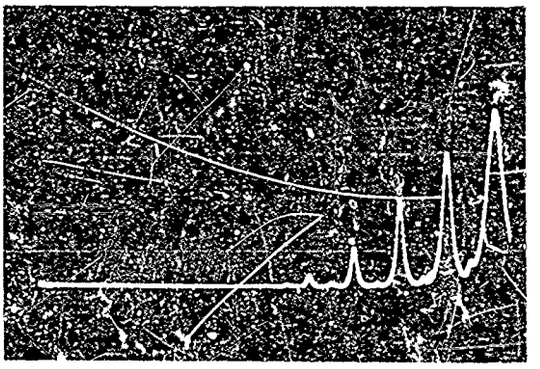

Figure B.12. Spectrum of AM receiver video output for sinusoidal signal with overmodulation.

Spectrum analysis of a 1000-Hz square wave taken to measure relative levels on a storage oscilloscope. Calibration is as follows:

20-kHz sweep range; 20 to 0 kHz left-to-right
40-dB gain for higher amplitude pulses
20-dB gain for lower amplitude pulses.

Therefore, calibration is 1 kHz between harmonics with a 20-dB difference in pulse height. This calibration is used as a reference in the following photos.

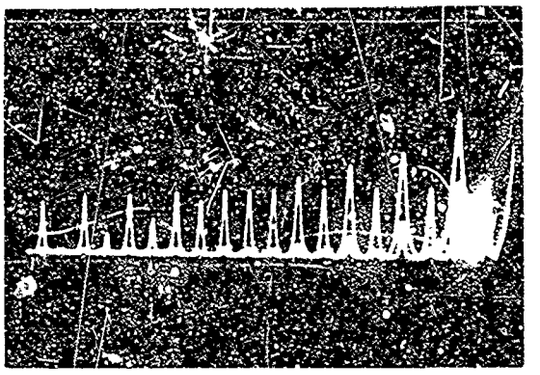

Figure B.13. Spectrum to calibrate frequency and amplitude levels on oscilloscope.

Shows 4- to 10-MHz CW carriers at the video output of the TR-711 receiver. IF input level = -47 dBm; 20-kHz IF bandwidth.
The harmonic spread shows the carriers to be 2 to 3 kHz off-tune from 10 MHz.

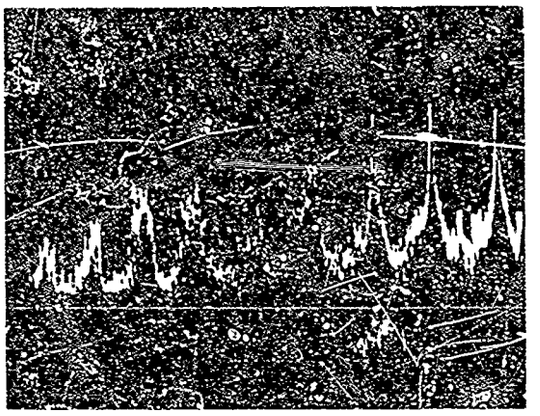

Figure B.14. Spectrum of four 10-MHz CW signals (20-kHz IF).

The same conditions as in fig. B.14 but with a 10-kHz IF bandwidth. Less noise is evident in the presentation compared with the 20-kHz IF.

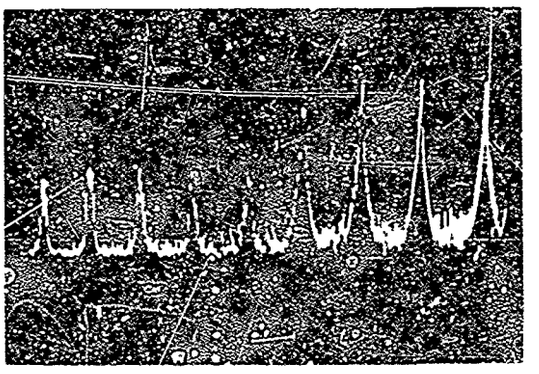

Figure B.15. Spectrum of four 10-MHz CW signals (10-kHz IF).

Shows the same carriers as in fig. B.14, except that they have been retuned to 10 MHz as critically as possible. This photo illustrates the high degree of interference to be expected from four on-tune carriers beating against each other. IF bandwidth is 20 kHz.

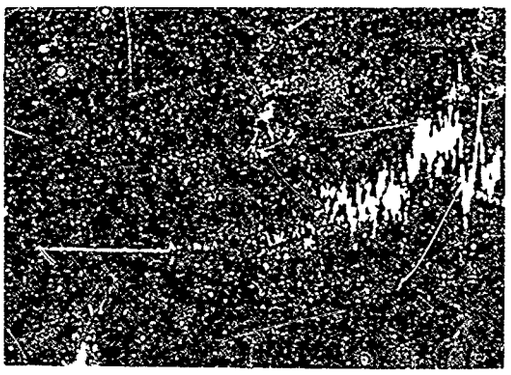

Figure B.16. Spectrum of four 10-MHz CW signals (20-kHz IF).

The same as fig. B.15, except the carriers have been retuned to 10 MHz again. IF bandwidth is now 10 kHz.

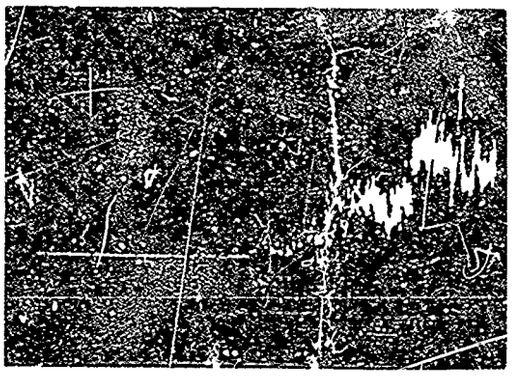

Figure B.17. Spectrum of four 10-MHz CW signals (10-kHz IF).

A spectrum analysis of the white noise source (20-kHz range) from a GR-1390B random noise generator modulating a carrier. Amplitude modulation was set at 95% with 1000 Hz, which had a peak amplitude equal to the highest measurable peaks of the noise source, as observed on a storage scope.
IF input = 10 MHz at -33 dBm at the playback input jack of the TR-711 receiver.
IF bandwidth = 20 kHz.

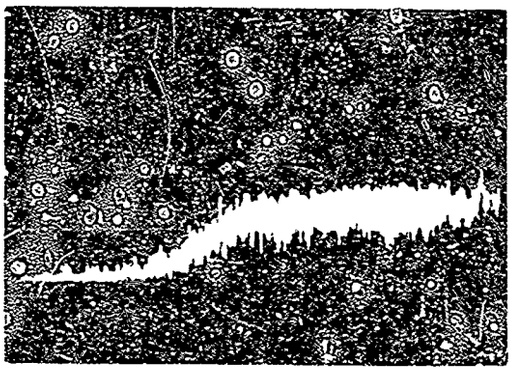

Figure B.18. Spectrum of AM white noise signals (20-kHz IF).

The same as fig. B.18, except for a 10-kHz IF bandwidth.

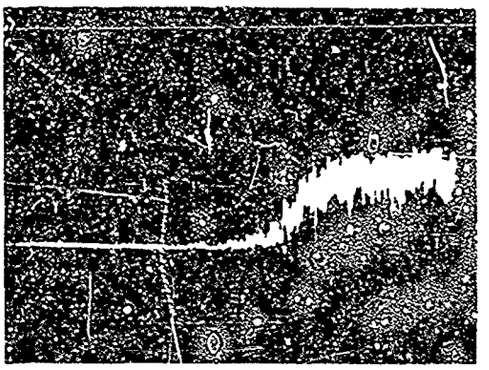

Figure B.19. Spectrum of AM white noise signals (10-kHz IF).

The spectrum analysis of 4-to 10-MHz carriers amplitude modulated by four different voice signals. Each carrier is separately modulated. The four signals are mixed in a coupler then fed to the playback input jack of the receiver.
IF input = 10 MHs at -33 dBm for each carrier
IF bandwidth = 10 kHs.

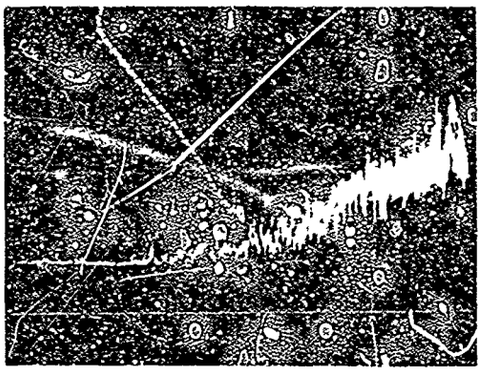

Figure B.20. Spectrum of four 10-MHz AM voice signals (10-kHz IF).

The same as fig. B.20, except IF bandwidth = 20 kHz.

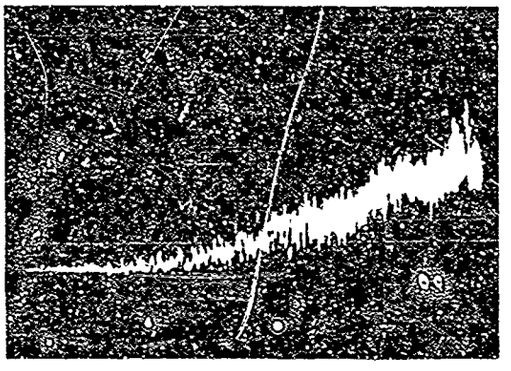

Figure B.21. Spectrum of four 10-MHz AM signals (20-kHz IF).

The output of the receiver when one 10-MHz carrier at -23 dBm is amplitude modulated by four voice recordings. Noise quieting to the left of 10 kHz (middle of photo) is due to higher carrier level. IF bandwidth = 20 kHz.

The slope of the spectrum in fig. B.22 is steeper than that displayed in fig. B.21. The rougher grain characteristics in fig. B.22 are due to the picture not being taken at precisely the same time and consequently not the same voice frequencies as the previous pictures.

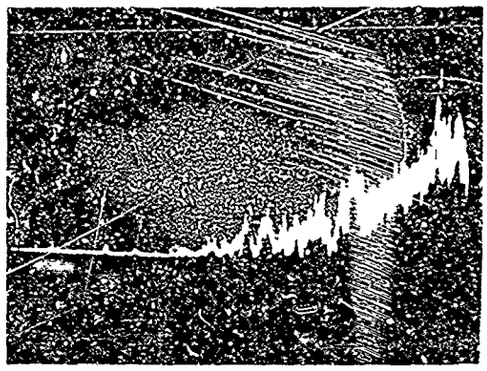

Figure B.22. Spectrum of one 10-MHz carrier, amplitude modulated by four voices (20-kHz IF).

The spectrum analysis of two 10-MHz FM carriers at -33 dBm with no modulation. 20-kHz IF bandwidth.

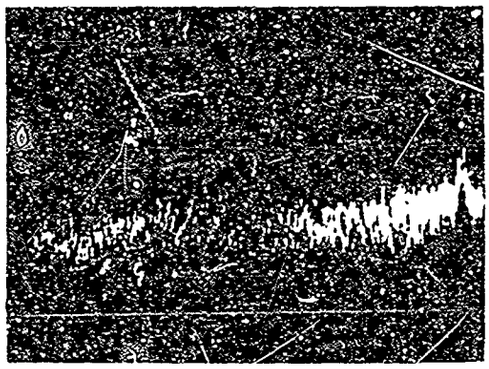

Figure B.23. Spectrum of two 10-MHz FM signals.

The spectrum analysis of one 10-MHz FM carrier modulated by the tape recording of a news broadcast.

IF input = -33 dBm.
20-kHz IF bandwidth.

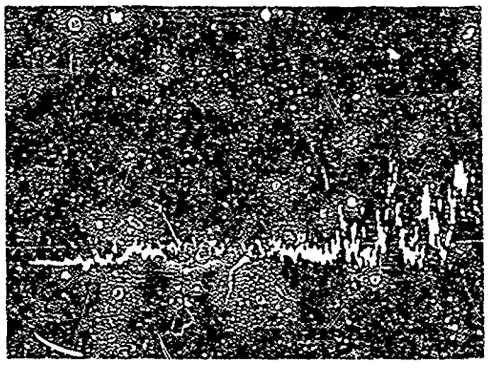

Figure B.24. Spectrum of one 10-MHz FM signal.

Spectrum analysis of two voice modulated 10-MHz FM carriers at -33 dBm. Video output of TR-711 receiver carriers are modulated by taped voice broadcasts.
IF bandwidth = 20 kHz. Input at playback jack of the receiver.

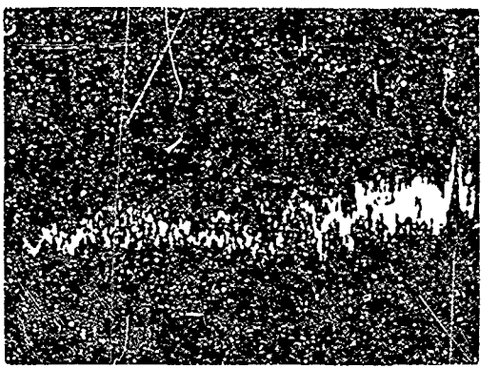

Figure B.25. Spectrum of two 10-MHz voice FM signals (equal power).

Condtions are similar to those in fig. B.25, except one FM carrier is at -33 dBm while the other has been increased to -23 dBm. This spectrum photo shows capture effect of stronger signal.

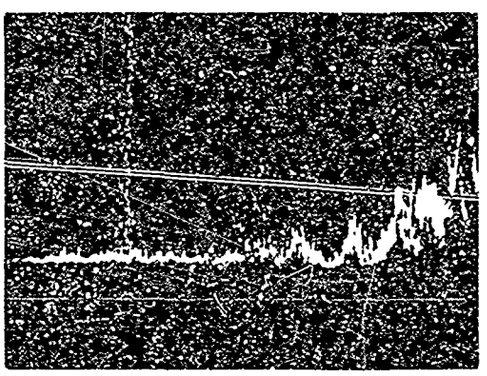

Figure B.26. Spectrum of two 10-MHz voice FM signal (unequal power).

A spectrum analysis of two voice signals modulating one FM carrier.

IF bandwidth = 20 kHz
Playback input, video output of the receiver
Carrier = 10 MHz FM at -33 dBm.

This photograph shows similarity to the spectrum presented in fig. B.26. In the region below 4 kHz the slope of the spectrum is similar, except for particular frequency features. Here again, dissimilar beat points on the voice tapes were photographed.

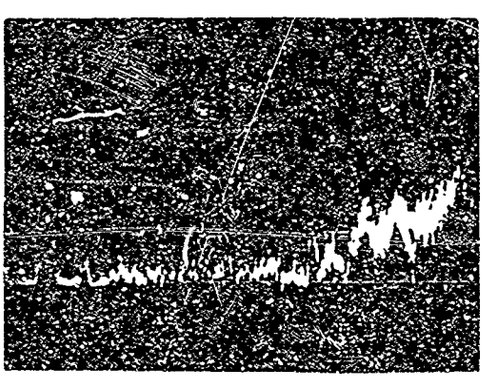

Figure B.27. Spectrum of one 10-MHz FM carrier with two voice signals.

Four voices modulating one FM carrier. Other features are the same as in fig. B.27. The finer grain feature of four voice frequencies beating against each other compared with two voices is apparent.

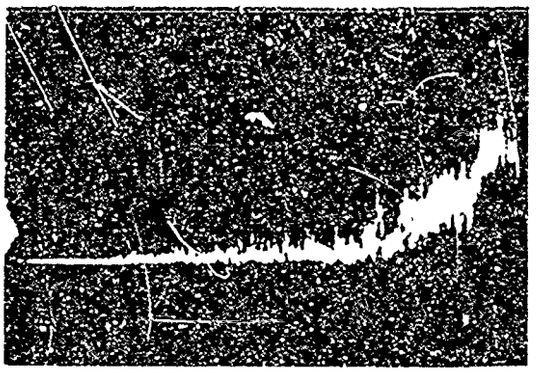

Figure B.28. Spectrum of one 10-MHz FM carrier with four voice signals.

An analysis of the four voices used in these tests being mixed and applied directly to the spectrum analyzer. There is no carrier. The general features are similar to the previous photo.

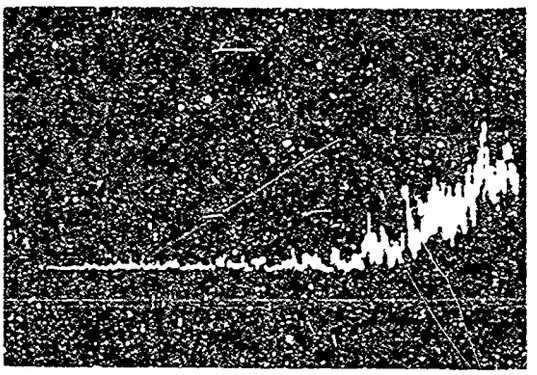

Figure B.29. Spectrum of four voice signals.

Spectrum analysis of noise from GR-1390B random noise generator through Philco flat filter; FM carrier at -33 dBm, 5-kHz deviation. Illustrates sharp-cutoff characteristics of filter of approximately 3800 kHz.

Video output of TR-711 receiver. IF bandwidth is 20 kHz.

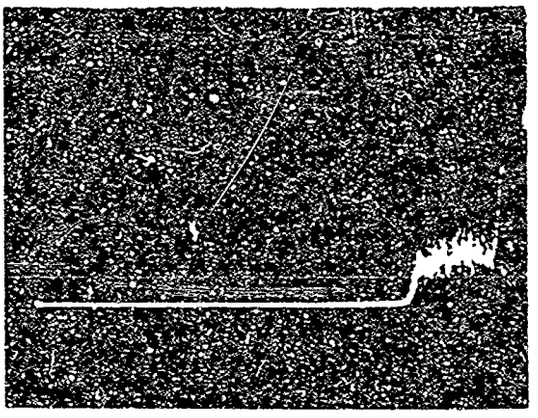

Figure B.30. Spectrum of FM white noise with flat filter.

Spectrum analysis of noise from random noise generator through Philco flat filter.
Amplitude modulation at 95%.
Carrier = -33 dBm.

Comparison of these two photos shows higher noise power level of 95% AM signal vs. 5-kHz deviation of FM signal.

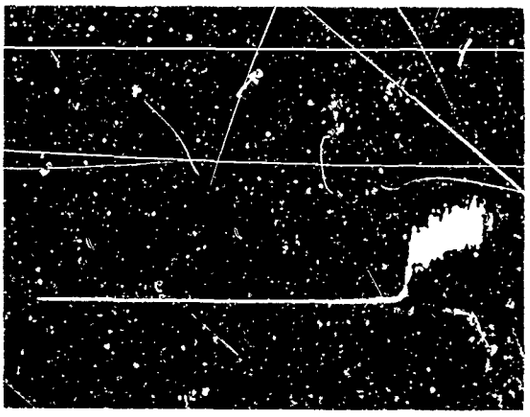

Figure B.31. Spectrum of AM white noise with flat filter.

The power properties of these signals are determined from their probability density functions (p.d.f.), which describe their amplitude distributions. The p.d.f.'s are well known for Gaussian noise and the sinusoidal signals. Davenport (1952) developed a modified Laplace distribution as a model for a speech signal, which was verified in the analysis by Hubbard et al. (1970). The peak power contained in these signals is defined as a quasi-peak value, which is a function of the fractional power excluded from the finite integrations performed over the p.d.f. The fractional power is denoted by α, and the quasi-peak powers $\hat{P}_B$ for these signals are given by

$$\hat{P}_B = 2\,\sigma^2 (\mathrm{erfc}^{-1}\alpha)^2 \qquad \text{(Gaussian)},$$

and $$\hat{P}_B = \lambda^2\,(\ell n\,\alpha)^2 \qquad \text{(Laplace, speech)}, \qquad \text{(B-33)}$$

$$\hat{P}_B = A^2 \cos^2 (\alpha\,\pi/2) \qquad \text{(Sinusoid)},$$

where σ^2 is the variance of the Gaussian distribution, λ^2 is one-half the variance of the Laplace distribution, A is the peak value of the sinusoid, and erfc^{-1} denotes the inverse complimentary error function.

The average power in these signals is also determined from their p.d.f.'s (Beckmann, 1967) and is found as

$$P_B = \sigma^2 \quad \text{(Gaussian)},$$
$$P_B = 2\lambda^2 \quad \text{(Laplace)},$$
and
$$P_B = A^2/2 \quad \text{(Sinusoid)}. \qquad \text{(B-34)}$$

We define the ratio of the peak power to the average power as Λ_B, and from (B-33) and (B-34) we find

$$\Lambda_B = 2(\text{erfc}^{-1}\alpha)^2 \quad \text{(Gaussian)},$$
$$\Lambda_B = \tfrac{1}{2}(\ln \alpha)^2 \quad \text{(Laplace)},$$
and
$$\Lambda_B = 2\cos^2(\alpha\pi/2) \quad \text{(Sinusoid)}. \qquad \text{(B-35)}$$

In practice, we are generally interested in small values of α for low distortion, and these characteristics are plotted in figure B.32. We see for $\alpha = 10^{-4}$ that the peak-to-average power ratio for a speech signal is approximately 4.5 dB higher than in the Gaussian case. In system design, this means that the peak power for speech in the baseband is 4.5 dB greater than required for a Gaussian baseband, for equal average powers in the two signals. The ratio Λ_B for speech is also approximately 13.25 dB higher than the sinusoidal signal with the same average power. These values are for no speech clipping. Licklider (1946) among others have shown that the intelligence of speech is not seriously affected when the signal is subjected to relatively large degrees of peak clipping. Clipping can be applied in system design to lower the peak power requirements for a speech baseband signal.

The peak and average power levels of the modulated waveforms in table B.2 were derived from the normalized amplitude factors. The results of these derivations, normalized by the average carrier power P_0 are presented in table B.3. The peak-to-average power ratio Λ_M for the modulated waveforms are also given in this table and are seen

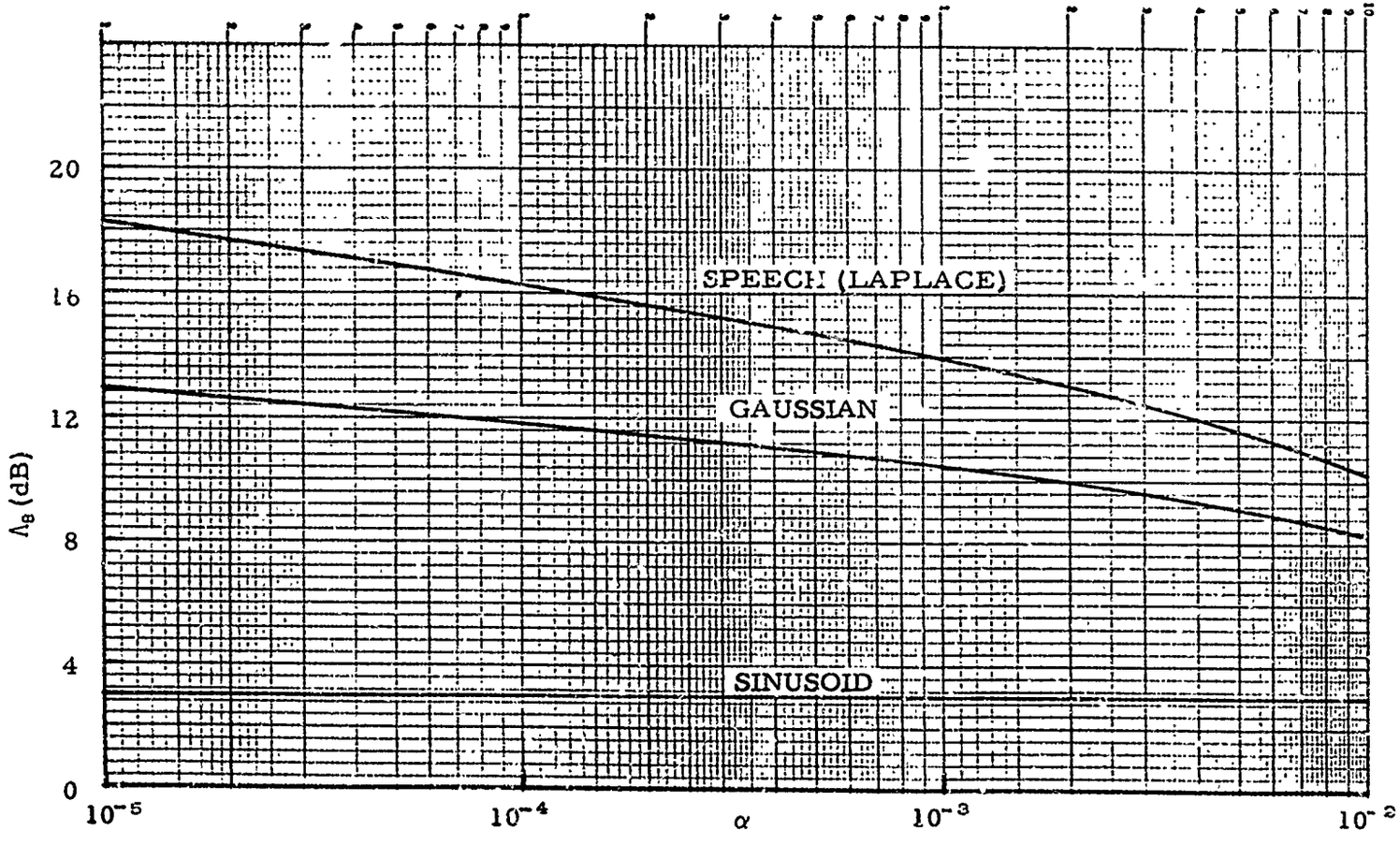

Figure B.32. Baseband signal peak-to-average power ratio for small α.

Table B.3. Power relationships for modulated waveforms with arbitrary baseband signals.

Modulation	Normalized Amplitude Factor $a(t)$	Normalized Average Modulated Carrier Power P_M / P_O	Normalized Peak Modulated Carrier Power $\hat{P}_M / P_O$	Peak-to-Average Modulated Carrier Power Ratio Λ_M
AM-DSB/SC	$M e_B(t)$	M^2 / Λ_B	$2M^2$	$2\Lambda_B$
AM	$1 + M\ e_B(t)$	$1 + M^2/\Lambda_B$	$2(1+M)^2$	$\frac{2(1+M)^2}{\Lambda_B + M^2}\Lambda_B$
AM-SSB/SC	$\sqrt{e_B^2(t) + \check{e}_B^2(t)}$	$2M^2/\Lambda_B$	$2\hat{a}^2$	$\frac{\hat{a}^2}{M^2}\Lambda_B$
PM	1	1	2	2
FM	1	1	2	2
PM-SSB	$\exp \pm[\beta_P \check{e}_B(t)]$	$\overline{a^2(t)}$	$2\hat{a}^2$	$2\hat{a}^2 / \overline{a^2(t)}$
FM-SSB	$\exp \pm [\beta_F \int \check{e}_B(t)\, dt]$	$\overline{a^2(t)}$	$2\hat{a}^2$	$2\hat{a}^2 / \overline{a^2(t)}$

to be dependent on the ratio (Λ_B) of the baseband signals derived above. Note that the SSB forms are incomplete and presented in terms of the amplitude factors. The statistics of the Hilbert transforms of the baseband signals are necessary to complete these expressions, but are not known. Additional information on this subject is given by Hubbard et al. (1970).

To illustrate the use of these derivations, consider the following example. For $\alpha = 10^{-4}$ in figure B.32, we find the values of Λ_B for the three baseband signals and compute the ratios Λ_M in two AM cases for $M = 0.8$. The results are presented in table B.4. As this table shows, for a speech baseband signal (Laplace), the AM peak-to-average power ratio is approximately 11 dB lower than for DSB/SC. It can be shown that the AM power ratio (Λ_M) is always less than that for DSB/SC for any baseband signals where $\Lambda_B > 1$. A sinusoidal baseband signal yields a lower Λ_M in DSB/SC signals for $M > 0.5$.

The performance of analog systems is in general based on S/N power ratios, as discussed in section 4. The most important signal power in these ratios is the average value, which is used in the comparison of system performance. Examples of these characteristics for an AM system with a linear amplitude detector and the basic FM

Table B.4 Λ_B and Λ_M factors in AM.

Baseband Signal	Λ_B (dB)	Λ_M (dB)	
		AM	AM-DSB/SC
Sinusoid	3	6.9	6
Gaussian	11.8	7.9	14.8
Laplace	16.2	8.1	19.2

system are given in section 4. The characteristics for other systems with both product and square-law detectors are given by Hubbard et al. (1970). All these performance characteristics are given in table B. 5. The symbols in this table not previously defined are as follows:

N_W = power density of white Gaussian noise (W/ Hz).

$(S/N)_i$ = input S/ N.

$(S/N)_o$ = output S/ N.

B = receiver bandwidth in Hz.

k_p = gain factor dependent upon the distribution of the modulating signal,

$= \frac{\overline{f^4(t)}}{[f^2(t)]^2}$, where f(t) is the modulating signal,

= 3/2 for a sinusoid.

B. 2. Summary of Discrete Modulation Forms

A general calss of discrete modulation methods are a series of pulse and/ or digital forms. Pulse modulation is based on the sampling theorem for band-limited signals and is implemented by changing some parameter of a uniform chain of pulses (carrier) in accordance with the information signal. As in the analog methods, modulation of a pulse train can be accomplished by varying either the amplitude or time parameters. These yield two basic classifications, known as pulse amplitude modulation (PAM) and pulse time modulation (PTM). PTM has the following subclassifications, defined in accordance with the time parameter which is varied:

(a) Pulse duration (PDM).

(b) Pulse position (PPM).

(c) Pulse frequency (PFM).

Table B. 5. Comparison of bandwidths and S/N for analog systems.

Modulation Method	Bandwidth Ratio (B/f_s)	Signal-to-Noise Ratio $N_i = N_w B$ (actual)	Signal-to-Noise Ratio $N_i = N_w f_s$ (actual)	Signal-to-Noise Ratio $N_i = N_w B$ (ideal)
AM-DSB/SC product detection	2	$(\frac{S}{N})_o = 2(\frac{S}{N})_i$	$(\frac{S}{N})_o = \frac{S_i}{N_w f_s}$	$(\frac{S}{N})_o = (\frac{S}{N})_i^2$
AM-SSB/SC product detection	1	$(\frac{S}{N})_o = (\frac{S}{N})_i$	$(\frac{S}{N})_o = \frac{S_i}{N_w f_s}$	$(\frac{S}{N})_o = (\frac{S}{N})_i$
AM Square-law detection general form	2	$(\frac{S}{N})_o = k_2 \frac{(\frac{S}{N})_i^2}{1+2(\frac{S}{N})_i}$	$(\frac{S}{N})_o = k_2 \frac{\frac{1}{4}(\frac{S_i}{N_w f_s})^2}{1+(\frac{S_i}{N_w f_s})}$	$(\frac{S}{N})_o = (\frac{S}{N})_i^2$
AM Square-law detection approximate form	2	$(\frac{S}{N})_o = k_2(\frac{S}{N})_i^2$ for $(\frac{S}{N})_i \ll 1$	$(\frac{S}{N})_o = \frac{k_2}{4}(\frac{S_i}{N_w f_s})^2$ for $(\frac{S}{N})_i \ll 1$	$(\frac{S}{N})_o = (\frac{S}{N})_i^2$
		$(\frac{S}{N})_o = \frac{k_2}{2}(\frac{S}{N})_i$ for $(\frac{S}{N})_i > 10$	$(\frac{S}{N})_o = \frac{k_2}{4}(\frac{S_i}{N_w f_s})$ for $(\frac{S}{N})_i > 10$	
AM Linear amplitude detection	2	$(\frac{S}{N})_o = 0.916(\frac{S}{N})_i^2$ for $(\frac{S}{N})_i < 1$ (unmodulated carrier)	$(\frac{S}{N})_o = 0.229(\frac{S_c}{N_w f_s})^2$ for $(\frac{S}{N})_i < 1$ (unmodulated carrier)	$(\frac{S}{N})_o = (\frac{S}{N})_i^2$
		$(\frac{S}{N})_o = 2(\frac{S}{N})_i$ for $(\frac{S}{N})_i > 10$	$(\frac{S}{N})_o = \frac{S_i}{N_w f_s}$ for $(\frac{S}{N})_i > 10$	
FM Wide Band $\beta_f > \pi/2$	$2\beta_f$	$(\frac{S}{N})_o = 3\beta_f^3(\frac{S}{N})_i$ for $(\frac{S}{N})_i > 10$	$(\frac{S}{N})_o = \frac{3}{2}\beta_f^2(\frac{S_c}{N_w f_s})$ for $(\frac{S_c}{N})_i > 10$	$(\frac{S}{N})_o = (\frac{S}{N})_i^{2\beta_f}$
FM Narrow Band $\beta_f < \pi/2$	$2(\beta+1)$	$(\frac{S}{N})_o = \frac{3}{2}\beta_f^2(\frac{B}{f_s})(\frac{S}{N})_i$ for $(\frac{S}{N})_i > 10$	$(\frac{S}{N})_o = \frac{3}{2}\beta_f^2(\frac{S_c}{N_w f_s})_i$ for $(\frac{S}{N})_i > 10$	$(\frac{S}{N})_o = (\frac{S}{N})_i^{2(\beta_f+1)}$

The principal advantage of pulse forms of modulation is their use in time division multiplex (TDM) systems, in which many information channels can be established by allocating specific transmission time slots to each. However, there is an inherent disadvantage in TDM compared with FDM. FDM systems can make use of a nonsimultaneous multiplex load advantage (Holbrook and Dixon, 1939), which conserves required power capacity as the number of channels increases. This is not possible in TDM, but may be somewhat compensated for by companding in TDM systems, where speech transmission is used (Schwartz et al., 1966; Stein and Jones, 1967).

A basic disadvantage in all pulse modes of modulation is that the transmission of a pulse requires a large amount of bandwidth. PDM therefore has a slight bandwidth advantage in that the duration or width of the transmitted pulse is changed with the message signal. However, in this form, all the information is actually contained at the trailing edge of the pulse, and a considerable amount of transmitted power is wasted, since it contains little information. For this reason, PPM is more efficient in terms of transmitter power; PAM is the most efficient in terms of bandwidth but suffers from variation in transmitted power.

All the above forms of pulse modulation are uncoded and essentially depend upon an analog form of the message signal, either directly or indirectly (as in sampled functions). Utility of the pulse forms is generally improved when they are applied in coded systems.

B.2.1 Quantizing and Coding

In their basic form, the pulse modulation schemes result in the transmission of a pulse train that has some parameter that varies directly with the modulating signal. The modulated parameter is thus allowed to assume all possible values of the information signal even though they

are sample values. In reception of these signals, the actual value of the sampled function becomes ambiguous because of additive noise and other transmission distortion. Thus, it is unnecessary to transmit all possible values of the sampled signal. If only certain discrete values are permitted, then the sampled signal becomes a quantized representation. Quantizing is done by normal sampling processes, but in addition the sampled value at the output of the quantizer assumes the nearest discrete value to the actual value. In this manner, an analog signal is transformed into a digital (discrete) form.

The advantage of quantizing is realized generally in the receiving and detection process. For example, assume a quantized PAM (QPAM) system in which the received signal has been contaminated by additive noise. If the noise is small compared with the quantized step used, the detection system can be designed, in essence, to correct for the noise and produce a new output pulse at precisely the correct quantized level. This feature is used to advantage in many systems that require repeaters over long-haul communication links. If we assume error-free output from each detector as above, the additive noise can be effectively eliminated. In contrast, analog systems with repeaters amplify and retransmit the additive noise, and its effect is compounded.

Quantizing produces a distortion of the original signal known as quantizing noise, which is an irreducable distortion in any given system and is the primary disadvantage of quantizing techniques. Quantization noise can be made negligible by increasing the number of discrete quantized levels. However, as the number increases, the quantized signal again approaches the exact-sampled case, and the quantizing advantage is somewhat lost. Quantization noise for two particular digital modulation processes are discussed further in section B. 2. 3.

In quantized systems, the number of allowable levels is finite. This leads into a new class of pulse modulation techniques, in which

the finite levels are coded before transmission. Coding techniques can be applied to any of the pulse modulation forms in which quantized sampling is used. They are classified generally as pulse-code modulation (PCM) and are the principal forms of discrete modulation of interest here. A wide variety of coding techniques are available for use in PCM, the most common of which is the binary system with only two levels (base N = 2). In these schemes, it can be demonstrated that a series of, say, n pulses can be used to represent N^n individual quantized signal levels. In transmission then, we exchange each individual quantized pulse for a particular sequence of n pulses. The bandwidth of transmission in coded systems must therefore obviously increase if n pulses are to be transmitted within the same time interval as the corresponding quantized pulse. An analogy between PCM systems and wideband FM can be made, i.e., each exchanges bandwidth for improved performance. As shown later, PCM techniques result in a S/N improvement similar to that in wideband FM.

If the information signal has a bandwidth of f_m, the sampling theory dictates the necessity of transmitting $2f_m$ code groups per second in the coded system. For n pulses/code group, the transmission rate becomes

$$r_r = 2nf_m \text{ pps} , \tag{B-36}$$

and again from the sampling theory we see that (B-36) will require a channel transmission bandwidth

$$B_c \geq nf_m \tag{B-37}$$

a value n times that required to transmit the basic quantized signal.

PCM techniques lend themselves to TDM. The most straightforward multiplex technique is to use a commutated sampling process, in which M individual channels are sequentially sampled and quantized. Thus, in a PCM-TDM system another bandwidth factor becomes important. If a

single channel requires a bandwidth of B_c as in (B-37), the TDM system will require a bandwidth

$$B_N = MB_c = M\, nf_s \ . \qquad \text{(B-38)}$$

TDM systems are somewhat difficult to implement in practice, because the encoding and decoding techniques must be synchronized. Otherwise, channels will not be properly separated in the detection process and garbled communication results. Most TDM systems rely on the transmission of frequent synchronizing information, or on extremely stable clocks that are periodically synchronized.

B.2.2 Digital Transmission

In any modulation form, the modulating signal and the information signal can be classified as analog or digital. The distinction between these signal forms should be clear. For example, PCM systems are basically digital, i.e., they result in a digital modulating signal. However, the information signal is in analog form and in most systems will be detected at the receiver as an analog signal. Since this class of practical pulse modulation schemes is of principal interest in current ATC studies, we are concerned with the modes of transmission for digital information and their performance. These factors are discussed in section 4.2.2 for the basic binary transmission systems. Their performance characteristics are given in figures 23 and 24 (sec. 4).

B.2.3 Digital Modulation

Because the development of digital modulation schemes for analog signals is quite recent, the accumulation of engineering experience and empirical data that assists evaluation and comparisons of analog modulation methods is not available for digital methods. An additional complication is the abundance of different methods that have been suggested, each with its advantages and limitations (Proc. IEEE, 1967).

The discussion here will be limited to PCM and delta modulation (DM) systems defined as follows: PCM, a system in which the input signal is sampled at equally spaced time intervals, with each sample quantized into one of L equally spaced voltage levels; DM, a system similar to PCM, in which the slope of the input signal, rather than the signal level, is quantized. Modifications of these methods have been proposed (Proc. IEEE, 1967) but are not considered here because of the scarcity of results.

Digital systems are limited by three types of noise: quantizing noise, overload noise, and the noise resulting from errors. The last is the most difficult to evaluate. Errors caused by pulse intermodulation can usually be reduced by proper pulse shaping and will not be considered further here. Errors related to the statistics of interfering Gaussian white noise have been considered for PCM and DM systems and are noted later in this section. As mentioned in section 4, the quantizing noise for PCM and DM systems have been calculated (Bennett, 1948; van de Weg, 1953). The results of these calculations, corrected by Hartman (Hubbard et al., 1970) for DM, are given in figure B.33. The parameters used to evaluate digital systems and the development of this figure are:

N = coding base,

L = number of quantizing levels,

n = number of elements the quantized signal into which is coded,

B_s = system bandwidth,

B_1 = bandwidth of the information signal, i.e., the baseband bandwidth,

f_s = sampling frequency,

f_m = maximum baseband frequency, and

f_t = test tone frequency.

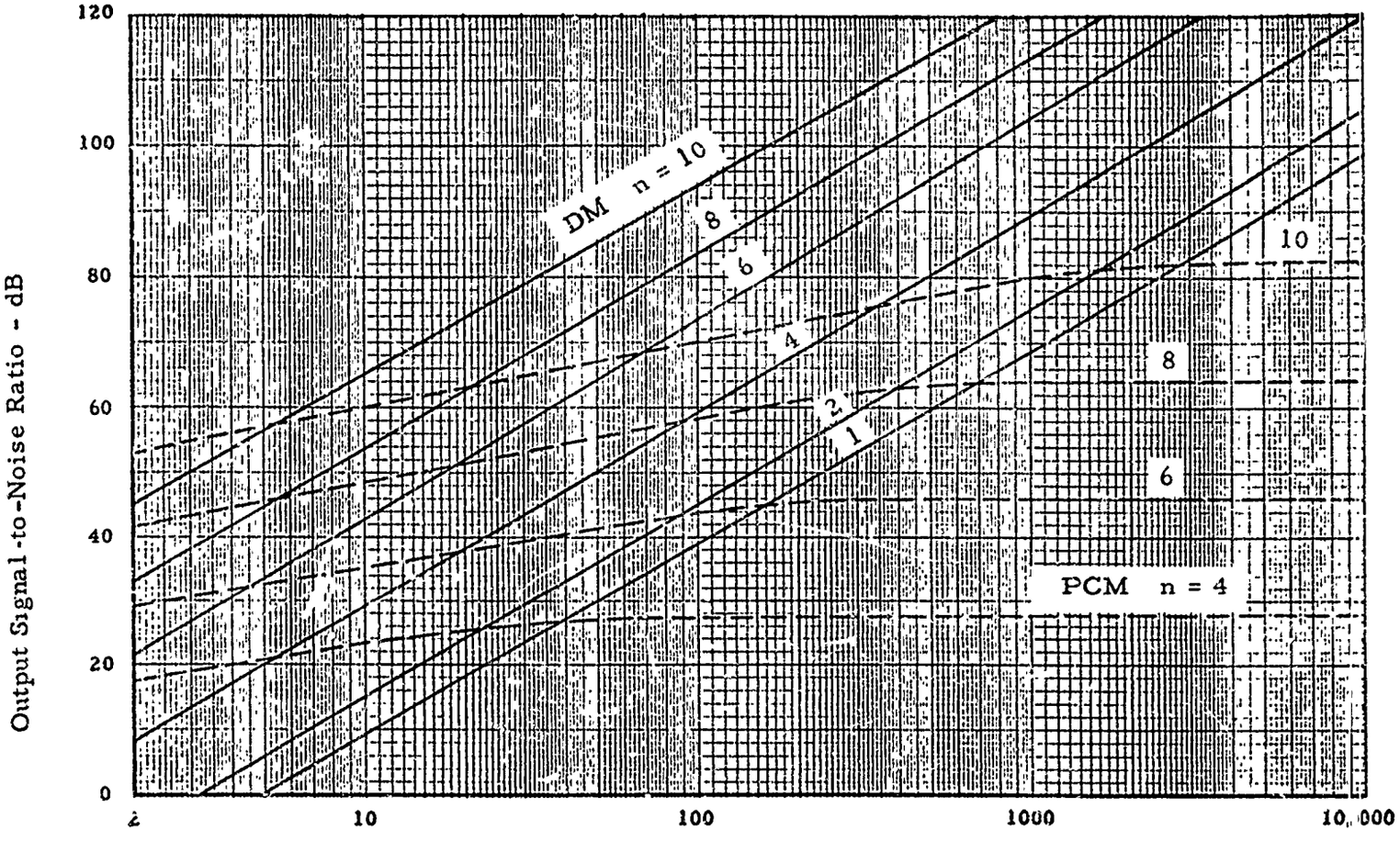

Figure B.33. Quantizing noise characteristics of PCM and DM binary systems.

Each of these curves is for a binary system (N = 2). The curve for DM for n = 2 is the same (within 0.5 dB) as the curve for N = 3, n = 1. Since the overall bandwidth of the system is $2nNf_s$, we see that the same S/N can be obtained in a smaller bandwidth. The conditions for which these curves have been calculated are (a) the input signal is white Gaussian noise, (b) the quantizing step is chosen so that for PCM the rms value of the signal is 1/4 the overload value, and for DM so that the rms value of the derivative of the signal is 1/4 the overload slope value. These curves do not include noise caused by overloading. The same curves for a full-load sinusoid of 800 Hz would be 9 dB higher for PCM and 17 dB higher for DM.

Zetterburg (1955) and de Jager (1952) have calculated the overload noise, or the point at which overload occurs for both DM and PCM systems. The overload noise in PCM systems has the same effect as clipping, and theory and data agree well. In DM, the agreement among different theories is not good, and the agreement between the data and any particular theory must be interpreted with this in mind. In any case, both PCM and DM systems can be designed to keep overload noise at a value less than the quantizing noise, and companding can be used advantageously in both systems.

The noise caused by errors has been calculated by Akima (1963) for PCM systems with a sine wave input at the Nyquist sampling rate, and the results of this work are mentioned in section 4.2.2. Combined with the prediction of errors caused by Gaussian noise in binary FSK systems, the S/N performance curves for PCM in figure 25 (sec. 4.2.2) were calculated by Akima (1963). A plot of the threshold levels in this figure for PCM n-ary system results in a curve that may be used for a performance comparison with other systems. This is shown in

figure B.34 (PCM-FS, N=2) in comparison with a typical curve for FM and AM-SSB. An additional threshold curve for an N-ary system where n=1 is also shown.

In using the results of figure B.34, we must remember that they are envelope characteristics of a family of performance curves. In other words, for each point on the curves an associated parameter must be taken into account. These parameters are

(a) n for PCM-FS N = 2,

(b) N for PCM-FS n = 1, and

(c) β (modulation index) for FM.

Unfortunately, the performance results for DM have not been similarly calculated because of the lack of knowledge of error noise characterization. A single point has been plotted for DM in figure B.34, based on a calculation by Wolf (1966). However, the validity of this point is questionable (see sec. 4.2.2), because Wolf assumes a Markov process as the input signal, which has infinite rms power (Hubbard et.al., 1970). Preliminary analysis indicates that the output S/N will be sensitive to the type of filter used to remove the DC component. Additional work is required before a meaningful analysis of the DM process can be completed.

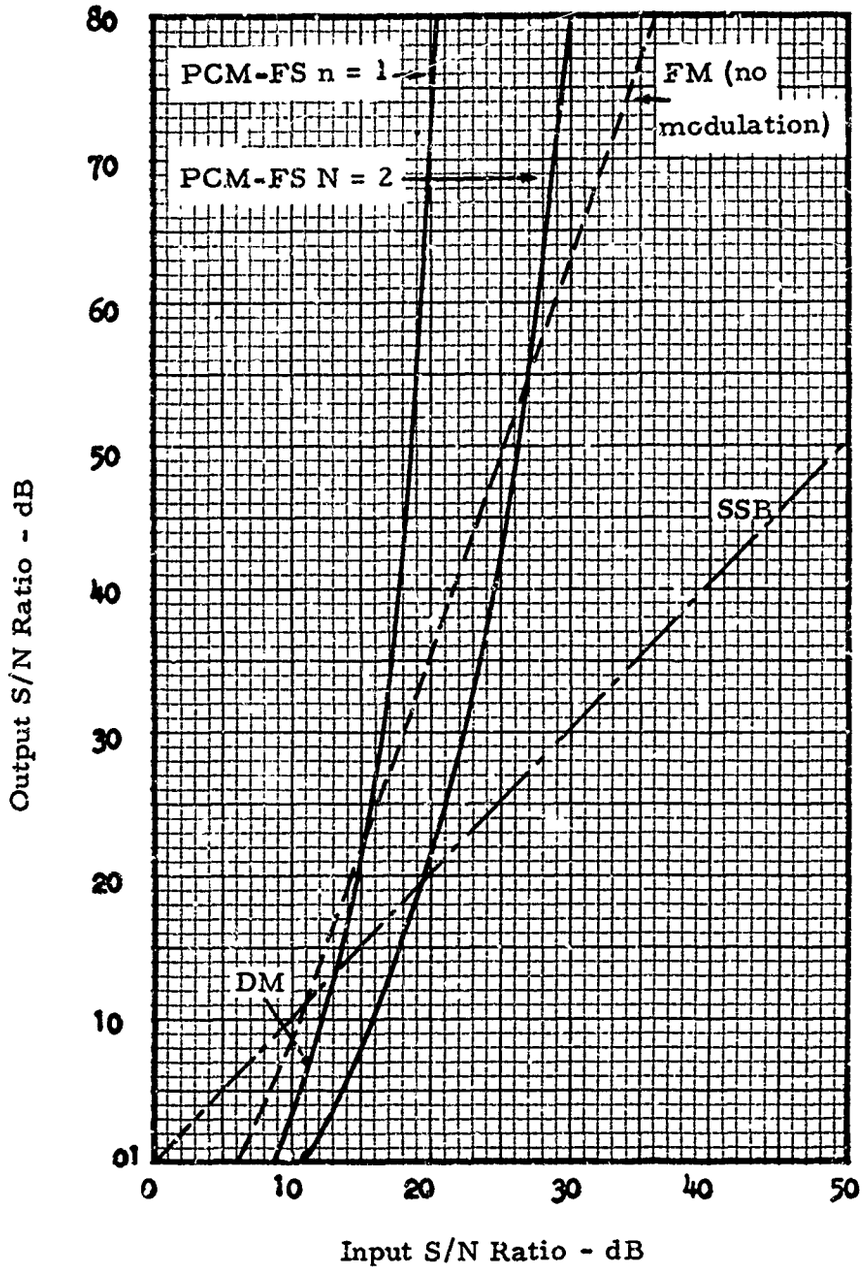

Figure B.34. Relative systems performance (after Akima, 1963).

APPENDIX C
System Performance Measurements

C.1 Discussion of SCI Tests and FM Capture Characteristics

Tests to determine required D/U have been made with the "speech communications index meter" (SCIM) (Kryter and Ball, 1964). Some were made to verify previous tests (figs. C.16 through C.33), while others were made to investigate the effects of two interfering signals upon a desired signal. Results of these tests appear in table 4 (sec. 4), which is a summary of the measurements. The earlier measurements are summarized in table 3 (sec. 4). A block diagram of the test equipment is shown in figure C.1. AGC curves for the TR-711 receiver are shown in figure C.34, the TMR-5 receiver is shown in figure C.35, and the CEI 960 receiver in figure C.36.

When inspecting table 3, one must take care to ascertain the test configuration in column 2 by checking the desired and undesired carrier frequencies reported in columns 3 and 5. This must be done to prevent a case of mistaken carrier (desired or undesired) identity. Required D/U for SCI = 0.4 and 0.85 is reported in this table.

One of the major difficulties encountered while performing these tests was the instability of the signal generators. According to manufacturers' specifications, the drift should not be more than 0.0025% and 0.015% respectively for each of the FM signal generators after a 10-min warm-up. The signal generators performed within these specifications over 90% of the time while the tests were being made. When frequency checks were made before and after each test, the frequency drift was discovered. The test would then be rerun when excessive drift was noted. Excessive drift here is defined as greater than ±2 kHz per carrier. The following factors must be considered:

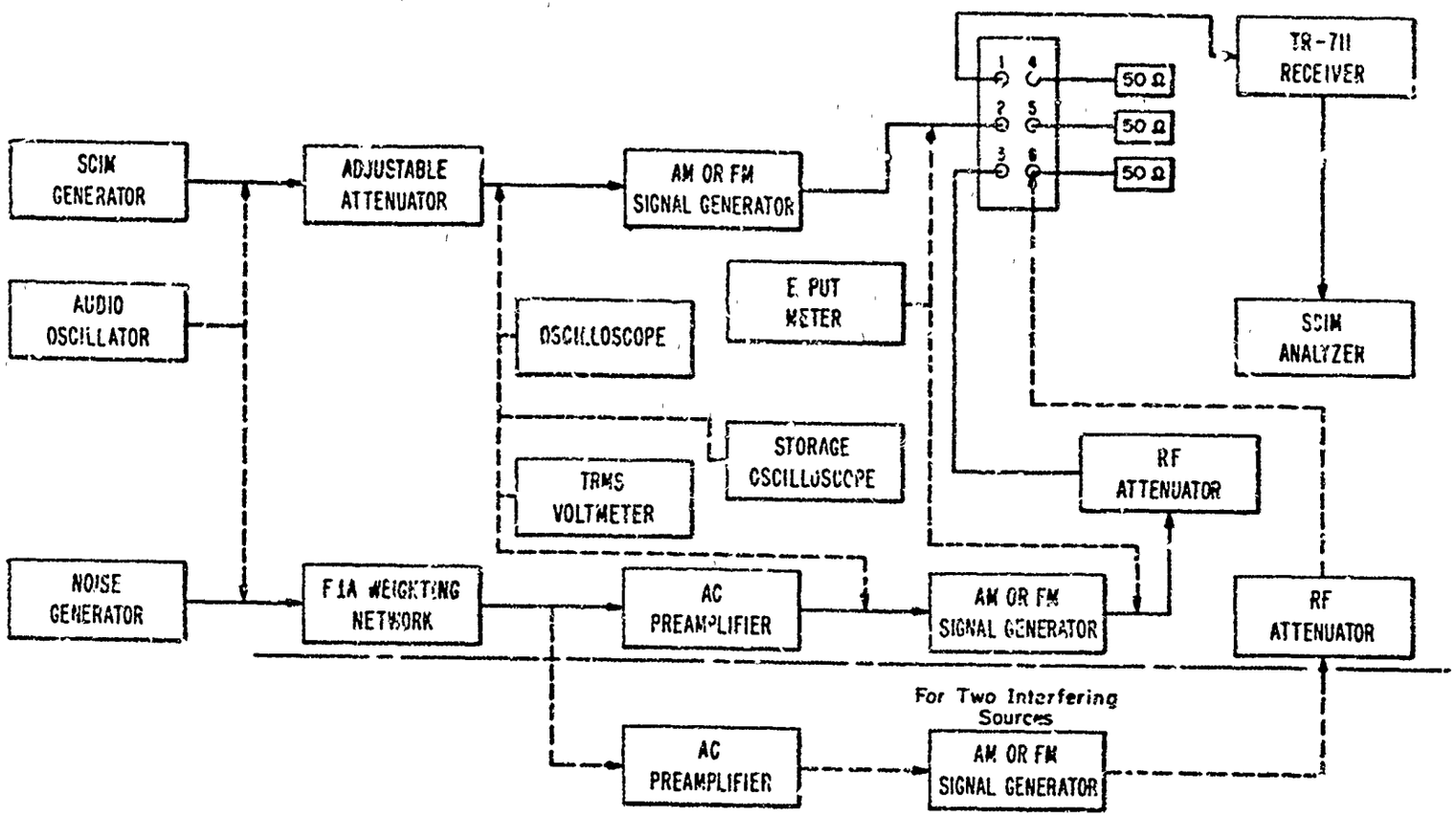

Figure C.1. Block diagram of SCIM tests.

(1) Drift of the carriers toward or away from each other when adjacent-channel configuration is used.

(2) Drift of the carriers away from each other, in a cochannel situation.

(3) Drift that takes place during a test run is undefined. How great is the drift on or off frequency as the test progresses? A continuous frequency monitor was not used on the carriers because of loading and power division of the signal from the generators.

If the carriers should drift toward each other, degradation of the SCI will take place. A 2-kHz drift of the adjacent undesired carrier toward the desired carrier would mean a degradation of the SCI equal to 3-dB higher interference level. This is derived from the inspection of bandpass characteristics of the 20-kHz IF filter in the TR-711 receiver (fig. C.2) at +0.020 MHz. Consequently, a total of 3-dB D/U degradation can occur just from drift caused by signal generator instability. Similar estimates can be made for the other IF's.

Another disconcerting effect was noted when the receiver was minutely detuned from the desired carrier and its modulating SCI signal. The SCIM test signal was monitored at all times at the video output of the receiver by an oscilloscope. During one test, the RF tuning knob was bumped at a point when the noise being introduced was becoming a major factor in the SCI readings; the SCI was dropping rapidly for a given D/U (fig. C.5). This detuning resulted in a 3-dB improvement in the protection ratio. Subsequent tests confirmed this idiosyncracy of the SCI analyzer. The 1-kHz SCI calibrating tone would be observed and the receiver detuned until a

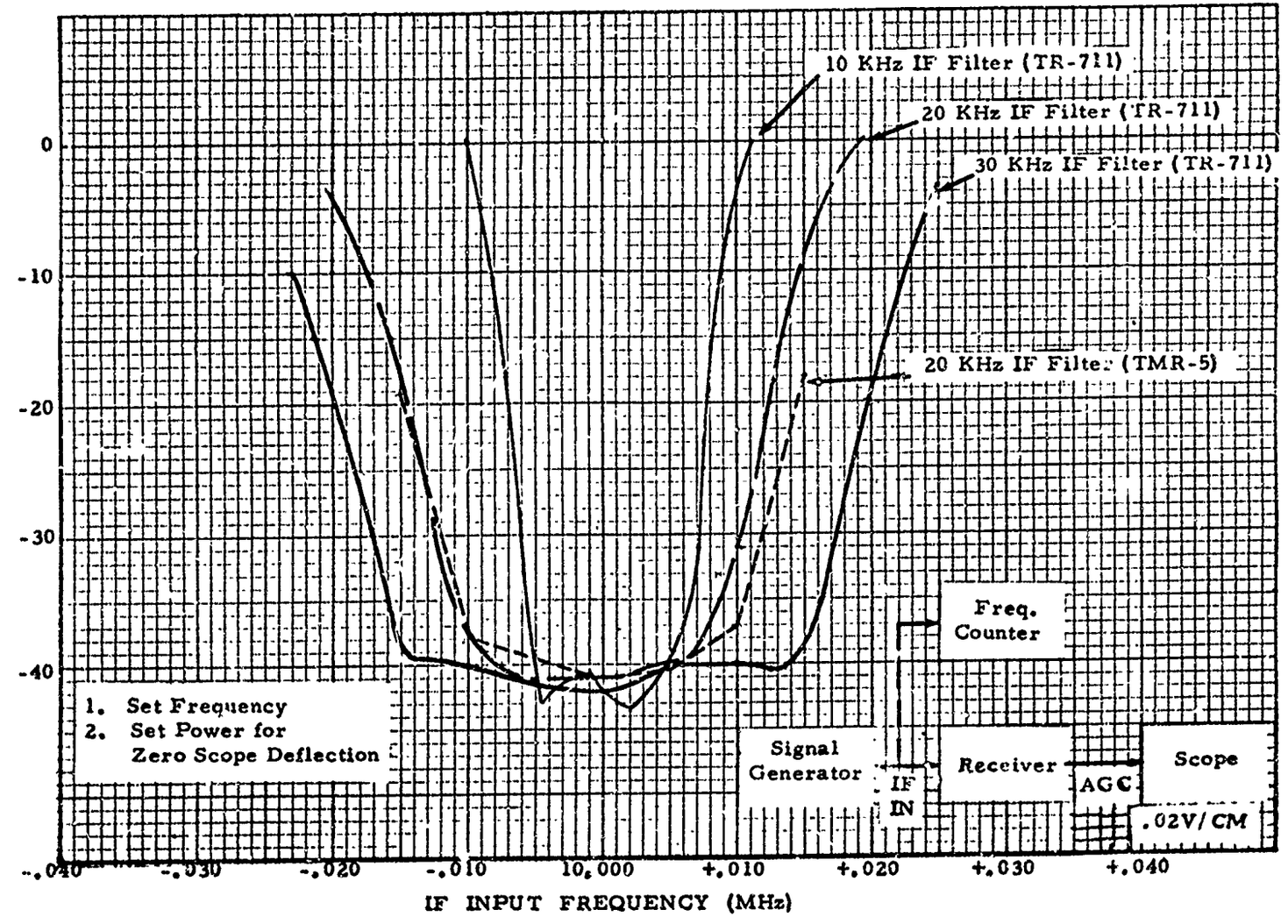

Figure C.2. IF bandpass characteristics of TR-711 and TMR-5 receivers.

slight amount of hash appeared on the tone. With a low carrier level (< -90 dBm), improved SCI readings resulted.

One of the basic problems encountered in these tests was the necessity of establishing a relatively high signal level (-87 dBm, -77 dBm) to reach a SCIM reading of .99. As the desired signal level was raised, it became necessary to increase the signal power level of the interfering signals, particularly in the adjacent channels.

A result of this "power escalation" is the front-end saturation of the receiver. According to Daghdady (1969), "all receivers start in the RF-to-baseband processing section with 'linear' stages purported to preselect and amplify a frequency range that includes the spectrum of the desired signal. Then, through frequency conversion processes followed by further linear filtering and amplification, the selected portion of the spectrum is narrowed down to the desired frequency channel, with the guard bands (if any) falling in the nominal cutoff regions. In practice, the degree of linearity of these receiver stages depends upon the input signal level, as well as upon the level of the interference present. Strong interference will usually cause the amplification, mixing, and filtering stages to be driven into non-linear modes of operation, causing a considerable increase in the receiver susceptibility to interference from all sources operating within the effective frequency response range of the antenna system.

Thus, one must recognize that so-called linear stages of selective amplification and frequency conversion in reality have limited dynamic ranges of linear response. A strong interference (anywhere in the spectrum) that drives these front-end stages into saturation will cause

(a) a drop in the level of the desired signal relative to attendant noises (so-called, desensitization) as delivered to the IF stages, and

(b) spurious by-products (in the IF range) of nonlinear interaction among signals present at the antenna terminals.

An illustration of the effect of dynamic range and the selection of LO and IF frequencies to minimize 'spurious responses' is shown in figure [C.3].

The response of the 'linear' stages is also usually regulated by automatic gain control (AGC) and automatic frequency control (AFC) to minimize dependence of their characteristics upon signal level and reduce susceptibility to frequency drifts. The presence of interference may influence the receiver response by affecting the AGC and AFC operations".

A possible solution for preventing receiver front-end saturation and intermodulation products has been suggested by Trott (1966) and Higgins (1968). Both authors recommend inserting a high-pass, low-pass, or symmertically balanced filter between the antenna and the receiver. Trott's paper describes commercially available notch filters that would be useful in eliminating particular interference sources, while Higgins uses network filter theory to design a cascaded high-pass, low-pass, and symmetrically tuned RC filter network that has a center frequency loss of 1 dB.

C.2. Description and Results of SCI Tests (Figs. C.4 through C.15)

The results displayed in figure C.4 show the prominent threshold effects of FM systems. With a D/U ratio change of 3 dB the SCI ranged from .99 to .45. This abruptness is a general characteristic of FM and appears for both the 20-kHz and 10-kHz IF filter tests. When comparing these results with those in figure C.8, we find a higher level of interference, when the interfering channel is amplitude

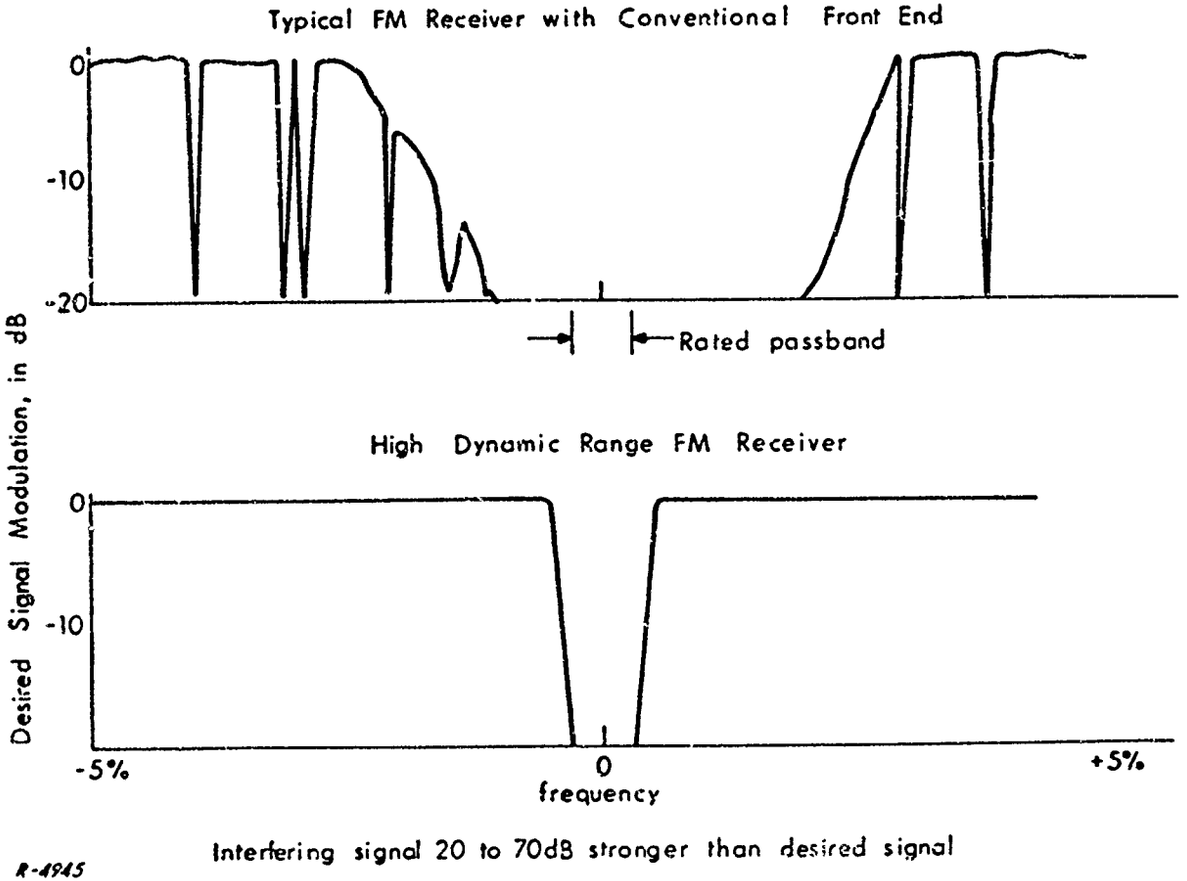

Figure C.3. Comparison of the effect of wide dynamic range and RF to IF frequency planning on receiver selectivity in the presence of strong interference (Baghdady, 1969, fig. 2).

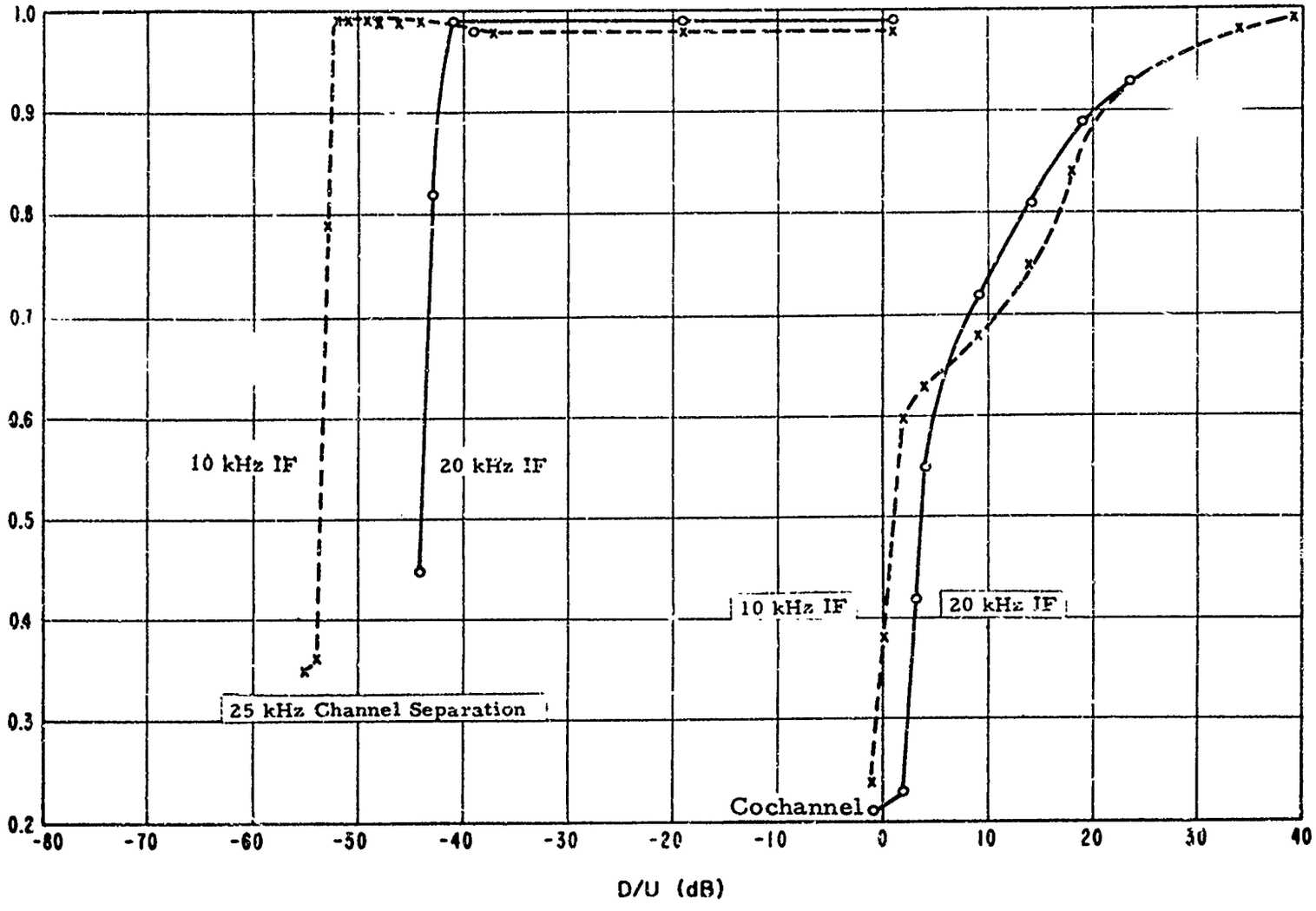

Figure C.4. Cochannel and adjacent channel FM interference to FM signals (FM_D / FM at RF).

modulated. This is true for the adjacent (25-kHz separation) and cochannel situations. In the adjacent channel tests illustrated in figures C.4 and C.8, a 4-dB improvement in protection ratio is noted in table 4 (sec. 4) when the interfering signal is frequency modulated and has a 20-kHz IF filter.

The wandering appearance of both sets of cochannel curves is attributed to carrier drifts and beats between the carriers as they come in and out of tune with each other.

Good agreement exists between the sets of curves shown in figures C.5 and C.6, where the desired signal was frequency modulated and interfering AM and FM signals on one side of the desired were transposed to determine a possible difference of interfering effects. Another objective of this set of tests was to determine whether there would be a difference in the protection ratio when the power level was increased similarly and simultaneously in the two interfering signals as compared to keeping one interfering power level constant while increasing the other.

The results in these figures indicate that the protection ratio for these configurations depends on the total combined AM and FM interfering power. They also indicate that whether AM or FM interference is immediately adjacent is not as important as indicated by other tests. The apparent stability of the signal generators for these particular tests is shown by the closeness of the three sets of results plotted here. A step in the D/U in figure C.5 is due to a slight detuning of the receiver and is discussed in section C.1.

The primary difference between the results shown in figure C.7 and those in figures C.5 and C.6 is that the interfering signals were placed on both sides of the desired carrier. Other than that, these tests were performed in the same way. Both interfering signals

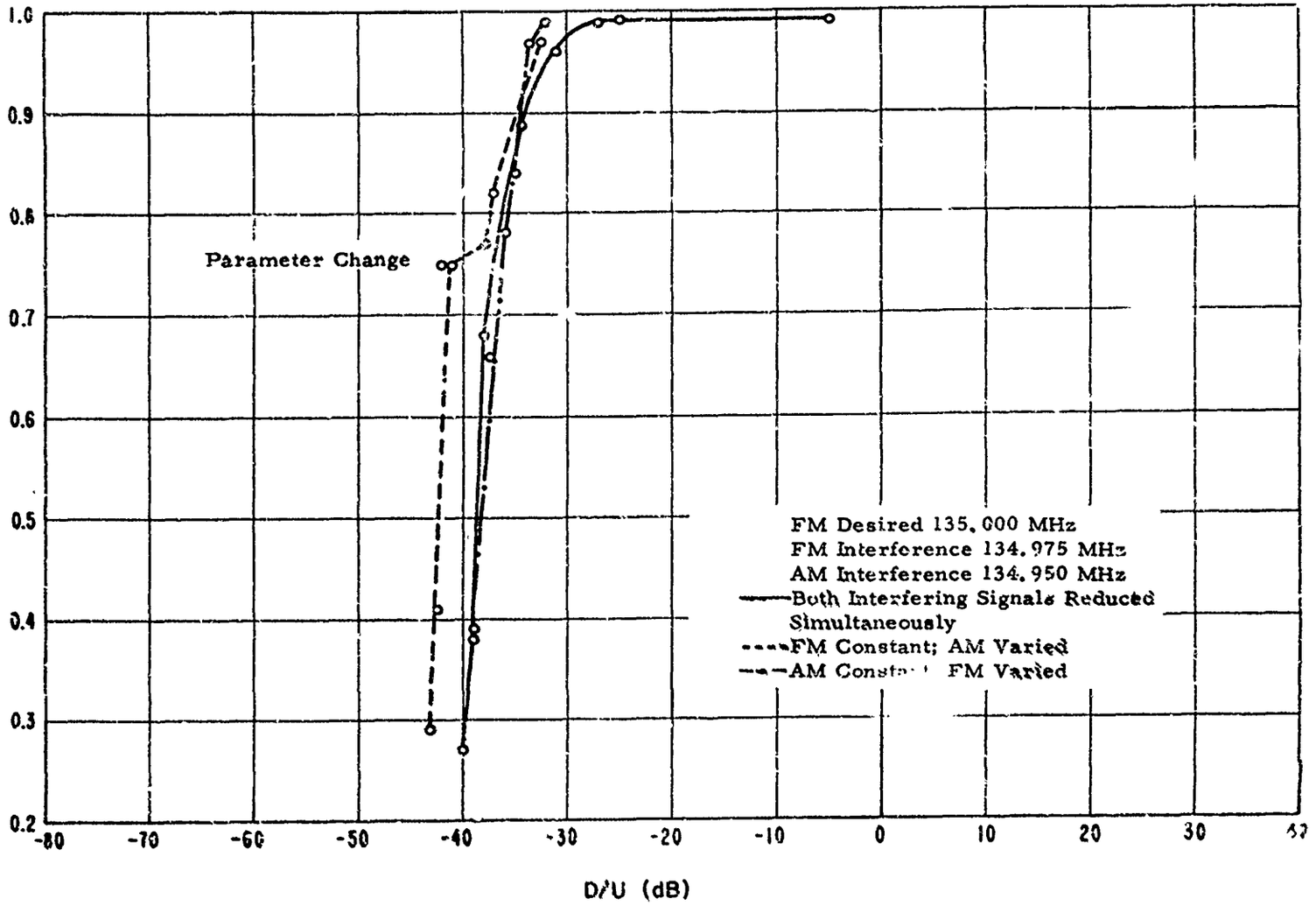

Figure C.5. Adjacent channel FM and AM interference to FM signals (FM_D / FM/ AM at RF).

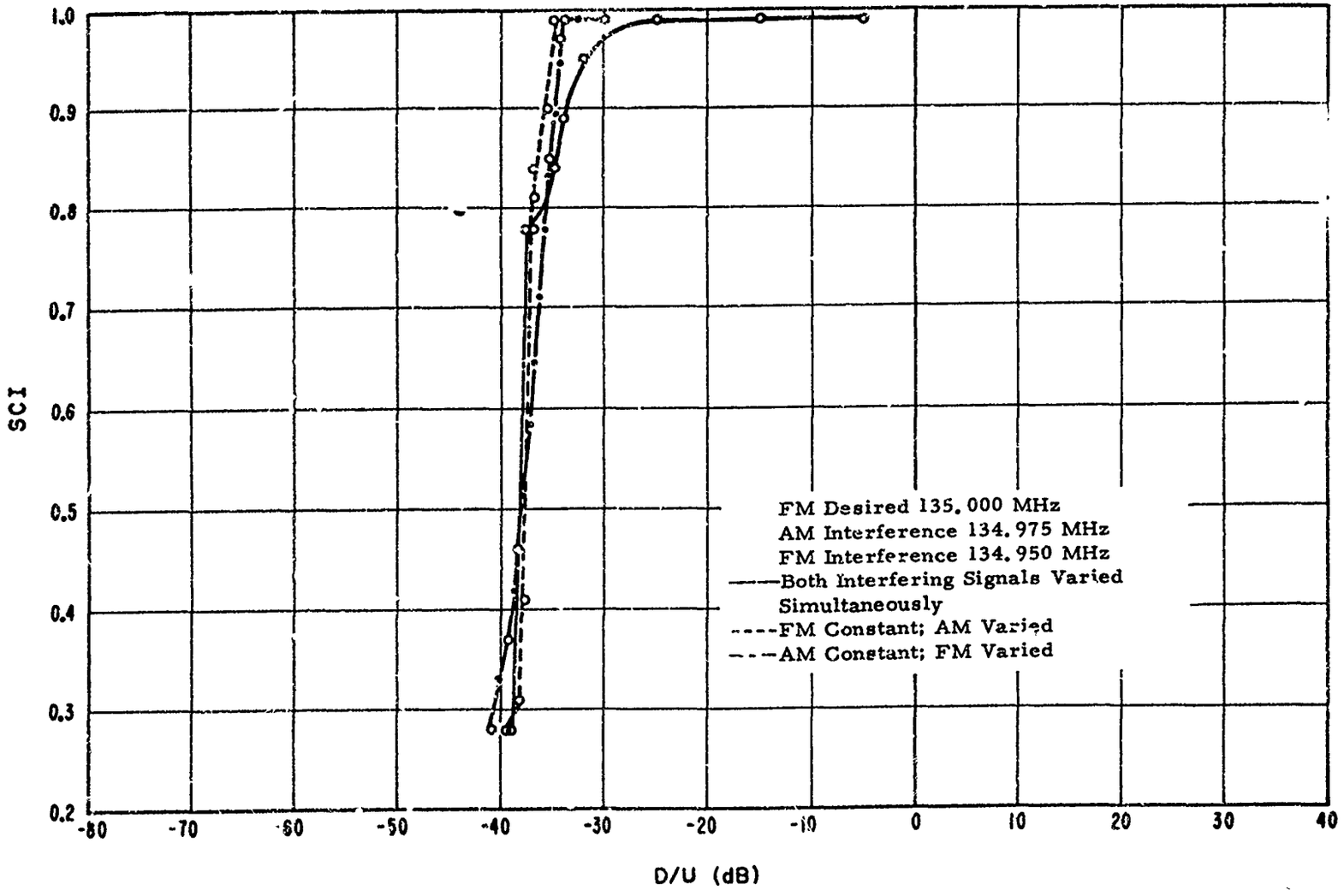

Figure C. 6. Adjacent channel AM and FM interference to FM signals (FM_D / AM/ FM at RF).

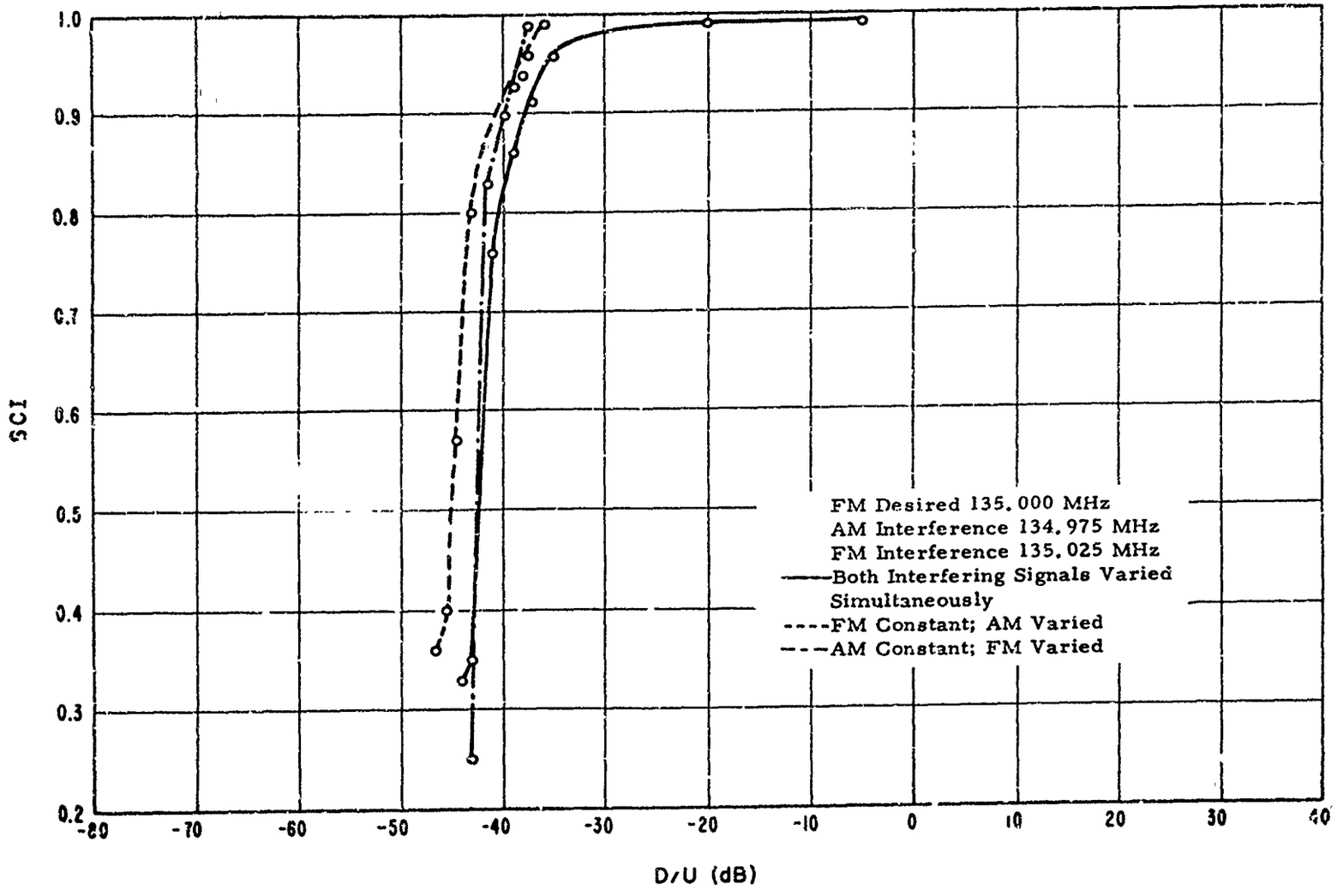

Figure C.7. Adjacent channel FM and AM interference to FM signals (FM/ FM_D / AM at RF).

were increased together, and then one was varied while the other was held constant in successive tests.

Surprisingly, the D/U in these tests is less (up to 5 dB) in comparison with the tests where both interfering signals were placed on one side of the desired signal. One possible explanation is frequency pulling/detuning exerted by the high-level interfering signals when placed on one side of the desired signal. AGC desensitizing in the RF tuner cannot be ignored either.

In another set of tests where the desired signal was amplitude modulated and the interfering FM signals were both on one side, higher D/U ratios were required as compared to straddling the desired signal (figs. C.13 and C.14). These results indicate that proximity of interfering adjacent channels does not necessarily result in an increase in the required protection ratios.

In figures C.8 and C.9, two sets of plotted data on similar tests, there is fair agreement between the tests with 20-kHz IF's and 25-kHz channel separation. In fact, for SCI = 4 there is a 2-dB difference, while for SCI = .85 there is only a 1-dB difference.

Unfortunately, when the 25-kHz channel separation test was performed with the 10-kHz IF, the results did not agree anywhere near as well. The probable reason is carrier frequency instability and indicates the closer frequency tolerances necessary when tests are performed with narrower bandwidths.

In the series of tests shown in figure C.10, the FM desired signal had AM interfering signals, + and -25 kHz on both sides. There is little difference in these results and those in figures C.8 and C.9, where single interfering sources were used. Here again, the total interfering power of the undesired signals appears to be the main criterion influencing the SCI.

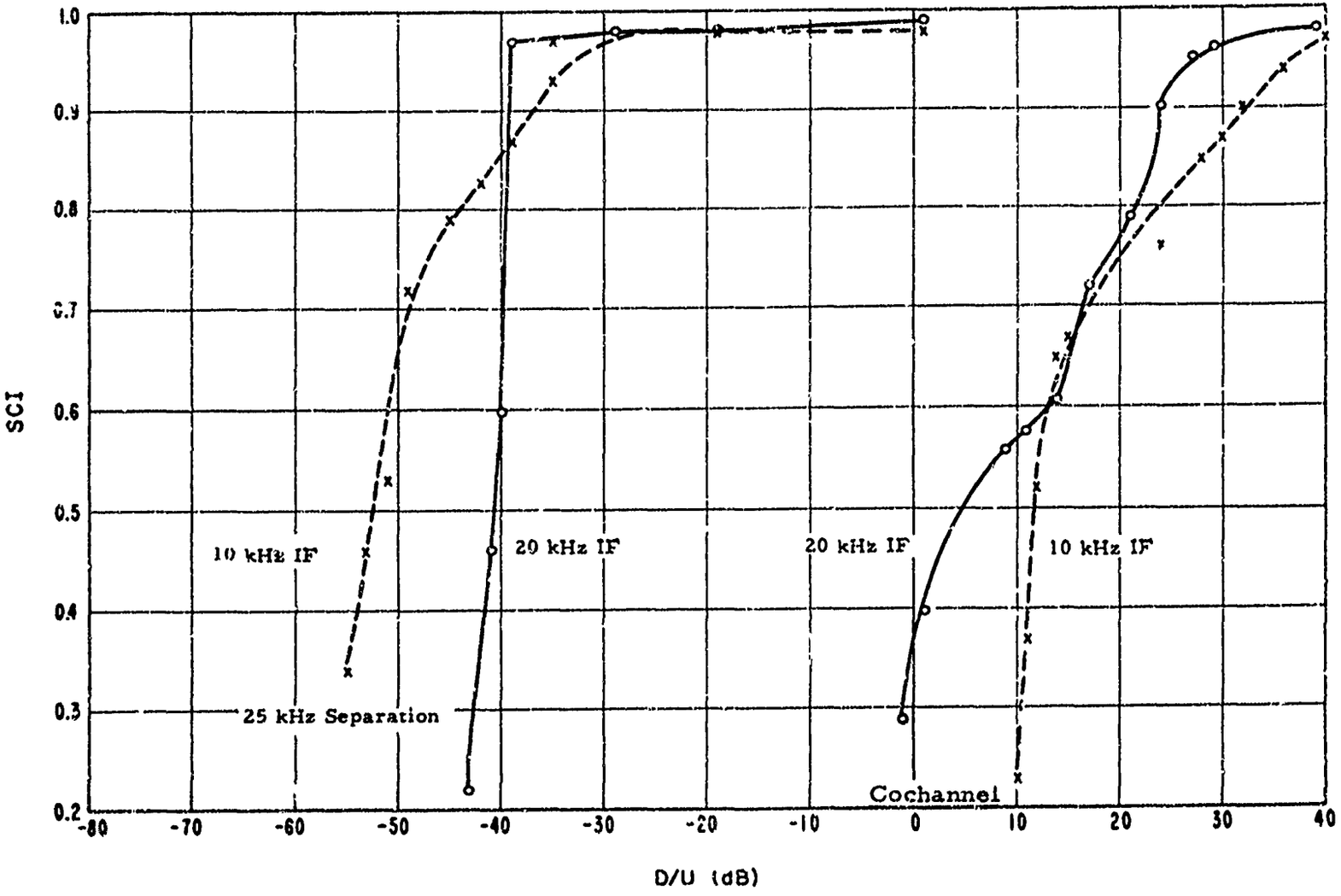

Figure C. 8. Cochannel and adjacent channel AM interference to FM signals (FM_0 / AM at RF).

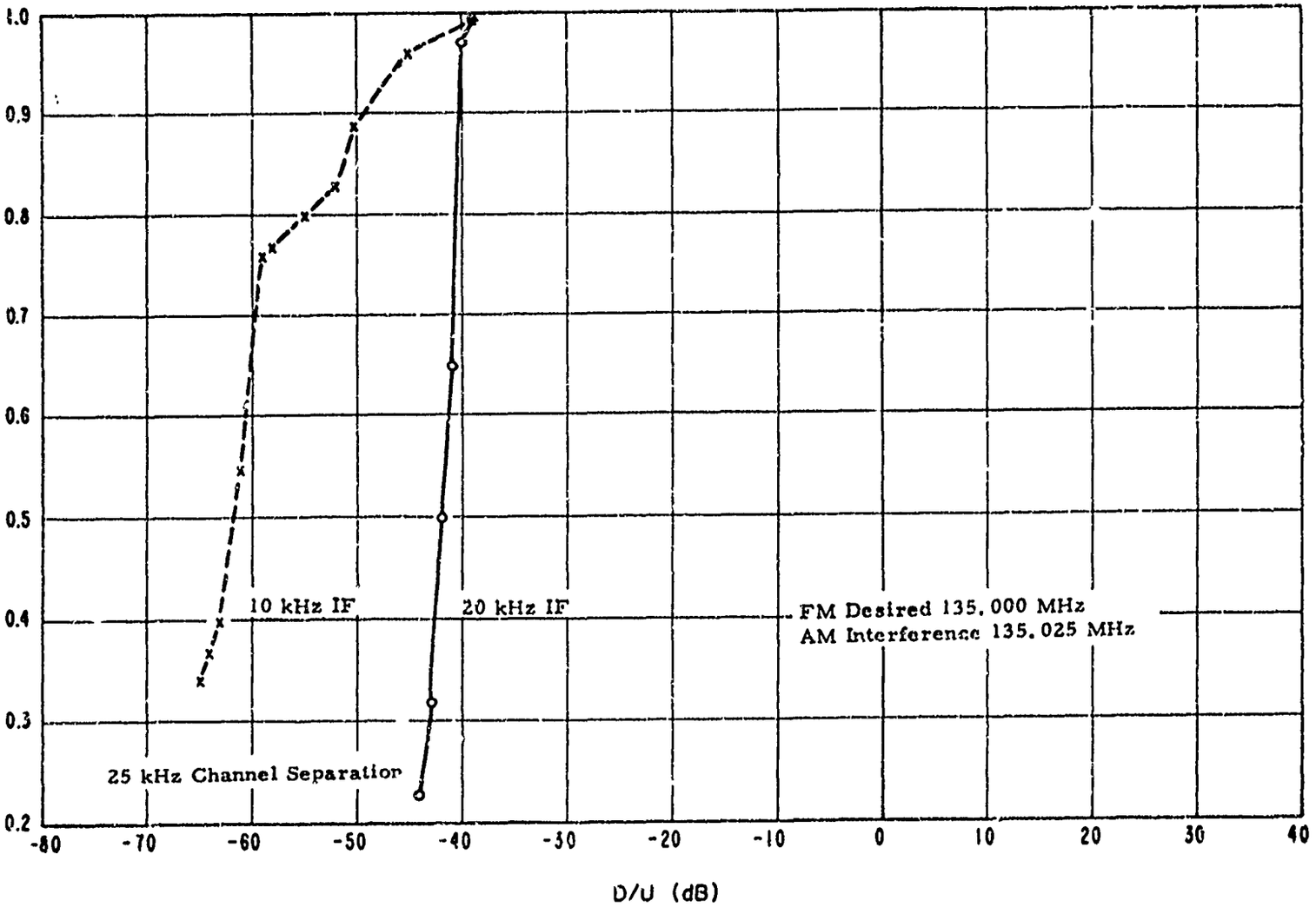

Figure C.9. Adjacent channel AM interference to FM signals (FM_0 / AM at RF).

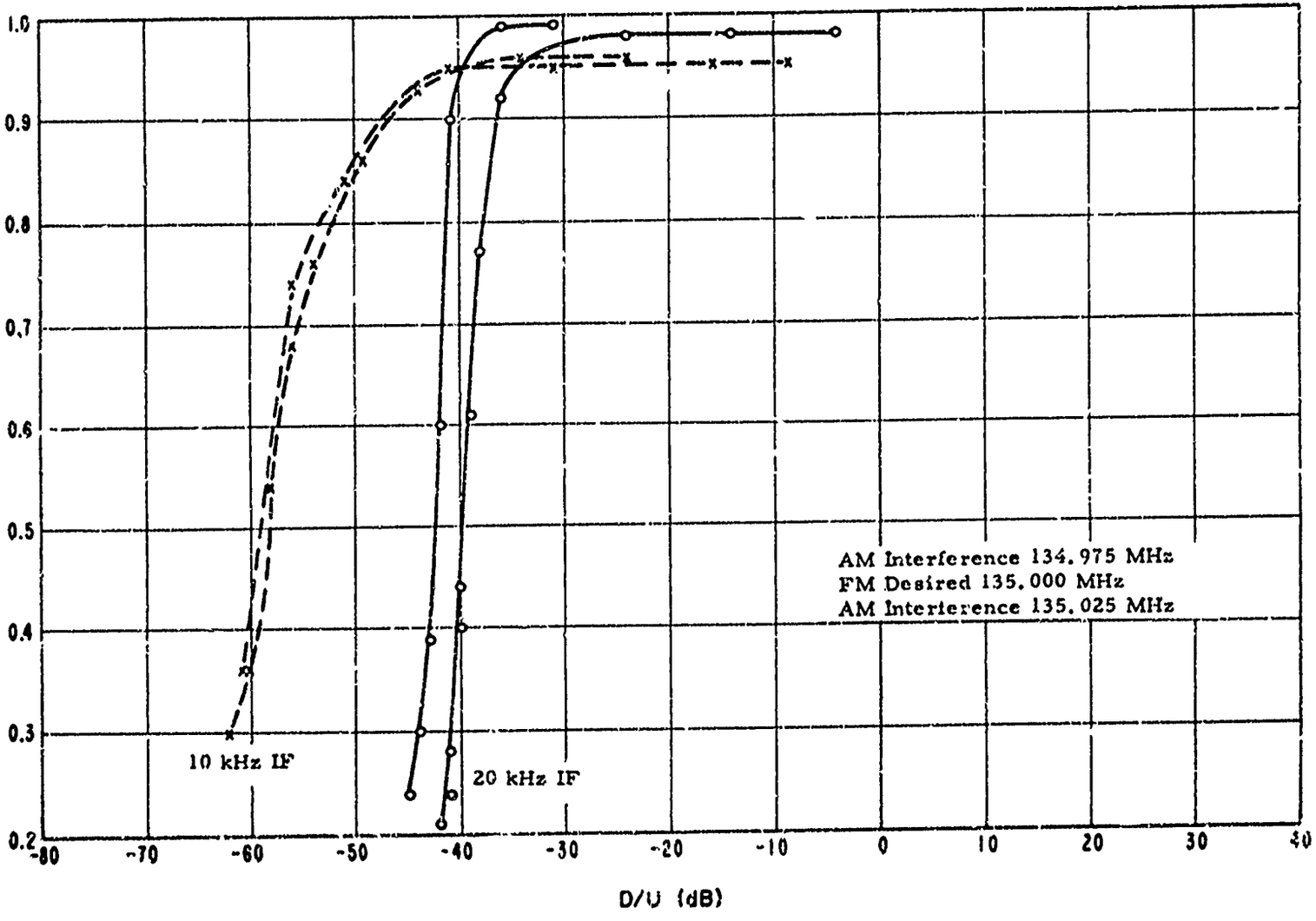

Figure C.10. Adjacent channel AM interference to FM signals (AM/ FM_D / AM at RF).

Two tests were performed with 10-kHz and 20-kHz IF's. In one set, both interfering signals were increased simultaneously. This is shown in the curves of figure C.10. When only one interfering AM source was increased, the lower D/U is indicated in this graph, particularly for 20-kHz IF. There is no significant difference for 10-kHz IF.

In all cases discussed so far, the desired signal was frequency modulated in various combinations with one or two AM or FM interfering signals. The D/U range for SCI of .4 was between -38 and -45 dB and for SCI = .85 between -35 and -43 dB, when tested with 20-kHz IF's. Considering the number of individual tests discussed here (15), and the various problems encountered, the results appear consistent.

Figure C.11 shows the result of a simple test configuration of an AM desired signal and one FM undesired signal. The D/U for SCI = .4 is -41 dB and for SCI = .85 it is -32 dB with 20-kHz IF's. For this particular test, the desired signal power had to be raised from -87 dBm to -77 dBm at the input to the receiver to achieve an SCI of .99 with no interference. Lower desired carrier levels resulted in SCI's of .85 and .89 at the upper extreme.

The test used to obtain the curves in figure C.12 consists of an AM desired signal with an FM undesired signal 25 kHz below and an AM undesired signal 25 kHz above the desired carrier frequency. As tabulated in table 4 (sec. 4), the SCI's are considerably lower than for figure C.11, where only one FM interfering signal was considered. A factor here is the lower desired carrier power used (-87 dBm), which resulted in a reduced SCI at the upper extreme. At an SCI of .85, the D/U was -17 dB (20-kHz IF). For this test it seems possible to achieve

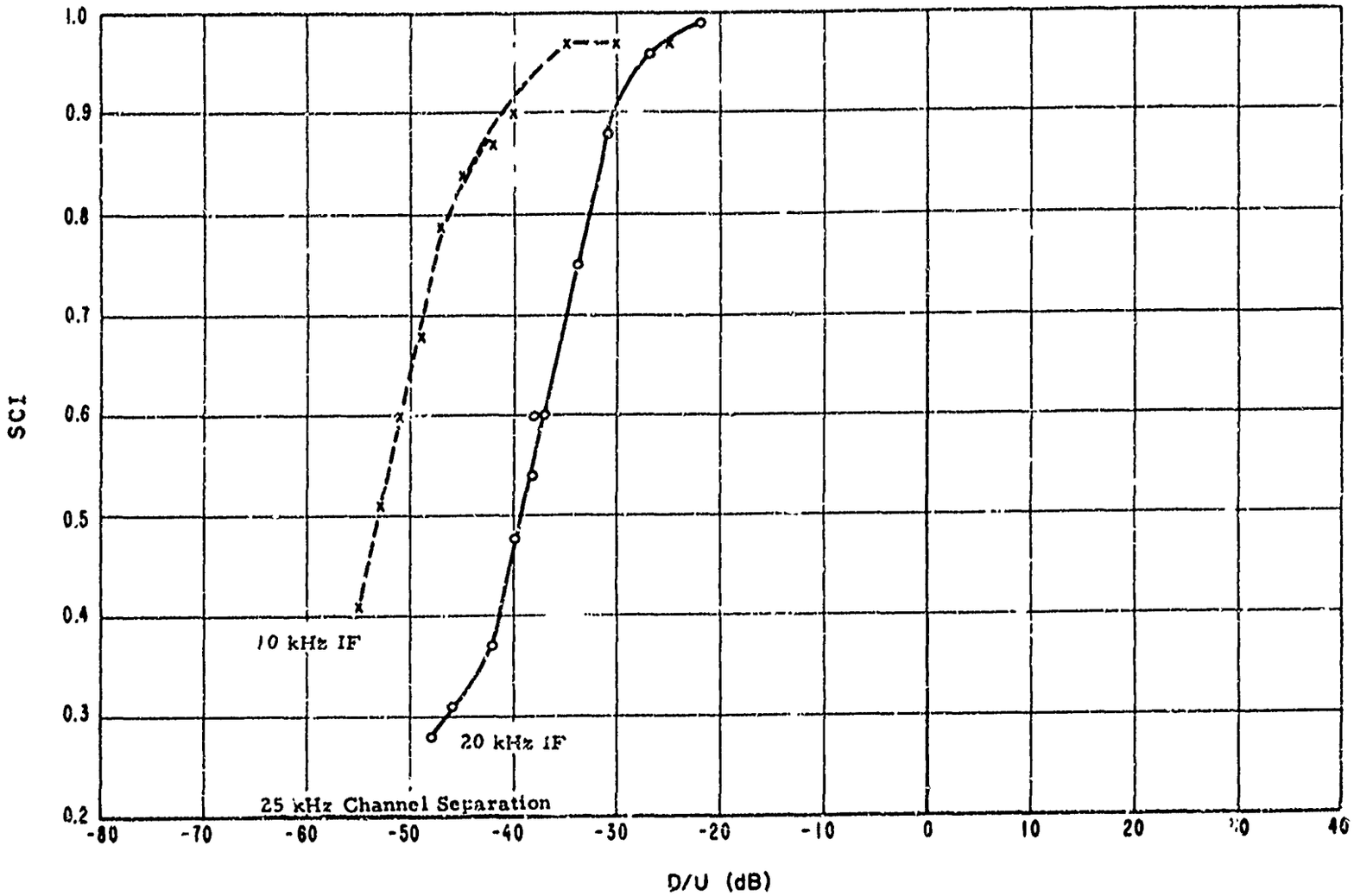

Figure C. 11. Adjacent channel FM interference to AM signals (AM_c / FM at RF).

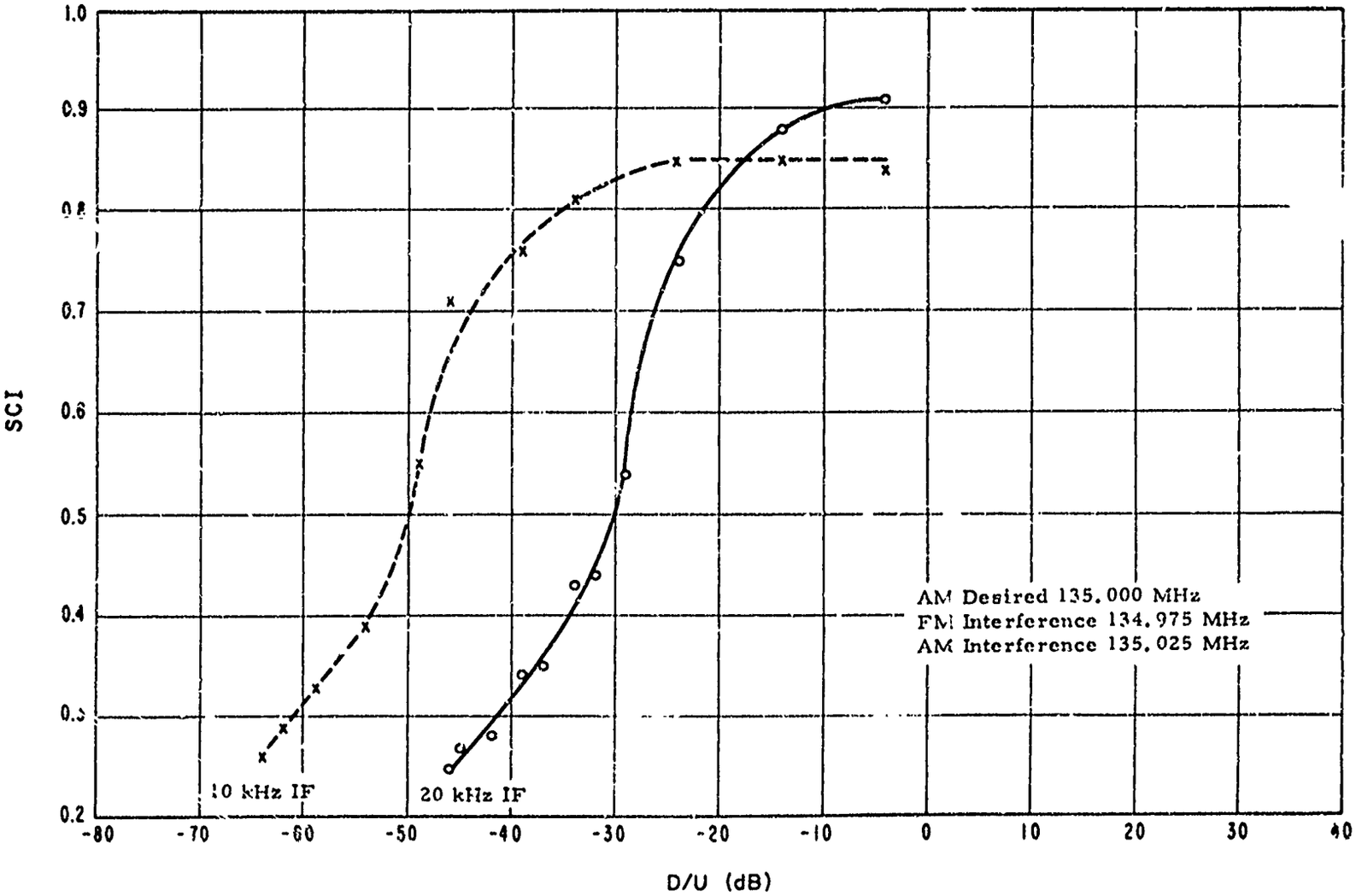

Figure C.12. Adjacent channel FM and AM interference to AM signals (FM/ AM_D / AM at RF).

a D/U ratio of -21 dB for a .85 SCI if the upper limiting SCI were increased to .99.

The results given in figure C.13 show a marked degradation when two interfering FM sources in 25-kHz channels are introduced rather than only one (fig. C.11), and there is a lower desired carrier level. There is a 13-dB and a 16-dB degradation for SCI = .4 and .85 respectively for a 20-kHz IF filter bandwidth. This degradation is also more severe than that displayed by adjacent AM and FM channel interference (fig. C.12). This could be due to detection of modulation energy (by the skirts of the AM receiver characteristics) from the FM interfering sources.

In the test associated with figure C.14, the AM desired signal competes with two interfering FM signals. One of the undesired signals is 25 kHz and the other 50 kHz lower than the desired signal.

When one interfering FM signal is varied and the other held constant and sufficiently attenuated, the signal that is varied will be the prime source of interference. For this test, one of the undesired carriers was attenuated 60 dB, while the effects of the other were noted. There should be less interference from an undesired signal 50 kHz from the desired signal than from one 25 kHz from the desired signal.

The results as recorded in table 4 (sec. 4) show a 13- and 14-dB improvement for the given SCI's when the signal located 50 kHz from the desired signal is kept 60 dB down, while the interference 25 kHz off is increased. It also can be said that with only the 50-kHz interference in effect and 25-kHz interference suppressed, there will be an improvement of 43 dB over that when both interfering sources are introduced for SCI = .85.

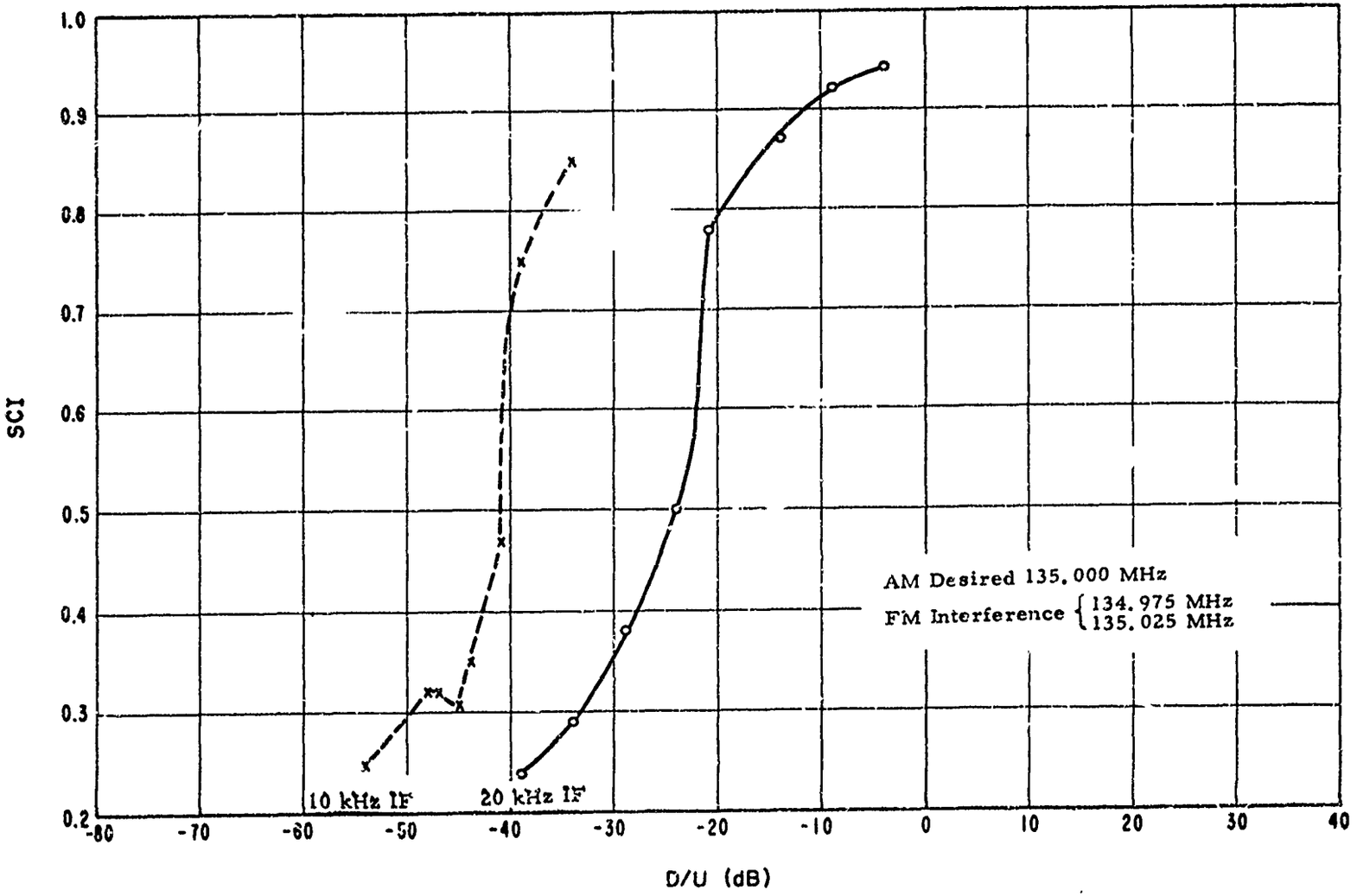

Figure C.13. Adjacent channel FM interference to AM signals (FM/ AM_D / FM at RF).

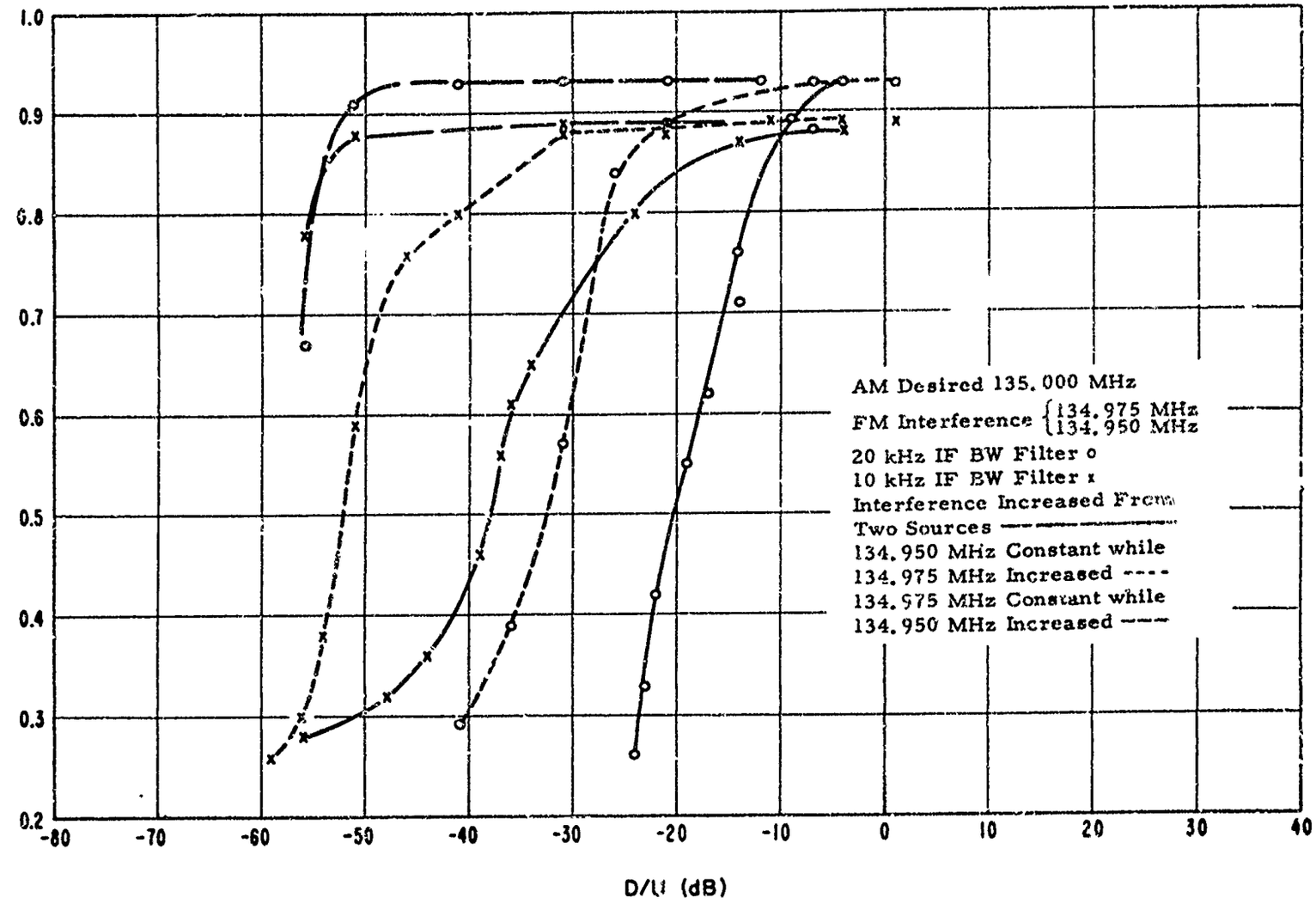

Figure C.14. Adjacent channel FM interference to AM signals (AM_D / FM/ FM at RF).

Assuming negligible frequency drift in all the tests, the worst case occurs where we have two FM signals 25 kHz and 50 kHz from the desired frequency. This is in contrast to two FM sources above and below the desired signal (fig. C. 7) where improved results are displayed.

Figure C. 15 shows the higher SCI scores possible when the RF input level is raised from -87 dBm to -77 dBm for similar IF bandwidths.

C. 3. Basic SCI Measurements (Figs. C. 16 through C. 33)

AM and FM system performance measurements with wide-band Gaussian noise comprise the basic data for this report. The same interference was used to evaluate performance subjectively in the ATC message and MRT tests and objectively by means of the SCI measure of performance. From this data, a relationship was derived between the subjective and objective performance of the systems (figs. 21 and 22).

The subjective data are plotted in figures 19 and 20; the objective data, in figures C. 16 and C. 17. Figures 21 and 22 also show a comparison between the subjective and objective results. Two independent objective measurements were performed in both systems. Two AM tests (test β-2, lines A and B) show agreement within about 1 dB, and the FM tests plotted in figure C. 17 (tests β-1B and 35) indicate very good agreement over the range of interest.

Figure C. 16, test 3, and figure C. 17, test 4, present the data obtained from a test performed with an RF noise generator as an interfering source. The noise power output of this instrument was not sufficient to allow measurements beyond a 0- to 10-dB range in D/U. However, the data are included for comparison with the results

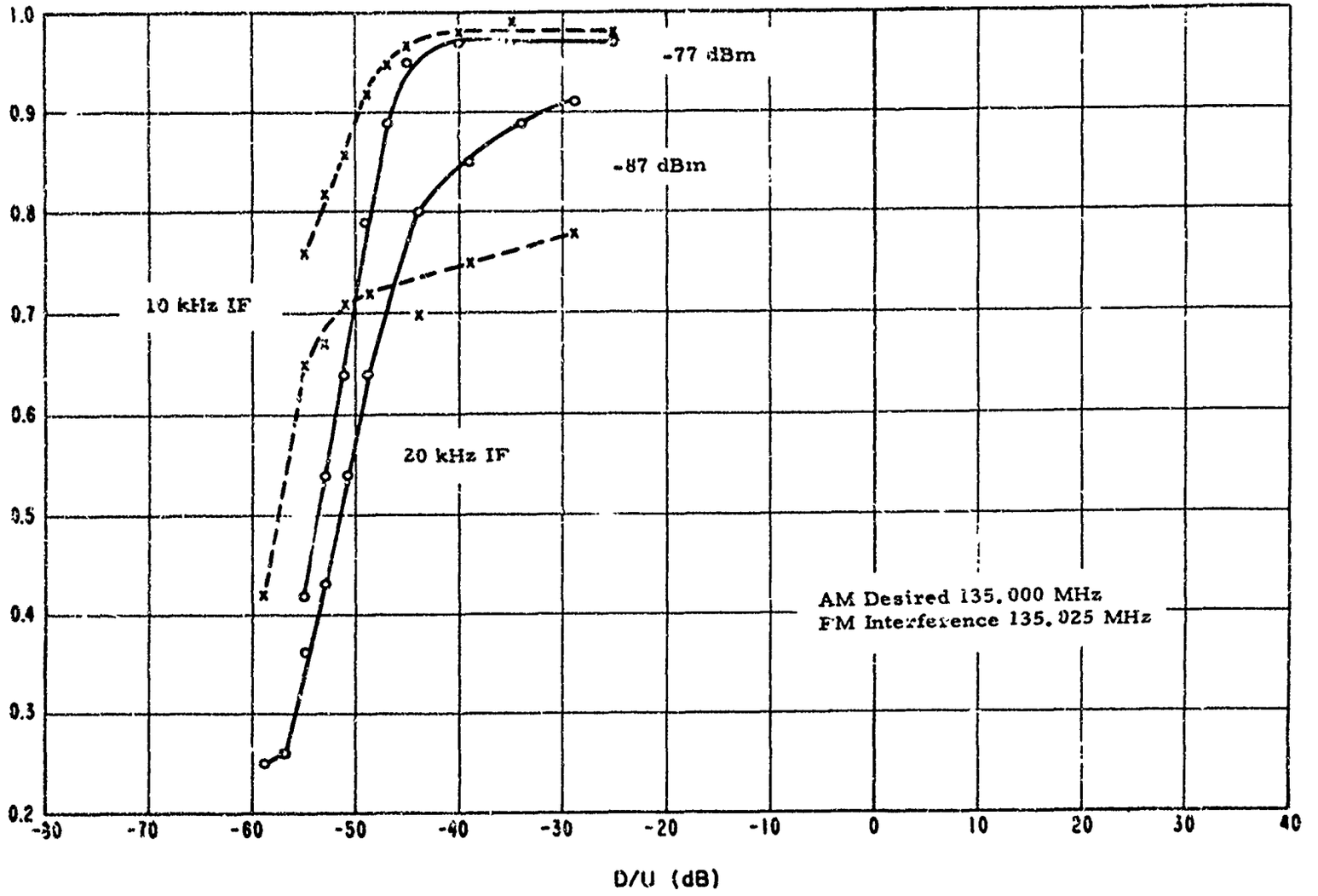

Figure C.15. Adjacent channel FM interference at two AM signal levels (AM_D / FM at RF).

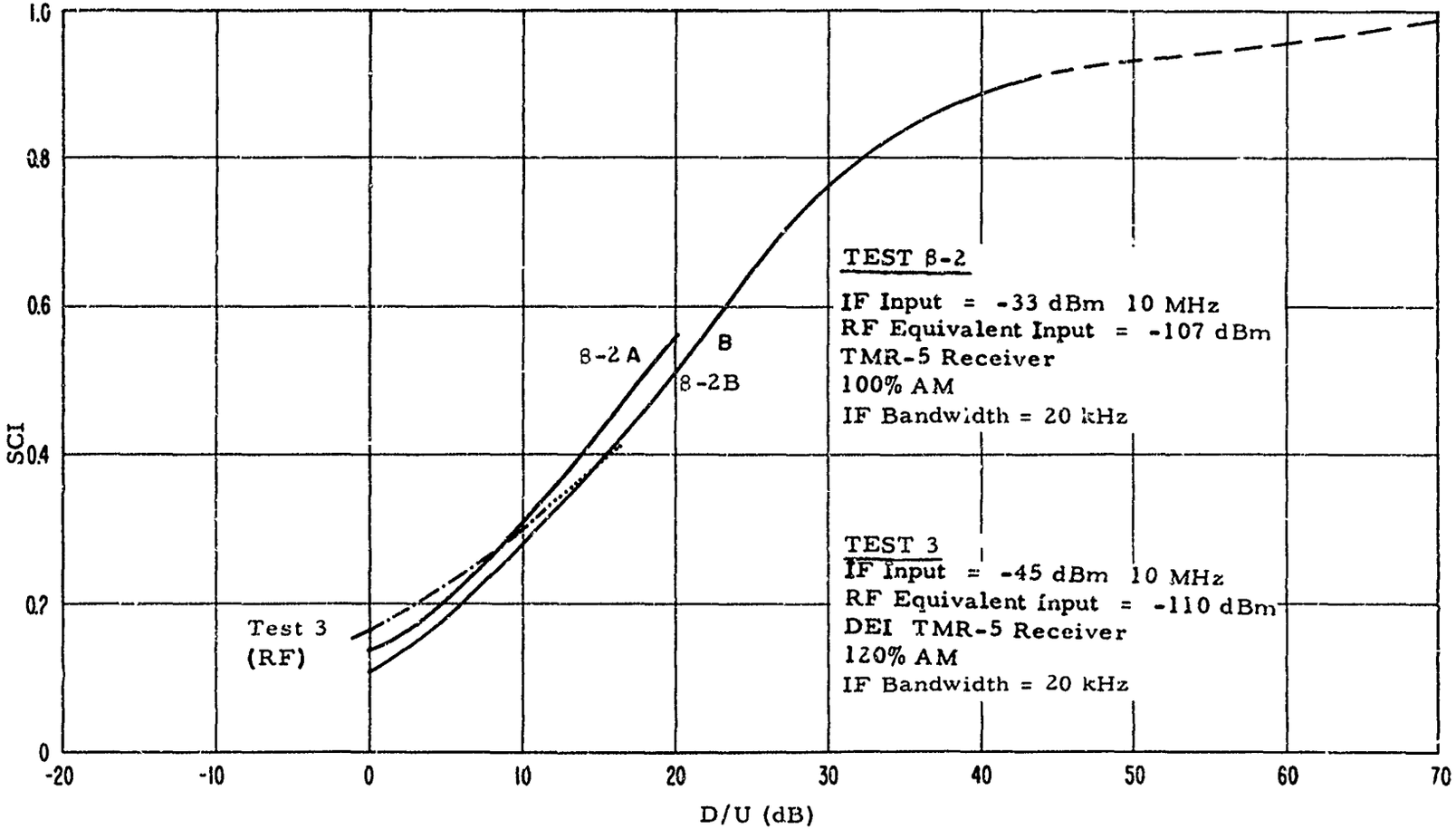

Figure C. 16. Wideband noise interference to AM signals (AM/ wideband noise at IF).

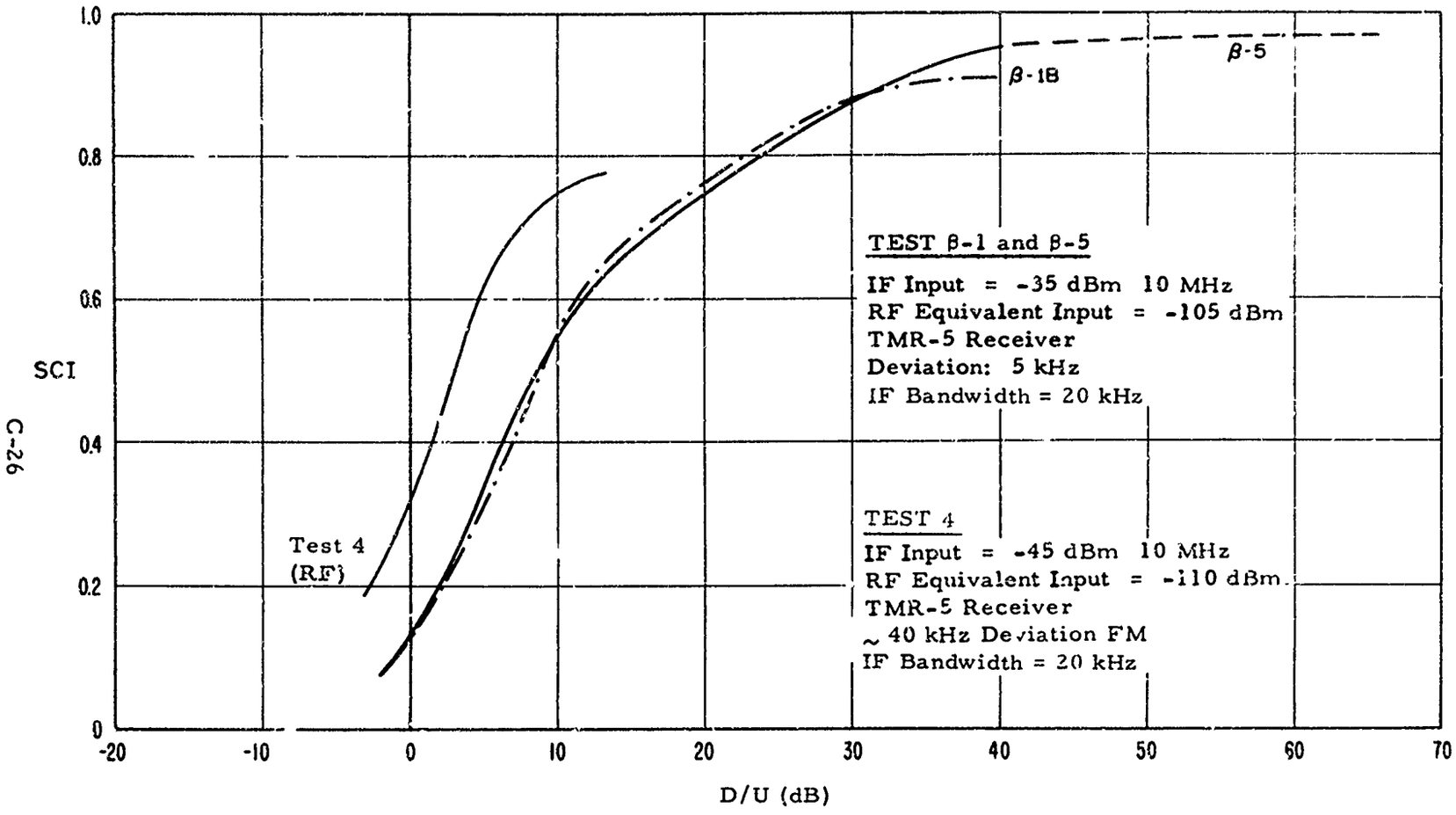

Figure C. 17. Wideband noise interference to FM signals (FM/ wideband noise at IF).

tests in which the wideband noise interference modulating a carrier was used.

To overcome the limitations of restricted RF noise power, a high modulation index FM spectrum was generated and used as an interfering signal source. A Gaussian random noise generator was used to frequency modulate a carrier at the IF with a frequency deviation of ~100 kHz or to a point where the modulation index was sufficient to suppress the carrier. The noise spectrum produced in this manner is considered proportional to the first order probability density function of the amplitude of the modulating signal (Woodward, 1952). Comparison of the results obtained with an RF noise source as an interference signal indicates that the method is valid for our test purposes (fig. C.16).

In figure C.17, the high deviation level for test 4 compensates for its lower signal level, when compared to a lower deviation ratio and higher signal level.

The AM/AM cochannel tests in figure C.19 demonstrate the effect of beat frequency interference. The 600-Hz off-tune condition is seen to require 10-dB higher protection ratio than either an on-tune or an off-tune condition where the resultant beat frequency appears outside the audio passband.

Tests 5 and 6 (figs. C.27 and C.20) are not considered entirely valid, as the desired signal FM deviation was inadvertently set to a high value. The 1-kHz test tone of the SCIM signal was used to set the peak deviation to 10 kHz. The speech-shaped noise peaks in this signal, however, are 12 dB higher than the test tone, and thus the resulting peak deviation would have been approximately 40 kHz, as indicated in table 3 (sec. 4), if the modulator had been assumed linear to that degree. It is not known precisely how the SCIM analyzer would

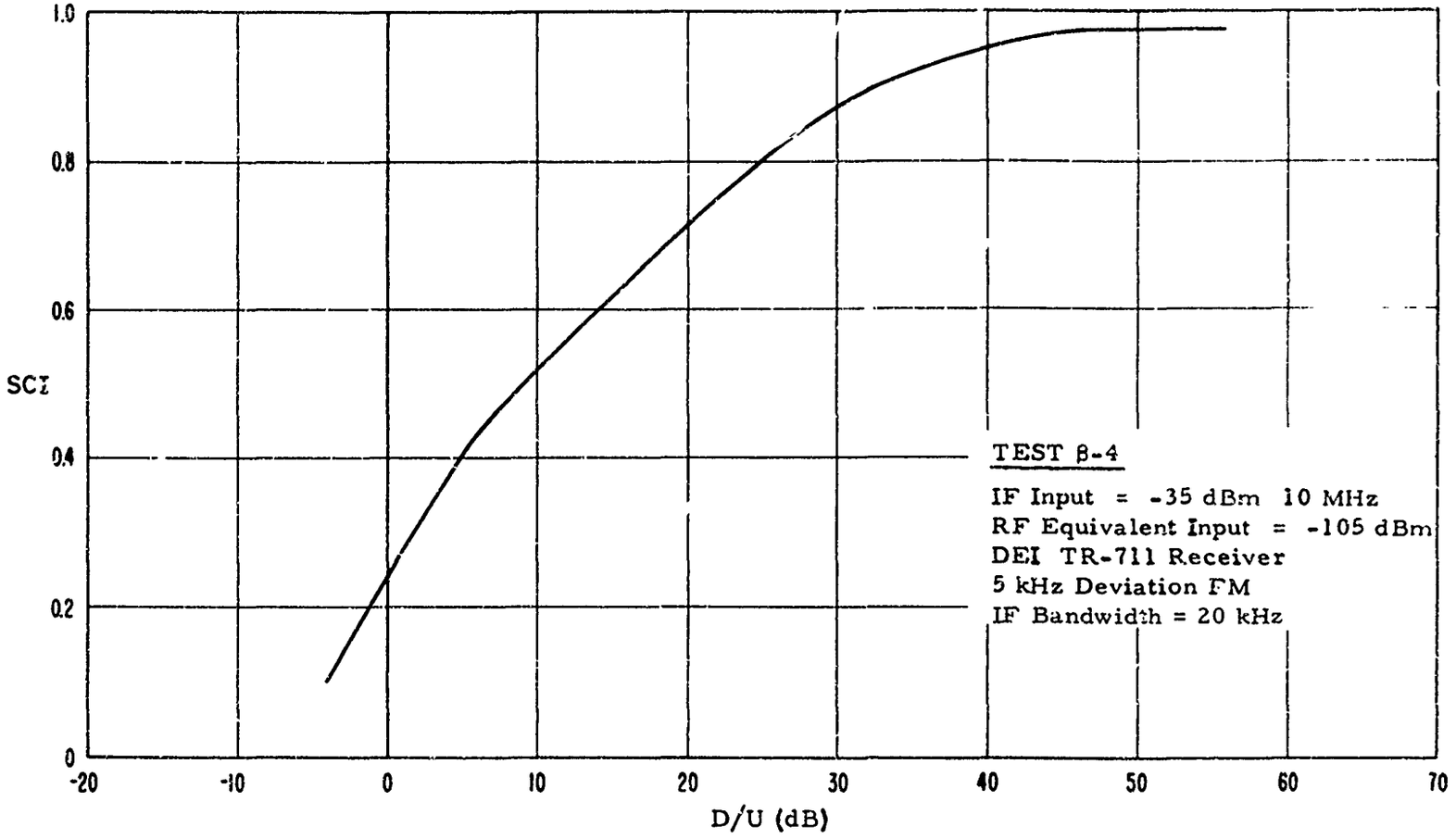

Figure C.18. Cochannel FM interference to FM signals (FM_D / FM cochannel at IF).

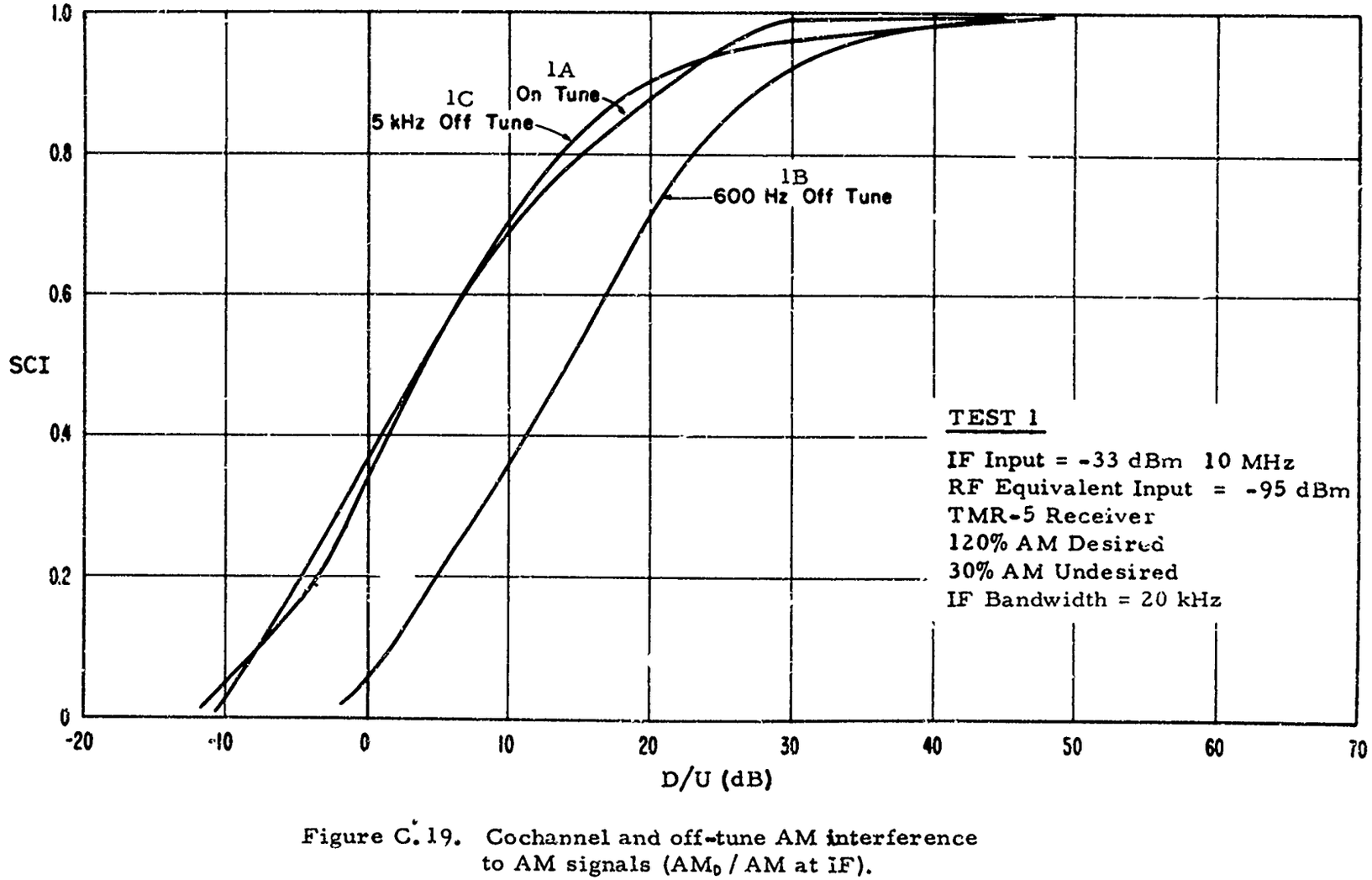

Figure C. 19. Cochannel and off-tune AM interference to AM signals (AM_0 / AM at IF).

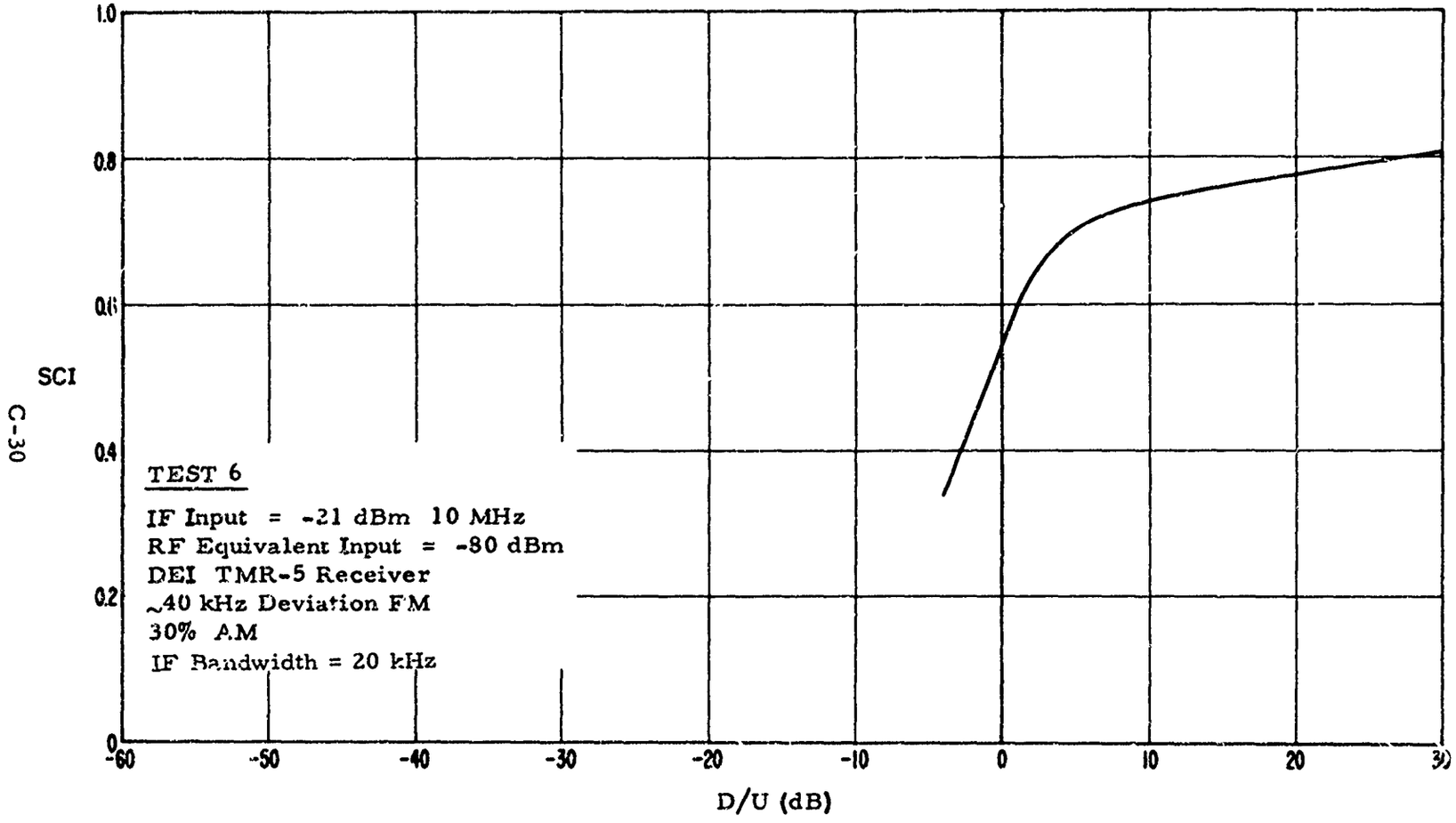

Figure C.20. Cochannel AM interference to FM signals (FM_D / AM cochannel at IF).

evaluate the distortion that would result after these wideband FM spectra have passed through a receiver bandwidth of 20 kHz.

These same comments apply to estimates of 120% amplitude modulation. When the 1-kHz test tone was set to 30% amplitude modulation, the resulting modulation of the speech-shaped noise peaks would be 120%.

Tests X-11 and X-12 in figure C.21 show the effects of increasing carrier level from -43 dBm to -33 dBm. These tests again illustrate the improved SCI readings caused by improved signal levels when the modulation characteristics remain the same.

The tests in figure C.21 were performed at the receiver IF frequency. Comparison of these results to results from tests at RF frequencies shows similar improved SCI scores when the carrier level is increased (figs. C.22 and C.23).

The results of measurements performed in the RF test range reveal the effect of receiver noise. Generally lower SCIM scores were obtained with lower levels of desired signals at high D/U (figs. C.22 and C.23). On the other hand, the performance curves are quite similar at lower D/U values regardless of the desired signal level. In these regions, the undesired external interference is dominant, and the internal receiver noise is effectively masked. Very good agreement between the RF and IF measurements is observed in these lower D/U regions of the performance curves.

The comments applying to figure C.20 apply to C.27 as well. The results are not considered entirely valid because the desired signal FM deviation was inadvertently set to a high value as explained in the comments for figure C.20.

The poor SCI scores in figure C.30 are a direct result of low desired carrier levels.

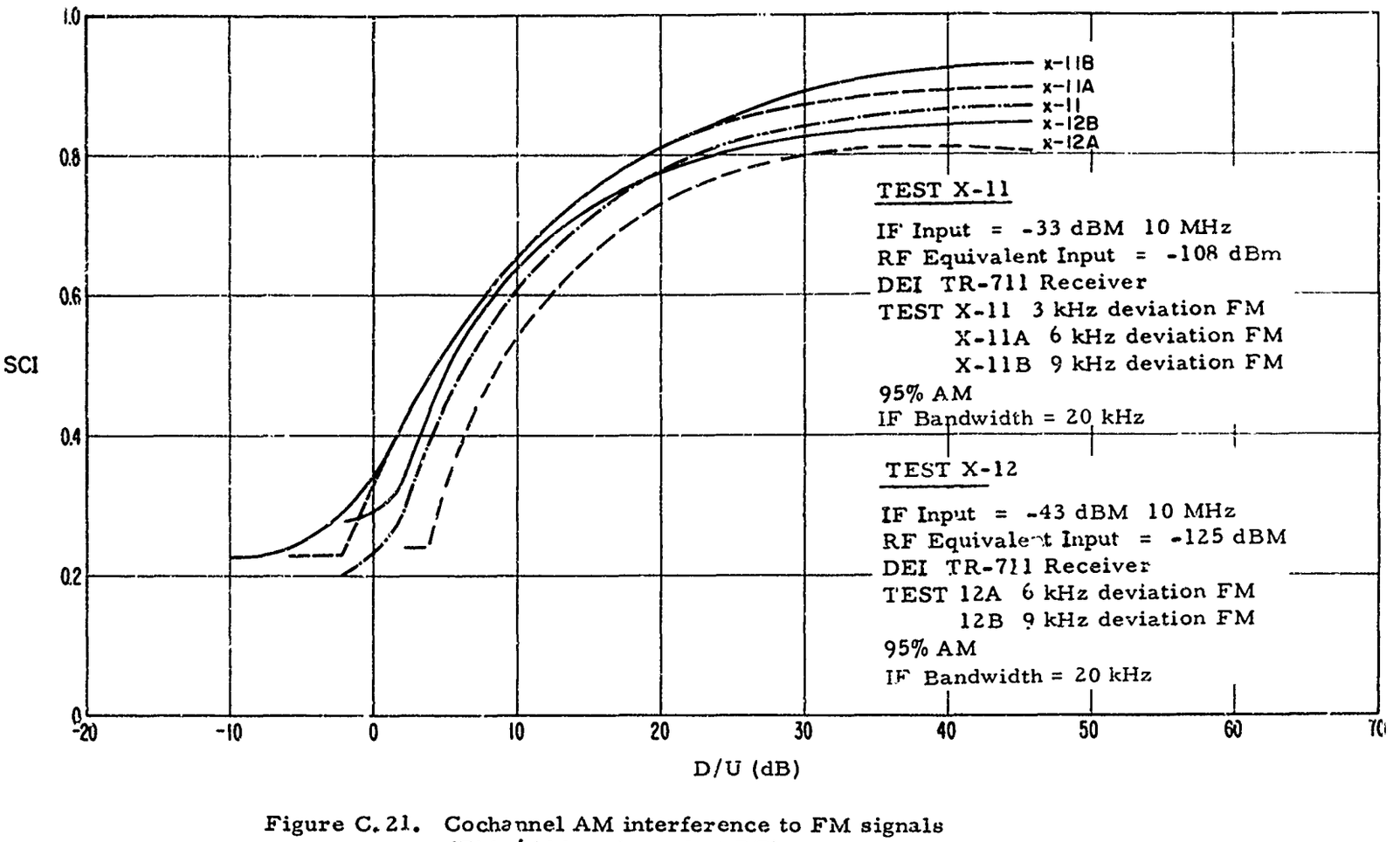

Figure C.21. Cochannel AM interference to FM signals (FM_0 / AM cochannel at RF).

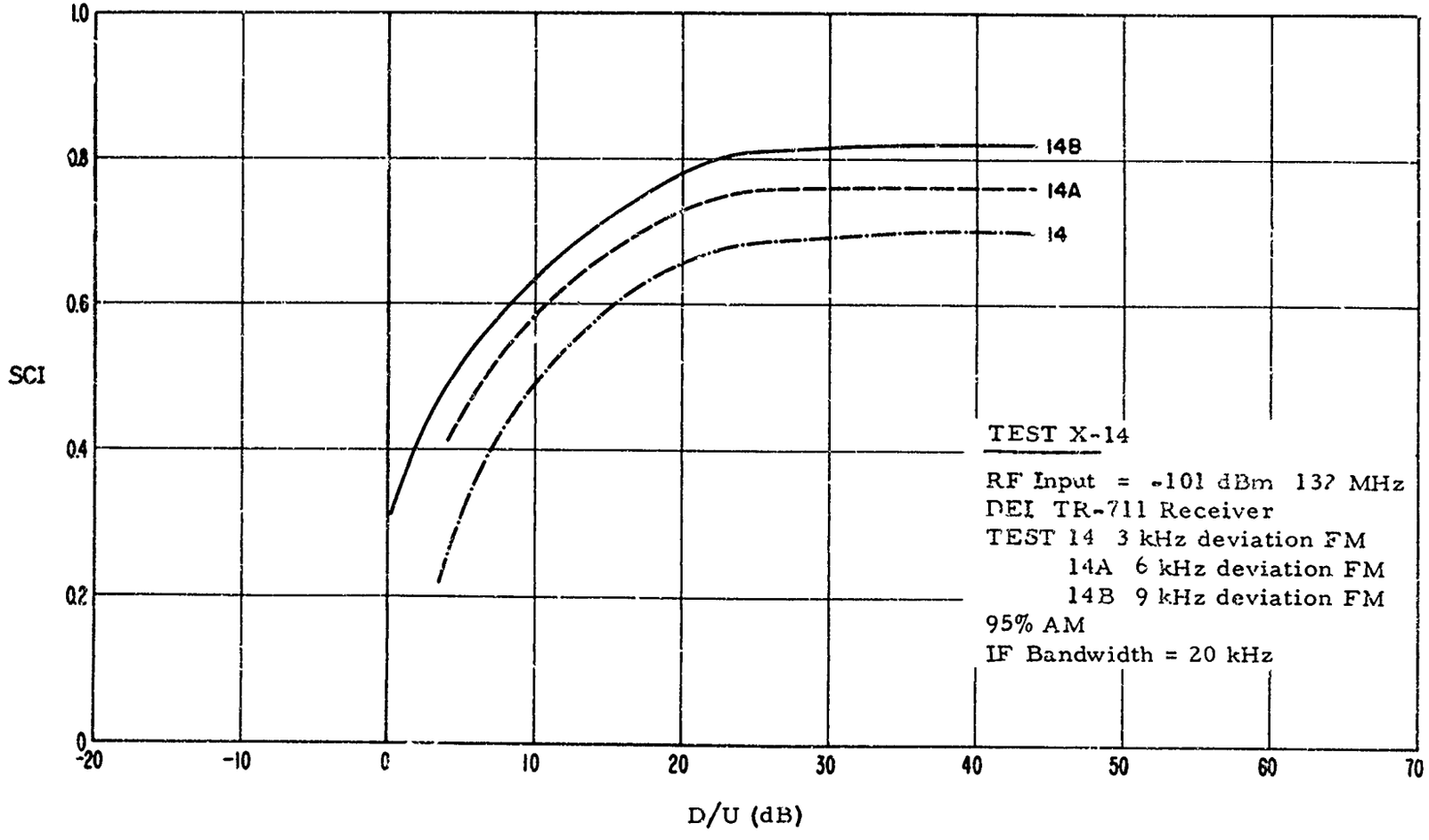

Figure C.22. Cochannel AM interference to FM signals (FM_D / AM cochannel at RF).

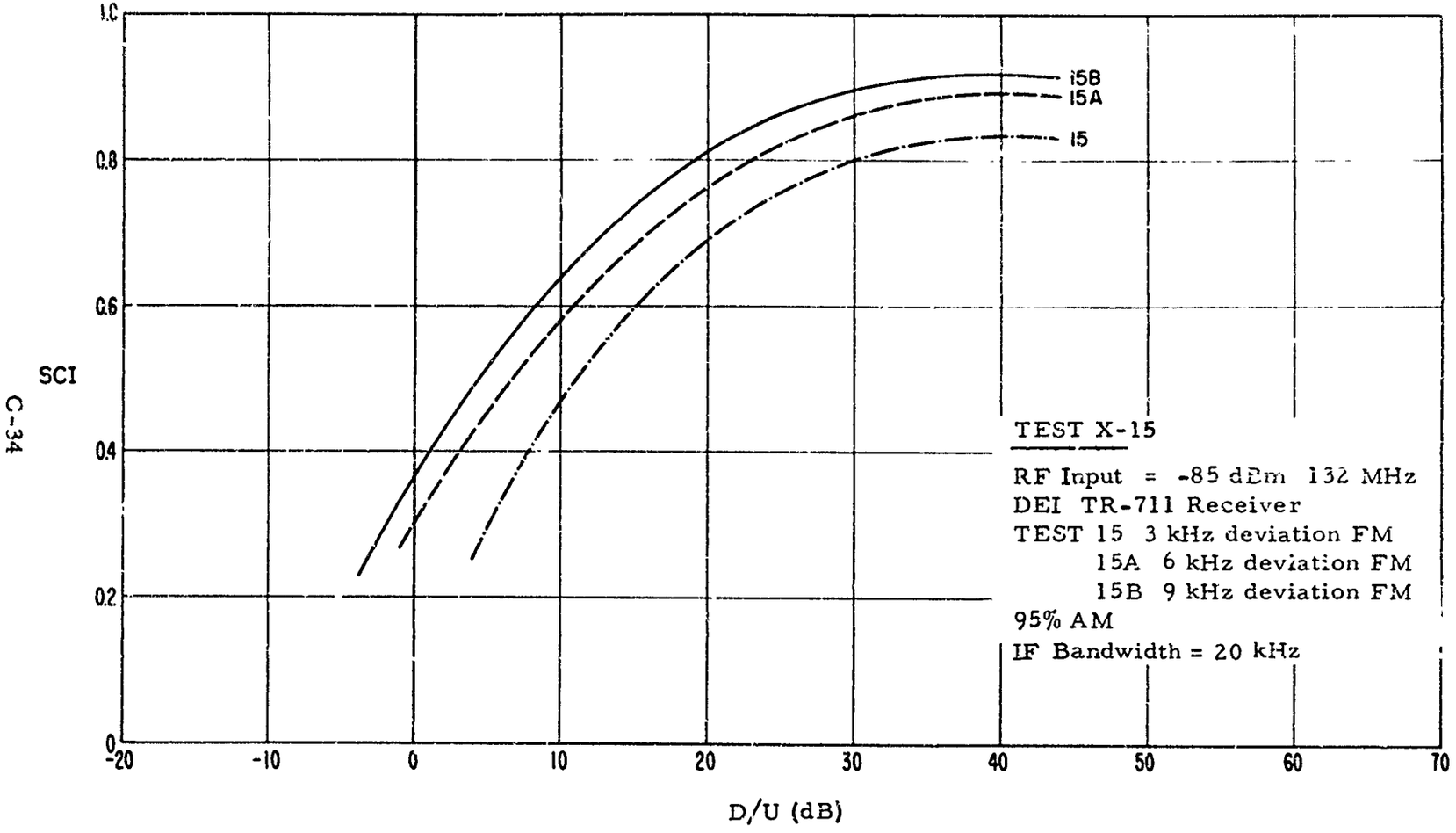

Figure C.23. Cochannel AM interference to FM signals (FM_D / AM cochannel at RF).

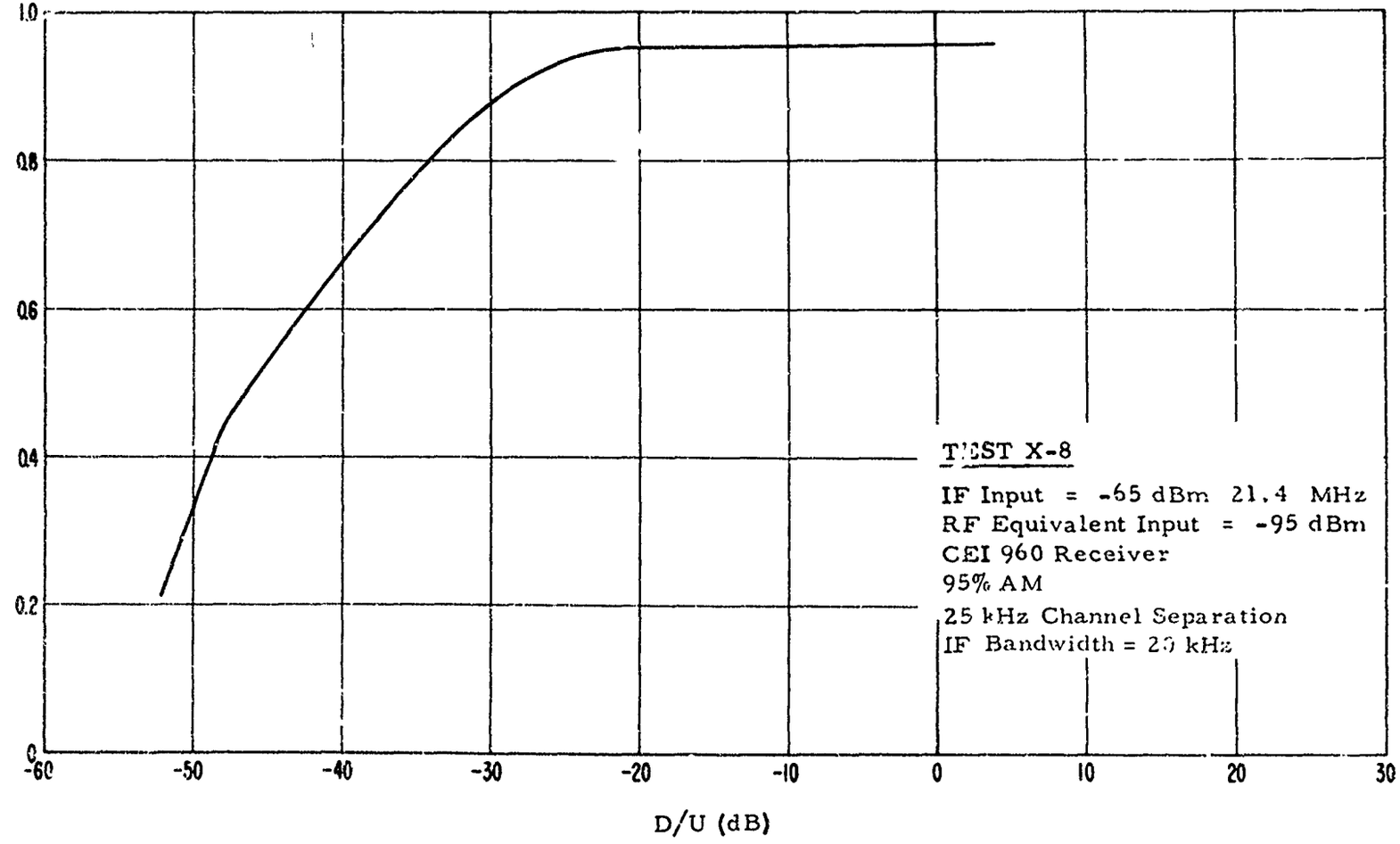

Figure C.24. Adjacent channel AM interference to AM signals (AM_0 / AM adjacent at IF).

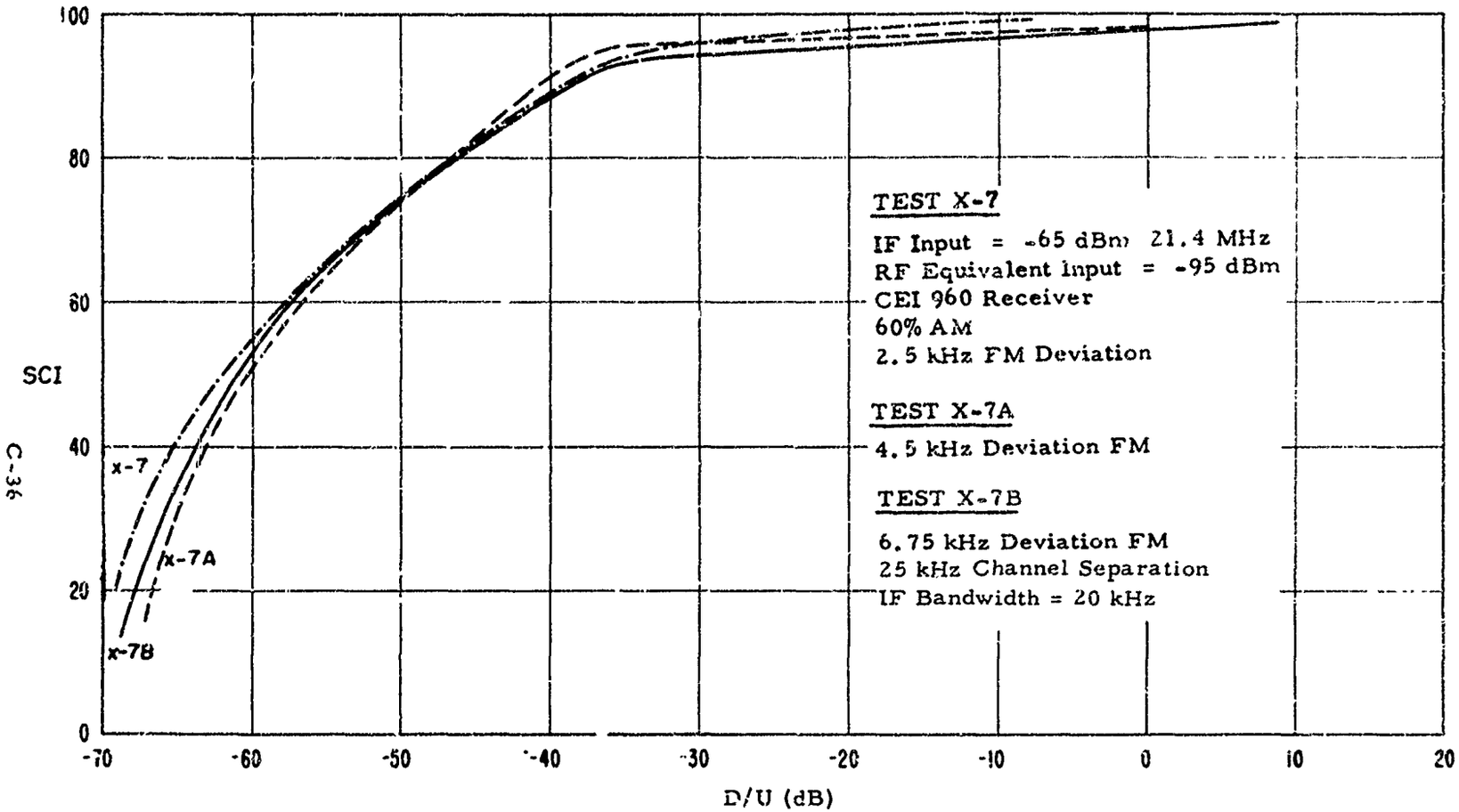

Figure C.25. Adjacent channel FM interference to AM signals (AM_0 / FM adjacent at IF), Test X.7.

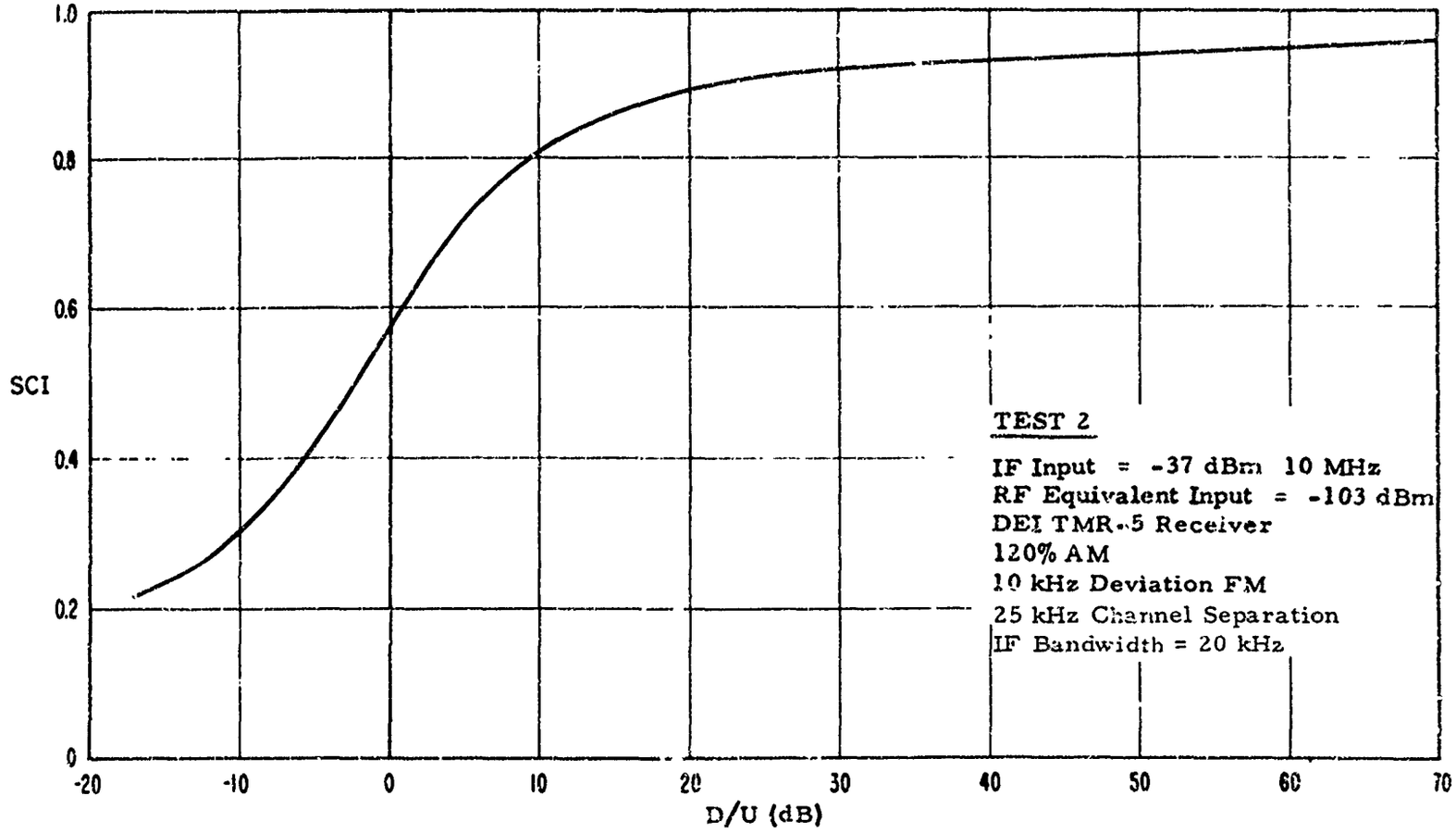

Figure C.26. Adjacent channel FM interference to AM signals (AM_b / FM adjacent at IF), Test 2.

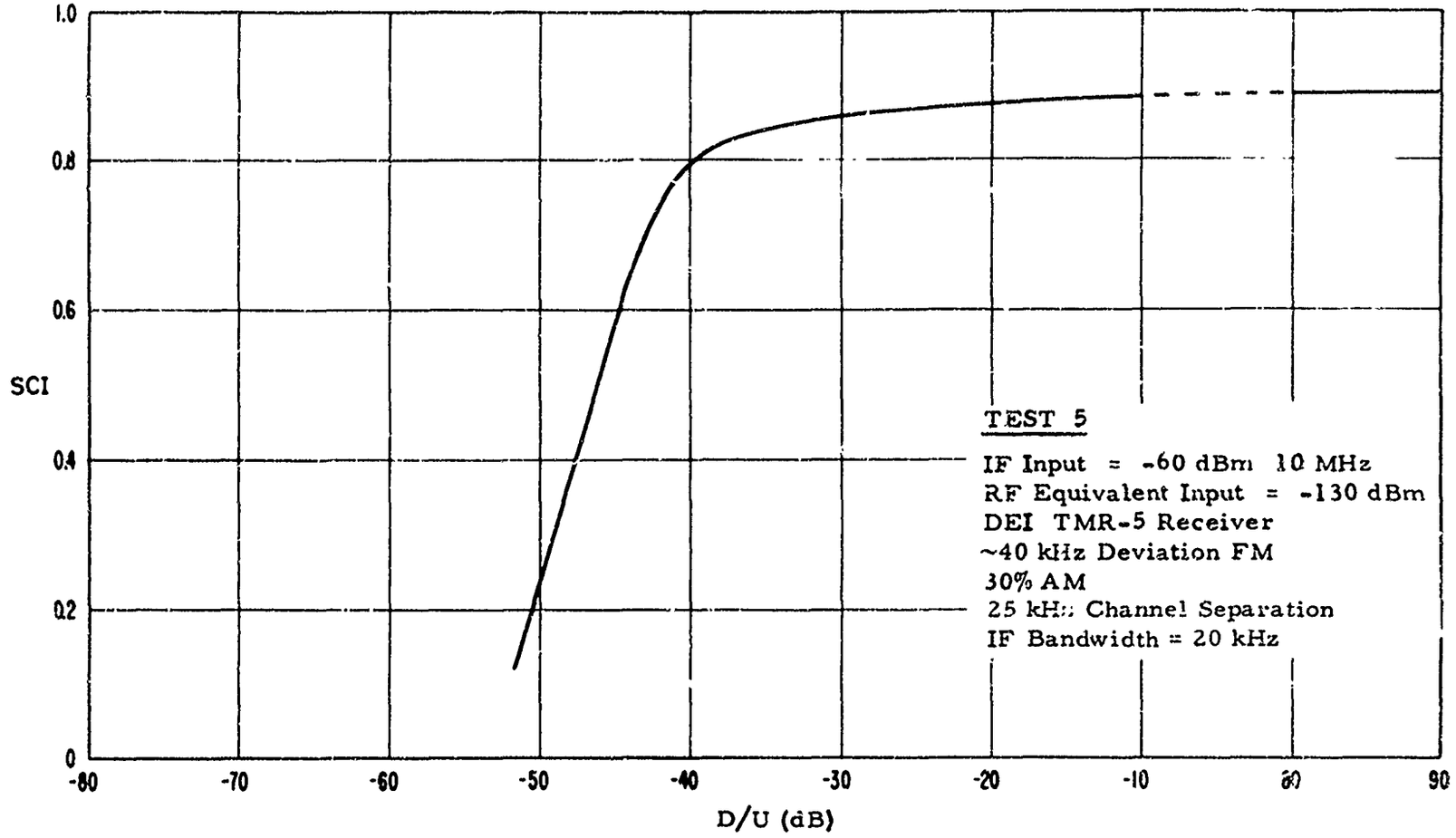

Figure C.27. Adjacent channel AM interference to FM signals (FM_D / AM adjacent at IF), Test 5.

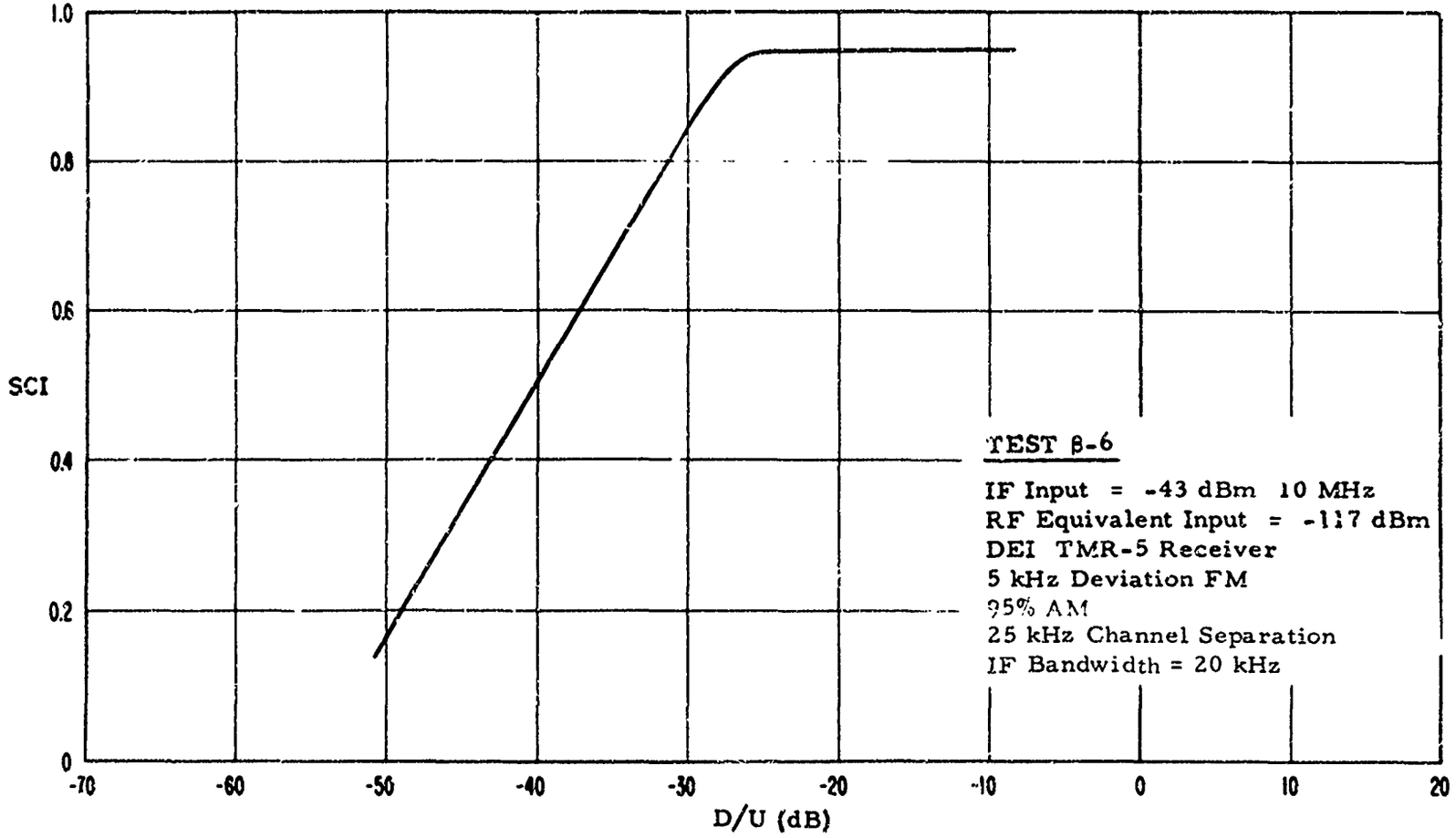

Figure C.28. Adjacent channel AM interference to FM signals (FM_D / AM adjacent at IF), Test 8-6.

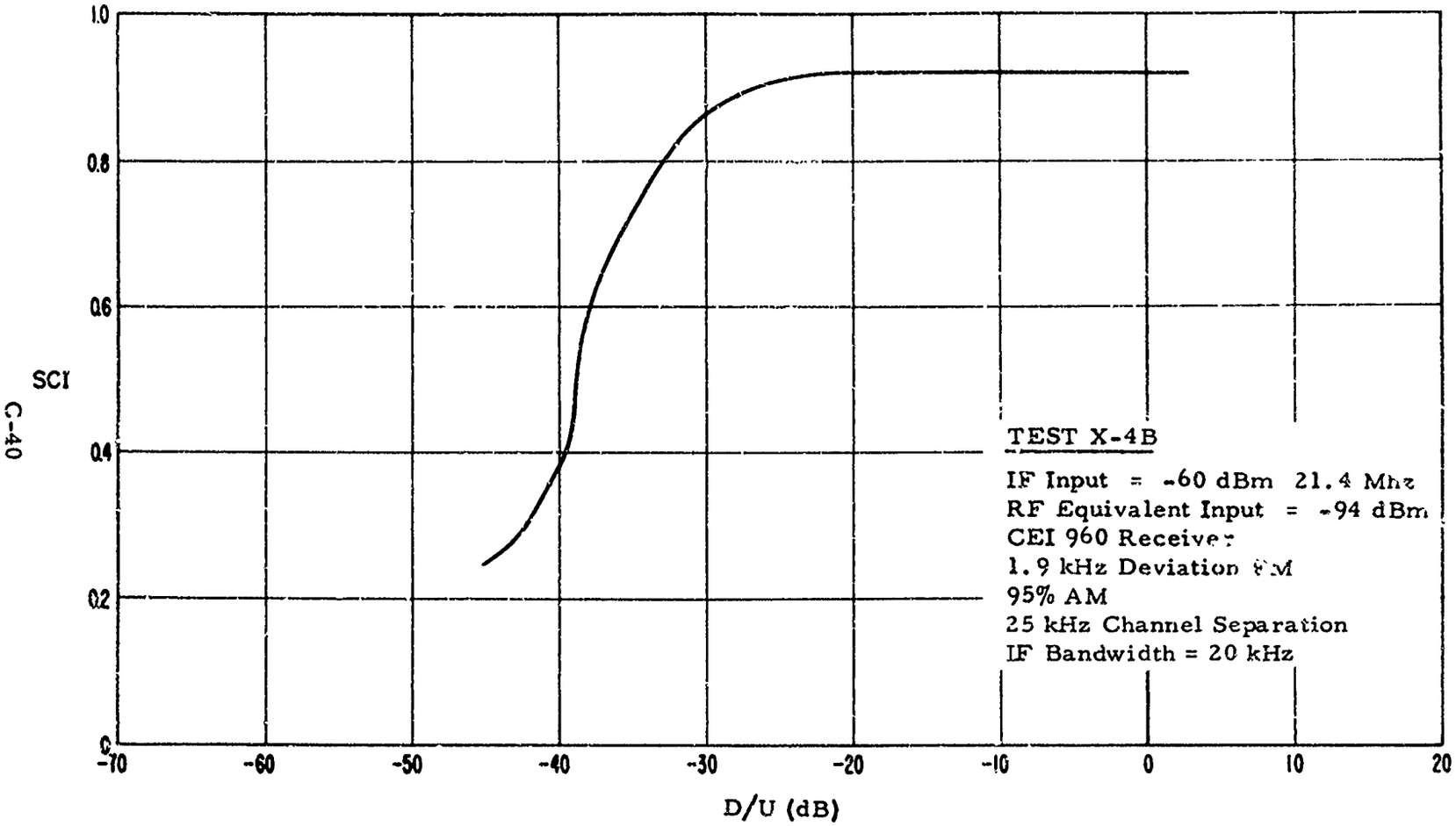

Figure C.29. Adjacent channel AM interference to FM signals (FM_0 / AM adjacent at IF), Test X-4B

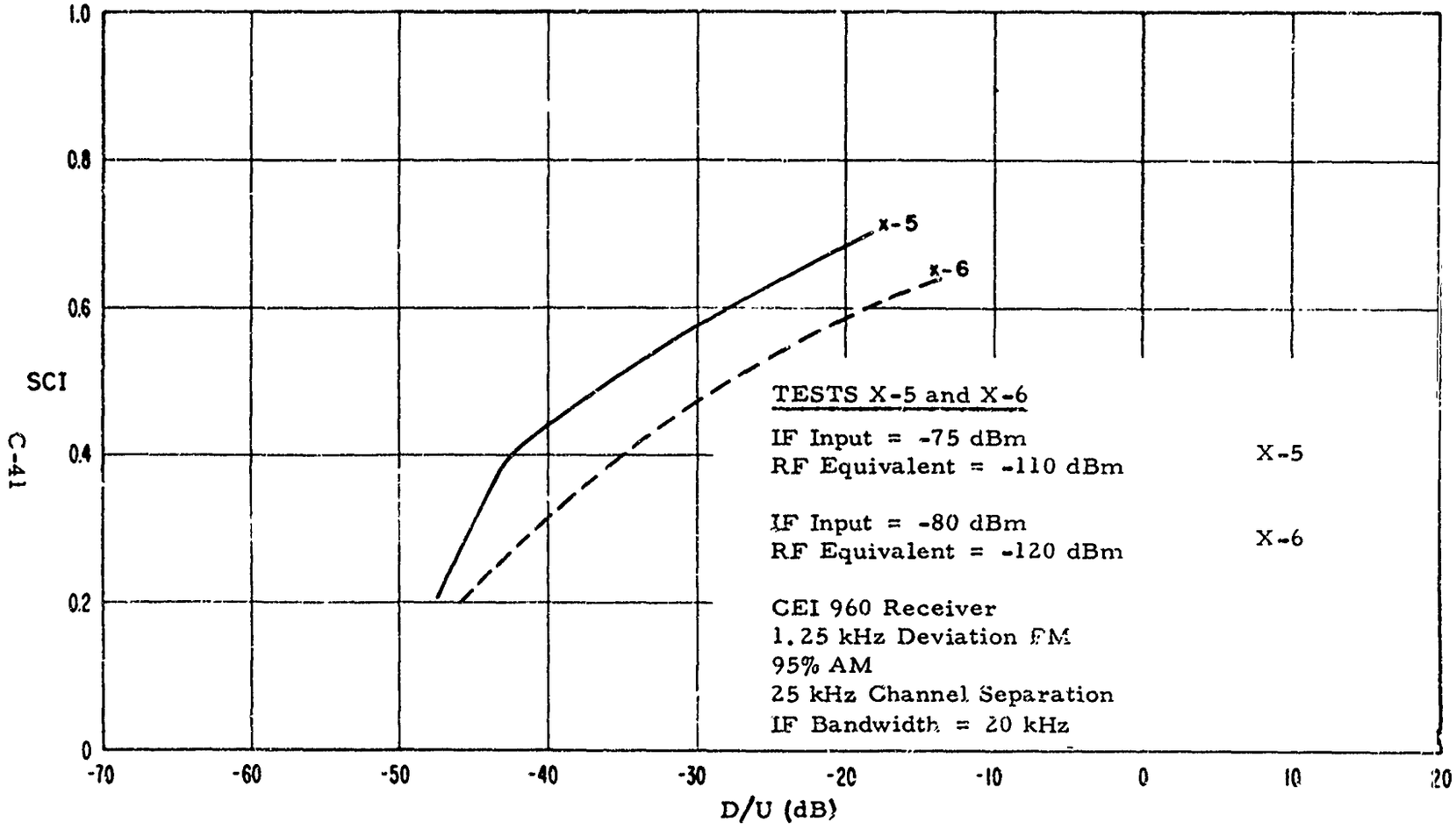

Figure C.30. Adjacent channel AM interference to FM signals (FM_D / AM adjacent at IF), Tests X-5 and X-6.

The tests in figures C.31 and C.32 again illustrate the improved SCI scores for a given D/U with a higher carrier level. For these tests, run at the TR-711 receiver IF frequencies, the SCI improvement is 0.1 for D/U at -25 dB and 6-kHz deviation.

Comparable improvements for RF tests are shown in figure C.33. Tests in figure C.32 were terminated at D/U = -30 dB because of inadequate interfering power available from the signal generator.

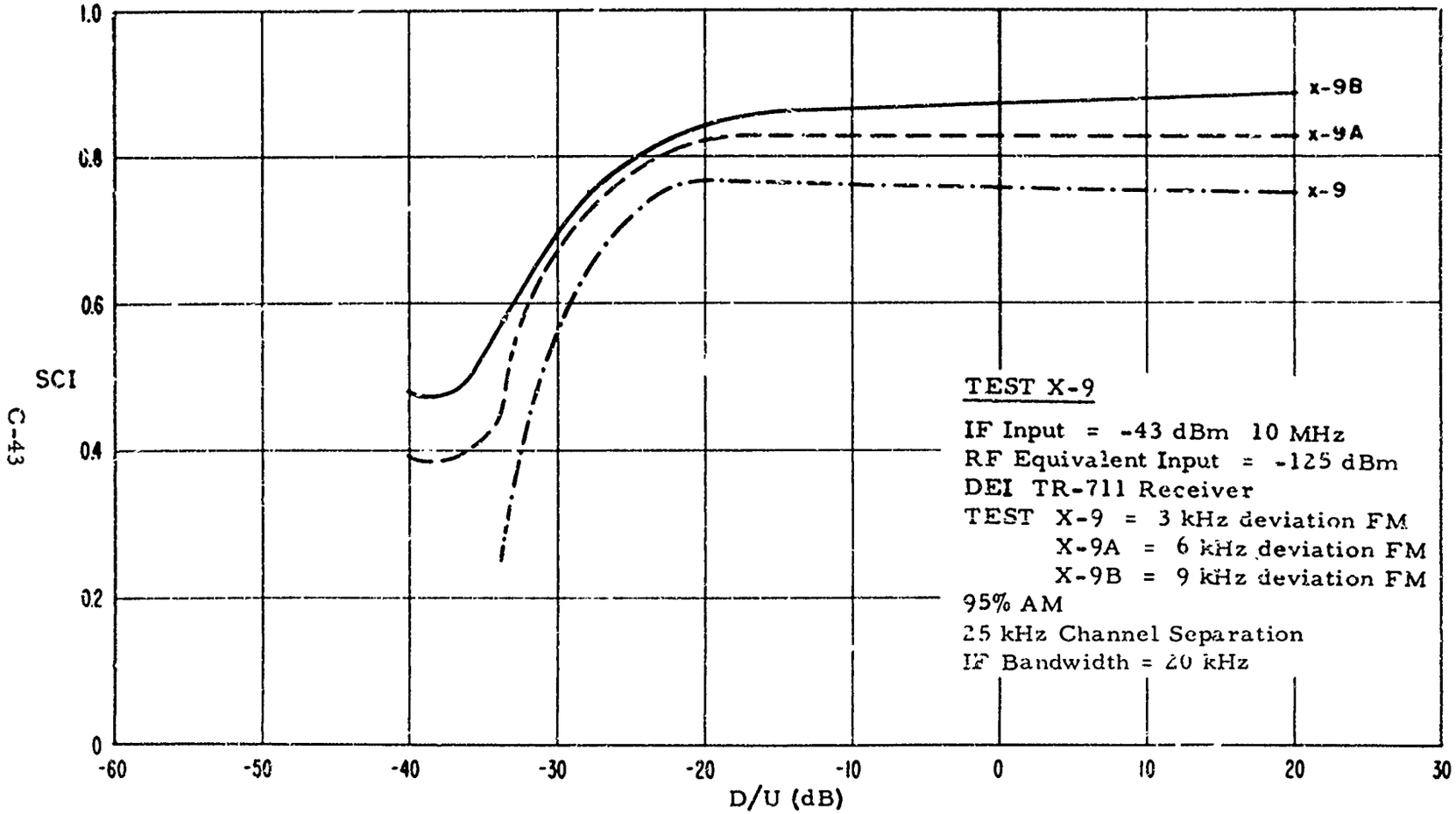

Figure C.31. Adjacent channel AM interference to FM signals (FM_0 / AM adjacent at IF), Test X-9.

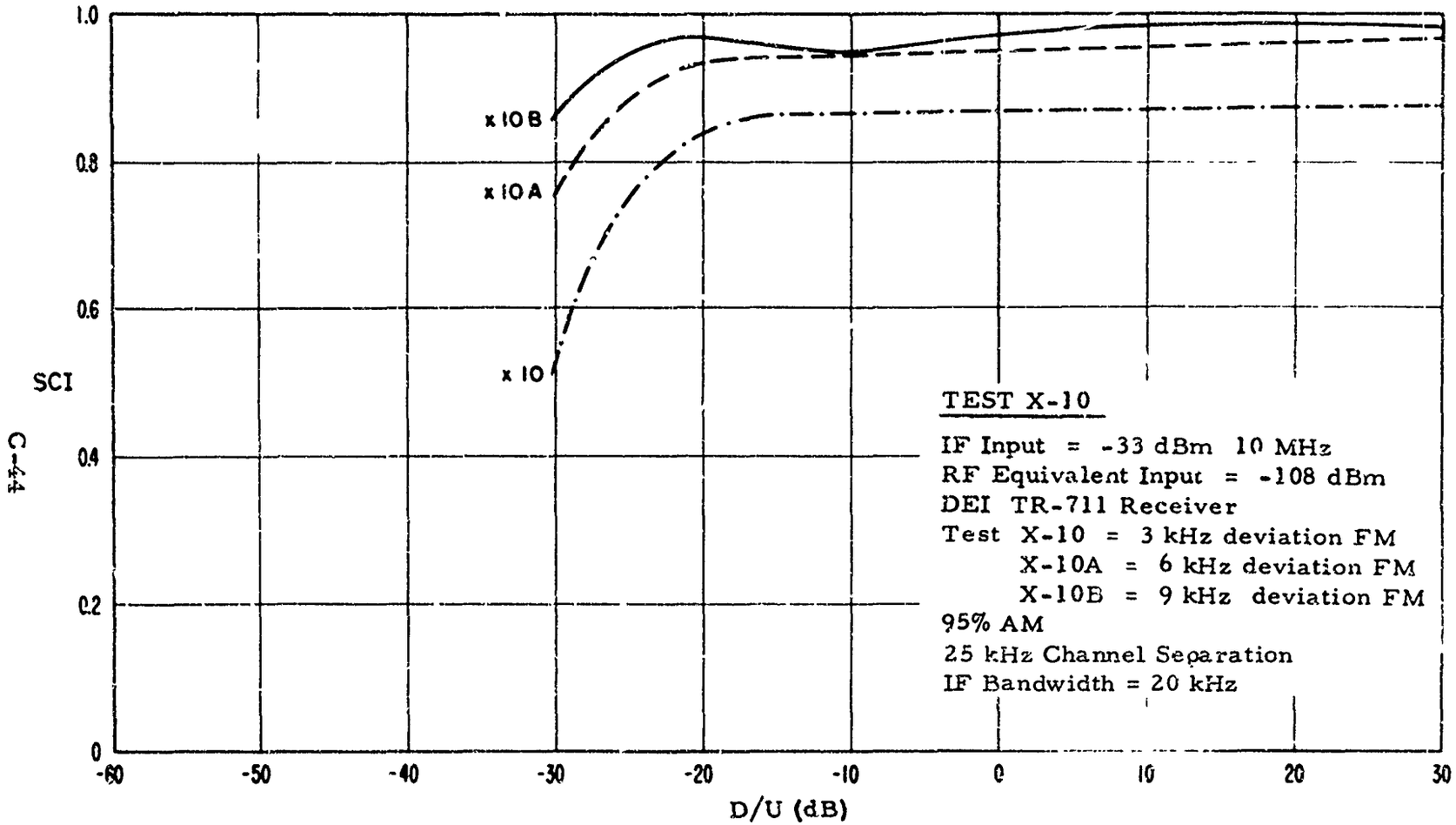

Figure C.32. Adjacent channel AM interference to FM signals (FM_D / AM adjacent at IF), Test X-10.

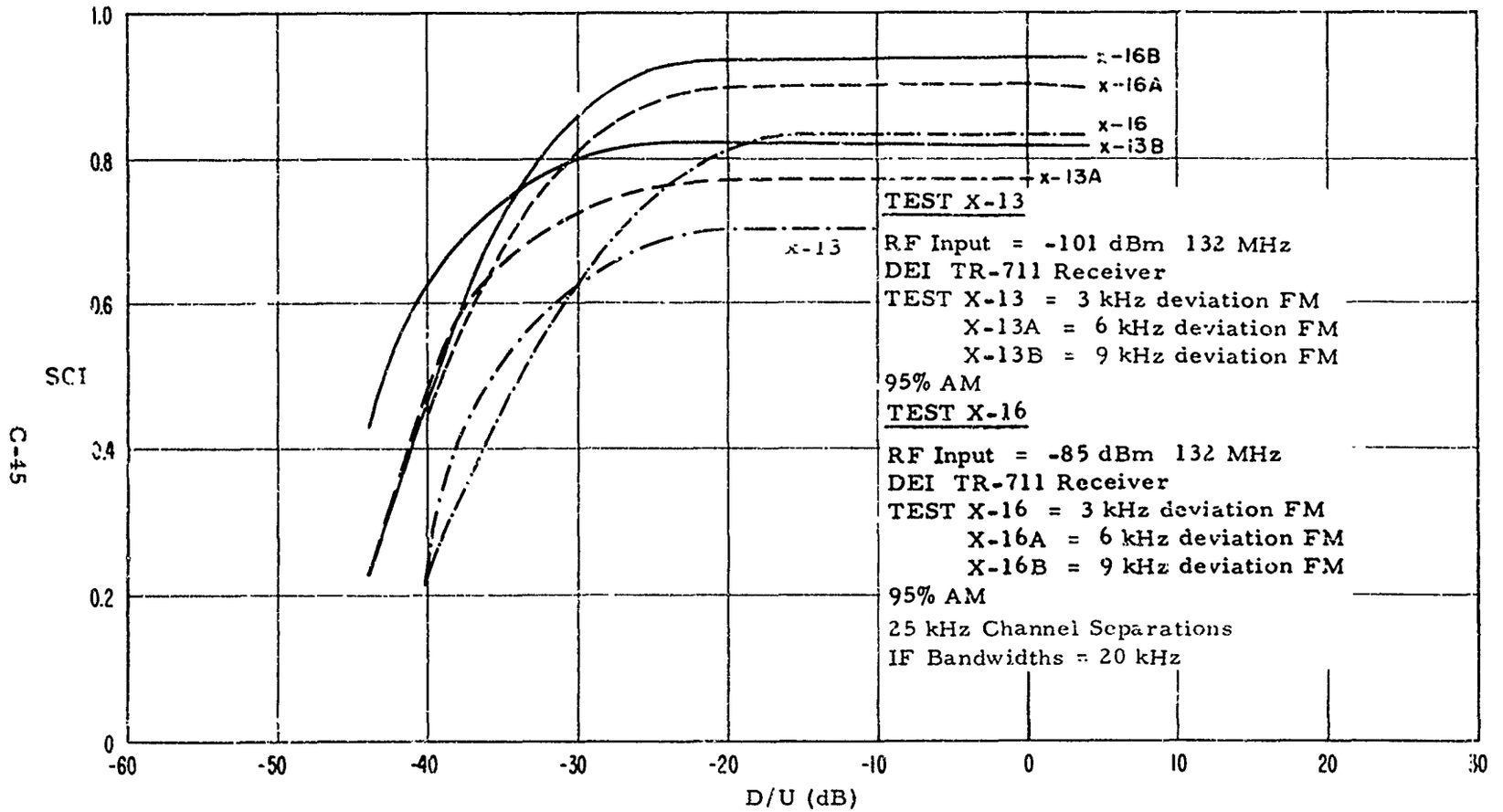

Figure C.33. Adjacent channel AM interference to FM signals (FM_D / AM adjacent at RF).

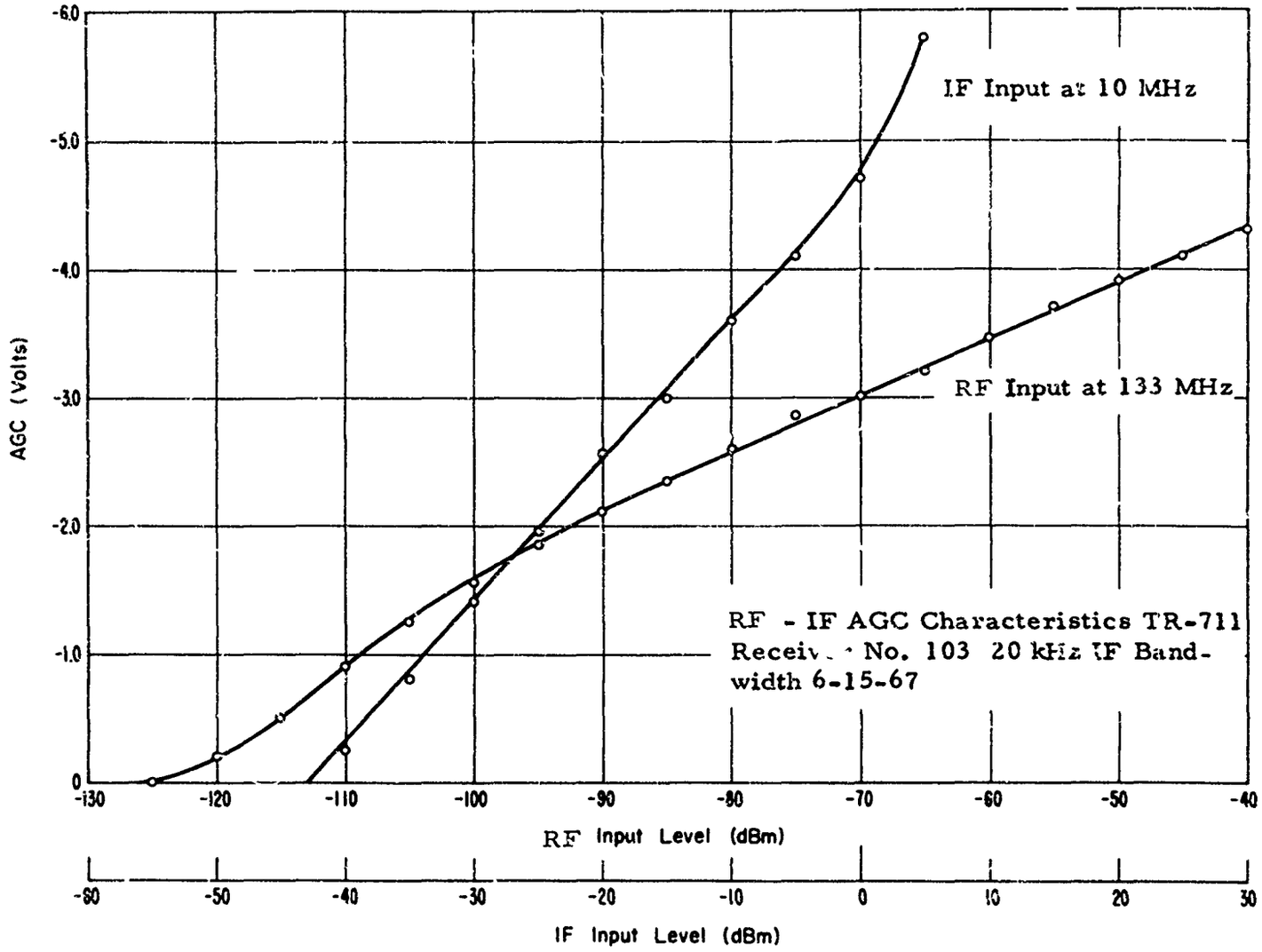

Figure C.34. Receiver AGC characteristics (TR-711).

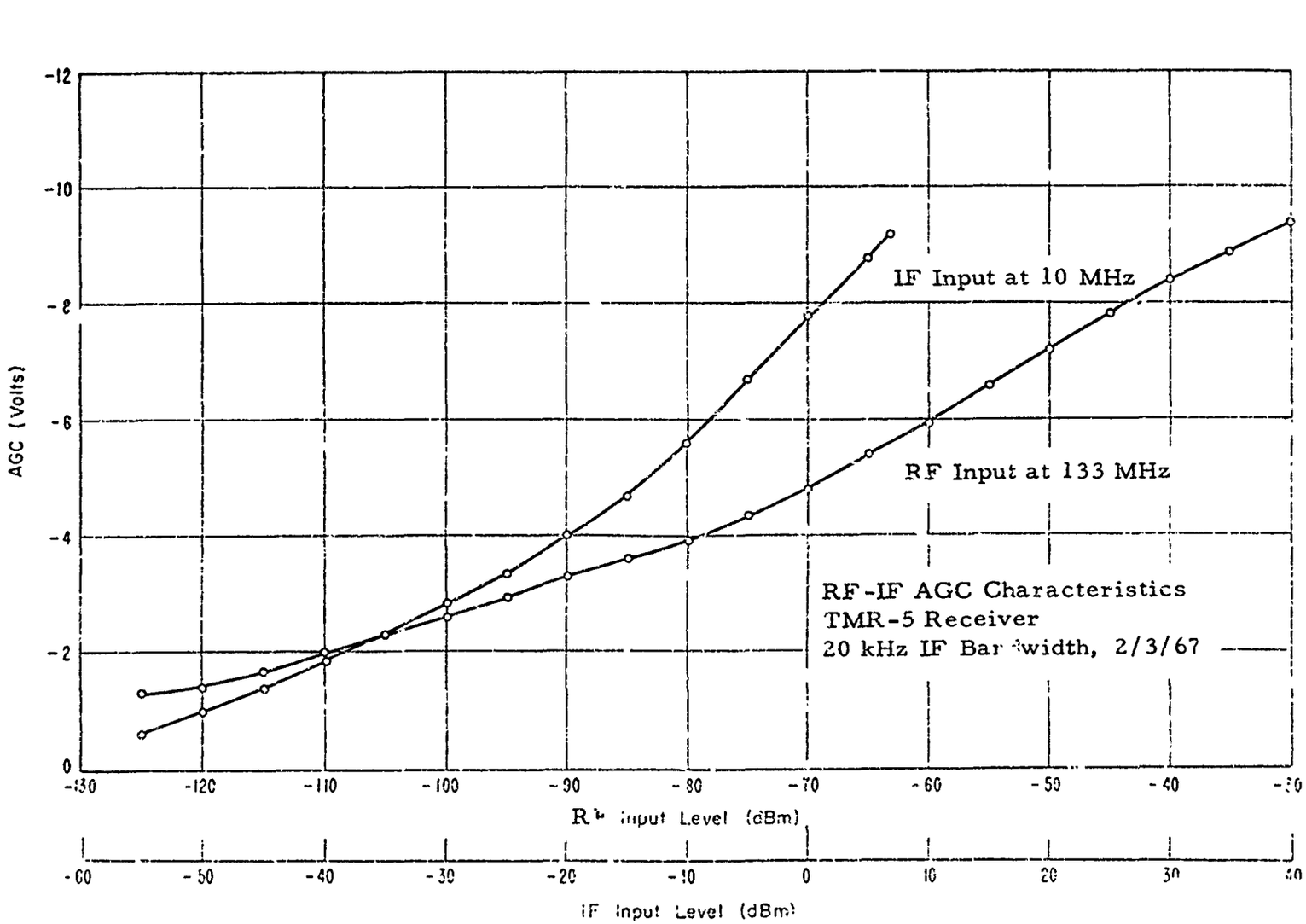

Figure C.35. Receiver AGC characteristics (TMR-5).

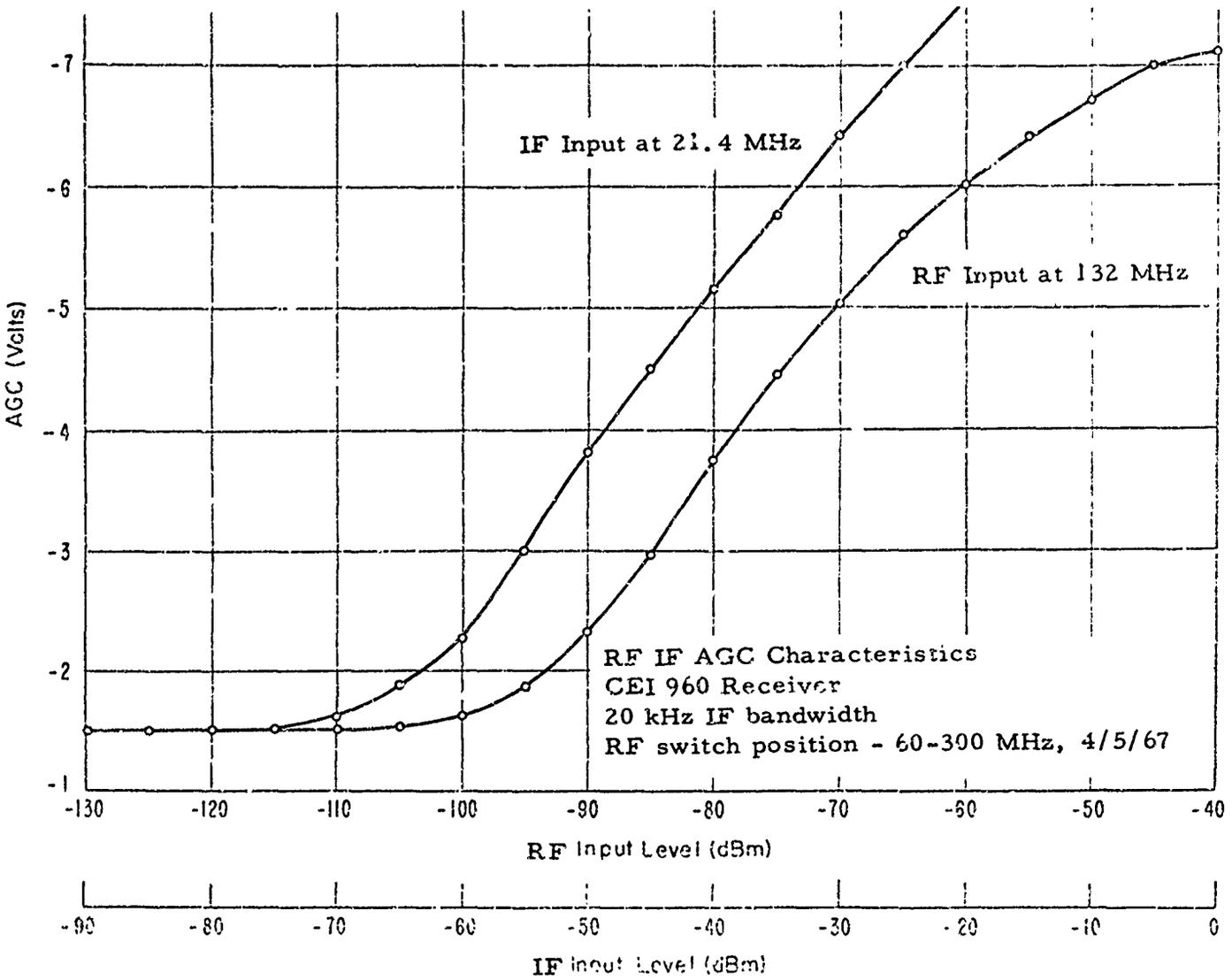

Figure C.36. Receiver AGC characteristics (CEI 960).

APPENDIX D
Addition of Powers Expressed in Decibels

The addition of powers expressed as ratios in decibels may be simplified by the conversion of the dB difference in the powers to a dB change to be applied to one of the powers as shown in figure D. 1.

In the usual case where the reference power is in the denominator of the power ratios, e. g., decibels referred to one watt the decibel change is added to the larger ratio.

If the reference power is in the numerator of the power ratio, e. g., S/ N ratio involving multiple noise sources or D/ U ratios involving multiple undesired signals expressed relative to the desired signal, the dB change is subtracted from the smaller ratio.

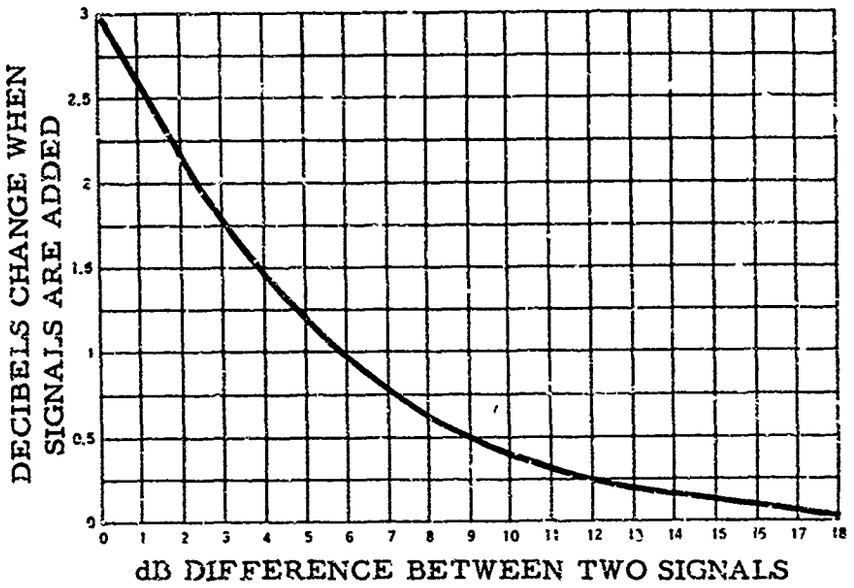

Figure D. 1. Chart to simplify the addition of signals expressed in decibels.

Example 1. (Reference powers in the denominator)

An example of determining the required protection ratio for figure C.4 (FM_0 / FM/ AM) follows. During the SCI measurements the FM desired signal was -87 dBm, the FM interference was -55 dBm and the AM interference was -50 dBm for an SCI of .77. Combining these three values requires taking the difference between the two interference values, reading the conversion from D.1, adding the difference to the greater of the two values and then subtracting from the desired signal.

(1) Determine the difference between -50 dBm and -55 dBm.

-50 - (-55) = 5

(2) Enter figure D.1 with 5 dB difference.
Read dB change of 1.2.

(3) Add 1.2 dB change to larger ratio.

-50 + 1.2 = -48.8 dB (undesired signal).

(4) Subtract undesired from desired signal.

-87 - (-48.8) = -38.2 dB (D/ U).

Example 2. (Reference power in the numerator)

If in example 1 the undesired signals were initially expressed relative to the desired signal, i.e. FM interference of -55 dBm as D/ U = -87 - (-55) = -32 dB; and the AM interference of -50 dBm as D/ U = -87 - (-50) = -37 dB the total ratio of desired to undesired signal may be calculated by:

(1) Determining the difference between -32 and -37 dB.

-32 - (-37) = 5 dB.

(2) Entering figure D.1 with the 5 dB difference and read a dB change of 1.2.

(3) Subtracting this change from the smaller ratio.

$$-37 - 1.2 = -38.2 \text{ dB (D/U)}.$$

The process may be continued irregardless of the number of signals involved as long as the reference power remains constant.

GPO 832-264